APPLICATIONS OF CLICK CHEMISTRY IN DRUG DISCOVERY, BIOCONJUGATION AND MATERIAL SCIENCE

by

XINGHAI NING

(Under the Direction of Geert-Jan Boons)

ABSTRACT

Click chemistry is a chemical philosophy introduced by Sharpless in 2001 and describes chemistry tailored to generate substances quickly and reliably by joining small units together. This dissertation has focused on the applications of click chemistry in three most relevant categories including drug discovery, bioconjugation, and materials science.

The first application is developing new anti-influenza drugs by using click chemistry. We designed the novel anti-influenza reagents based on the Altermune method, which would stimulate the immune system to attack influenza viruses using a Linker Molecule(LM), which can recognize the viruses and also be recognized by immune system. The LM then redirects the immune response to the influenza viruses. The second application is developing a new bioconjugation strategy basing on the "click philosophy". We developed a new click reagent, 4-dibenzocyclooctynol, which reacts exceptionally fast with azido compounds to give stable triazoles in the absence of any catalyst. A biotin-modified derivative is ideally suited for visualizing and tracking glycoconjugates of living cells that are metabolically labeled with azido-containing monosaccharides. In addition, we also developed a novel quantitative isotopic and chemoenzymatic tagging (QUIC-Tag) containing 4-dibenzocyclooctynol for monitoring the

dynamics sialylation *in vivo* using quantitative mass spectrometry-based proteomics. Because sialic acid is a terminal glycan residue with a notably increased expression in cancers, this method will help to delineate the molecular basis for aberrant glycosylation in cancer and could ultimately be applied for diagnostic and therapeutic.

The third application is preparing new nano-drug delivery sysytems. We tried to develop novel multifunctional micellar nanosystems for targeted drug delivery device. To achieve these goals, we successfully conjugated targeting moieties on the nanoparticle surface by using click chemistry. These freestanding polymer particles with targeting ligands can be used as carriers for drug and imaging agents for biomedical applications.

INDEX WORDS: Click chemistry, Click reaction, Drug discovery, Influenza Virus, Anti-influenza, Altermune Method, Bioconjugation, Cu^I-free click, Cell imaging, quantitative isotopic and chemoenzymatic tagging (QUIC-Tag), Material Science, Drug delivery, Nanoparticles, Micelles, Magnetic Nanoparticles, MRI.

APPLICATIONS OF CLICK CHEMISTRY IN DRUG DISCOVERY,

BIOCONJUGATION AND MATERIAL SCIENCE

by

XINGHAI NING

B.S., Shandong University, P.R. China, 2000

M.S., Peking Union Medical College (PUMC), P.R. China, 2003

A Dissertation Submitted to the Graduate Faculty of the University of Georgia in

Partial Fulfillment of the Requirements for the Degree

DOCTOR OF PHILOSOPHY

ATHENS, GEORGIA

2008

APPLICATIONS OF CLICK CHEMISTRY IN DRUG DISCOVERY,

BIOCONJUGATION AND MATERIAL SCIENCE

by

XINGHAI NING

Major Professor: Geert-Jan Boons

Committee: Bingqian Xu

                  Yan Geng

Electronic Version Approved:

Maureen Grasso

Dean of the Graduate School

The University of Georgia

December 2008

DEDICATION

This dissertation is dedicated to my parents and in-laws, wife Zhirui Wang and my other family members for their unconditional support and encouragement.

ACKNOWLEDGEMENTS

I would like to thank Professor. Geert Jan Boons for giving me an opportunity to work in his lab and for his support and supervision throughout my research. I would like to thank Dr. Margreet Wolfert for doing all the bioassays of my compounds without which my projects wouldn't be complete and also explaining me all the basics of the assays. I would like to thank my committee members Dr. Xu and Dr. Geng for their suggestions and help. I would like to thank Dr. John Glushka for helping me with the NMR instruments and clarifying doubts about the spectrum. It has been my greatest pleasure to work with Dr. Andre Venot, who is the most experienced person in our lab. I not only learned how to carry out experiments, but also how to judicially use various chemicals and keep the hood and surroundings clean, and follow safety precautions. I would like to thank Dr. Therese Buskas, Dr. Jana Rauvolfova, Dr. Jun Guo, and Dr. Xiuru Li for their help in my projects. I also want to express my appreciation toward all my lab mates who have been very friendly, helpful,resourceful, and supportive.

I would like to specially thank my wife Zhirui Wang for her inspiration, encouragement, and support at all times of my PhD life without which it would not have been easy to accomplish this task. Also, I want to thank my parents, my parent in laws, and my other family members for their constant support and encouragement.

Finally I would like to thank Saeid for his technical help with computer and other software related issues and CCRC staff members who have been very friendly and helpful.

TABLE OF CONTENTS

LIST OF FIGURES

ABBREVIATIONS

Å…………………………………………………………………........Angstrom

Ac……………………………………………………………………... Acetyl

Ac$_2$O…………………………………………………….........Acetic anhydride

AcOH……………………………………………………………….. Acetic acid

BH$_3$·NHMe$_2$………………………………………………..Dimethylamine borane

BF$_3$·Et$_2$O……………………………………………….Borontrifluoride diethylether

Bn……………………………………………………………………Benzyl

BSA…………………………………………………………...Bovine serum albumin

BuOH…………………………………………………………………Butanol

C……………………………………………………………………Carbon

Cbz…………………………………………………………………Carboxybenzyl

CC……………………………………………………………Click Chemistry

C$_6$H$_5$CH-(OMe)$_2$…………………………………………….Benzaldehyde dimethylacetal

CDAP…………………………………………………… Cyano dimethyl aminopyridinium

CHCl$_3$……………………………………………………………..Chloroform

CHF………………………………………………………........ Congestive heart failure

CH$_3$CN………………………………………………………........... Acetonitrile

CHO……………………………………………… ………………Chinese hamster ovary

CT……………………………………………………………Computed tomography

CSA………………………………………………………Camphor Sulfonicacid

HPAEC-PAD…………………………High performance anion exchange chromatography pulsed amperometric detection

HSQC……………………………………………...Heteronuclear single quantum coherence

Hz………………………………………………………………………………..Hertz

Kdo……………………………………………..............3-deoxy-D-manno octulosonic acid

IDCT………………………………………………Iodonium di-sym-collidine triflate

KLH………………………………………………………………..Keyhole lymphocyte

M………………………………………………………………………….. Molar, Mega

Man………………………………………………………………......... Mannose

MALDI-TOF-TOF………Matrix assisted laser desorption ionization spectroscopy-time of flight

MeOH…………………………………………………………………… Methanol

MgSO$_4$………………………………………………….......... Magnesium sulfate

MRI………………………………………………………… ….magnetic resonance imaging

MS………………………………………………………………........... Molecular sieves

NIS…………………………………………………………........... *N*-iodosuccinimide

NaH…………………………………………………………………….... Sodium hydride

NaHCO$_3$…………………………………………………………........ Sodium bicarbonate

NaN$_3$………………………………………………………………........ Sodium azide

NaOH…………………………………………………………........... Sodium hydroxide

NaOMe………………………………………………………….......Sodium methoxide

Na$_2$S$_2$O$_3$…………………………………………………….......... Sodium bisulfite

NH$_3$………………………………………………………………….........Ammonia

NO………………………………………………………………….......... Nitric oxide

NM…………………………………………………………………………………..Nano meter

NH_2NH_2……………………………………………………….........................Hydrazine

NMR……………………………………………………………….Nuclear magnetic resonance

PCL……………………………………………………………………Polycaprolactone

Pd…………………………………………………………………………...........Palladium

$Pd(OH)_2$……………………………………………………………Palladium hydroxide

PEG………………………………………………………………....Polyethylene glycol

PS…………………………………………………………………...........Polysaccharide

PBS………………………………………………………………….........Phosphate buffered saline

PCC……………………………………………………………........... Pyridinim chlorochromate

PMe_3………………………………………………………………… Trimethyl phosphine

TBDMS…………………………………………………………........... Tert-butyl dimethylsilyl

TEM…………………………………………………………………Transmission electron microscopy

TFA……………………………………………………………………. Trifluroacetic acid

Tf_2O…………………………………………………………………Triflic anhydride

TfOH………………………………………………………………….. Triflic acid

TLC…………………………………………………………………Thin layer chromatography

THF……………………………………………………………….......... Tetrahydrofuran

TMS…………………………………………………………………….. Trimethyl silyl

TMSOTf……………………………………………………... Trimethylsilyl trifluromethane sulfonate

TOCSY…………………………………………………………..Total correlation spectroscopy

UV……………………………………………………………………….Ultraviolet

Zn…………………………………………………………………………... Zinc

CHAPTER 1

INTRODUCTION AND LITERATURE REVIEW

1.1 INTRODUCTION

Secondary metabolites produced in Nature have diverse architectures with extensive carbon-hetero atom bond C-X-C bond networks. These compounds often possess important biological activities that make them potential therapeutic agents.[1] However, drug discovery based on these natural products is generally slow, costly, and hindered by complex synthesis. The recent development of combinatorial chemistry and high-throughput screening has aided in the rapid generation of compounds in search of biological function but relies heavily on the success of the individual reactions to construct molecular frameworks.[2] Therefore, a set of criteria defining reliable reactions known as "Click Chemistry" was proposed to meet the demands of modern day chemistry and in particular, the demands of drug discovery.[3]

Click Chemistry was coined by Sharpless in 2001 for an approach to synthesis that prizes the use of a few key chemical reactions to generate substances that contain particular chemical groups by joining small units together. The reactions have a strong energetic driving force that ensures that the starting compounds react every time, quickly, efficiently, and without creating unwanted byproducts. This was inspired by the fact that Nature also link compounds together by joining small modular units. It is, indeed, noteworthy that over recent years, complicated reactions requiring either complex apparatus, harsh experimental conditions, or complex-purification techniques, have been less frequently studied than in the last century and gradually replaced by simpler tools. In this context, the straightforward "click" reactions have become

tremendously popular in both academic and industrial research, as evidenced by a nearly exponential growth in the amount of related publications. A literature search via SciFinder Scholar®, performed on October 1st of 2008, revealed a total of 1015 publications containing the keywords "click chemistry" or "click reaction", which included journal articles, reviews, preprints, abstracts, patents, and dissertations. As shown in Figure1.1, publications in this area have quickly increased over the past 5 years.
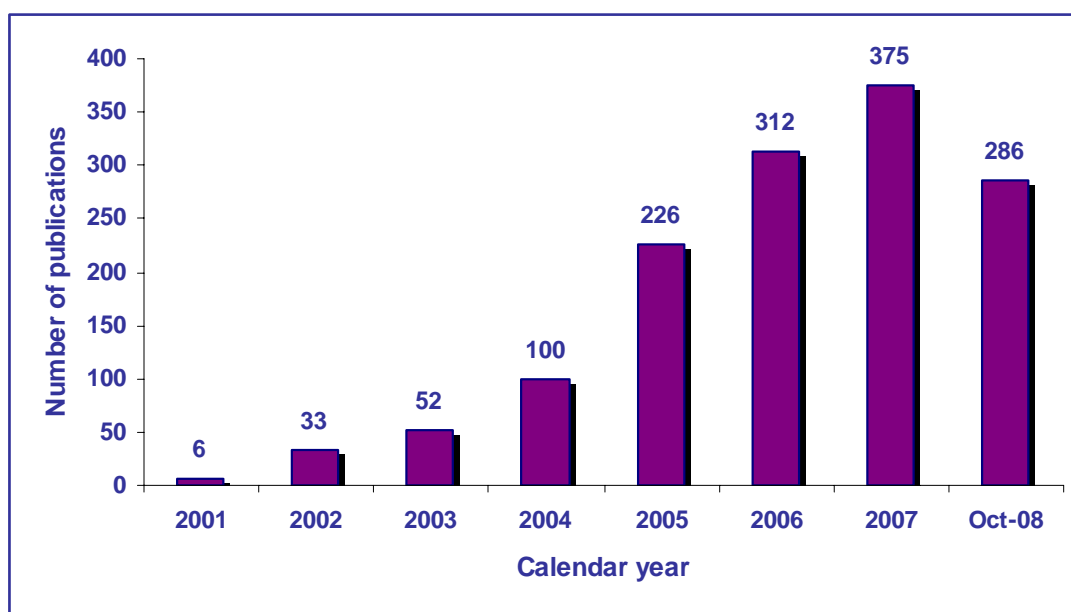
Figure 1.1 Number of publications containing the key words "click chemistry" or "click reaction" from 2002–2008. The literature search was performed via SciFinder Scholar® on Oct. 1, 2008 and included journal articles, abstracts, preprints, dissertations, patents, and reviews.

1.2 THE CLICK CHEMISTRY PHILOSOPHY

Examination of the biomolecules created by Nature, reveals an overall preference for carbon–heteroatom bond connecting units over carbon–carbon bond; for example, nucleic acids, proteins and polysaccharides are condensation polymers of repeating subunits (nucleotide, amino acid and monosaccharide units) linked through carbon–heteroatom bonds. This strategy of

making large oligomers from relatively simple building blocks can be described as Nature's way of performing combinatorial chemistry with remarkable modularity and diversity. All nucleic acids are created from 8 building blocks that are joined *via* reversible heteroatom links. In addition, enzymes ensure that chemical processes can overcome large enthalpic hurdles by division into a series of reactions each with a small energy hurdle. Following Nature's lead, and limiting the search for new substances to those which can be generated by joining small units together through heteroatom links, Sharpless *et al.* defined click chemistry.[4]

In 1996 Guida calculated the size of the pool of drug candidates at 10^{63}, based on the presumption that a candidate consists of less than 30 non-hydrogen atoms, weighs less than 500 daltons, is made up of atoms of hydrogen, carbon, nitrogen, oxygen, phosphorus, sulfur, chloride and bromide, and is stable at room temperature and stable towards oxygen and water.[5] Click chemistry in combination with combinatorial chemistry, high-throughput screening speeds up new drug discoveries by making each reaction in a multistep synthesis fast, efficient and predictable.

A click reaction satisfies many criteria: it can be applicable modularly and widely in scope, obtain high chemical yields, produce minimal byproducts that can be removed by chromatographic methods, and be stereospecific (but not necessarily enantoselective) when applicable. In addition, it has simple reaction conditions, involves readily available starting materials, reagents, and a benign solvent (preferably water), and allows simple isolation of products by crystallization or distillation but not preparative chromatography. In practice, click reactions tend to have large negative free energies and hence involve carbon-heteroatom bond-forming processes. Thus, unlike many conventional synthetic reactions, the power of click chemistry lies in its simplicity and ease of use.

Although meeting the requirements of a click reaction is a tall order, four major reaction classes have been identified, which step up to the mark (Figure 1.2):

• Cycloaddition-- these especially refer to 1,3-dipolar cycloadditions, but also include hetero-Diels-Alder cycloadditions[6].

• Nucleophilic ring-openings—these refer to the openings of strained heterocyclic electrophiles, such as aziridines, epoxides, cyclic sulfates, aziridinium ions, episulfonium ions, etc.[6]

• Non-aldol carbonyl chemistry—examples include the formations of ureas, thioureas, hydrazones, oxime ethers, amides, aromatic heterocycles, etc.[4] Carbonyl reactions of the aldol type generally have low thermodynamic driving forces, hence they have longer reaction times and produce side products, and therefore cannot be considered click reactions[4].

• Additions to carbon-carbon multiple bonds—examples include epoxidations, aziridinations, dihydroxylations, sulfenyl halide additions, nitrosyl halide additions, and certain Michael additions.[6,7]
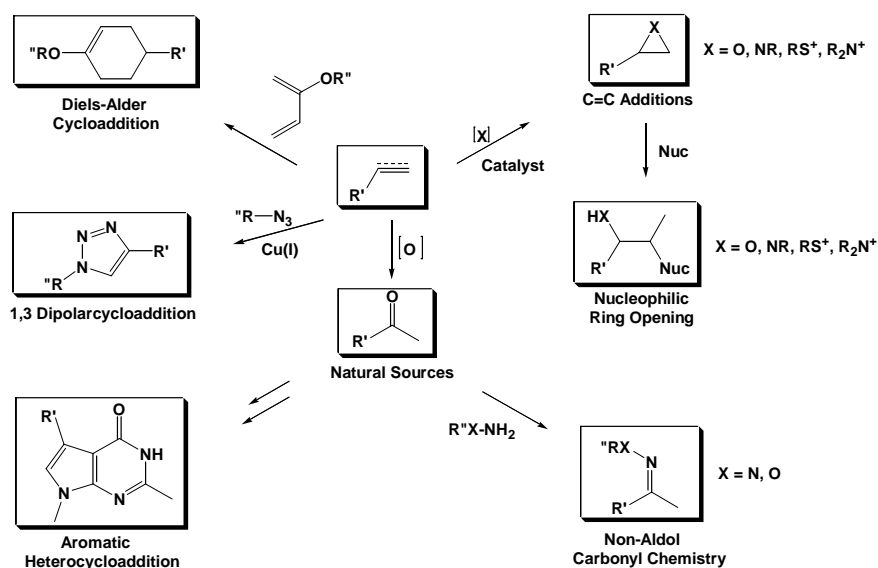
Figure 1.2 Major classifications of click chemistry reactions

The cream of the crop

Of all the reactions which meet the click requirements, the copper (I) catalyzed variant [8,9] of the Huisgen 1,3-dipolar cycloaddition (CuAAC) [10-12] has certainly been the "cream of the crop" of click reactions, so much that it is now undoubtedly the premier example of the click chemistry reaction. The formation of 1,2,3-triazoles by 1,3-dipolar cycloaddition of azides and alkynes was first reported by Arthur Michael at the end of the 19th century and significantly developed by Rolf Huisgen in the 1960s.[10,11,13] In the absence of a transition-metal catalyst, these reactions are not regioselective, relatively slow, and require high temperatures to achieve acceptable yields (Figure 1.3A). Various attempts to control the regioselectivity have been reported without much success until Meldal and co-workers, in early 2002, reported that the use of catalytic amounts of copper(I), which can bind to terminal alkynes, leads to fast, highly efficient, and regioselective azide-alkyne cycloaddition (AAC) at room temperature in organic medium (Figure 1.3B).[8] Shortly after, Sharpless and co-workers manifested that CuAAC can be successfully performed in polar media, such as methanol or pure water.[9] Furthermore, the reaction is compatible with various functional groups such as esters, acids, alkenes, alcohols, and amines and requires no protecting groups, and proceeds with almost complete conversion and selectivity for the 1,4-disubstituted 1,2,3-triazole (*anti*-1,2,3-triazole). No purification is generally required. These two important breakthroughs led to a remarkable renaissance of Huisgen cycloadditions in synthetic chemistry. Due to the reliability and generality of the copper(I)-catalyzed azide-alkyne cycloaddition to generate *N*- heterocyclic pharmocophores, several reports have confirmed the wealth of applications of this practical and sensible chemical approach in the areas of bioconjugation,[15,16] polymer and materials sciences[20-23] and drug discovery.[24] Numerous authors demonstrated that CuAAC is a true example of efficient and versatile click chemistry.[14]

Figure 1.3 The Cu(I) catalyzed Huisgen 'click reaction' results in exclusive formation of the 1,4-triazole, whilst the thermally induced Huisgen cycloaddition usually results in an approximately 1 : 1 mixture of 1,4- and 1,5-triazole stereoisomers.

Mechanism of CuAAC

In general, cycloadditions proceed through an associated mechanism. However, experimental kinetic data[15] and molecular modeling[16] performed on the Huisgen 1,3-dipolar cycloaddition reaction seem to favor a stepwise reaction pathway.[17] Based on experimental evidence[17] and the fact that the copper-catalyzed reaction is thought to proceed in a stepwise manner starting with the generation of copper(I) acetylide (5) (Figure1.4). There are actually several different kinds of Cu-acetylide complexes that can be formed, depending on the reaction conditions utilized; compound **5** represents just one possibility.[16] The π complexation of Cu^I lowers the pKa of the terminal alkyne by as much as 9.8 pH units, allowing deprotonation to occur in an aqueous solvent without the addition of a base.[18] If a non-basic solvent such as acetonitrile was to be used, then a base, such as 2,6-lutidine or *N,N'*-diisopropylethylamine (DIPEA), would have to be added[19]. In the following step, density functional theory calculations show a preference for the stepwise addition (5 → 6 → 7 → 8) over the concerted cycloaddition (5 → 8) by approximately 12 to 15 kcal mol^{-1}, leading to the intriguing six-membered

metallocycle 7. Once 8 forms, one final protonation releases the Cu^I catalyst from the 1,2,3-triazole product , to undergo a second catalytic cycle with different substrates.[16]
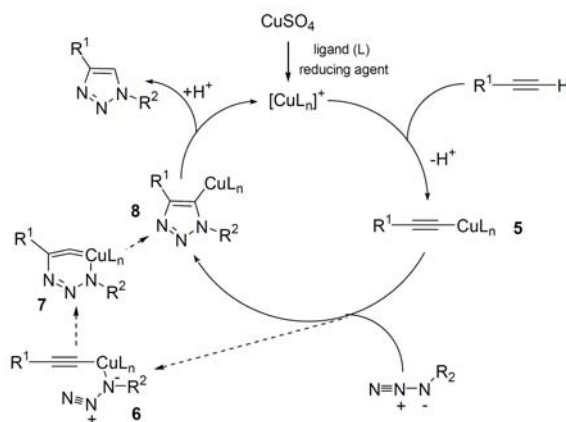
Figure 1.4 Proposed catalytic cycle for the Cu^I-catalyzed ligation

Catalysts for click reaction

There are many systems to generate the Cu^I catalyst for click reaction. One of the most common techniques is to reduce Cu^{II} salts, such as $CuSO_4$, *in situ* to produce Cu^I salts. Sodium ascorbate is typically used as the reducing agent in at least five equivalent excess,[18] but other reducing agents, such as hydrazine[22] and tris(2-carboxyethyl)phosphine (TCEP)[25] have been used with 1 equivalent. The advantages of this strategy are that it can be performed in water without requiring deoxygenated atmosphere.[16,23] The reaction requires neither a base, nor protecting groups and it is environmentally safe.[4]

A second method to form the catalyst is to directly add Cu^I salts. A lot of compounds have been employed over the past few years, including CuBr, CuI, CuOTf·C_6H_6, [Cu(NCCH$_3$)$_4$][PF$_6$], etc.[9]. This method does not require a reducing agent, but it has to be done without oxygen and in an organic solvent (or a mixed solvent), meaning that protection groups will probably be needed along with a base.[23] It has been demonstrated that using excess amounts of DIPEA produce the best results.[9, 21] Still, Cu^I salts are not as reliable as the Cu^{II} procedure.

Oxidizing copper metal with an amine salt is the third way to generate the catalyst.[16,19] There are some disadvantages at this strategy. Longer reaction times are needed, as well as large excess amounts of copper, and it requires a slightly acidic environment to dissolve the metal, which may damage acidic-sensitive functional groups present in the reactants.[18]

Besides copper, one research group has attempted to use three different catalyst: $NiCl_2$, $PtCl_2$, and $PdCl_2$ which are transition metals, which can insert into alkynes as the catalyst.[26,27] Although all of these transition metals displayed catalytic activity, none were better than CuI, and they all produced products in acceptable yields (Figure 1.5A). In 2005, another group reported a different catalyst, $Cp*RuCl(PPh_3)_2$, as a novel catalyst for click chemistry. Contrary to all previously mentioned catalysts, $Cp*Ru$ complexes form only 1,5-substituted 1,2,3-triazoles[28] (Figure 1.5B). In addition, they can catalyze reactions with both terminal and internal alkynes.[29] These novel results of $Cp*Ru$ complexes continue a significant step-forward in the development of click chemistry.
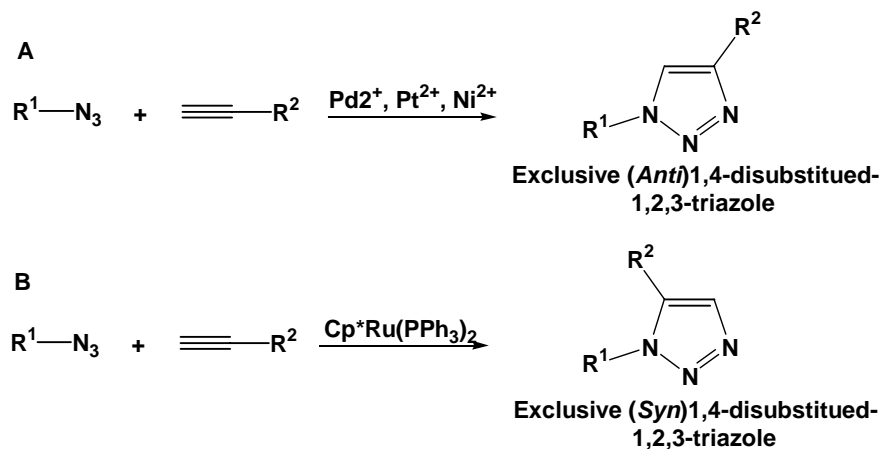
Figure 1.5 Different types of catalysts were used in click reaction. A) Using Pd^{2+}, Pt^{2+} and Ni^{2+} catalysts in the click reaction for exclusively forms 1,4-substituted 1,2,3-triazoles. B) Using a $Cp*Ru$ catalyst in the click reaction exclusively forms 1,5-substituted 1,2,3-triazoles. These catalysts can also work on internal alkynes (not shown), contrary to all other known catalysts.

Finally, comparing metal-catalysis click reaction, some studies have shown that 1,3-dipolar cycloadditions do not always need a catalyst to proceed (shown in Figure 1.6). The reaction can work readily at ambient conditions by using electron deficient alkynes (Figure 1.6A).[30] However, electron deficient alkynes are very reactive toward nucleophiles including amine and thiol and produce a lot of side products,[31] which have made these types of reactions depart from the field of click chemistry.
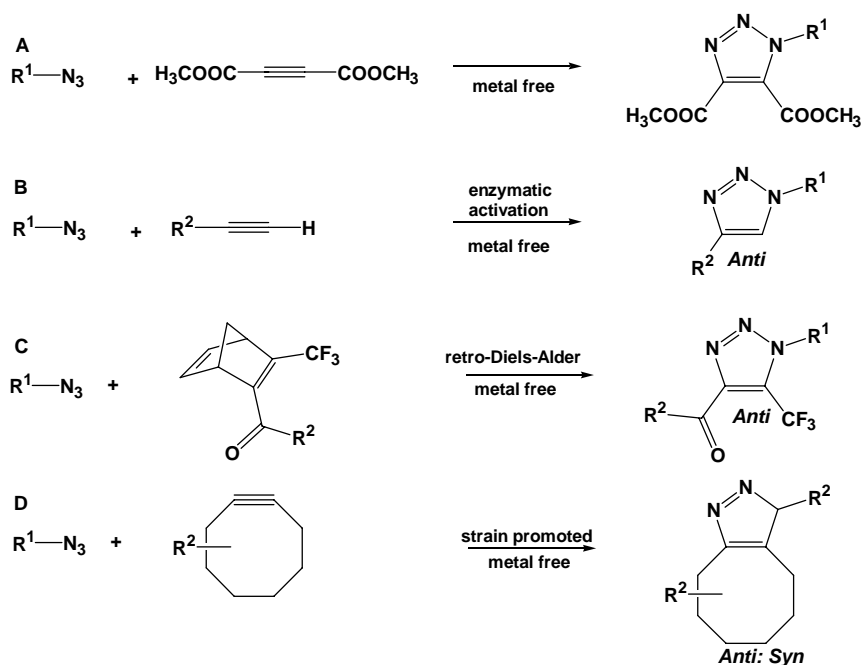
Figure 1.6 General scheme of metal-free ''click'' chemistry cycloaddition reactions.

Other studies have demonstrated that copper-free azide-alkyne cycloadditions are appropriate reactions for the target-guided synthesis of enzyme inhibitors (Figure 1.6B).[32] In this case, the sluggishness of standard Huisgen cycloadditions at 37 °C was elegantly turned into an advantage, as slow kinetics are required in this application. Moreover, in this strategy, the regiospecificity of the "click" reaction is not induced by an added catalyst but by confinement in the binding pocket of the enzyme. However, such an approach is rather specific and cannot be extended to more standard ligation reactions.

Furthermore, Cornelissen *et al.* investigated an elegant metal-free strategy for preparing a 1,2,3-triazole linkage.[33] This method does not rely on substituted alkynes but on oxanorbornadienes, which react with organic azides in a tandem [3+2] cycloaddition-retro-Diels-Alder reaction (Figure 1.6C). It was demonstrated that this particular reaction is faster at room temperature than standard Huisgen azide-alkyne cycloadditions. Hence, this approach was successfully used for modifying model peptides and proteins. However, one drawback of this method is the formation of a relatively toxic byproduct (*i.e.* furan) during the retro-Diels-Alder step.

In addition, an interesting copper-free azide-alkyne cycloaddition strategy has been recently proposed by Bertozzi and co-workers and relies on the use of strained cycloalkynes (Figure 1.6D).[31, 34, 35] Taking a cue from the work of Wittig and Krebs, who found that the reaction of cyclooctyne and phenyl azide "proceeded like an explosion to give a single [triazole] product".[36] Such high reactivity is a consequence of the geometrical deformation of the alkyne bond arising from ring strain (18 kcal/mol), which causes them to react readily with azides.[31] While this method leaves no side products and requires no cytotoxic catalysts, it requires the prerequisite of connecting the alkyne of interest to an eight-member ring. An additional concern with the cyclooctyne method is that it is not regioselective, which defies the very definition of click chemistry, which requires click reactions to be regiospecific, however the method exhibits some click features in the sense that it is chemoselective and readily applicable in physiological conditions.

1.3 APPLICATIONS OF CLICK CHEMISTRY

Since its debut in 2001, click chemistry has stimulated an explosive growth in publications describing a wealth of applications of this practical and sensible chemical approach. In the

beginning, click chemistry was introduced to fit the demands of drug discovery, Its applications are increasingly found in all aspects of drug discovery, ranging from lead finding to proteomics and DNA research. Among all the publications identified through SciFinder Scholar®, 16% are drug discovery related (Figure 1.7). Interestingly, click chemistry philosophy has recently provided a powerful tool in material sciences, leading to an excess of novel, tailor-made biomacromolecules with extraordinary structural characteristics and properties. Many different synthetic strategies were reported to achieve the coupling of synthetic polymers with nucleic acids, peptides, sugars, proteins or even viruses and cells by using the alkyne–azide click cycloadditions. In addition, biological applications of click chemistry, especially in bioconjugation sciences, are also emerging as a great interest click-field. One reason is that in many fields of studies, such as nanomedicine, bioconjugation plays a central role. *In vivo* and *in vitro* bioconjugation applications benefit from the unprecedented reliability of the copper-catalyzed azide–acetylene union, the inertness of the reactants under physiological conditions and the mild condition under which the biologicals and other fragile structures present will not loss their functions. In the following sections, an in-depth look will be taken at some of its applications relating to key areas where click chemistry has had significant impact, and is thus divided into the three most apposite classes: (i) drug discovery, (ii) bioconjugation, and (iii) materials science.
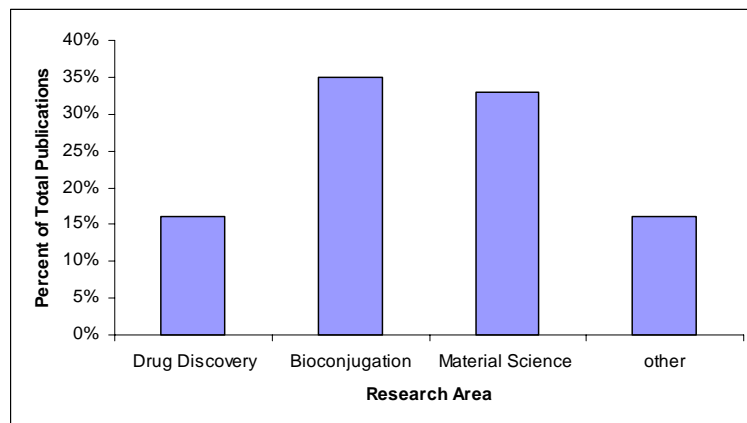
Figure 1.7 Major classifications of the applications of click chemistry. Analysis was performed based on a literature search via SciFinder Scholar® on Oct. 1, 2008. The search included journal articles, abstracts, dissertations, patents, preprints, and reviews. It is intended for this chart to represent a general overview and should not be taken literally.

1.3.1 Click chemistry and drug discovery

Click chemistry is being used increasingly in pharmaceutical sciences, ranging from lead discovery and optimization, and detection in biological systems, such as nucleotides, proteins and whole organisms. Several early applications of it are highlighted here.

In situ click chemistry

Usually the approaches for lead compound discovery involve the synthesis of a collection of compounds and subsequent biological screening. The procedure would be promoted if the biological target could choose its best ligand itself. Indeed, the target would act as the ideal template to generate the perfect hit. These fragment-based approaches, also termed target-guided synthesis (TGS), show great promise in lead discovery applications by combining the synthesis and screening of libraries of small-molecules in a single step. Irreversible, target-guided synthesis of high-affinity inhibitors from reactants has potential to come out as a reliable lead discovery mean. Recently, Sharpless demonstrated the efficacy of the 1,3-Huisgen cycloaddition

towards this application.[37] This reaction has the special properties which make it perfectly suited for the discovery of lead compounds through *in situ* target directed synthesis, they are: (1) the reaction is kinetically slow at room temperatures. However, at room temperature, an enzyme could bring azide and alkyne-containing molecules in close proximity so as to overcome the high energetic barrier allowing the Huisgen reaction to occur. In this manner, only compounds which fit correctly into the active site of the enzyme should react to give new potent ligands of the enzyme, and active site of the enzyme would act as the reaction chamber; (2) no any third participants such as catalysts or other reagents are needed in the reaction. The reaction proceeds cleanly without the formation of by-products; (3) bioorthogonality, *i.e.* both azide and alkyne functionalities are inert in the presence of biomolecules, and can survive in biological conditions. By contrast, other approaches have to employ highly reactive reagents (e.g. aldehydes and hydrazines; thiols and α-chloroketones etc.) and reversible reactions for the *in situ* assembly of inhibitors inside a target's binding pocket[38-41]. Click chemistry has been successfully utilized to a selection of biological targets to find improved inhibitors.

This strategy was used to identify extremely potent inhibitors of acetylcholinesterase (AChE) which is involved in neurotransmitter hydrolysis of acetylcholine at the synaptic cleft in the central and peripheral nervous systems and a pharmacological target for many clinically relevant conditions, including Alzheimer's disease. This enzyme was chosen for study for two reasons. First, much structural data of AChE were available: the enzyme's active site is located at the base of a narrow gorge, ~20 Å in depth,[42] and peripheral binding site exists at the rim of the gorge, near to the enzyme surface.[43,44] Second, small molecule ligands for both parts of the active site and inhibitors that bind both parts of the active site are known. The design of building blocks was based on the tacrine and phenanthridinium, two known site specific ligands. A set of

building blocks derivatized with a terminal alkyne or an azide were incubated with the enzyme. The enzyme chose the TZ2/PA6 pair to form product in a highly regioselective fashion: the TZ2PA6 syn-6 triazole (Figure 1.8). This compound has potency greater than all known non-covalent organic AChE inhibitors, with an impressive Kd of 77 femtomolar. By contrast, chemical synthesis in the absence of enzyme provided roughly a 1:1 mixture of syn- and anti-6 regioisomers, the 1,4-isomer was found to be a weaker inhibitor compared to the 1,5-disubstituted triazole. Thus, the results approved that AChE itself, served as the reaction chamber, synthesizing its own inhibitor by equilibrium-controlled sampling of various possible pairs of reactants in its gorge until the clicking between azide and acetylene essentially 'stablize' the pair that fits best into the binding pocket. As no catalyst was used in this approach, it is commonly coined "*in situ* click chemistry".
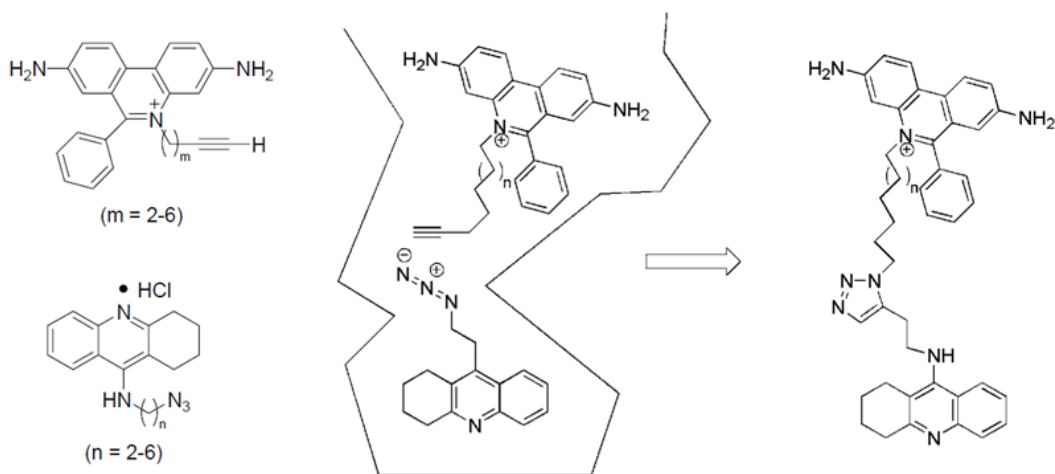
Figure 1.8 *In situ* click chemistry. Building blocks for acetylcholinesterases TGS modified with either an alkyne or an azide group await in the active site of the enzyme for azide-or alkyne-containing partners that can fit the enzyme. No catalyst is required for the reaction. The TZ2PA6 1,5-disubstituted triazole formed and it has potency greater than all known non-covalent organic AChE inhibitors.

The strategy of *in situ* CC has been utilized further with other enzymes, such as HIV-1 protease[45] and carbonic anhydrase (CA).[46] The two systems were studied in almost the same way as the AcHE system but with some important differences that expanded the research fields of *in situ* lead discovery. Firstly, in the case of HIV-1 protease, the *in situ* experiment was set up using an HIV-1 protease and two complementary azide and alkyne fragments which only weakly bind to the enzyme generate a potent inhibitor of this enzyme when connected with click-formed 1,4-disubstituted triazole. The reaction was confirmed to be catalysed by the enzyme active site with the usual control experiments, the reaction formed the 1,4-disubstituted triazole as a major product compared to the 1,5-disubstituted triazole in the presence of the enzyme, ratio between two products is 18:1. Thus, these results demonstrated that the enzyme can indeed guide specificity *in situ* to choose a potent inhibitor. The applicability of this system was also used for carbonic anhydrase inhibitors, strongly demonstrating that this powerful technique can be used to many drug targets. Only the alkyne building blocks, an acetylenic benzenesulfonamide including structure of 4-carboxybenzenesulfonamide which shows the inhibitory nature towards CA, showed binding affinity for the target, thus acting as an anchor for the azide building blocks. A set of selected azide functionalised compounds which cover six different structural themes did not show binding affinity. After *in situ* click reaction, one potent CA inhibitor connecting with 1,4-disubstituted triazole displayed hits. This result demonstrated that an inhibitor with increased binding affinity can be produced from a fragment which shows moderate binding coupled with a fragment that shows no binding, strongly widening the scope of *in situ* CC. Indeed, the *in situ* CC approach has been used into a microfluidic chip device, Tseng *et al.* demonstrated that *in situ* reactions can be performed in 96-well plates with reduced consumption of target proteins and reagents, as well as reduced reaction times.[45]

Drug discovery based on the CuAAC

CuAAC reaction has ideal properties including simple reaction conditions, tolerance of function groups (azide and alkyne), and fast speed (10^6-fold faster than Huisgen's 1,3-dipolar cycloaddition reaction), which fit the requirements of drug discovery. Two building blocks are reliably connected together by formation of a 1,4-disubstituted 1,2,3-triazole linkage. The triazole in this case could act as an inactive linker or spacer, although it cannot be excluded that, at times, it may act as a pharmacophore on its own. This ligation process works best in aqueous media without requiring protecting groups for most common functional groups, so reaction mixtures can be screened *in situ* (*i.e.* without prior purification).

Fucosyltransferase inhibitors

CuAAC is very reliable reaction and products can be used to screen leading compounds directly from the reaction mixture. Based on this common sense, Wong *et al* developed a novel high throughput strategy, which led to the discovery of a novel and selective inhibitor of Human r-1,3-Fucosyltransferase (Fuc-T), an enzyme which catalyzes final glycosylation step in the biosynthesis and expression of many important saccharides by transferring an L-fucose moiety from guanosine diphosphate β-L-fucose (GDP-fucose) to a specific hydroxyl group of sialyl N-acetyl-lactosamine (Figure 1.9). Fucosylated saccharides play an important role in inflammation, thus selective inhibitors of these enzymes might provide potential anti-inflammatory drugs by blocking the synthesis of fucosylated end-products. Previous strategies employed to identify inhibitors of Fuc-T generally relied upon the design of acceptor, donor and transition state analogues. Difficulties arise, however, due to the complexity of the transition state composition, which consists of sugar donor, acceptor, divalent metal, and nucleotide. Using the CuAAC approach, a new inhibitor of this enzyme was identified in a very simple and rapid manner. In

detail, a range of azide fragments were synthesized, which comprised hydrophobic residues and alkyl chain linkers of varying length. These were then coupled with an alkyne GDP core in water, without the use of protecting groups. Water can act as a protecting group itself and, indeed, the troublesome dianionic phosphate linkage gave no problem. The obtained compounds were so pure that they were screened directly for biological activity, yielding three hit compounds. Hit follow-up, conducted on purified compounds against a panel of fucosyl and galactosyl transferases and kinases, revealed one of these as the most potent inhibitor of human α-1,3-fucosyltransferase VI that has been found to date. However, this direct approach, where the reaction mixture can be directly screened in the biological assay, is not always applicable and requires some forewarnings. For example, a copper catalyst is toxic to living systems and not compatible with some appropriate biological screening.
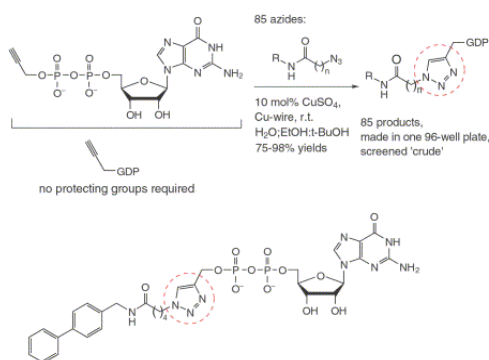
Figure 1.9 CuAAC in microtiter plate for *in situ* screening.

CuAAC in fragment-based drug discovery

Fragment-based drug discovery (FBDD) is a recently developed drug discovery strategy which enables high-throughput identification of small molecule inhibitors using a minimal number of compounds as building blocks.[47] The approach is powerful especially against protein targets which possess not only one binding site in their active sites. Traditional FBDD integrates biophysical techniques, such as X-ray crystallography, nuclear magnetic resonance spectroscopy,

isothermal calorimetry with fragment library design and a range of computational methodologies for an efficient hit-to-lead process. Currently, a novel method is used to assist the assembly of compounds: the in situ screening method based on the click chemistry pioneered by Sharpless *et al.*[48] The click chemistry approach is highly versatile since it requires neither special equipment nor mutations in the target proteins, making it easily adaptable by most research laboratories. To this end, it has been used successfully in the discovery of inhibitors against tyrosine phosphatase (PTP), SARS 3CL protease, and matrix metalloprotease (MMP).[49] For example, Yao *et al.* demonstrated that the triazole linker can be used to generate divalent inhibitors, where the molecule interacts with two different binding sites of the same target. This has been employed to identify inhibitors of protein tyrosine phosphatase (PTP), a large and structurally diverse class of signaling enzymes which causes obesity and diabetes.[50] Recently, much effort has been made in attempts to discover potential small molecule-based drugs, that target PTP in vivo with high efficacy and minimum side effects.[51] In this instance, because N-phenyloxamic acid was demonstrated that it could bind the primary site of PTP, it was chosen as a core group. Aromatic rings with different polarity and alkyl linkers of different lengths were chosen as potential peripheral groups. A library of 66 compounds was synthesized in water and the products with triazole groups obtained were directly screened as inhibitors without purification. Six were hits and one had activity in the micromolar range and was found to be more selective (Figure 1.10).
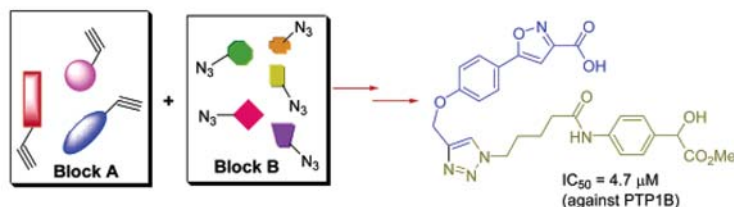
Figure 1.10 "CuAAC" was carried out for rapid assembly of 66 different bidentate compounds. Subsequent in situ enzymatic screening revealed a potential PTP1B inhibitor.

A similar idea was exploited to identify selective matrix metalloprotease (MMP) inhibitors. MMPs are a family of zinc-containing metalloproteases, which play critical roles in a variety of physiological processes, such as maintaining normal cellular function and development. MMPs are responsible for a variety of human diseases, including Alzheimer's disease, arthritis, heart diseases and cancer.[52] One of the most widely exploited platforms of MMP inhibitors is the peptide-based succinyl hydroxamate.[53] Small moleculess containing zinc-binding groups (succinyl hydroxamates) normally exhibit selective inhibition not only to MMPs but also to most metalloproteases. Therefore, it is a challenge to develop highly efficient synthetic strategies that allow rapid formation and screening of small molecule inhibitors possessing both high potency and good selectivity toward MMPs. However, Yao *et al.* demonstrated a click chemistry approach for the rapid assembly/synthesis of a small molecule library based on different succinyl hydroxamates, and subsequent in situ screening to identify candidate hits, which possess selective inhibitory activity against MMPs over other metalloproteases. In this case, library design was based on the succinyl hydroxamate, which is well known to interact with a zinc ion present in the active site of the enzyme. Eight substituted succinyl bearing a variety of alkyl, cycloalkyl, and aromatic side chains were chosen as warhead. These were reacted with 12 different azides bearing a hydrophobic moiety by using a parallel combinatorial approach. Two of them were inhibitors of MMP 7 with selective activity in the micromolar range (Figure 1.11).[54] This approach thus lays the foundation for future exploration of more potent and selective MMP inhibitors, in high throughput, using click chemistry.
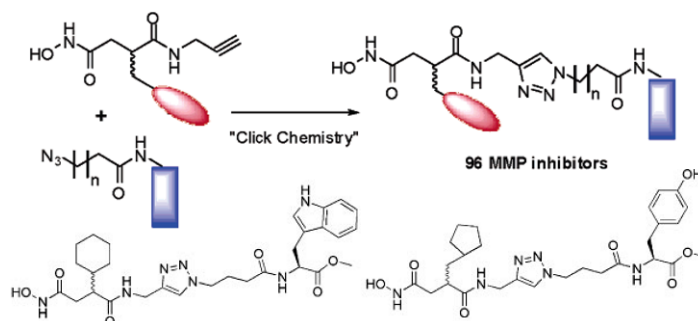
Figure 1.11 A panel of 96 metalloprotease inhibitors was assembled using "click chemistry" and two of them were indentified as inhibitors of MMP 7 with selective activity in the micromolar range.

Synthesis of glycoconjugates

Carbohydrates are the most abundant of the four major classes of biomolecules. They play a central role in living things, such as the storage and transport of energy (starch, glycogen) and structural components (cellulose in plants, chitin in animals). Additionally, carbohydrates and their derivatives fill numerous roles in the working process of metabolism, cell–cell interaction, cell migration processes, and pathogen defence, providing great opportunities for attractive drug discovery.[55] In spite of this great potential, carbohydrate-based drug discovery does not develop quickly. Carbohydrates make poor lead compounds due to their well-known modest affinities for the respective enzymes or receptors, poor pharmacological properties, and difficult syntheses. However, multivalent carbohydrates are attractive synthetic targets since they often bind much stronger to the respective receptors than their monovalent counterparts. This multivalent principle came form Nature to increase the affinity of weakly bound sugars to biologically relevant levels. Many kinds of linkages of sugars to scaffold molecules have been utilized over the years and impressive affinity increases have been reported.[56] CuAAC promises to greatly simplify and accelerate the discovery of high-affinity multivalent carbohydrates as known as it has already been utilized in numerous systems.

Inspired by the fact that Nature increases weakly-bound sugars to biologically relevant levels through multivalency[57] Santoyo-Gonzalez and co-workers used the uncatalyzed Huisgen cycloaddition to conjugate sugars to scaffold molecules with the purpose of preparing a series of multivalent, triazole-linked multivalent carbohydrates in 2001.[58] The reaction was performed for very long reaction times (30 h to 6 days) in refluxing toluene and naturally generated both the 1,4- and 1,5-linked regioisomeric 1,2,3-triazoles for each linkage. Subsequent studies reported by the same group in 2003, demonstrated the employment of the copper-catalyzed method, which greatly improved reaction rates and regioselectivity of the synthesis of the 1,2,3-triazole-based systems.[59] Complete regioselectivity and yields of more than 80% were achieved. Microwave irradiation could shorten the reaction times from several hours to a few minutes at room temperature.

CuAAC reactions have also been utilized to conjugate multiple sugars with a central aromatic plarform[60] and a similar strategy to generate compounds which show potential antitumoral activity. For example, taking advantage of preliminary data which indicated that a β-D-glucosamine hexamer showed mild antitumoral potential,[61] a C3 symmetric (1-6)-N-acetyl-β-D-glucosamine octadecasaccharide was syntesized through triazole-linkage in order to employ the multivalent concept (Figure 1.12B). As expected, the trivalent octadecasaccharide had better antitumor activity compared to the monovalent controls.[62]
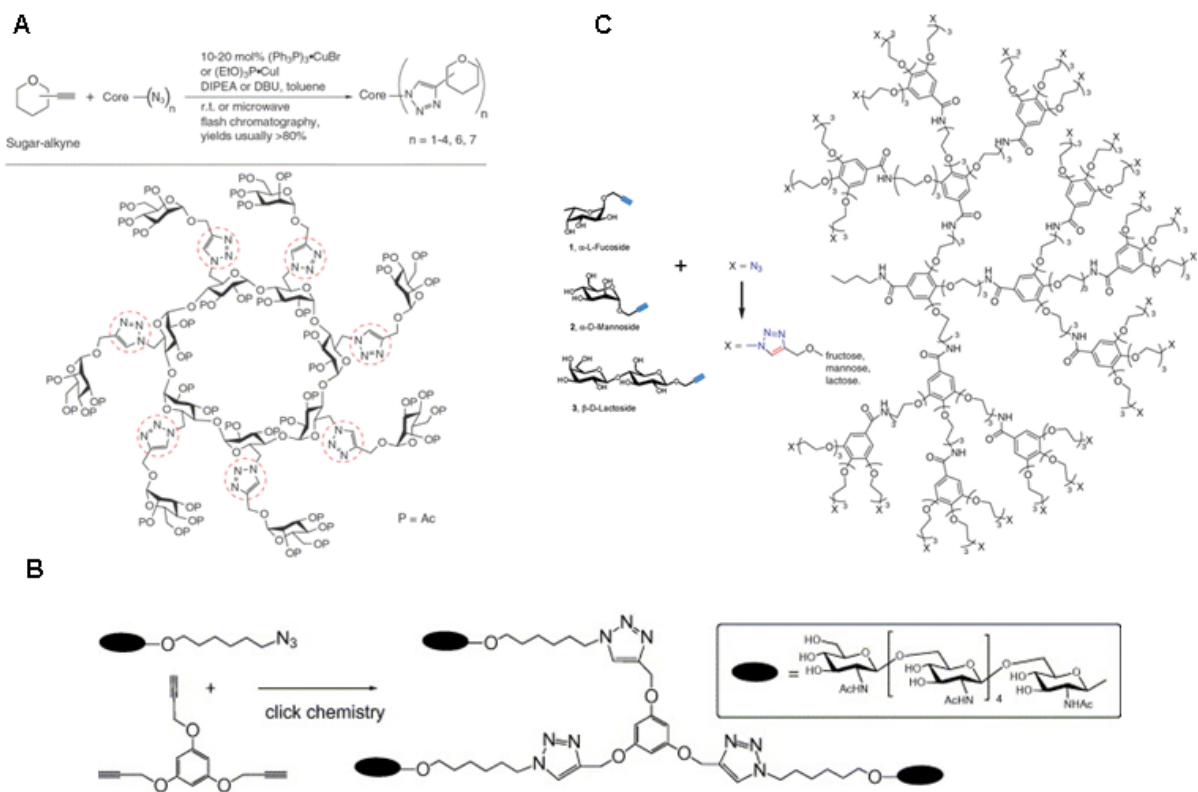
Figure 1.12 Click reaction was used to synthesize glycodendrimers.

Related to the glycodendrimers shown above, Riguera and coworkers utilized click chemistry to functionalize larger dendrimer systems,[63] which were designed basing on the previously prepared dendrimers[64] consisting of the relative 3,4,5-trihydroxy-benzoic acid repeating unit. These types of dendrimers display significant rigidity, are easily variable, and have considerable distances between the azide containing endgroups, which might be favorable for multivalent binding to biological enzymes. This cooperative effect, generally referred to as the "cluster effect",[65] has opened up the possibility of inhibiting or promoting carbohydrate-receptor interactions with synthetic multivalent glycoconjugates.[66] There appears to be a preference to have the alkyne on the dendrimer and the azide on the functional molecule, but Riguera and coworkers report one case of the azide on the periphery of the dendrimer and the alkyne on the carbohydrate (Figure 1.12C).[67] In this case, they resolved to place azide and alkyne

functional groups on the dendrimer and the carbohydrate partners, respectively. Azide-terminated dendrimers were preferred to those incorporating terminal alkynes due to the potential bias of the latter to Cu(II)-catalyzed intradendritic oxidative coupling.[68] With the advent of the click reaction, a more easy preparation allows the atom economical incorporation of up to 27 unprotected fucose, mannose, and lactose residues to generate the large systems (weight average molecular mass, Mw 18 kDa), requiring only catalytic amounts of Cu in *tert*-BuOH/H_2O mixtures for 72 h at room temperature. The resulting large glycodendrimers are isolated in reproducible high yields (up to 92%), after purification of the reaction mixture by ultrafiltration.[14] The functionalization of dendrimers with sugars is a particular focus due to the synergistic fit of click chemistry with sugar chemistry as the reaction can be water based with no protecting groups on the sugar required. The general use of click reaction to decorate substrates with sugars is likely to be a significant ongoing research field. What is particularly notorious in the dendrimer field is the mixing of the divergent and convergent methods of dendrimer synthesis in many of the reports using the click reaction. There are examples of divergently made dendrons being linked together at the focus as a last reaction[69,70] and convergently made dendrimers going through a reaction on the periphery in the last step.[14, 68, 71] All this is made possible by the selectivity inherent in the click reaction.

1.3.2 Click chemistry and bioconjugation

Bioconjugation encloses a broad field of science at the interface between chemistry and molecular biology. Bioconjugation techniques are the process of coupling two biomolecules together in a covalent linkage. The most common bioconjugations are modification of biopolymers (such as protein, oligosaccharides and nucleic acids) by incorporation of fluorophores, ligands, chelates, radioisotopes, and affinity tags, or coupling a complex

carbohydrate with a peptide, and modifications such as connecting two or more proteins together such as the coupling of an antibody to an enzyme. The power of bioconjugation extends to the labeling of biomolecules *in vivo*. The use of bioconjugations is quickly becoming common practice, and an estimated 30 biopharmaceuticals generated form bioconjugations are currently in clinical trials till May 1st, 2007.[72] This popularity stems from the fact that bioconjugation reactions can serve many purposes and satisfy many functional requirements including being used to reduce immunogenicity, increase aqueous solubility, improve stability, and increase circulation time. Currently, there are only a handful of reactions which have been identified as useful tools in this context. Generally, these 'coupling-type' reactions have two complementary components which are orthogonal to the functionality present in biological systems. Examples include carbonyl based formation of thiazolidines, oximes and hydrazones, and photochemically initiated free radical reactions, which have broader reactivity. The Diels–Alder reaction and Staudinger ligation[4] have also been recognized as important.

Click chemistry is the latest strategy called upon in the development of state of the art exponents of bioconjugation. Although the applicability of click chemistry towards bioconjugation was first indicated in the work of Meldal *et al* in 2002, which demonstrated to synthesize the first "peptidotriazoles" on sold phase by using Cu(I) catalysed variant of the Huisgen cycloaddition reaction, the click reaction has now become the ideal bioconjugation method. One reason for this is that 1,2,3-triazoles is ideal linkers. They are extremely water soluble, making *in vivo* administration much easier. Actually, many evidences approved that triazole group displays structural and electric similarity with the amide bond, mimicking a Z or an E-amide bond depending on its substitution patterns (the 1,4-disubstituted triazole moiety shows similarity with a Z-amide bond, on the other hand, the 1,5-substitution pattern mimics the

E-amide bond), but they are not subject to the same hydrolysis reactions.[18] They are also stable in typical biological conditions such as aqueous and mildly reducing.[48] In addition, as the triazole is rigid ring, this advantageous property ensures that the two linked substances are not interacting with each other.[18] If the linker was flexible then the substances would easily aggregate and/or react with each other. Finally, azides and alkynes can be introduced into organic compounds easily, and their bioorthogonal properties and tolerance to a wide range of solvents (including water) can exclude most side reactions at unintended sites of the substances which is a major problem in bioconjugation reactions. In conclusion, *in vivo* and *in vitro* bioconjugation applications benefit from the unprecedented reliability of the azide–alkyne union, the inertness of the reactants under physiological conditions, and the mild reaction conditions. After the discovery and development of the click reaction in water, more and more scientists realized the potential introduction of varying functionality into the biomolecular environment. As a result, lot of biomolecules such as DNA, peptides, proteins, oligosaccharides and glycoconjugates have been labeled to study biological systems.

Activity-based protein profiling (ABPP)

One of the great challenges of biology is how to understand the function of proteins in their natural surrounding, including their regulation pathway. Proteomic approaches provide a way to study proteins, particularly their structures and functions.[73] However, these techniques are mainly designed to compare protein levels, and therefore the activity of these proteins can only be assumed. In order to overcome these limitations, activity-based protein profiling (ABPP) techniques start to be established and fine-tuned.[74] ABPP is a chemical strategy that utilizes active site-directed chemical probes with broad target selectivity to label active proteins within various enzyme classes and allows the visualization of proteins expressed at low levels, and

provides the information of an indication of activity more than of abundance which allows for the discovery of new drug targets.[75] The chemical probes contain a functional group that covalently reacts with specific classes of enzymes such as serine hydrolases.[76] These site-directed probe are usually composed of two different elements: the molecule that brings selectivity to the binding and the label that can then be visualized (e.g., fluorescent probe, antibody-recognizable tag, etc.). The approach allows for the rapid detection and isolation of the enzymes covalently attached to the probe from a complex mixture of proteins. However, the isolation of these probes is preceded by homogenisation of the cell tissue. As a consequence of this homogenisation, there is potential loss of information relating to the differences in protein activity in the relevant physiological setting (disruption of cell tissue may cause differences in concentrations of substances affecting protein activity). One potential solution would be to carry out the ABPP *in vivo*. However, until the development of the copper(I)-catalyzed azide-alkyne cycloaddition, ABPP experiments were conducted *in vitro* because the bulky chemical tags inhibited cellular uptake and caused the enzymes to be profiled outside their natural biological environments, thereby, preventing measurements in living organisms.[32] The discovery of the copper-catalyzed click reaction offered a solution to this problem by allowing enzymes to be profiled *in vivo*.

Cravatt and co-workers have demonstrated that the use of an azide containing a phenyl sulfonate ester reactive group allowed the in vivo profiling of glutathione S-transferases, aldehyde dehydrogenases, and enoyl CoA hydratases.[77] The small azide reactive group is easily up taken by the cell and covalently labels active proteins. These functionalities can form an inert handle which can be 'clicked' with bulkier reporter tags (*i.e.* only the relatively small azide and alkyne activity based probes are administered *in vivo*, followed by *in vitro* analysis, using click

reaction to attach the reporter tags before analysis) (Figure 1.13).The procedure was developed and tested to evaluate whether it could be used in the identification of targets of enzyme inhibitors *in vivo*, and secondly to test if homogenisation did affect enzyme activity profiles. The Cravatt strategy was performed even in live animals, allowing ECH-1 to be tracked in the heart muscle of mice one hour after treatment with an alkyne reactive fragment and labeling of the unique protein with the fluorescent tag from the crude heart-homogenate by using click reaction. This is the first experiment which determines protein expression levels in living organisms, since tagging occurs before cell death, this new *in vivo* ABPP method provides more reliable results which can possibly provide more information to understand the function of proteins.
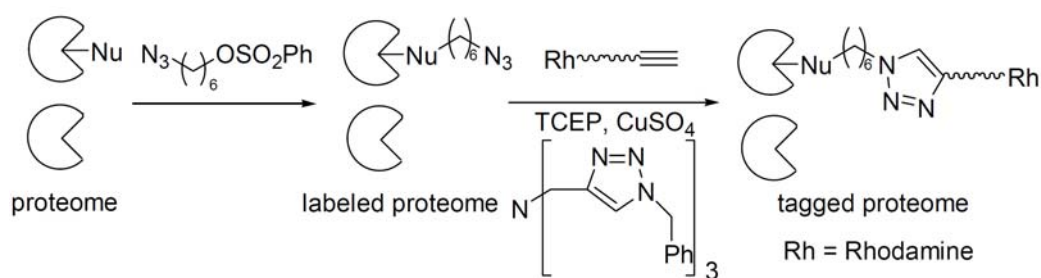
Figure 1.13 Schematic representation of click chemistry ABPP.

Labeling DNA

Oligonucleotides, an important class of biomolecules, have found many applications to many research fields including gene therapy[78], as molecular probes[79], as antisense agents to treat diseases like leukemia[80], etc. The versatility of oligonucleotides can be increased by adding different functional groups at either the 3′-end, 5′-end, or an internal position. The newly added functional moieties can act as handles for bioconjugation with different biological molecules. DNA bioconjugation methods must be able to bear aqueous conditions, give high yields, and the resulting linkage must be stable in biological conditions[81]. Click chemistry is perfect for the requirements.

Using click reaction to post-synthetically decorate alkyne modified DNA, Carell *et al* demonstrated to form high density functionalisation of modified DNA, which was synthesised by standard means using phosphoramidite chemistry, with the incorporation of the modified uridine nucleosides (Figure 1.14).[82] Different molecules with azides which represented potentially useful labels (Figure 1.14) were chosen for conjugation, such as azido-sugars which are semiprotected aldehydes used for Ag staining, coumarin which shows fluoresence only after generating the triazole, and a fluorescein tag with an azide which is used in a variety of biophysical applications. The DNA was successfully tagged using the click reaction with the added ingredient tris(benzyltriazolylmethyl)amine, a ligand which stabilizes the Cu(I) oxidation state and protects the coupled triazole product from degradation.[83] All of two labelling nucleosides resulted in fully labelled DNA strands. These studies demonstrated that the click reaction was a highly reliable and complete method to form high-density functionalization of oligodeoxyribonucleotides.
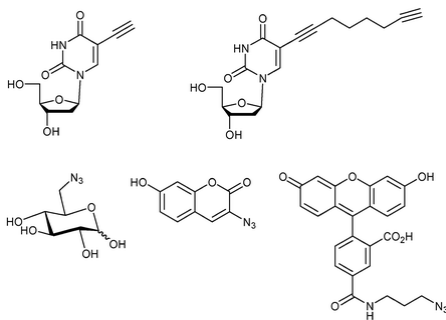
Figure 1.14 Uridine nucleosides with alkynes and tag molecules with azides used in the high-density functionalisation DNA.

Seo *et al*. demonstrated another example of labeling the 5′-end of single-stranded DNA with a fluorophore.[81] In this case, no catalyst was used in the reaction, the 5′-end terminal alkyne modified oligonucleotide was coupled with the fluorophore containing an azido functional group in a high yield, but, leading to a mixture of 1,4-substituted and 1,5-substituted 1,2,3-triazole products. The advantages of this method are that it proceeds in high yield under relatively mild

conditions, no adding additives (e.g. catalysts or reagents) or the formation of by-products, allowing purification of the labeled DNA unnecessary. Seela *et al.* labeled DNA one step further and synthesized nucleosides containing a single terminal alkyne on their aromatic nucleobase.[84] Several oligonucleotides were subsequently formed by using solid phase synthesis. The evidence of successfully labeling oligonucleotides had been indicated by that conjugation the reporter molecules began to show fluoresence.

Labeling polysaccharides

Polysaccharides are another major class of macromolecules which regulate a variety of events, including cell-cell recognition, fertilization, metastasis, and immunological response.[85,86] Despite these important biological functions, moderate affinity towards target receptors and enzymes and poor pharmacological properties make them seldom used as lead compounds/ targeting moieties.[48] Chemical modifications of the carbohydrates can improve both of these properties, but only low product yields can be achieved because of restricted alcohol functional groups and the steric bulkiness of polysaccharides. Due to the easy introduction of azide functional groups and high reliability of the click reaction, Liebert *et al.* demonstrated the use of click reaction to modify the cellulose surface.[87] Based on the previously reported fact that the 1,2,3-triazoles would interact with biological targets via hydrogen bonding and dipole interactions, this should increase the overall affinity of cellulose towards its target proteins. The azide functional groups were first introduced into cellulose through two simple steps: tosylation and azide displacement of the secondary alcohol groups in high yields. Three different small molecules, methylpropiolate, 2-ethynylaniline and 3-ethynylthiophene with terminal alkynes were then reacted with the azide-celluloses in separate reactions using the click reaction. All reactions were successful in high yields. Another example was shown by Hafrén *et al.*[88] In this

29

case, celluloses with terminal alkynes were synthesized by using 5-hexynoic acid in one step and then reacted with 3-Azidocoumarin in presence of copper catalyst. Upon reaction, the coumarin-cellulose compound began to show blue fluoresence, indicating that the reaction was successful. These reports clearly indicate that polysaccharides can be modified through the click reaction in high yields.

Labeling CPMV

The click reaction has also found application in the case of complex and multimeric biological systems such as viruses, bacteria, and cells. Considering their high degree of complexity, these highly organized structures display a challenging target when compared to the simpler biological entities that were mentioned above. Additional precautions are necessary to avoid damaging activities. The majority of researches deal with the conjugation with small molecular compounds such as dyes by using click chemistry. One particularly striking application of CC was reported by Finn *et al.*,[89] in their studies on the conjugation of fluorescein dye molecules onto the cowpea mosaic virus(CPMV) which is frequently used as a scaffold. CPMV can be made inexpensively on a gram scale and it is easy to separate from small unreacted reagents. Furthermore, it contains 60 identical copies of an asymmetric two-protein unit, each of which contains one cysteine and one lysine.[25,89] These 60 cysteines and lysines can be manipulated and attached to various functional groups and biomolecules, as evidenced by countless studies.[91,92] In their study, via traditional bioconjugation methods, a total of 60 azides per virus particle were attached. In this case, the virus particle was decorated with an azide functionality.

In initial studies, three different functionalized virus particles were labeled by fluorescein through the click reaction (Figure 1.15A). This work discovered three important conclusions:

firstly, reductants such as ascorbate and *p*-hydroquinone disassemble the virus capsid; secondly, although the virus was stable to Cu(II), it was decomposed by triazole formation in the presence of Cu(II); and thirdly, the tris(benzyltriazolylmethyl)amine ligand could protect the virus from disassembly. However, later studies by the same group reported on the attachment of a wide variety of substrates including complex sugars, peptides, poly(ethylene oxide) polymers and the iron carrier protein to CPMV using click chemistry.[92] Interestingly, during these studies a new water-soluble sulfonated bathophenanthroline ligand was employed to modify the CPMV virus capsid. Compared to the tris(benzyltriazolylmethyl)amine ligand under otherwise identical conditions, a much lower concentration of labelling substrate was required. In another study, conducted by Wang *et al.*, fluorescein dye derivatives were conjugated to both azide-functionalized and alkyne-functionalized CPMV via click chemistry in 100% yield.[89] A few years later, they were successful in attaching three hemicyanine dyes to CPMV using the same reaction.[25]
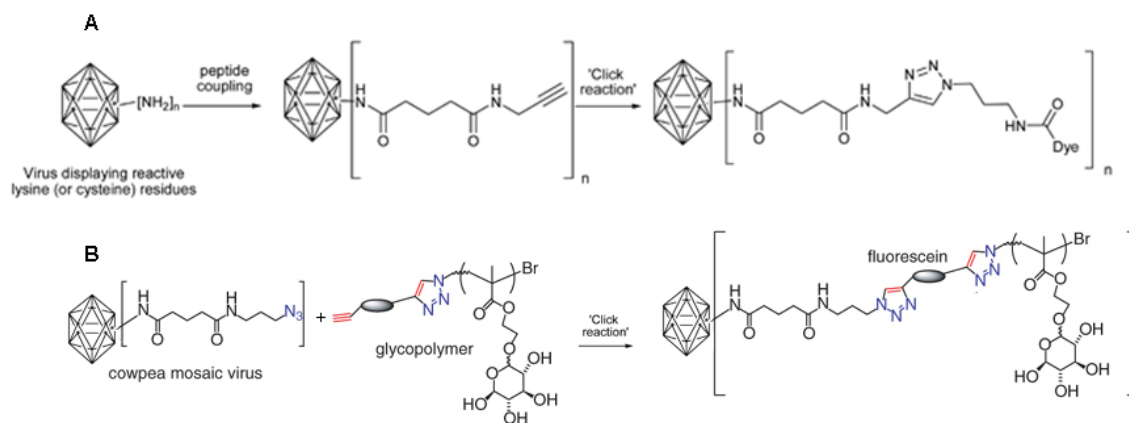
Figure 1.15 Functionalisation of cowpea mosaic virus particles.

More recently, Finn *et al* demonstrated on the formation of virus–glycopolymer fluorescent bioconjugates by an elegant combination of the click reaction and atom transfer radical polymerization (ATRP) (Figure 1.15B).[93] In this case, ATRP was used to synthesize a

glycopolymer using an azide functionalized initiator. The glycopolymer was subsequently coupled to a dialkynyl functionalized fluorescein molecule via click reaction, yielding the corresponding fluorescent alkynyl-terminated glycopolymer. The final connection of the polymer with the virus used the water-soluble sulfonated bathophenanthroline ligand, under inert atmosphere with copper(I) triflate and TRIS buffer. The average number of glycopolymer chains covalently bound to CPMV capsid was calculated to be 125±12, which closely corresponds to the 150 azido groups present on the exterior of the virus shell after reaction with the NHS heterobifunctional linker. Such a structure can also be used as a bio-templated star polymer where the multi-valency of the virus provides the core for attaching many arms of glyco-polymers.

Labeling *E.coli*

The proteins expressed on the surfaces of microbial cells are useful in various fields, including protein engineering, adsorbents for bioremediation, whole cell catalysts, screening for antibody fragments, etc[94,95]. Although there are only 20 naturally-occurring amino acids, certain amino acids with synthetic derivatives could be used to expand the set of amino acids expressed on the surface proteins which could be further handled and they provide quite useful applications. In this field, some research groups have already showed remarkable success[95].

Tirrell and coworkers[126] reported that click chemistry can be used for the selective labeling of the cell surfaces of E. coli bacteria. It had previously been shown that an azide-containing synthetic amino acid, azidohomoalanine (AHA) can replace methionine residues in proteins.[96] In their studies, AHA was metabolically incorporated into the porin C (OmpC), a protein with three methionine residues[97] that is abundant in the outer membrane of *E. coli* bacteria. Once AHA had been incorporated into OmpC for both strains, bacterial cells with azide groups to the

extracellular milieu were successfully biotinylated under the special click conditions developed by the Finn group, with a biotinylated alkyne reagent. The biotin decorated cells could in fact subsequently be stained with avidin and, therefore, discriminated from cells lacking the unnatural amino acid. In another ground-breaking example, a mutant *E. coli* containing nine methionine residues per OmpC was also created for comparison. The cells were successfully biotinylated and the mutant *E. coli* could bind with the large molecule avidin.

Labeling mammalian cells with strain-promoted click reaction

Ideal bioconjugation methods can be performed without affecting living tissues, and do not need assistant catalysts (the mandatory copper catalyst shows considerable cell toxicity) and ligands including tris(benzyltriazolylmethyl)amine, and tris(2-carboxyethyl)phosphine (TCEP). Based on the idea of "click" chemistry, the Bertozzi group developed new substituted cyclooctynes (Figure 1.16) which react with azido derivatives. In a first report, substituted cyclooctynes successfully react with various small molecular compounds including benzyl azide, 2-azido ethanol or *N*-butyl α-azidoacetamide via [3+2] cycloaddition.[99] The group initially utilized this modified reaction towards labeling of biomolecules in living systems. More specifically, the [3+2] cycloaddition was performed at physiological conditions using cyclooctyne derivatives bearing a biotin moiety and an azide-functionalised GlyCAM-Ig, which was formed from expression of the recombinant glycoprotein GlyCAM-Ig in Chinese hamster cells (CHO) in the presence of peracetylated *N*-azidoacetylmannosamine (Ac$_4$ManNAz), leading to incorporation of *N*-azidoacetylsialic acid (SiaNAz) into its glycans. Biotinylation was observed for GlyCAM-Ig modified with SiaNAz, followed by staining with FITC avidin. Consequently, the cells displayed a dose-dependent increase in fluorescence upon treatment with the cyclooctyne probe. These strained cycloalkynes were stable in mild acidic and basic

conditions and the reaction proceeded without any apparent cytotoxicity. However, in comparison to CuAAC, these cycloalkynes gave rather slow cycloaddition kinetics, as well as having the limited water solubility.
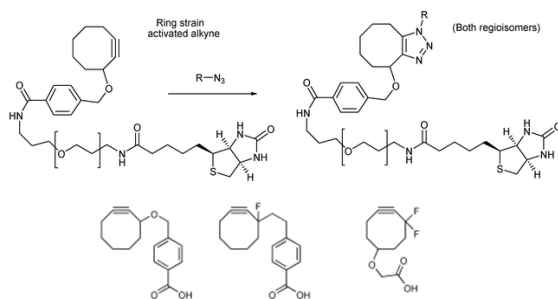
Figure 1.16 Cyclooctynes fragment utilised in strain promoted click reaction.

This situation was dramatically improved by introducing electron-withdrawing substituents, which would lower the energy of the alkyne's lowest unoccupied molecular orbital (LUMO) and hence increase the rate of cycloaddition with azides on the α position of the triple bond (Figure 1.16).[34,35] For instance, fluoro substituents were selected for several reasons. Firstly, they are relatively inert in a biological environment; secondly, the use of fluorine, a ε electron-withdrawing group, avoided creating a Michael, which would improve the reagent's bioorthogonality. Recently, the same group reported that a difluorinated cyclooctyne, termed DIFO, lead to very fast and efficient azide-alkyne cycloadditions and this active reactivity did not decrease specific reactivity with azides.[34] These reactions produce a racemic mixture of regioisomers, but exhibit some "click" features in the sense that they are chemoselective and readily applicable in physiological conditions. Moreover, strain-promoted and fluorine-activated cycloadditions exhibit better reactivity than CuAAC. More importantly, the surface of mammalian cells could be labeled with fluorescent dyes within minutes utilizing this strategy and the labeled glycans within the cells into cell compartments could be tracked *in vivo*. Thus, cyclooctyne-based ligations could become more and more important tools in chemical biology.

1.3.3 Click chemistry and polymer and material science

The metal catalyzed azide/alkyne "click" reaction, which originally focused on drug discovery and bio-conjugation has vastly increased in broadness and application in the field of material science. Although the first applications of the click reaction in material science was published 2004, according to a SciFinder search in Oct 2008, the click reaction has had a huge impact on the field of material science, more than 300 papers including original papers, reviews and patents, have been published in the context of click chemistry and material science. Because the click reaction has ideal properties including high efficiency reaction coupled with a high functional group tolerance and solvent insensitivity (also highly active in water), working equally well under homogeneous and heterogeneous conditions such as solid/liquid, liquid/liquid, or even solid/solid interfaces, as well as moderate reaction temperatures (25-70 °C), it provide a super solution to many problems exiting in material science, such as: a) a poor degree of functionalization with multiple functional groups; b) purification problems; c) incomplete reaction on surfaces and interfaces; and d) harsh reaction conditions leading to the damage of associates and assemblies. In the following part, a survey assembles recent applications of this reaction in the field of material science.

Dendrimers

Dendrimers are repeatedly branched species which continue to receive much attention because of their unique properties and applications in medicinal and materials chemistry. Difficulties of purification are major dendrimer synthesis problems, which has been addressed by the reliability of click reaction. The initial report of triazole-based dendrimers by Fokin *et al.* utilized a convergent pathway of dendrimer synthesis using the reaction of two azides with a bis-alkyne alkyl chloride (Figure 1.17).[100] Individual "branches" were first generated by sequential "

click reactions˙ onto a bis-alkynyl scaffold and the resultant bis-triazole alkyl chloride was converted into an azide. Subsequently, the first generation dendrimer was ˙clicked˙ onto another bis-alkynyl core to give the second generation dendrimer *etc.*, resulting in a number of products including 3rd and 4th generation dendrimers. Standard aqueous reaction conditions and organic-solvent-based microwave conditions were used to synthesize lower generation and higher generations depending on the periphery end groups individually, and the reactions were mostly driven to completion, greatly simplifying purification at each stage. Dendrimers have also been formed divergently using copper sulfate and ascorbate in different solvents including water, ethanol and DMSO.[101]
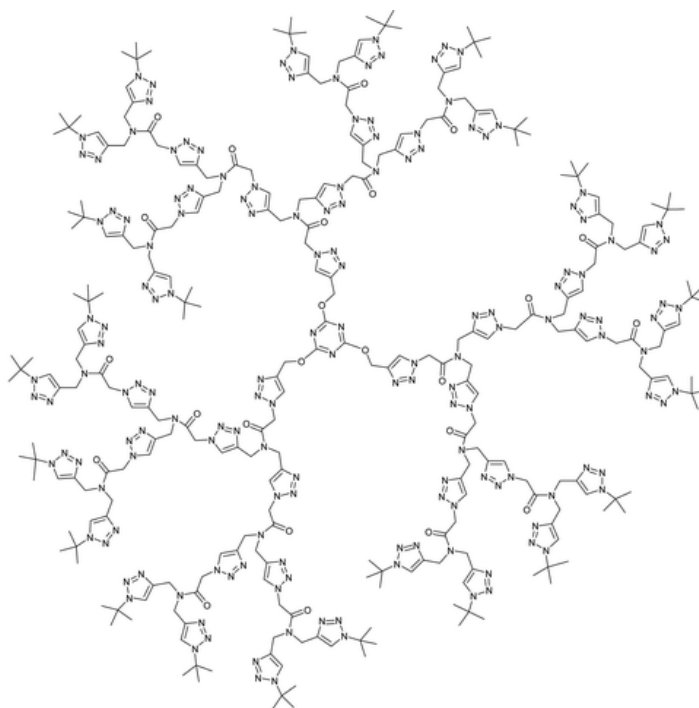
Figure 1.17 dendrimer synthesis via click reaction.

Click chemistry has been further adopted in the synthesis of chain-end functionalization of dendrimers containing sugar binding units. The general use of the click reaction to decorate dendrimers with sugars is a significant ongoing research field. There are some cases of

convergently made dendrimers through a reaction on the periphery in the last reaction.[68,71,102] All of them were made possible by the orthogonal properties of click reaction. Click chemistry has also been used to syntesize bivalent dendrimers with both coumarin fluorescent and mannose units.[103]

Polymer

The click reaction is a coupling reaction like urethane formation, esterification and etherification. The fundamental porperties of click reaction-high efficiency, reliability and ease of work-up—make it an ideal method for polymer synthesis. There are many published reports involving polymers and the click reaction which probably reflects the urgency to discover the scope and limits of the method's application to polymer science. Currently, there are two major directions in the use of click reaction in polymer science, the integration of ATRP and the click reaction and polymer synthesis/functionalization.

Less efficient transformations generally suffer from incomplete reactions as a result of the steric inaccessibility of the reaction site in a polymer structure. The emergence of click chemistry drastically changed the scientific community's view on polymer synthesis. Due to its extremely high reaction efficiency and tolerance to many functional groups, click chemistry has become the hallmark of linker chemistry. It is one of the most efficient ways to join two moieties together and has thus been utilized to conjugate well-defined homopolymers to form block copolymers. Recently, Van Camp *et al*. reported a synthetic system for diverse amphiphilic copolymer structures by incorporating with ATRP and the click reaction (Figure1.18). Using a formal strategy, polymers containing alkyne functionalities and polymers with azide functionalities, e.g. poly(acrylic acid) and poly(1-ethoxyethyl acrylate), were first formed through ATRP. They were then subsequently "clicked" together to generate block copolymers.[104] In addition, Opsteen *et al*.

used similar approach to synthesize polystyrene (PS), poly(tert-butyl acrylate) (PtBA), poly(methyl acrylate) (PMA) block copolymers via click chemistry.[105] Using an initiator with a triisopropylsilyl (TIPS) protected acetylene, the three homopolymer blocks were obtained through ATRP and the terminal bromides were subsequently converted to azides. Following TIPS deprotection, the heterotelechelic homopolymers were conjugated together through click reactions. Clearly, the click reaction has provided the second strategy of block copolymer synthesis. In addition, any two homopolymer blocks can be joined together to form block copolymers by using click reaction. All of this opens the door to synthesize a block copolymer library, allowing the synthesis of diverse copolymers with very unique properties quickly and easily, which could potentially lead to great useful in the field of pharmaceutical sciences.
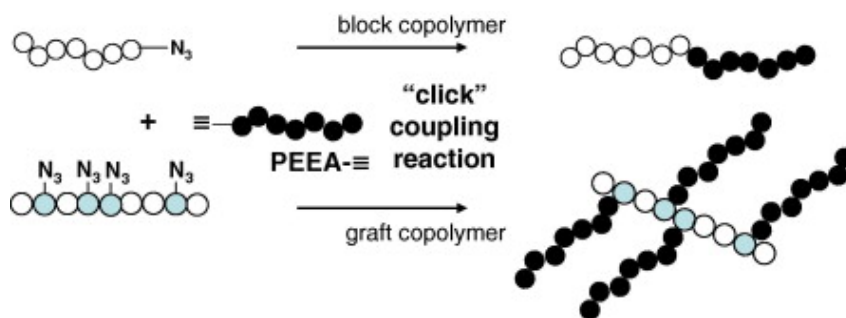
Figure1.18 Using "click" chemistry to synthesize block and graft copolymers.

Another case showed that the functionalization of polymers by click reaction provides the basis for more complicated processes in the arena of polymer synthesis and functionalization. Haddleton *et al.*[106] investigated the use of click reaction in the development of novel neoglycopolymers (sugar derived polymers). These compounds are receiving much attention due to their potential medical applications and favourable interactions with protein receptors or enzymes. Polymer backbones with an alkyne of both homo- and co-polymer types were synthesized, followed by "clicking" with azido-sugar residues to generate model glycopolymers in quantitative yield. Interestingly, a novel 'co-click' system was developed using a mixture of

two azide containing sugar moieties (β-galactoside and α-mannoside) and an alkyne bearing a homopolymer chain to decorate a polymer in which contained both α-mannoside and β-galactoside units connected with the polymer backbone through a triazole linker (Figure 1.19).
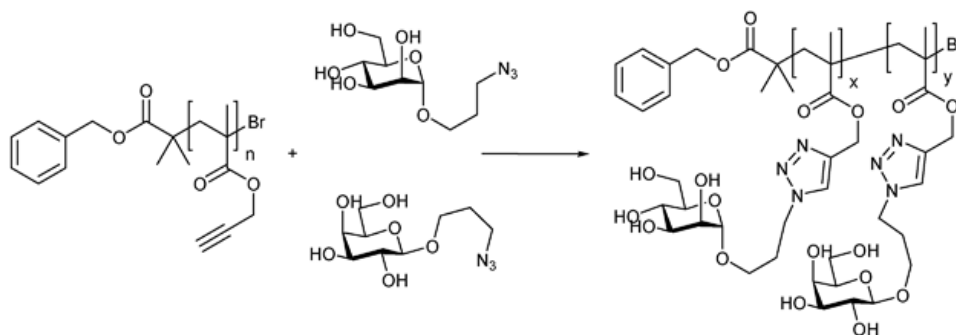
Figure 1.19 Neoglycopolymers were synthesized by using click reaction.

Nanotubes

Click chemistry has been applied to the highly fashionable field of nanotechnology. An interesting application of click reactions has been demonstrated using single walled carbon nanotubes (SWNTs), allotropes of carbon with a nanostructure that can have a length-to-diameter ratio more than 1,000,000. These cylindrical carbon molecules have novel properties that make them potentially useful in many applications in molecular electronics, sensors, field emission devices, and components in high-performance composites. They exhibit unique electrical properties, extraordinary strength and flexibility, which suggests they will have a potential role in nanotechnology engineering. However, the insolubility of these structures presents problems when it comes to solution phase processing. Sidewall modification with polymeric structures has been shown to improve solubility, and functionalization with polymers allows control over the final properties of the nanotube–polymer conjugate. As showed recently, the use of highly reactive dipolarophiles (such as azomethine ylides,[107] nitrile imines,[108] and nitrile oxides[109] leads to cycloaddition reactions onto the surface of single-walled carbon nanotubes (SWCNTs).[110]

However, slow reactions are often observed, which lead to reaction times in the range of several days. Adronov *et al.* used click reaction to successfully fix a telechelic PS polymer by a grafting-to approach onto the surface of SWCNTs (Figure1.20).[111] The ˈclick reactionˈ enabled high density functionalization, by incorporation of a small alkyne bearing reactive species on to the surface of the nanotube, followed by conjugating of these fragments to polystyrene chains containing terminal azide. As demonstrated extensively by solubility change and thermogravimetric analysis, a significant attachment of the PS polymer was achieved. The group can decorate the carbon nanotube to such a density that the complex material consisted of about 45% polymers. The materials synthesised exhibited high solubility in a range of organic solvents.

PS = Polystyrene
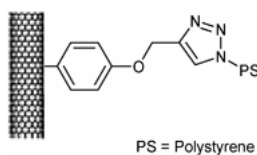
Figure1.20 Carbon nano-tubes were functionalized by using click reaction.

Nanoparticles

In nanotechnology, the nanoparticle is defined according to size: In terms of diameter, fine particles cover a range in size from 10 to 1000 nanometers, while ultrafine particles, on the other hand, are sized between 1 and 100 nanometers. Over the past few decades, nanoparticle systems including quantum dots, gold nanoparticles, magnetic nanoparticles, liposomes and micelles have all been extensively investigated for applications of imaging and drug/gene delivery.[112,113] Nanoparticles have some special properties such as small size and high loading rate, which make them easily and allow efficient drug accumulation at target sites. In addition, nanoparticular delivery systems combing with drug targeting offer several further important advantages: they reduce drug dose, minimize side-effects, protect drugs against degradation, increase the retention time, and enhance drug stability.[115]

Surface modifications of nanoparticles can significantly improve their physical-chemical properties and therapeutic efficacy. They can change hydrophobicities, nanoparticle zeta potentials, and targeting capabilities. There are several techniques, such as physical adsorption, electrostatic binding, specific recognition, and covalent coupling, that have been used to modify surfaces, each has its own advantages and disadvantages. However, chemical modification of surface by using click reaction attracted more and more attentions from interfacial scientist. One of the important properties of the click reaction is high reactivity at an interface, which leads to the potential applications of a high efficiency for the modification of surfaces. Moreover, since recent chemical reactions for surfaces and interfaces modifications are incomplete or insufficient chemical reactions, the click reaction changed the views of the interfacial scientist, enabling easy access to modified surfaces of reproducible and reliable surface densities. Therefore, a lot of click reactions on self-assembled monolayers (SAMs),[115-126] polymeric surfaces,[78,127-131] layer by layer assemblies,[131,132] nanopaticles,[133,134] polymersomes[135-137] and liposomes[130-140] and the functionalization of crosslinked resins with terminal alkyne/azido groups have been reported. Thus a large variety of nanoparticles (Au,[116,141-143] CdSe,[144] Fe_2O_3,[145-147] SiO_2[148]) as well as viruses[149], micelles and liposomes[150] have been surface-modified by this method. Compared to conventional surface-function methods, the click reaction enables an elegant, efficient and fast methodology to modified nanoparticles in a simple mode.

Polymeric Micelles

Polymeric micelles, an aggregate of surfactant molecules dispersed in a liquid colloid, are water-soluble biocompatible nanocontainers with great potential for delivery vehicles for therapeutic, imaging, or diagnostic agents. Although polymeric micelles are simple and effective delivery systems that have been developed in clinical treatments for a variety of cancers, they

still have several challenges such as control of drug release and stability. To improve micelle properties, many different methodologies have been developed.[151,152] One of the most interesting methods was investigated by Wooley's group, who reported a novel method to stabilize polymeric micelles. In this case, the well-defined core-crosslinked polymeric micelles were prepared by using multi-functional dendritic crosslinkers (Figure 1.21).[153] Firstly, amphiphilic diblock copolymers of poly(acrylic acid)-b-poly(styrene) (PAA-b-PS) were functionalized with terminal alkynes throughout the hydrophobic polystyrene block segment to generate micelles that were click-readied for crosslinking. Azide functionalized 1st generation dendrimers were then conjugated with the alkynyl groups of the micelles to form core crosslinked micelles by using click reaction. It was calculated that about 3.4 polymer chains were clicked to each dendrimer. The remaining clickable functionalities, both azides and terminal alkynes, could be utilized for further chemical modifications, such as conjugating fluorescent tags.
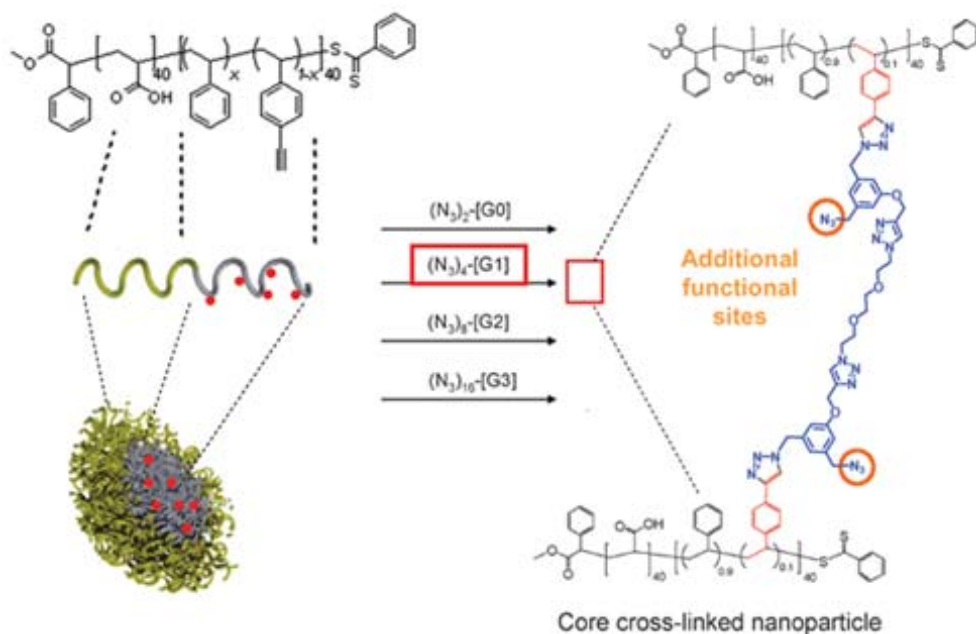
Figure 1.21 Synthesis of polymer nanoparticles from azido-terminated dendrimers and alkynyl-functionalized micelles.

42

In addition to crosslinking micelles, click reactions on their surface constitute another issue, which was addressed recently by the same group. The modification of systems in an easy, room temperature-controlled process with (biorelated) ligands is important, mainly due to their dynamic properties, which requires reactions at room temperatures. In their studies, they could introduce clickable functionalities selectively throughout either the core or shell of micelles[154]. Poly(acrylic acid) within the micelle shell was modified to display either azido or alkynyl functionalities via amidation chemistry after obtaining a poly(acrylic acid)-*b*-polystyrene copolymer micelle. Repeating the amidation conjugation reaction once more, the unreacted acrylic acids were bonded together by a diamine linker, crosslinking the shell of the micelle in an intramicellar fashion. Following similar chemistry, a shell-crosslinked micelle containing clickable functionalities in the polystyrene core was also formed. Fluorescent dyes had been conjugated on the crosslinked micelles by using the click reaction to demonstrate the availability and reactivity of the functional groups (azides or terminal alkynes). While the methodologies shown above are very appealing, they are still in their early stages of development for applications of click reaction in micelles.

Liposomes

Since liposomes were first described by Bangham and co-workers in the late 1950s[154], they have attracted a lot attentions form pharmaceutical scientists to develope it as drug delivery systems. Over the past decade, US Food and Drug Administration (FDA) have approved liposomal formulations for treatments for a variety of cancers[155]. However, this particular drug carrier still needs to be optimized to attain its full potential in several aspects: Their surfaces need to be modified to escape form the phagocytic cells of the reticular endothelial system (RES), drug release mechanisms need to be improved so that the drug can exclusively and completely

delivered to the disease target site, and more efficient methods for linking targeting moieties, such as antibodies and peptides, to liposomal surfaces need to be developed. Although the first two issues have been addressed,[156-158] the last still remains a problem. Many strategies rely on chemical reactions that are not well-controlled, which often lead to unwanted products. As already mentioned above, the click reaction is a highly useful and reliable conjugation method. Thus, some reports can be found in the literatures relating click chemistry and liposomal conjugations.

Recently, Hassane *et al.*[138] demonstrated a novel method for linking mannose ligands to the surfaces of preformed liposomes via the click reaction. The resulting liposomes bearing mannose ligands can be used as vehicles to target specific cells, such as human dendritic cells.[159] In this case, a lipid anchor with a terminal alkyne functionality was first conjugated to liposomes. Then an unprotected mannosyl derivative with an azide group was clicked to the surface of the liposome in one step. The group found that if the Cu(I) oxidation state was protected from degradation pathways by using a stabilizing agent, the reaction will be greatly accelerated and gave high yields. The results showed that the click reaction did not damage the integrity of the bilayers and did not significantly change the particle size.[160]

Metal nanoparticles-Gold and Magnetic

The application of gold nanoparticles in pharmaceutical research has become a well-developed research field, and more and more scientific literature relating to gold nanoparticles have been published. Because they have special chemical and physical properties, they have been utilized to target polynucleotides[162] and label antibodies[161] in cancer cell diagnostics[163] and drug delivery systems[164]. The most popular strategies rely on attaching biological molecules through a non-covalent linkage, which have important disadvantages.[143] For example, due to

weaker bonds of non-covalent interactions, it is very easy to break apart the nanoparticle-biological molecule conjugate. Thus, covalent bonds must be used for long-term conjugation. Recently, Brennan *et al*. demonstrated that covalent-bond bioconjugations could be performed on gold nanoparticles easily and rapidly by using click chemistry (Figure 1.22A).[143] In this study, gold nanoparticles bearing azide groups at the surface were first prepared. A lipase enzyme, a 30 kDa globular recombinant protein, which was modified to express a single terminal alkyne, was allowed to click with the nanoparticles. Several lipases were covalently attached to each nanoparticle without any nonspecific binding as verified through gel electrophoresis. In addition, the enzyme activity of the lipases remained intact. In addition, Fleming *et al*. conjugated several different alkynyl derivatives such as aniline, ferrocene, and PEG to gold nanoparticles through the click reaction following a similar procedure.
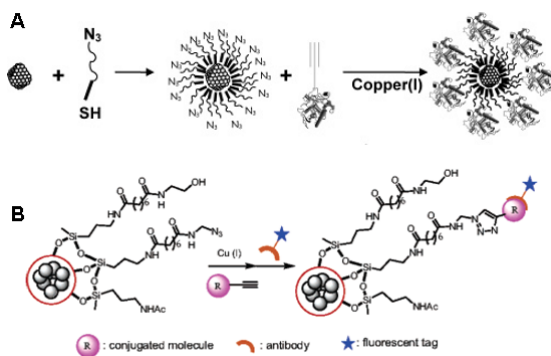
Figure 1.22 Click reaction on metal nanoparticles.

Magnetic nanoparticles are another kind of nanoparticles which have a wide variety of applications in pharmaceutical sciences due to their super properties, including injectability, good biocompatibility, and highly specific accumulation in target tissues under a local magnetic field.[165] Lin *et al*.[167] successfully conjugated several different organic molecules to magnetic particles by using the click reaction (Figure 1.22B). The molecules included the Tn antigen, biotin, the flag peptide, 2,4-dinitrophenol (DNP), and the maltose binding protein (MBP), all of

which had been modified to carry a terminal alkyne. The magnetic nanoparticles counterparts were functionalized with an azide group. Fluorescent tests showed that all of the bioconjugations were successful without nonspecific binding of the 1,2,3-triazole or unreacted azide. Additionally method has been shown by Lin *et al.* in their studies. For example, ligands with either a phosphonic acid or a carboxylic acid group at one terminus were strongly conjugated to the surface of a γ-Fe$_2$O$_3$ nanoparticle, and either an acetylene or azide group at the other terminus to supply a functional group for modification.[147] Both 5-chloropentyne and benzyl azide were then successfully clicked onto the nanoparticles. In addition, an acetylene terminated polymeric ligand was also successfully conjugated to the nanoparticles, which improve the versatility of the strategy.

1.4 CONCLUSION AND OUTLOOK

In the relatively short period since initial reporting of click chemistry, it has found a home in the tool box of chemists as evidenced by the dramatic and diverse impact in many fields of modern chemistry. The chemists, sometimes forced to accept the extensive use of protecting-group strategies and insufficient reaction progress, have been searching for click-type reactions for long time. Now, with the emergence of the azide/alkyne-1,3-dipolar cycloaddition click reaction, great progress in this direction has been made. Ever since the foundations of the click reaction were laid, there has been an explosive growth in publications describing a wealth of applications of this practical and sensible chemical approach. The versatility of click reaction seems endless, yet we are still in the early developmental stages of it. Certainly, new and other types of click reaction, which meet 'click' criteria, will come into view in the future and place strong, hands-on chemical items to our chemistry "tool box". With them in the hand, scientists can build the scientific world in a brick-type fashion by simple chemical reactions.

1.5 REFERENCES

1. D. Barton, K. Nakanishi Comprehensive Natural Products Chemistry. Sankawa, U, Ed.; Elsevier; New York 1999

2. P. Seneci, Solid-Phase Synthesis and Combinatorial Technologies. Wiley: New York, 2000

3. Stein, R.B. Henerson, J. S. Fruton, Heterocylic Compounds. R.C. Elderfield, Wiley&Sons, Inc.: London, 1950, Vol. 1

4. H. C. Kolb, M. G. Finn and K. B. Sharpless, *Angew. Chem., Int. Ed.*, 2001, 40, 2004

5. W.C. Guida et al. *Med. Res. Rev*. 1996, 3

6. C. D. Hein, X. Liu, D. Wang, *Pharmaceutical Res.*, 2008, 25, 10, 2216

7. J.-F. Lutz, H. G. Börner, K. Weichenhan, *Macromol. Rapid Commun.* 2005, 26, 514

8. C. W. Tornoe, C. Christensen, M. Meldal, *J. Org. Chem.* 2002, 67, 3057

9. V. V. Rostovtsev, L. G. Green, V. V. Fokin, K. B. Sharpless, *Angew. Chem. Int. Ed.* 2002, 41, 2596

10. R. Huisgen, *Angew. Chem. Int. Ed. Engl.* 1963, 2, 565.

11. R. Huisgen, *Angew. Chem. Int. Ed. Engl.* 1963, 2, 633.

12. R. Huisgen, " *1,3-Dipolar Cycloaddition Chemistry* ", A. Padwa, Ed., Wiley, New York 1984

13. A. Michael, *J. Prakt. Chem.* 1893, 48, 94.

14. a. J. P. Collman, N. K. Devaraj, C. E. D. Chidsey, *Langmuir* 2004, 20, 1053; b. D. D. Díaz, S. Punna, P. Holzer, A. K. McPherson, K. B. Sharpless, V. V. Fokin, M. G. Finn, *J. Polym. Sci. Part A* 2004, 42, 4392; c. B. Helms, J. L. Mynar, C. J. Hawker, J. M. J. Fréchet, *J. Am. Chem. Soc.* 2004, 126, 15020; d. P. Wu, K. B. Sharpless, V. V. Fokin, *Angew. Chem.* 2004, 116, 4018; *Angew. Chem. Int. Ed.* 2004, 43, 3928-3932

15. B. M. Mykhalichko, O. N. Temkin, and M. G. Mys'kiv. *Russ. Chem. Rev*. 2000, 69, 957

16. F. Himo, T. Lovell, R. Hilgraf, V. V. Rostovtsev, L. Noodleman, K. B. Sharpless, and V. V. Fokin. *J. Am. Chem. Soc*. 2005, 127, 210

17. V. O. Rodionov, V. V. Fokin, and M. G. Finn. *Angew. Chem., Int. Ed. Engl*. 2005, 44, 2210

18. V. D. Bock, H. Hiemstra, and J. H.-V. Maarseveen. *Eur. J. Org. Chem*. 2006, 51

19. W. S. Horne, C. D. Stout, and M. R. Ghadiri. *J. Am. Chem. Soc*. 2003, 125:9372

20. R. Chinchilla, and C. Najera. *Chem. Rev*. 2007, 107, 874

21. W. S. Horne, C. D. Stout, and M. R. Ghadiri. *J. Am. Chem. Soc*. 2003, 125, 9372

22. P. L. Golas, N. V. Tsarevsky, B. S. Sumerlin, and K. Matyjaszewski. *Macromolecules*. 2006, 39, 6451

23. H. A. Orgueria, D. Fokas, Y. Isome, P. C.-M. Chane, and C. M. Baldino. *Tetrahedron Lett*. 2005, 46, 2911

24. S. Chassaing, M. Kumarraja, A. S.-S. Sido, P. Pale, and J. Sommer. *Org. Lett*. 2007, 9, 883

25. W. H. Zhan, H. N. Barnhill, K. Sivakumar, H. Tian, and Q. Wang. *Tetrahedron Lett*. 2005, 46, 1691

26. M. A. Bennett. *Chem. Rev*. 1962, 62, 611

27. F. R. Hartley. *Chem. Rev*. 1973, 73, 163

28. L. L. Zhang, X. Chen, P. Xue, H. H. Y. Sun, I. D. Williams, K. B. Sharpless, V. V. Fokin, and G. Jia. *J. Am. Chem. Soc*. 2005, 127, 15998

29. G. C. Tron, T. Pirali, R. A. Billington, P. L. Canonico, G. Sorba, and A. A. Genazzani. *Med. Res. Rev*. 2007, 28, 278

30. Z. Li, T. S. Seo, and J. Ju. *Tetrahedron Lett*. 2004, 45, 3143

31. N. J. Agard, J. A. Prescher, and C. B. Bertozzi. *J. Am. Chem. Soc*. 2004, 126, 15046

32. R. Manetsch, A. Krasinski, Z. Radic, J. Raushel, P. Taylor, K. B. Sharpless, H. C. Kolb, *J. Am. Chem. Soc.* 2004, 126, 12809; b. V. P. Mocharla, B. Colasson, L. V. Lee, S. Röper, K. B. Sharpless, C.-H. Wong, H. C. Kolb, *Angew. Chem.* 2005, 117, 118; *Angew. Chem. Int. Ed.* 2005, 44, 116

33. S. S. van Berkel, A. J. Dirks, M. F. Debets, F. L. van Delft, J. J. L. M. Cornelissen, R. J. M. Nolte, F. P. J. T. Rutjes, *ChemBioChem.* 2007, 8, 1504.

34. J. M. Baskin, J. A. Prescher, S. T. Laughlin, N. J. Agard, P. V. Chang, I. A. Miller, A. Lo, J. A. Codelli, C. R. Bertozzi, *Proc. Natl. Acad. Sci. USA* 2007, 104, 16793

35. N. J. Agard, J. M. Baskin, J. A. Prescher, A. Lo, C. R. Bertozzi, *ACS Chem. Biol.* 2006, 1, 644

36. G. Wittig, A. Krebs, *Chem. Ber.* 1961, 94, 3260-3275; A. T. Blomquist, L. H. Liu, *J. Am. Chem. Soc.* 1953, 75, 2153

37. K. B. Sharpless and R. Manetsch, *Expert Opin. Drug Disc.*, 2006, 1, 525.

38. D. Rideout, *Science* 1986, 233, 561

39. D. Rideout *et al.*, *Biopolymers* 1990, 29, 247

40. R. Nguyen and I. Huc, *Angew. Chem. Int. Ed. Engl.* 2001, 40, 1774

41. J-M. Lehn and A.V. Eliseev, *Science* 2001, 291, 2331

42. J.L. Sussman *et al.*, *Science* 1991, 253, 872

43. J.P. Changeux, *Mol. Pharmacol.* 1966, 2, 369

44. P. Taylor and S. Lappi, *Biochemistry* 1975, 14, 1989

45. M. Whiting, J. Muldoon, Y.-C. Lin, S. M. Silverman, W. Lindstrom, A. J. Olson, H. C. Kolb, M. G. Finn, K. B. Sharpless, J. H. Elder and V. V. Fokin, *Angew. Chem., Int. Ed.*, 2006, 45, 1435

46. J. Wang, G. Sui, V. P. Mocharla, R. J. Lin, M. E. Phelps, H. C. Kolb and H.-R. Tseng, *Angew. Chem., Int. Ed.*, 2006, 45, 5276

47. Arkin, M. R.; Wells, J. A. *Nat. Rev. Drug Discovery* 2004, 3, 301

48. Kolb, H. C.; Sharpless, K. B. *Drug Discovery Today* 2003, 8, 1128

49. Wu, C.-Y. et al. *Proc. Natl. Acad. Sci. U.S.A.* 2004, 101, 10012

50. Johnson, T. O.; Ermolieff, J.; Jirousek, M. R. *Nat. Rev. Drug Discovery* 2002, 1, 696.

51. Bialy, L.; Waldmann, H. *Angew. Chem., Int. Ed.* 2005, 44, 3814.

52. Overall, C. M.; Kleifeld, O. *Nat. Rev. Cancer* 2006, 6, 227

53. Whittaker, M.; Floyd, C. D.; Brown, P.; Gearing, A. J. H. *Chem. Rev.* 1999, 99, 2735

54. Nelson, A. R.; Fingleton, B.; Rothenberg, M. L.; Matrisian, L. M. *J. Clin. Oncol.* 2000, 18, 1135

55. Wong, C.-H., ed. Carbohydrate-based Drug Discovery., pp. 980, Wiley-VCH (2003)

56. P. I. Kitov, J.M. Sadowska, G. Mulvey, G. D. Armstrong, H. Ling, N. S. Pannu, R. J. Read, D. R. Bundle, *Nature* 2000, 403, 669

57. M. Mammen *et al.*, *Angew. Chem. Int. Ed. Engl.* 1998, 37, 2755

58. F. G. Calvo-flores, J. Isac-Garcia, F. Hernandez-Mateo, F. Perez-Balderas, J. A. Calvo-Asin, E. Sanchez-Vaquero, F. Santoyo-Gonzalez, *Org. Lett.* 2000, 2, 2499

59. F. Perez-Balderas, M. Ortega-Munoz, J. Morales-Sanfrutos, F. Hernadez-Mateo, F. G.Calvo-Flores, J.A.Calvo-Asin, J. Isac-Garcia, F. Santoyo-Gonzalez, *Org. Lett.* 2003, 5,1951

60. Pe´rez-Balderas F, Ortega-Mun˜oz M, Morales-Sanfrutos J, Herna´ndez-Mateo F, Calvo-Flores FG, Calvo-Ası´n JA, Isac-Garcı´a J, Santoyo-Gonza´lez F. Org Lett 2003, 5, 1951

61. Yang F, Du Y. Carbohydr Res 2003, 338, 495

62. Chen Q, Yang F, Du Y. Carbohydr Res 2005, 340, 2476

63. Fu X, Albermann C, Zhang C, Thorson JS. Org. Lett. 2005, 7, 1513

64. E. Fernandez-Megia, J. Correa, I. Rodriguez-Meizoso, R. Riguera, *Macromolecules* 2006, 39, 2113

65. Lundquist, J. J.; Toone, E. J. *Chem. Rev.* 2002, 102, 555.

66. Fan, E.; Zhang, Z.; Minke, W. E.; Hou, Z.; Verlinde, C. L. M. J.; Hol, W. G. J. *J. Am. Chem. Soc.* 2000, 122, 2663.

67. E. Fernandez-Megia, J. Correa, I. Rodriguez-Meizoso, R. Riguera, *Macromolecules* 2006, 39, 2113.

68. Joosten, J. A. F.; Tholen, N. T. H.; Maate, F. A. L.; Brouwer, A. J.; van Esse, G. W.; Rijkers, D. T. S.; Liskamp, R. M. J.; Pieters, R. J. *Eur. J. Org. Chem.* 2005, 3182.

69. J. W. Lee, J. H. Kim, B. K. Kim, *Tetrahedron Lett.* 2006, 47, 2683.

70. J. W. Lee, J. H. Kim, B. K. Kim, W. S. Shin, S. H. Jin, *Tetrahedron* 2006, 62, 894.

71. D. T. S. Rijkers, G. W. van Esse, R. Merkx, A. J. Brouwer, H. J. F. Jacobs, R. J. Pieters, R. M. J. Liskamp, *Chem. Commun.* 2005, 4581.

72. A. H. Dent. *Pharm. Tech. Eur*. 2007, 19, 39, 43

73. Anderson NL, Anderson NG. *Electrophoresis* 1998, 19, 1853

74. Speers AE, Cravatt BF. *ChemBioChem* 2004, 5, 41

75. Cravatt, B. F.; Sorensen, E. J. *Current Opin. Chem. Biol*. 2000, 4, 663

76. Liu, Y.; Patricelli, M. P.; Cravatt, B. F. *Proc. Natl. Acad. Sci. U.S.A.* 1999, *96*, 14694

77. Speers, A. E.; Adam, G. C.; Cravatt, B. F. *J. Am. Chem. Soc*. 2003, *125*, 4686

78. H. K. Tewary, and P. L. Iversen. *J. Pharm. Biomed. Anal.*, 1997, 15, 1127

79. M. Schena, D. Shalon, R. W. Davis, and P. O. Brown. *Science,*1995, 270, 467.

80. A. M. Gewirtz. *Curr. Opin. Hemat*. 1998, 5, 59

81. T. S. Seo, Z. Li, H. Ruparel, and J. Ju. *J. Org. Chem*. 2003, 68, 609

82. J. Gierlich, G. A. Burley, P. M. E. Gramlich, D. M. Hammond and T. Carell, *J. Org. Lett.*, 2006, 8, 3639.

83. T. R. Chan, R. Hilgraf, K. B. Sharpless and V. V. Fokin, *Org. Lett.*, 2004, 6, 2853

84. F. Seela, V. R. Sirivolu, and P. Chittepu., *Bioconjugate Chem*. 2008, 19, 211

85. G. M. Cooper. *The Cell Surface. The Cell: A Molecular Approach, 2nd edn*. Sinauer, Sunderland, MA, 2000.

86. D. B. Werz, and P. H. Seeberger, *Chem. Eur. J*. 2005, 11, 3194

87. T. Liebert, C. Hänsch, and T. Heinze. *Macromol. Rapid Commun*. 2006, 27, 208

88. J. Hafrén, W. Zou, and A. Córdova. *Macromol. Rapid Commun*. 2006, 27, 1362

89. Q. Wang, T. R. Chan, R. Hilgraf, V. V. Fokin, K. B. Sharpless and M. G. Finn, *J. Am. Chem. Soc.*, 2003, 125, 3192

90. Q. Wang, E. Kaltgrad, T. Lin, J. E. Johnson, and M. G. Finn. *Chem. Bio*. 2002, 9, 805

91. Q. Wang, T. Lin, L. Tang, J. E. Johnson, and M. G. Finn. *Angew. Chem., Int. Ed. Engl*. 2002, 41, 459

92. S. S. Gupta, J. Kuzelka, P. Singh, W. G. Lewis, M. Manchester, M. G. Finn, Bioconjug. Chem. 2005, 16, 1572

93. S.S. Gupta, K.S. Raja, E. Kaltgrad, E. Strable, M. G. Finn, Chem. Commu. 2005, 4315

94. W. Chen, and G. Georgiou. *Biotechnol. Bioeng*. 2002, 79, 496

95. J. A. Link, and D. A. Tirrell. *J. Am. Chem. Soc*., 2003, 125, 11164.

96. K. L. Kiick, E. Saxon, D. A. Tirrell, and C. R. Bertozzi. *Proc. Natl. Acad. Sci. U.S.A.*, 2002, 99, 19

97. A. Basle, G. Rummel, P. Storici, J. P. Rosenbusch, and T. Schirmer. *J. Mol. Bio.*, 2006, 362, 933

98. J. M. Baskin, C. R. Bertozzi, *QSAR Comb. Sci.* 2007, 26, 1211

99. B. K. Marcus, and W. E. Cormier. Going green with zeolites. *Chem. Eng. Prog.*, 1999, 95, 47

100. P. Wu, A. K. Feldman, A. K. Nugent, C. J. Hawker, A. Scheel, B. Voit, J. Pyun, J. M. J. Fréchet, K. B. Sharpless and V. V. Fokin, *Angew. Chem., Int. Ed.*, 2004, 43, 3928

101. M. J. Joralemon, R. K. O'Reilly, J. B. Matson, A. K. Nugent, C. J. Hawker, K. L. Wooley, *Macromolecules* 2005, *38*, 5436.

102. M. Malkoch, K. Schleicher, E. Drockenmuller, C. J. Hawker, T. P. Russell, P. Wu, V. V. Fokin, *Macromolecules* 2005, *38*, 3663.

103. P. Wu, M. Malkoch, J. N. Hunt, R. Vestberg, E. Kaltgrad, M. G. Finn, V. V. Fokin, K. B. Sharpless and C. J. Hawker, *Chem. Commun.*, 2005, 5775

104. W. Van Camp, V. Germonpre, L. Mespouille, P. Dubois, E. J. Goethals, and F. E. Du Prez. *React. Functl. Polym.* 2007, 67, 1168

105. J. A. Opsteen, and J. C. M. Van Hest. *J. Polym. Sci., Part A: Polym. Chem.* 2007, 45, 2913

106. V. Ladmiral, G. Mantovani, G. J. Clarkson, S. Cauet, J. L. Irwin and D. M. Haddleton, *J. Am. Chem. Soc.*, 2006, 128, 4823

107. J. Li, H. Grennberg, *Chem. Eur. J.* 2006, 12, 3869; Y. Wang, Z. Iqbal, S. Mitra, *Carbon* 2005, 43, 1015

108. M. Alvarado, P. Atienzar, P. de la Cruz, J. L. Delgado, H. Garcia, F. Langa, *J. Phys. Chem. B* 2004, 108, 12691

109. M. Alvaro, P. Atienzar, L. Echegoyen, *J. Am. Chem. Soc.* 2006, 128, 6626

110. N. Tagmartarchis, M. Prato, *J. Mater. Chem.* 2004, 14, 437

111. H. Li, F. Cheng, A. M. Duft and A. Adronov, *J. Am. Chem. Soc.*, 2005, 127, 14518

112. J. Panyam, and V. Labhasetwar. *Adv. Drug Delivery Rev.*2003, 55, 329

113. E. Katz, and I. Willner. *Angew. Chem., Int. Ed. Engl.* 2004, 43, 6042

114. P. Couvreur, G. Barratt, E. Fattal, P. Legrand, and C. Vauthier. *Crit. Rev. Ther. Drug Carrier Syst.* , 2002, 19, 99

115. R. Zirbs, F. Kienberger, P. Hinterdorfer, W. H. Binder, *Langmuir* 2005, 21, 8414

116. W. H. Binder, L. Petraru, R. Sachenshofer, R. Zirbs, *Monatsh. Chem.* 2006, 137, 835

117. X. L. Sun, C. L. Stabler, C. S. Cazalis, E. L. Chaikof, *Bioconjugate Chem.* 2006, 17, 52

118. Y. Zhang, S. Luo, Y. Tang, L. Yu, K. Y. Hou, J. P. Cheng, X. Zeng, P. G. Wang, *Anal. Chem.* 2006, 78, 2001

119. J. P. Collman, N. K. Devaraj, T. P. A. Eberspacher, C. E. D. Chidsey, *Langmuir* 2006, 22, 2457

120. N. K. Devaraj, R. A. Decreau, W. Ebina, J. P. Collman, C. E. D. Chidsey, *J. Phys. Chem. B* 2006, 110, 15955

121. T. Lummerstorfer, H. Hoffmann, *J. Phys. Chem. B* 2004, 108, 3963

122. J. K. Lee, Y. S. Chi, I. S. Choi, *Langmuir* 2004, 20, 3844

123. R. D. Rohde, H. D. Agnew, W. S. Yeo, R. C. Bailey, J. R. Heath, *J. Am. Chem. Soc.* 2006, 128, 9518

124. J.-C. Meng, C. Averbuj, W. G. Lewis, G. Siuzdak, M. G. Finn, *Angew. Chem. Int. Ed.* 2004, 43, 1255

125. S. Prakash, T. M. Long, J. C. Selby, J. S. Moore, M. A. Shannon, *Anal. Chem.* 2007, 79, 1661

126. R. V. Ostaci, D. Damiron, S. Capponi, G. Vignaud, L. Leger, Y. Grohens, E. Drockenmuller, *Langmuir* 2008, 24, 2732

127. D. E. Bergbreiter, P. N. Hamilton, N. M. Koshti, *J. Am. Chem. Soc.* 2007, 129, 10666

128. B. S. Lee, J. K. Lee, W. J. Kim, Y. H. Jung, S. J. Sim, J. Lee, I. S. Choi, *Biomacromolecules* 2007, 8, 744

129. Y. Li, W. Zhang, J. Chang, J. Chen, G. Li, Y. Ju, *Macromol. Chem. Phys.* 2008, 209, 322

130. G. K. Such, J. F. Quinn, A. Quinn, E. Tjipto, F. Caruso, *J. Am. Chem. Soc.* 2006, 128, 9318

131. G. K. Such, E. Tjipto, A. Postma, A. P. R. Johnston, F. Caruso, *Nano Lett.* 2007, 7, 1706

132. D. E. Bergbreiter, B. S. Chance, *Macromolecules* 2007, 40, 5337

133. R. K. O'Reilly, M. J. Joralemon, K. L. Wooley, C. J. Hawker, *Chem. Mater.* 2005, 17, 5976

134. R. K. O'Reilly, M. J. Joralemon, C. J. Hawker, K. L. Wooley, *J. Polym. Sci., Part A: Polym. Chem.* 2006, 44, 5203

135. J. A. Opsteen, R. P. Brinkhuis, R. L. M. Teeuwen, D. W. P. M. Lowik, J. C. M. v. Hest, *Chem. Commun.* 2007, 3136

136. S. F. M. v. Dongen, M. N. Sanne, S. Jeroen, J. L. M. Cornelissen, R. J. M. Nolte, J. C. M. v. Hest, *Macromol. Rapid Commun.* 2008, 29, 321

137. B. Li, A. L. Martin, E. R. Gillies, *Chem. Commun.* 2007, 5217

138. F. S. Hassane, B. Frisch, F. Schuber, *Bioconjugate Chem.* 2006, 17, 849

139. S. Cavalli, A. R. Tipton, M. Overhand, A. Kros, *Chem. Commun.* 2006, 3193

140. H.-J. Musiol, S. Dong, M. Kaiser, R. Bausinger, A. Zumbusch, U. Bertsch, L. Moroder, *Chem. Bio. Chem.* 2005, 6, 625

141. R. Voggu, P. Suguna, S. Chandrasekaran, C. N. R. Rao, *Chem. Phys. Lett.* 2007, 443, 118.

142. D. A. Fleming, C. J. Thode, M. E. Williams, *Chem. Mater.* 2006, 18, 2327

143. J. L. Brennan, M. Brust, *Bioconjugate Chem.* 2006, 17, 1373

144. W. H. Binder, R. Sachsenhofer, C. J. Straif, R. Zirbs, *J. Mater. Chem.* 2007, 17, 2125

145. W. H. Binder, H. C. Weinstabl, *Monatsh. Chem.* 2007, 138, 315

146. W. H. Binder, D. Gloger, H. Weinstabl, G. Allmaier, E. Pittenauer, *Macromolecules* 2007, 40, 3097

147. M. A. White, J. A. Johnson, J. T. Koberstein, N. J. Turro, *J. Am. Chem. Soc.* 2006, 128, 11356

148. R. Ranjan, W. J. Brittain, *Macromolecules* 2007, 40, 6217.

149. Q. Zeng, T. Li, B. Cash, S. Li, F. Xie, Q. Wang, *Chem. Commun.* 2007, 1453

150. A. Gole, C. J. Murphy, *Langmuir* 2008, 24, 266

151. F. Henselwood, and G. Liu. Water-soluble nanospheres of poly(2-cinnamoylethyl methacrylate)-block-poly(acrylic acid). *Macromolecules*. 1997, 30, 488

152. B. Loppinet, R. Sigel, A. Larsen, G. Fytas, D. Vlassopoulos, and G. Liu. *Langmuir*., 2000, 16, 6480

153. R. K. O'Reilly, M. J. Joralemon, C. J. Hawker, and K. L. Wooley. *New J. Chem*. , 2007, 31, 718

154. R. K. O'Reilly, M. J. Joralemon, K. L. Wooley, and C. J. Hawker. *Chem. Mater*., 2005, 17, 5976–5988

155. A. D. Bangham, D. H. Heard, R. Flemans, and G. V. Seaman. *Nature (London)*., 1958, 182, 642

156. T. M. Allen, and P. R. Cullis. *Science (Washington, D.C.)*. 2004, 303, 1818; M. L. Immordino, F. Dosio, and L. Cattel. *Int. J. Nanomed*. 2006, 1, 297

157. X. Guo, and F. C. Szoka Jr. *Acc. Chem. Res*. , 2003, 36, 335

158. L. Nobs, F. Buchegger, R. Gurny, and E. Allemann. *J. Pharm. Sci.*, 2004, 93, 1980

159. M. J. Copland, M. A. Baird, T. Rades, J. L. McKenzie, B. Becker, F. Reck, P. C. Tyler, and N. M. Davies. *Vaccine*. 2003, 21, 883

160. S. Gal, I. Pinchuk, and D. Lichtenberg. *Chem. Phys. Lipids*. 2003, 126, 95

161. P. W. Faulk, and M. G. Taylor. *Immunochem.*, 1971, 8, 1081

162. B.-S. Tan, X.-H. Cao, and Z.-H. Mo. *Chongqing Daxue Xuebao, Ziran Kexueban.*, 2003, 26, 58

163. X. Huang, I. H. E.-Sayed, and M. A. E.-Sayed. *Proc. SPIE-Int. Soc. Opt. Eng.*, 2005, 5929

164. G. Han, P. Ghosh, M. De, and V. M. Rotello. *NanoBiotech.*, 2007, 3, 40

165. A. Ito, M. Shinkai, H. Honda, and T. Kobayashi. *J. Biosci. Bioeng.*, 2005, 100, 1

166. A. H. Lu, E. L. Salabas, and F. Schüth. *Angew. Chem., Int. Ed. Engl.*, 2007, 46, 1222

167. P.-C. Lin, S.-H. Ueng, S.-C. Yu, M.-D. Jan, A. K. Adak, C.-C. Yu, and C.-C. Lin. *Org. Lett.*, 2007, 9, 2131

CHAPTER 2

SYNTHESIS OF NEW SIALOSIDES TRIMERS AS NEW POTENT ANTI-INFULENZA VIRUS THERAPY AGENTS BASED ON THE ALTERMUNE METHOD

ABSTRACT

The term "influenza", usually also called "flu or grippe ", refers to a disease caused by certain strains of the influenza virus, which is isolated as small and spherical particles[1]. Influenza can induce many different illness patterns including mild common cold symptoms, life-threatening pneumonia and secondary bacterial infections. The complications of influenza require different treatment and may need urgent medical attention. However, the current influenza antiviral drugs are not able to inhibit all of influenza viruses, in particular the virus in infected people. Therefore, the development of efficient anti-influenza anti-viral drugs attracts more and more attention from pharmaceutical scientists. We designed the novel anti-influenza reagents based on the Altermune Method, which is stimulating the immune system to attack a disease using a Linker Molecule, which can be recognized by immune system and target the disease sites, and then induce the immune response to disease locations.

2.1 INTRODUCTION

Altermune Method

The Human immune system, which is the integrated body system of organs, tissues, cells, and cell products such as antibodies, works to ward off infection and disease. The immune system comprises two sections: Innate immunity, which consists of hereditary components that provide an immediate "first-line" of defense to continuously ward off pathogens[2]; and Adaptive

(acquired) immunity, which produces antibodies (a type of protein) and T-cells specifically to target particular pathogens and make the body develop a specific immunity to particular pathogens[3]. In vertebrates, the innate and adaptive immune systems interact each other and there is an important reciprocal interplay that operates between these systems. In these animals the cells and molecules of the innate immune system provide immediate protection and then set in motion the activation of the adaptive immune response. The adaptive immune response in turn "revs" up innate immune mechanisms of host defense.

With the further study to the therapy and precaution strategies based on the immune system, scientists presented the Altermune Method to fight infection and disease based on the ability of the body's immune (natural internal defense) system[4].

The Altermune Method is the development of a new chemical method for redirecting our immune system temporarily from one target to another. The method is stimulating the immune system to attack a disease by using a Linker Molecule which can be recognized by immune system and target the disease sites, and then induce the immune response to disease locations (Figure 2.1).
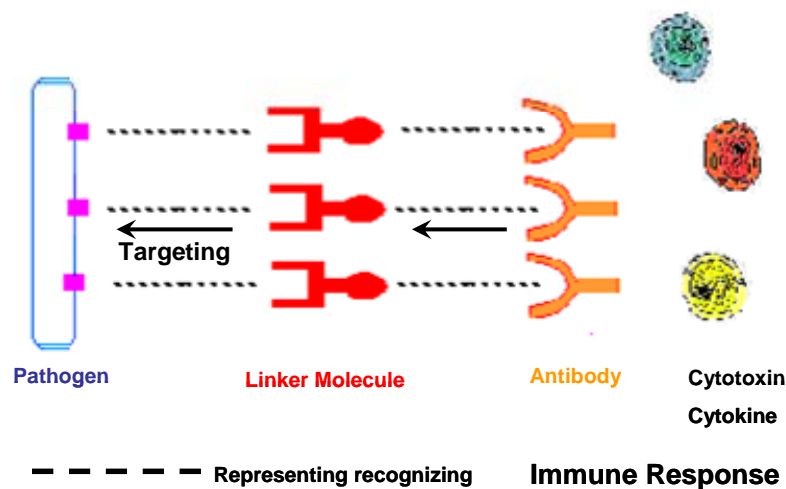
Figure 2.1   Altermune strategy

At this point, the Altermune Method is mostly used for therapy or prevention of cancer and virus infection, in particular in the vaccine research[4]. The main reason is that the cancer cells and the virus-infected cells are similar with human normal cells, which are the obstacles for the researchers to find the proper drug, which do not effect normal cells. So we can use the Linker molecules specifically recognizing cancer cells, virus-infected cells or virus to induce the immune system to attack the cells and pathogens.

In the altermune method, a key part is the Linker Molecule, which must be developed so that it will bind itself tightly to a specific pathogen, to which the immune system is presently naïve. In addition, the Linker Molecule must bind, through immunogenic epitope, to the antibodies or T-cell receptors (TCRs) created by the immune system. Accordingly, the Linker Molecule for the Altermune Method constitutes three parts, a targeting moiety, an immunogenic moiety and a linker linking the two moieties or carrier carrying the two parts. (Figure 2.2) The various targeting moieties are associated with particular diseases, and the immunogenic moiety needs to be recognized by the immune system to cause an immune response.

Linker (carrier)

Targeting moiety: binding to the pathogen

Immunogenic moiety
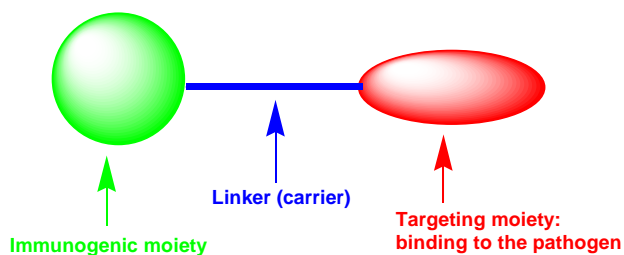
Figure 2.2 Linker molecule

1. Immunogenic moiety-- α-Gal epitope

Carbohydrates play a critical role in cell surface during the proliferation of cancer. The terminal α-Gal residue, particularly in conjunction with other sugar-containing oligosaccharides, plays a dominant role in recognition and antibody response in autoimmune processes[5-7]. Anti-Gal is a natural IgG antibody found to be present in large amounts in human serum and constitutes as

much as 1% of the circulating IgG in humans. Anti-Gal IgG binding with α-Gal could trigger the antibody-dependent cell-mediated cytotoxicity by human blood monocytes and macrophages. In addition, the IgM isotype of anti-Gal is believed to be responsible for the complement activation that leads to complement-mediated lysis of the xenograft cells.[8]

Recent studies have revealed that the natural anti-Gal antibody has distinct specificity to recognize carbohydrate epitopes bearing a Galα1-3Galβ terminus (Figure 2.3). Particularly, the Galαl→3Gal epitope, as a unique glycosidic structure, has been evolutionarily conserved in many mammalian species and found to be present on various normal and malignant tissues. However, the Galαl→3Gal epitope has not been detected in human tissues.[22] Furthermore, most studies show that 80-100% of the natural antibodies in humans utilize a single determinant, Galαl-3Galβ1-4GlcNAc (2). Therefore, Galαl-3Galβ1-4GlcNAc would be made a perfect immunogenic moiety, which can trigger the autommune response and have no risk for unspecific interactions.
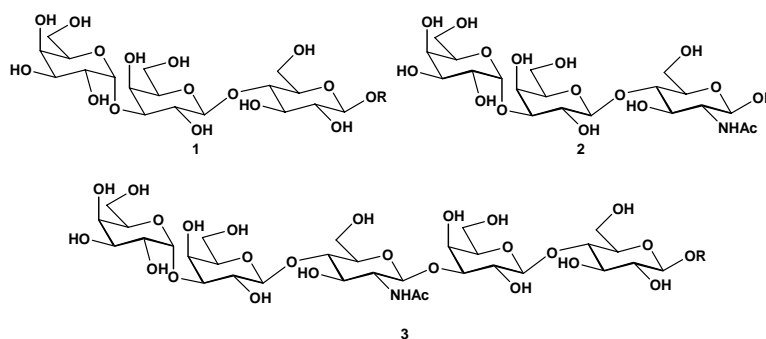
Figure 2.3 Carbohydrate epitopes bearing a Galα1-3Galβ terminus

2. Targeting moiety--Choosing multivalent sialic acid as targeting moiety

The binding of influenza virus particle to the surface receptors of a host cell is mediated by two virus-encoded glycoproteins, hemagglutinin (HA) and neuraminidase (NA). HA, the major surface antigen of the virus, is important for the binding of virions to the receptors of the host

cell and for fusion between the host cell and the virion envelope.[9] NA, which is the minor surface antigen, is a glycosidase that cleaves sialic acid from the terminal position of glycoproteins and it is responsible for releasing virions from the surface of the host cell.[10] Herein, HA plays a key role in initiating viral infection by binding to sialic acid-containing receptors on host cells, and thus, mediating the subsequent viral entry and membrane fusion. In fact, the pocket of sialic acid binding site is the only surface exposed of the HA that has no changes. Residues lining this depression are highly conserved in comparison with the hypervariable antibody binding sites. Based upon this knowledge, it is possible to use a sialic acid (Figure 2.4) that mimics the cell receptor and thus preferentially binds to the virus, and was not influenced by variations of HA.
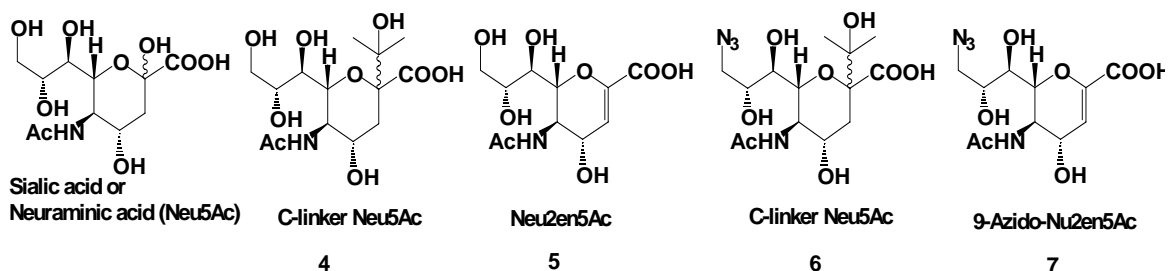
Figure 2.4 Structures of sialic acid derivatives

In addition, the influenza NA removes sialic acid from the HA of progeny virus particles and catalyzes cleavage of the α-glycosidic linkage of Neu5Ac, then facilitating the release of the virus from infected cells. Additionally, NA shares the specificity of the HA to act effectively. George M. et al compared the neuraminidase-resistant HA inhibition between the acrylamide copolymers containing a C-Glycoside and O-glycoside of N-acetylneuraminic acid[11]. The results showed that maximum inhibition capacity of the C- and O-glycosidic polymers is very similar. So in order to reduce the cleavage of Neu5Ac by NA, we chose the C-glycosidic Neu5Ac **4**, which show good affinity to HA[11], as the targeting moiety.

Furthermore, studies of the X-ray crystal structure of influenza HA bound to sialic acid revealed the location of the enzyme active site.[12] On the basis of the X-ray crystallographic structural information for influenza HA, several novel inhibitors were founded[13] including Neu2en5Ac (5-acetamido-2,6-anhydro-3,5-dideoxy-D-*glycero*-D-*galacto*-non-2-enonic acid, 2,3-dehydro-2-deoxy-*N*-acetylneuraminic acid (Figure 2.4), which mimics the sialic acid binding transition-state to HA and therefore demonstrate stronger binding activity to the HA. Thus, we explored the feasibility of using Neu2en5Ac **5** (Figure 2.4) as targeting moiety.

The X-ray crystal structure of sialic acid bound to influenza HA shows that the 9-hydroxy group has weak interactions with the protein.[14] Based on this information, C9 position modified derivatives of Neu2en5Ac were synthesized and showed high affinity for influenza HA, in addition, several had also good antiviral properties.[15] Therefore, we chose the C9 position as a conjugation sites and designed compounds **6** and **7** as targeting moieties.

The fact that individual receptor on virus surface only has weak binding to individual cell surface ligand, has to be considered when designing the targeting part of the Linker Molecule. To this end, multivalent substrates appear to be more attractive since they can offer more strong binding to the respective receptors than their monovalent counterparts. Inspired by this strategy[16] derived from Nature, we designed a triazole-linked multivalent sialic acid (Figure 2.5) to function as the targeting molecule, which can be synthesized via the click reaction, to enhance the binding of virus and Linker Molecule.
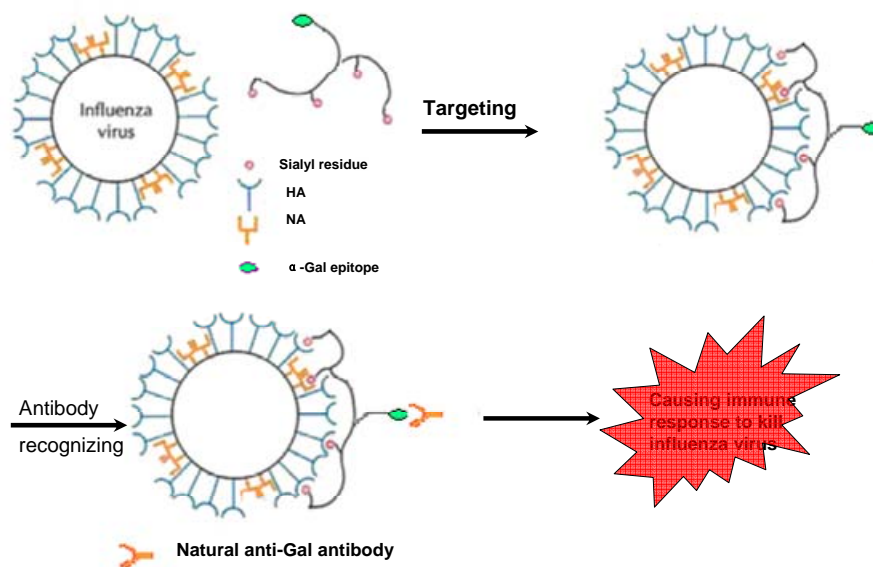
Figure 2.5 Polyvalent targeting strategy

3. The carrier of neuraminic acids and trisaccharides

Polyvalent sialic acid was chosen as the targeting moiety, therefore, the carrier molecules should be able to conjugate several *N*-acetyl neuraminic acid with one trisaccharide. Dendrimers are attractive molecules owing to their multifunctional properties. 3,4,5-Trihydroxybenzoic acid (gallic acid) as trivalent core and tetra-ethylene glycol derivatives with terminal alkynes as hydrophilic spacers were used to scaffold the dendritic backbones (Figure 2.6). The tetra-ethylene glycol was chosen as they are commercially available and can provide sufficient spacing to allow sialic acid moieties to be readily accessible by receptor sites.
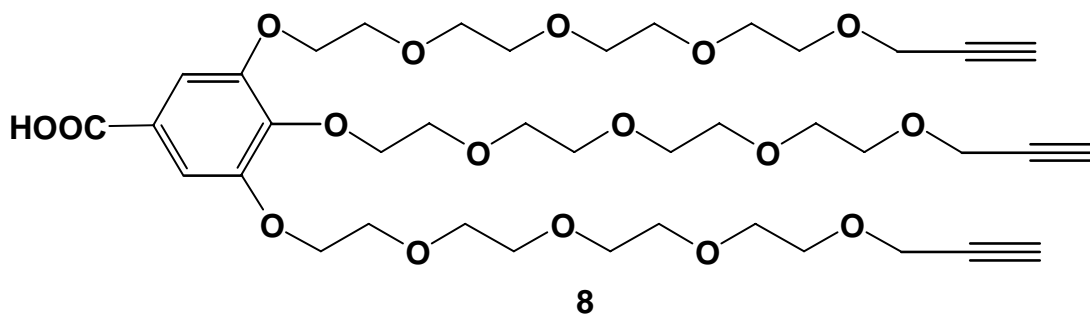
Figure 2.6 Gallic acid carrier molecules

4. The targeting molecule designing

Based on all the information discussed above, we finally designed the target molecules (shown in Figure 2.7). This molecules are constituted with three parts: immunogenic moiety (α-Gal epitope), targeting moiety (multivalent sialic acid), and carrier (gallic acid) carrying the two parts together.
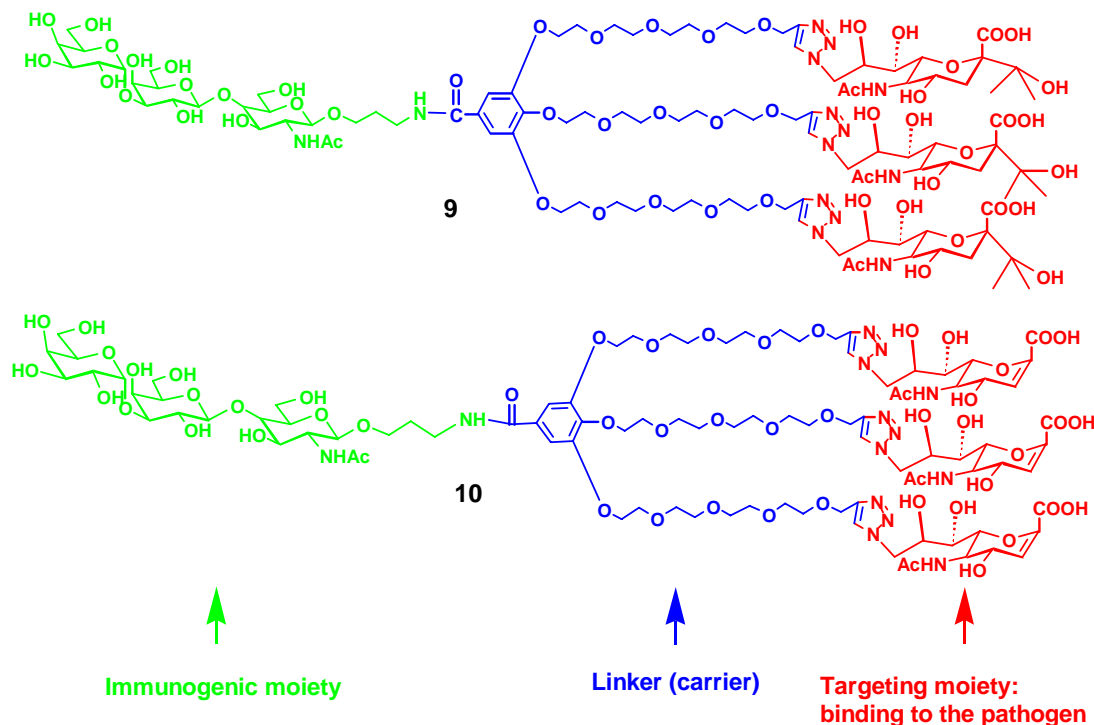
Figure 2.7 targeting molecules

2.2 RESULTS AND DISCUSSION

Retrosynthesis of target molclues

The retrosynthetic analysis of targeting compound **9** and **10** is shown in Scheme 1. Fully protected target compound **11** could be divided into three building blocks: protected trisaccharide **12** with a free amine functional group, bifunctional carrier **8** with free carboxylic acid and terminal alkyne functional moieties, and protected C-glycosidic sialic acid **13** with an azide group at C-9(Scheme 2.1A). The three building blocks have different functional groups,

therefore they can be conjugated together using the click reaction and amide bond formation. Similarly, fully protected target compound **14** can be synthesized from trisaccharide **12**, carrier **8**, and Neu2en5Ac **15** using same strategy as for compound **11**(Scheme 2.1B).
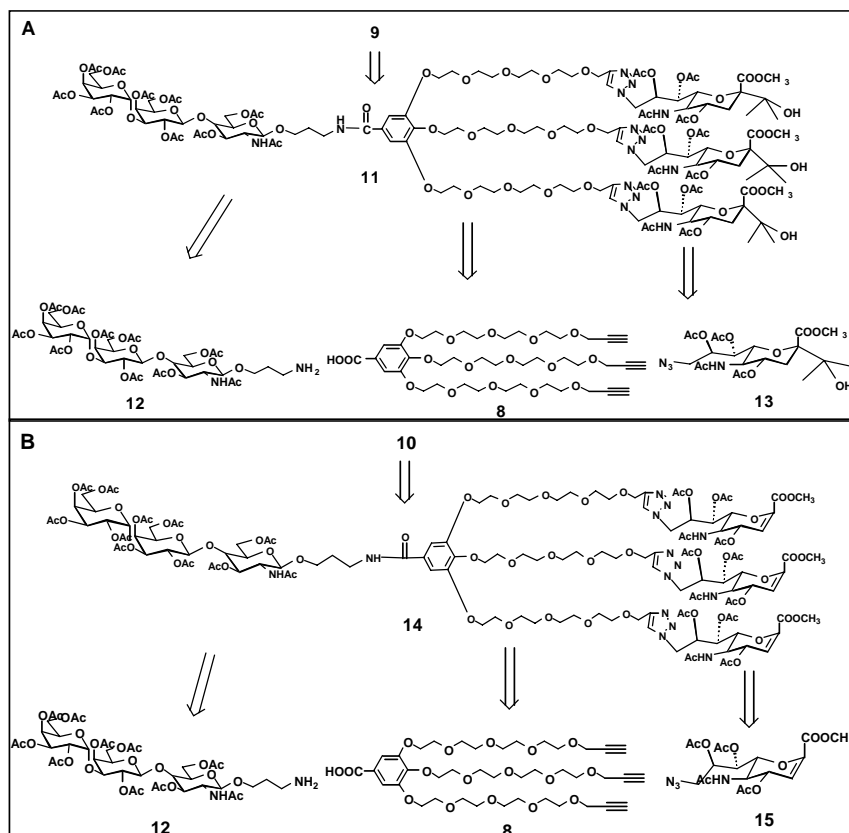
Scheme 2.1 Retrosynthesis of target molclues

Synthesis of the trisaccharide 12

1. Retrosynthetic analysis of the one-pot synthesis of the α-Gal derivative

Construction of the spacer-containing α-Gal epitope trisaccharide **1** was envisaged to proceed by a "one-pot glycosylation" (OPG) strategy, which distinguishes the reactivity difference of a pair of the glycosylation donors or acceptors so as to carry out two glycosylation steps sequentially without purification of the first-step coupling product. Designing building blocks is the key step in our one-pot synthesis. The retrosynthetic analysis of α-Gal epitope **16** is

shown in Scheme 2.2. Fully protected trisaccharide **17** could be divided into three building blocks: a non-reducing end galactosyl donor **18**, a hydroxy bridging galactosyl **19**, and reducing end glucosaminyl block **20**. A decreasing order of reactivity for the three building blocks in each one-pot reaction is essential for execution of the one-pot oligosaccharide synthesis. The non-reducing end unit should have the highest reactivity among the three building blocks, and the reducing end component should have no reactivity due to its *O*-glycoside. The selection of protecting groups was based on the "armed-disarmed effect",[17,18] major stereoelectronic factors causing the reactivity differences. To charge these building blocks with different reactivities, different protecting groups were used according to the reactivity order of thioglycosides based on the method which Wong group developed.[17, 18] Thus, three functional building blocks **18**, **19** and **20** were designed and synthesized by literature procedures[17, 19, 20] for the one-pot glycosylation of the α-Gal epitope. The synthesis of three units was performed as depicted in Scheme 2.3, 2.4 and 2.5.
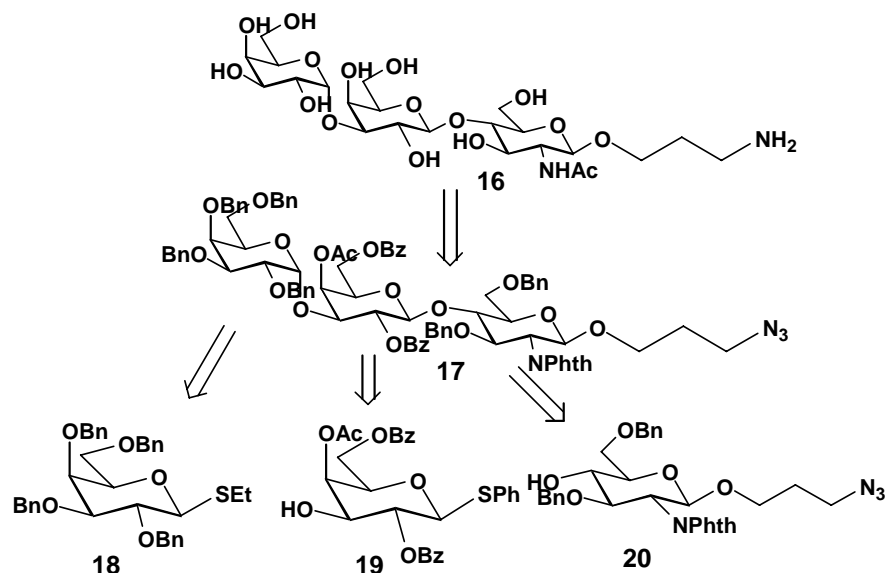
Scheme 2.2 Retrosynthetic analysis of the one-pot synthesis of α-Gal derivative
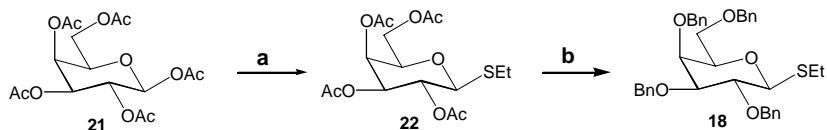
Scheme 2.3 Reagents and conditions. a) EtSH, BF$_3$.Et$_2$O, CH$_2$Cl$_2$; b) i. NaOCH$_3$, CH$_3$OH; ii. NaH, BnBr, DMF.
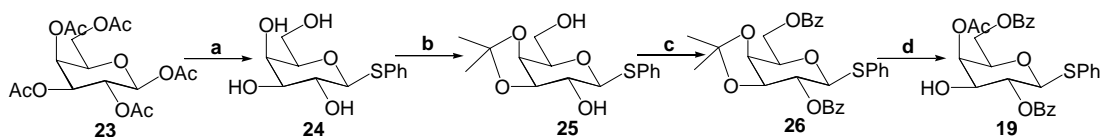
Scheme 2.4 Reagents and conditions. a) NaOCH$_3$, CH$_3$OH; b) 2,2-dimethoxypropane, CSA; c) BzCl, pyr., CH$_2$Cl$_2$; d) i. AcOH/H2O (4:1); ii CH$_3$C(OEt)$_3$, CF$_3$COOH, CHCl$_3$; (iii) MeCN, H$_2$O.
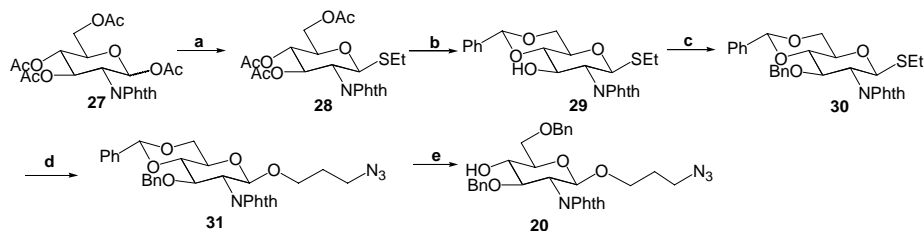
Scheme 2.5 Reagents and conditions. a) NaOH, phthalic anhydride, H$_2$O, overnight, rt, quantitative; b) Ac$_2$O, pyridine, DMAP, overnight, rt, 72%; c) EtSH, CHCl$_3$, BF$_3$·Et$_2$O, 0 °C→rt, reflux 3 h, 70%; d) i. NaOMe, CH$_3$OH, 90%; ii. PhCH(OMe)$_2$, *p*-TsOH, CH$_3$CN, rt, 87%; iii. BnBr, NaH, DMF, 0 °C, 2 h, 74%; e) 3-azidopropanol, NIS, TfOH, CH$_2$Cl$_2$; f) NaBH$_3$CN, HCl–Et$_2$O, MS-3 Å, 0–5 °C, 1 h, 76%.

The one-pot synthesis of fully protected α-Gal epitope and the preparation of its deprotected product 12

With all building blocks in hand, we began to assemble the target oligosaccharides using the OPG strategy. The synthesis of the trisaccharide is depicted in Scheme 2.6. Iodonium di-sym-collidine triflate (IDCT)-mediated chemoselective glycosidation strategy was chosen for the first

glycosylation. The more reactive armed ethyl 2,3,4,6-tetra-*O*-benzyl-β-D-thiogalactoside **18** was first activated by IDCT, which is readily generated by reaction of iodine, silver triflate and collidine, in the presence of disarmed phenyl 4-*O*-acetyl-2,6-di-*O*-benzoyl-β-D-thiogalactoside **19** in a mixture of CH_2Cl_2 at 0 °C and coupled with the less reactive building block **19**. After complete consumption of donor (monitored by TLC), the third building block **20** along with 2 molar equivalent of NIS and TfOH were then added. The resulting trisaccharide **17** was obtained in 37% isolated yield. Complete deprotection of **17** involved three steps: the phthalimido group and benzoylester were converted into NHAc and an *N*-acetyl acetylester, respectively by treatment with $NH_2NH_2 \cdot H_2O$ followed by reacetylation with acetic anhydride in pyridine; the acetyl group was removed by $NaOMe/CH_3OH$; the benzyl, benzylidene and benzyl carbamate protecting groups were removed with Pd–C catalyzed hydrogenolysis to afford trisaccharide **16** (in the form of acetate) in 70% isolated yield. The hydroxyl groups of trisaccharide **16** could then be selectively acetylated with acetyl chloride under acidic conditions directly to afford the final building block **12**.
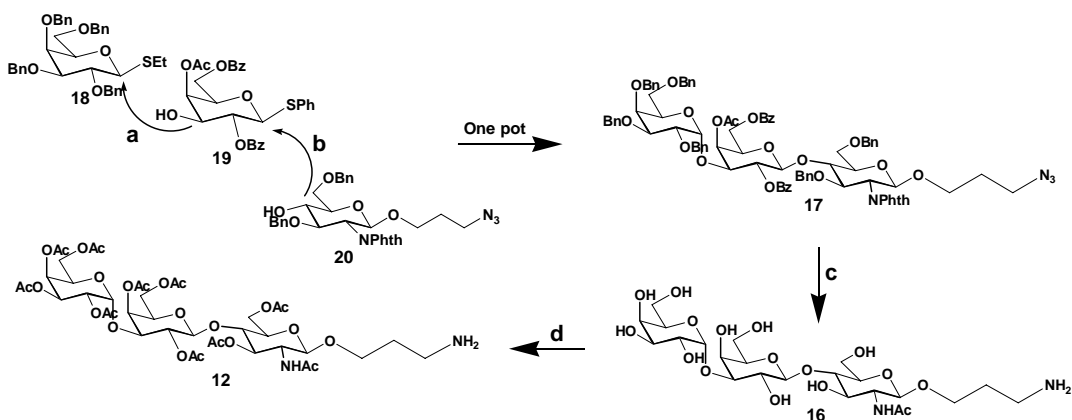
Scheme 2.6 Reagents and conditions. a) IDCT, CH_2Cl_2, 0 °C; b) NIS, TfOH, CH_2Cl_2, 0 °C, 37% ; c) i. NH_2NH_2, nBuOH, reflux; ii. Ac_2O, CH_3OH; iii. $NaOCH_3$, CH_3OH, 94%; iv. H_2, Pd/C, HCl, tBuOH/H_2O 11/4 v/v, quant; d) AcOH, AcCl, rt, 56%.

Synthesis of carrier

Gallic acid based carriers were synthesized using commercially available tetra-ethylene glycol as spacer arms. The bifunctional PEG spacers with an alkyne and tosylate group **36** was synthesized from tetra(ethylene glycol) (**34**, PEG$_4$) as shown in Scheme 2.7. First, PEG$_4$ **34** was converted to *mono*-alkyne-PEG$_4$ **35** by reaction with 1.1 equivalent of propargyl bromide in the presence of sodium hydride. Treatment of **35** with *p*-toluenesulfonyl chloride afforded alkyne-PEG$_4$-tosylate **36** in good yield. Methyl ester of gallic acid **33** were prepared from gallic acid using standard procedure; (Shown in Scheme 7). The white solid ester was then carefully O-alkylated with a slight excess of alkynetosylate spacer **36** using K$_2$CO$_3$ as base (DMF at 80 ℃) to afford the key dendrimer **37** in 77%. The methyl ester was hydrolyzed under basic condition (NaOH, CH$_3$OH) to afford carrier **38** almost quantitatively (Scheme 2.7).
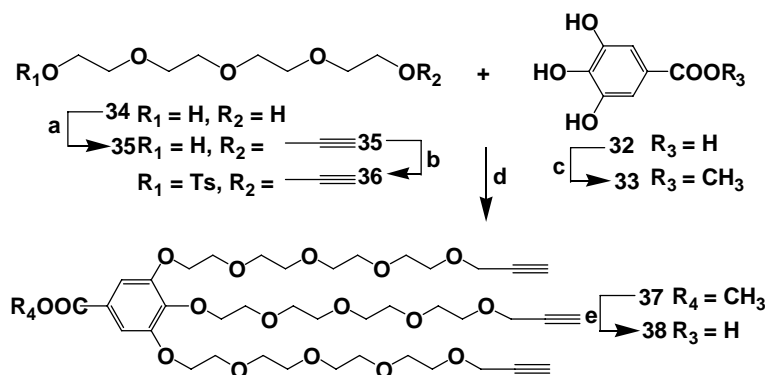
Scheme 2.7 Reagents and conditions: a) Propargyl bromide, NaH, THF, rt, 65%; b) TsCl, DMAP, Py, rt, 61 %; c) CH$_3$I, K$_2$CO$_3$, acetone, reflux, 81%; d) K$_2$CO$_3$, DMF, 80 ℃, 77%; e) NaOH, CH$_3$OH, 99%;

Synthesis of Neu2en5Ac 15

We used N-acetylneuraminic acid hydrochloride as starting material to synthesize the target compound **15** (Scheme 2.8). The synthetic process includes the esterification of **39** with methanol and acidic resins, to give the methyl ester **40**, which is then treated with acetyl chloride

to afford the **41**. The unsaturated derivative **42** was synthesized *via* elimination of HCl from the β-chloride derivative **41** in 62% yield. Compound **42** was treated with NaOMe and then with *p*-toluenesulfonyl chloride to produce tosyl derivative **43** in 69% yield. Compound **43** was converted to azide derivative **44** by treatment with sodium azide, and then acetylated to afford **15**.
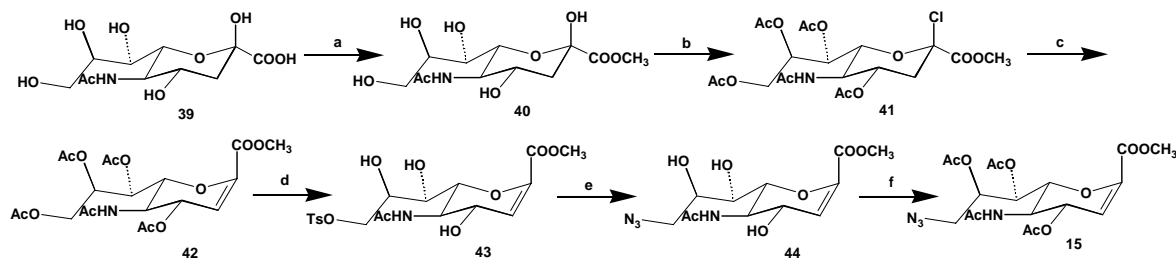
Scheme 2.8 Reagents and conditions: a) CH$_3$OH, ion exchange resin Amberlite® IR 120-H, rt, 84%; b) AcCl, rt, quantitative; c) TEA, CH$_2$Cl$_2$, rt, 62%; d) i. NaOCH$_3$, CH$_3$OH, ii. TsCl, Py, rt, 69%; e) NaN3, DMF, 70 °C, 65%; f) Ac$_2$O,Py, rt, 88%.

Synthesis of C-glycosidic sialic acid 13

The synthesis of C-glycosidic sialic acid **13** is shown Scheme 2.9. Treatment of **41** with thiophenol in dichloromethane in the presence of TEA readily gave **42**, which were converted in excellent yields into the sulfones **43** using ruthenium trichloride hydrate and sodium metaperiodate in the biphasic system carbon tctrachloride-acetonitrile-water. C-glycoside **47** was synthesized by using samarium iodide under Barbier conditions,[23] which has been previously used to prepare C-glycosides of hexoses. Through a simple, high-yielding reaction, this same chemistry could be used to couple different ketones or aldehydes with peracetylated sialic acid sulfone and form α-C-glycosides of Neu5Ac. Compound **47** was treated with NaOMe to give compound **48**, which reacted with *p*-toluenesulfonyl chloride and then was treated with sodium azide at 70 °C, the crude product can be acetylated to afford the compound **13** (41% in 3 steps).
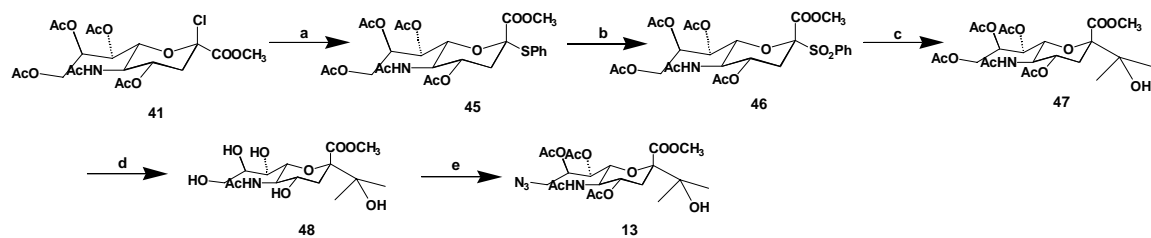
Scheme 2.9 Reagents and conditions: a) PhSH, TEA, CH_2Cl_2, rt, 78%; b) $RuCl_3$, $NaIO_4$, CCl_4, H_2O, rt, 91%; c) acetone, SmI_2, THF, rt, 62%; d) i. $NaOCH_3$, CH_3OH, rt, 88%; e) i. TsCl, Py, rt, 69%, ii. NaN3, DMF, 70 °C, iii. Ac_2O,Py, rt, 41% in 3 steps.

Synthesis of final compound 9 and 10

With all building blocks **8**, **12**, **13** and **15** in hand, we began to assemble the final compounds. Synthesis of compound **9** and **10** are depicted in Scheme 2.10 and 2.11 respectively. Due to its high reliability and mild reaction condition, click reaction was utilized to form sialic dentrimer **51**, trisaccharide **12** was conjugated with compound **51** to afford compound **11** by using standard amide bond forming conditions (DCC, DMAP, DIPEA) in good yields. Final compound **9** was reached by treatment of **11** with LiOH in H_2O and methanol. By using same strategy, final compound **10** was formed in good yield.
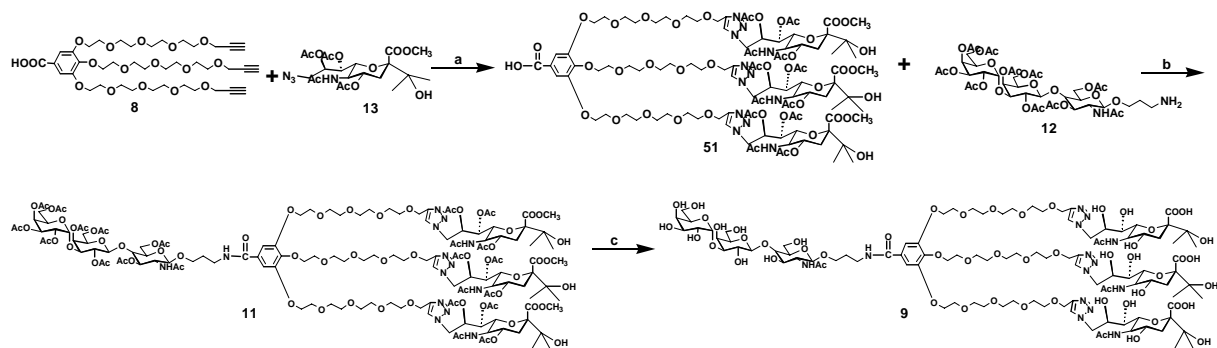
Scheme 2.10 Reagents and conditions: a) CuI, DIPEA, DMF, rt, 68%; b) DCC, DMAP, DIPEA, CH_2Cl_2, rt, 61%; c) LiOH, CH_3OH, H_2O, rt, 61%.
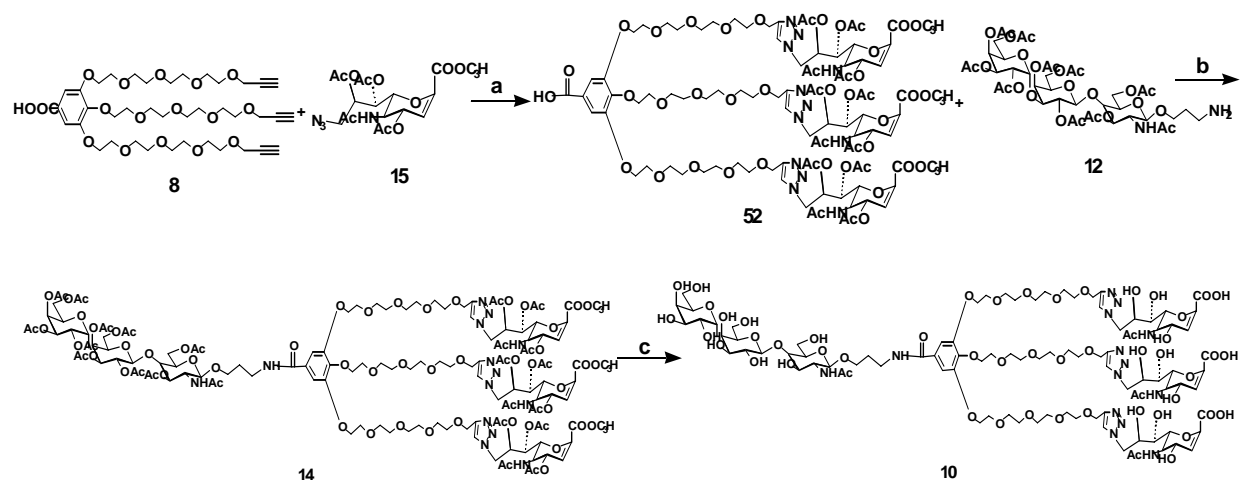
Scheme 2.11 Reagents and conditions: a) CuI, DIPEA, DMF, rt, 65%; b) DCC, DMAP, DIPEA, CH₂Cl₂, rt, 55%; c) LiOH, CH₃OH, H₂O, rt, 60%.

CONCLUSIONS

There is a clear need for more rapid, specific and efficient anti-influenza antiviral drugs for influenza. In our studies we synthesized the anti-influenza antiviral drugs basing on the altermune method by using click reaction. We believe this to be the first synthesis of the anti-influenza agents based on the altermune method, which is a new chemical method for redirecting our immune system temporarily from anti-Gal to influenza virus. Furthermore, the Altermune Method showed a lot of advantages comparing common anti-influenza approaches: 1. we chose the conversed sites of HA as target for the linker molecule. In this way the antigenic mutation of HA on influenza virus does not affect the binding between Linker Molecules and HA, and then influence the effectiveness of drugs, whereas the resistant of influenza virus to vaccine or other drugs are limited in the prevention and treatment of influenza. 2. The strategy of the Altermune Method does not block the HA or NA, but induce the immune response to viruses. As long as there is some binding of the molecule and HA, the trisaccharide moiety of the molecule can stimulate the immune system to kill the viruses.

2.3 EXPERIMENTAL PROCEDURES

General procedures

^{1}H NMR spectra were recorded in CDCl$_3$ or D$_2$O on Varian Merc-300 or Varian Inova-500 spectrometers equipped with Sun workstations at 300 K. TMS (δ_H 0.00) or D$_2$O (δ_H 4.67) was used as the internal reference. ^{13}C NMR spectra were recorded in CDCl$_3$ or D$_2$O at 75 MHz on a Varian Merc-300 spectrometer, respectively, using the central resonance of CDCl$_3$ (δ_C 77.0) as the internal reference. COSY, HSQC, HMBC and TOCSY experiments were used to assist signal assignment of the spectra. The different monosaccharide units are referred to as a, b, c, and d, respectively, with a denoting the reducing end monosaccharide. Mass spectra were obtained on Applied Biosystems Voyager DE-Pro MALDI-TOF (no calibration) and Bruker Daltonics 9.4T (FTICR, external calibration with BSA). Optical rotatory power was obtained on Jasco P-1020 polarimeter at 300 K. Chemicals were purchased from Aldrich or Fluka and used without further purification. CH$_2$Cl$_2$, acetonitrile and toluene were distilled from calcium hydride; THF from sodium; and CH$_3$OH from magnesium and iodine. Mariculture keyhole limpet hemocyanin (mcKLH), maleimide activated bovine serum albumin (BSA-MI), and succinimidyl 3-(bromoacetamido)propionate (SBAP) were purchased from Pierce Endogen, Rockford, IL. Aqueous solutions are saturated unless otherwise specified. Molecular sieves were activated at 350 ℃ for 3 h in vacuo. All reactions were performed under anhydrous conditions under argon and monitored by TLC on Kieselgel 60 F254 (Merck). Detection was by examination under UV light (254 nm) and by charring with 10 % sulfuric acid in methanol. Silica gel (Merck, 70-230 mesh) was used for chromatographies. Iatrobeads 6RS-8060 was purchased from Bioscan.

Preparation of IDCT Silver triflate (560 mg, 2.2 mmol), 2,6-di-*tert*-butyl-4-methylpyridine (1.16 g, 5.7 mmol) and 4 Å molecular sieves were added to freshly distilled CH$_2$Cl$_2$ (1 mL) and

cooled to −78 °C under Ar. The Iodine (550 mg, 2.2 mmol) in freshly distilled CH_2Cl_2 (2 mL) was added to the mixture under Ar. The reaction was allowed to warm to the room temperature, and the reaction mixture was filtered through celite and crystallization was induced by the addition ether. The resulting solid was filtered and dried in vacuo.

Ethyl 2,3,4,6-tetra-*O*-acetyl-1-thio-β-D-galactopyranoside (22) [23] A suspension of D-galactose (1.8 g, 10.0 mmol) in Ac_2O (4.82 mL, 51.0 mmol) was placed in an ice bath with continuous stirring. To this cold suspension was added $BF_3 \cdot OEt_2$ (1.9 mL, 15.0 mmol) in one portion. An exothermic reaction started immediately and the mixture was allowed to stir for 30 min. After completion of the reaction (as indicated by TLC, hexane-EtOAc 1:1), ethanethiol (1.6 mL, 15.6 mmol) was added and the reaction mixture was allowed to stir for another 5 h. The reaction was quenched by addition of 100 mL aq $NaHCO_3$ and the mixture was extracted with 200 mL CH_2Cl_2. The organic layer was washed with 50 mL water, dried ($MgSO_4$), and concentrated under reduced pressure. Purification of the crude reaction product by column chromatography on silica gel using hexane-EtOAc (3:1) as the eluant furnished pure ethyl 2,3,4,6-tetra-*O*-acetyl-1-thio-β-D-galactopyranoside **22**, which could be crystallized from Et_2O–hexane (3.9 g, 90%). ^{1}H NMR (300 MHz, $CDCl_3$): δ 5.43 (1H, dd, J = 1.1, 3.3 Hz, *H*-4), 5.24 (lH, t, *H*-2), 5.05 (lH, dd, J = 10.0 Hz, *H*-6a), 4.50 (lH, d, J = 9.8 Hz, *H*-1), 4.14 (2H, m, *H*-6b,*H*-3), 3.93 (lH, m, *H*-5), 2.73 (2H, m, SC*H*₂), 2.16, 2.07, 2.05, 1.99 (12H, 4s, 4 X COC*H*₃), 1.29 (3H, t, J = 7.5 Hz, CH_2C*H*₃).

Ethyl 2,3,4,6-Tetra-O-benzyl-1-thio-β-D-galactopyranoside (18) [24] A solution of **22** (580 mg, 1.48 mmol) in CH_2Cl_2-methanolic 10 mM sodium methoxide (l: l, 15 mL) was stirred for 12 h at room temperature, neutralized with acetic acid (1 mL), and concentrated. Sodium hydride dispersion (570 mg, 12 mmol) was slowly added to a solution of the residue and benzyl bromide

(1.06 mL, 8.9 mmol) in dry DMF (10 mL) at 0 °C. The mixture was allowed to warm to room temperature, and after 12 h methanol (5 mL) was added to destroy excess benzyl bromide. After 45 min the solution was neutralized with acetic acid, diluted with CH_2Cl_2 (50 mL), washed with water (2 X 50 mL), dried, and concentrated. Column chromatography (hexane-EtOAc, 10: l) of the residue gave 18 as a syrup (780 mg, 90%). ^{1}H NMR (300 MHz, CDCl$_3$): δ 7.40–7.18 (20H, m), 4.89 (1H, d, J = 10.8 Hz, C*H*HPh), 4.73 (1H, d, J = 12.4 Hz, C*H*HPh), 4.68 (1H, d, J = 12.4 Hz, C*H*HPh), 4.67 (1H, d, J = 12.1 Hz, C*H*HPh), 4.60–4.56 (2H, m, C*H*$_2$Ph), 4.53–4.51 (3H, m, C*H*$_2$Ph, *H*-1), 4.13 (1H, dd, J = 9.7, 4.7 Hz, *H*-3), 4.03 (1H, t, J = 9.9 Hz, *H*-2), 3.85 (2H, m, *H*-5, *H*-4), 3.82 (1H, dd, J = 11.0, 4.9 Hz, H-6b), 3.72 (1H, dd, J = 10.8, 1.4 Hz, *H*-6a), 2.67–2.53 (2H, m, SC*H*$_2$), 1.25 (3H, t, J = 7.4 Hz, CH$_2$C*H*$_3$).

Phenyl 1-Thio-β-D-galactopyranoside (24) [25] Pentaacetate Galactopyranose **21** (10.0 g, 25.7 mmol) was dissolved in anhydrous CH_2Cl_2 (150 mL) and cooled to 0 °C. Thiophenol (3.43 mL, 33.4 mmol) was added to the mixture with stirring for 30 min. Then BF$_3$·Et$_2$O (9.77 mL, 77.0 mmol) was slowly injected into the mixture. The reaction mixture was stirred for 4 h, and then diluted and washed with aq NaHCO$_3$ and brine. After drying over MgSO$_4$, the solvents were removed in vacuo, and the crude product was purified by sicica gel column chromatography (1:5 EtOAc–hexanes) to afford phenyl 2,3,4,6-Tetra-*O*-acetyl-1-thio-β-Dgalactopyranoside (9.7 g, 86%). The product (9.7 g, 22.0 mmol) was dissolved in anhyd CH$_3$OH (100 mL), and NaOMe powder was added in small portions to pH 9. The mixture was stirred for 2 h and the solution was neutralized using acetic acid. The solvent was removed in vacuo to afford **24** as a amorphous solid (5.0 g, 88%). ^{1}H NMR (300 MHz, D$_2$O): δ 7.58–7.55 (2 H, m, aromatics), 7.42–7.35 (3 H, m, aromatics), 4.76 (1 H, d, J = 9.6 Hz, H-1), 3.97 (1 H, d, J = 3.2 Hz), 3.76–3.59 (5 H, m); ^{13}C NMR (75 MHz, D$_2$O): δ 133.0, 131.4, 129.6, 88.3, 79.3, 74.3, 69.5, 68.9, 61.2.

Phenyl 3,4-*O-iso*propylidene-1-thio-β-D-galactopyranoside (25) [26] Compound **24** (5.99 g, 22.0 mmol) was dissolved in a 1:1 mixture of dry CH_2Cl_2 and dimethoxypropane (30 mL). TsOH·H_2O (250 mg) was then added to the solution. The reaction mixture was stirred for 3 h and then concentrated in vacuo and diluted with CH_2Cl_2. The solution was washed with aq $NaHCO_3$ and brine, dried over $MgSO_4$. The solvent was removed in vacuo. Purification by column chromatography (2:1 EtOAc-hexanes) afforded compound **25** (3.43 g, 50.0%). ^{1}H NMR (300 MHz, $CDCl_3$): δ 7.53–7.50 (2 H, m), 7.33–7.26 (3 H, m), 4.46 (1 H, d, J = 10.4 Hz, H-1), 4.17 (1 H, dd, J = 5.6, 2.0 Hz), 4.13-4.08 (1 H, m), 3.99–3.94 (1 H, dd, J = 11.2, 7.2 Hz), 3.88–3.85 (1 H, m), 3.79 (1 H, dd, J = 11.2, 3.6), 3.56 (1 H, dd, J = 10.4, 7.2 Hz), 1.41 (3 H, s), 1.32 (3 H, s); ^{13}C NMR (75 MHz, $CDCl_3$): δ 132.6, 132.2, 129.3, 128.3, 110.7, 87.9 (C-1), 79.5, 74.1, 71.7, 62.8, 28.6, 26.6.

Phenyl 2,6-di-*O*-benzoyl-3,4-*O*-isopropylidene-1-thio-β-D-galactopyranoside (26) [27] Benzoyl chloride (0.9 mL, 7.8 mmol) was added to a solution of **25** (800 mg, 2.6 mmol) in anhydrous pyridine (4.8 mL) with stirring and cooling in ice-water. The mixture was stirred for 30 min at rt, when TLC (1: 1 hexane-EtOAc) showed the reaction to be complete. After the addition of methanol (1 mL), the solution was concentrated, and the residue was crystallized from ethanol to give **26** (1.15 g, 86%). ^{1}H NMR (300 MHz, $CDCl_3$): δ 8.15 and 7.73-7.10 (15 H, 2 m, aromatics), 5.41 (1 H, dd, J = 10.0, 6.8 Hz, *H*-2), 4.85 (1 H, d, *H*-l), 4.80 (1 H, dd, J = 4.0, 12.0 Hz, *H*-6a), 4.67 (1 H, dd, J = 8.0 Hz, *H*-6b), 4.45 (1 H, dd, J = 6.0 Hz, *H*-3), 4.39 (1 H, dd, J = 2.5 Hz, *H*-4), 4.29 (1 H, m, *H*-5), 1.63 and 3.38 (6 H, 2 s, C*H*$_3$,).

Phenyl 4-*O*-acetyl-2,6-di-*O*-benzoyl-1-thio-β-D-galactoside (19) [28] Compound **26** (520 mg, 1.0 mmol) was dissolved in 5mL 50% TFA in H_2O and kept rt for 2 h. Then the solution was concentrated in vacuo to give a white solid which was used in the next step without further

purification. To the solution of the residue in CHCl$_2$ (5 mL) was added CH$_3$C(OEt)$_3$ (510 mg, 3.1 mmol) and TFA (one drop). The mixture was stirred for 20 min at rt. Acetonitrile (5 mL) and H$_2$O (1 mL) were added and the mixture stirred for 30 min. Concentration of the mixture in vacuo, followed by silica gel flash chromatography (EtOAc/petrol 3:7), gave **19** as needles (510 mg, 95%). ^{1}H NMR (300 MHz, CDCl$_3$): δ 7.12–7.21, 7.45–7.60, 8.05–8.08 (15H, 3 × m, aromatics), 5.52 (1H, d, J = 3.5 Hz, *H*-4), 5.30 (1H, dd, J = 10.0, 9.8Hz, *H*-2), 4.90 (1H, d, J = 10.0 Hz, *H*-1), 4.50 (1H, dd, J = 11.5, 7.6 Hz, *H*-6a), 4.44 (1H, dd, J = 11.5, 5.2 Hz, *H*-6b), 4.11 (1H, dd, J = 9.8, 3.5 Hz, *H*-3), 4.06 (1H, dd, J = 5.2, 7.6 Hz, *H*5), 2.71 (1H, s, O*H*), 2.21 (3H, s, C*H*$_3$). ^{13}C NMR (75 MHz, CDCl$_3$): δ 20.73, 62.69, 69.99, 71.59, 72.62, 74.95, 86.43, 127.96–133.54, 166.03, 166.70, 170.82.

Ethyl 3,4,6-Tri-*O*-Acetyl-2-deoxy-2-phthalimido-1-thio-β-D-glucopyranoside (28) [29]

BF$_3$·OEt$_2$ (3.8 mL, 29.1 mmol) was added dropwise to a solution of **27** (10.0 g, 20.9 mmol) in EtSH (2.2 mL, 29.1 mmol) and anhydrous CH$_2$Cl$_2$ (100 mL) at 0 °C. The reaction was stirred for 1 h at 0 °C and then at room temperature for 4 h. Et$_3$N (5 mL) was added to quench the reaction. The solution was evaporated in vacuo and the residue purified by silica gel chromatography (1:1 EtOAc–hexanes) to give **28** (7.4 g, 74 %). ^{1}H NMR (300 MHz, CDCl$_3$): δ 7.70-7.90 (4 H, m, aromatics), 5.84 (1 H, t, J = 10.2 Hz, *H*-4), 5.49 (1 H, d, J = 10.6 Hz, *H*-1), 5.18 (1 H, t, J = 9.8 Hz, *H*-3), 4.40 (1 H, t, J = 10.2 Hz, *H*-5), 4.14-4.36 (2 H, m, *H*-6a), 3.87-3.91 (1 H, m, *H*-2), 2.62-2.73 (2 H, m, SC*H*$_2$), 2.11 (s, 3 H, CH$_3$), 2.04 (3 H, s, C*H*$_3$), 1.87 (3 H, s, C*H*$_3$), 1.22 (3 H, t, J = 7.4 Hz, C*H*$_3$).

Ethyl 4,6-*O*-Benzylidene-2-deoxy-2-phthalimido-1-thio- β -D-glucopyranoside (29) [30] A solution of **28** (4.8 g, 10.0 mmol) in CH$_3$OH (100 mL) was treated with NaOMe (200 μL) at room temperature. After being stirred for 2 h, dry ice was added to quench the reaction. The

solution was concentrated in vacuo to give a white solid which was used in the next step without further purification. The residue was dissolved in DMF (50 mL), then treated with TsOH·H$_2$O (0.46 g, 2.4 mmol) and dimethoxytoluene (4.7 mL, 30.0 mmol). The reaction mixture was stirred overnight at 70 °C. The solvent was evaporated in vacuo and the residue was dissolved in EtOAc (100 mL) and washed with saturated NaHCO$_3$ and brine. The organic layer was dried with anhydrous MgSO$_4$, concentrated in vacuo and the residue purified by silica gel chromatography (1:2 EtOAc-hexanes) to afford **29** (3.71 g, 84 %) as white foam. ^{1}H NMR (300 MHz, CDCl$_3$): δ 7.68-7.85 (4H, m, aromatics), 7.35-7.53 (5H, m, aromatics), 5.59 (1H, s, PhC*H*), 5.39 (1H, d, *J* = 10.6 Hz, *H*-1), 4.62 (1H, m, *H*-5), 4.25-4.45 (2 H, m, *H*-3, *H*-4), 3,798 (1 H, t, *J* = 9.4 Hz, *H*-2), 3.53-3.70 (2 H, m, *H*$_2$-6), 2,782 (1 H, d, *J* = 3.2 Hz, O*H*), 2.67-2.73 (2 H, m, SC*H*$_2$), 1.21 (3 H, t, *J* = 7.4 Hz, C*H*$_3$). ^{13}C NMR (75 MHz, CDCl$_3$): δ 14.7, 24.0, 55.3, 68.6, 69.5, 70.3, 81.8, 82.1, 101.8, 123.3, 123.8, 126.3, 128.3, 129.3, 131.6, 134.2, 136.9, 168.2.

Ethyl 3-*O*-benzyl-4,6-*O*-benzylidene-2-deoxy-2-phthalimido-l-thio-β-D-glucopyranoside (30) [31] A mixture of compound **29** (1.31 g, 2.97 mmol) and 60% NaH in oil (300 mg, 7.48 mmol) in dry THF (30 mL) was stirred at 60°C for 1 h. Benzyl bromide (798 mL, 6.68 mmol) was added, and stirring was continued at 60°C overnight. Small pieces of ice were then added for quenching, and the solution was evaporated in vacuo, extracted with 1:1 ether-EtOAc, washed with water and brine, dried (MgSO$_4$), and concentrated in vacuo. Silica gel flash chromatography (1:2 EtOAc-hexanes) of the residue on silica gel afforded **30** (1.30 g, 82.5%). ^{1}H NMR (300 MHz, CDCl$_3$): δ 7.85-6.87 (14 H, m, arometics), 5.63 (1 H, s, PhC*H*), 5.34 (1 H, d, *J* = 10.5 Hz, *H*-1), 4.758 and 4.548 (2 H, 2d, *J* = 12.2 Hz, C*H*$_2$Ph), 4.44 (1 H, d, *J* = 8.5 Hz, *H*-4), 4.426 (1 H, m, *H*-2), 4.297 (1 H, t, *J* = 10.2 Hz, *H*-5), 3.87-3.66 (3 H, m, *H*-6a, *H*-6b and *H*-3), 2.652 (2 H, m, SC*H*$_2$CH$_3$), 1.165 (3 H, t, *J* = 7.2 Hz, SCH$_2$C*H*$_3$).

3-Azidopropyl 3-*O*-benzyl-4,6-*O*-benzylidene-2-deoxy-2-phthalimido-β-D-glucopyrano

-side (31) [32] A solution of **30** (3.7 g, 7 mmol) and 3-azidopropan-1-ol (2.12 g, 21 mmol)

containing 4 Å MS in CH_2Cl_2 (50 mL) at 0 °C was treated with NIS (2.2 g, 10 mmol) and TfOH

(100 μL, 0.3 mmol). The mixture was kept at 0 °C for 15 min, and Et_3N (2 mL) was added. The

reaction mixture was filtered and washed with aq. $NaHCO_3$. The organic layer was dried with

$MgSO_4$, filtered, and concentrated in vacuo. Silica gel column chromatography of the residue

(1:5 EtOAc-hexanes) afforded **31** (3.35 g, 5.9 mmol, 84%) as a white foam. ^{1}H NMR (300 MHz,

$CDCl_3$): δ 7.74–6.89 (14H, m, aromatics), 5.62 (1H, s, C*H*Ph), 5.20 (1H, d, $J = 8.8$ Hz, *H*-1),

4.80 (1H, d, $J = 12.4$ Hz, C*H*Ph), 4.50 (1H, d, $J = 12.4$ Hz, C*H*Ph), 4.43 (2H, m, *H*-2, *H*-3), 4.20

(1H, dd, $J = 11.0, 8.8$ Hz, *H*-2), 3.82 (3H, m, *H*-4, H_2-6), 3.72 (1H, m, *H*-5), 3.41 (2H, m, O–

C*H*$_2$–CH$_2$), 3.12 (2H, m, C*H*$_2$N$_3$), 1.71 (2H, m, CH$_2$–C*H*$_2$–CH$_2$). ^{13}C NMR (75 MHz, $CDCl_3$): δ

167.1, 137.4, 136.9, 133.4, 131.6, 130.8, 128.5, 128.3, 127.6, 127.4, 126.8, 125.5, 124.5, 122.7,

100.5, 98.3, 82.3, 74.0, 73.3, 68.0, 65.7, 65.5, 60.5, 58.5, 55.2, 47.2, 28.1.

3-Azidopropyl 3,6-Di-*O*-benzyl-2-deoxy-2-phthalimido-β-D-glucopyranoside (20) [33]

Compound **31** (2.85 g, 5 mmol) was treated with TfOH (1.27 mL, 15.0 mmol) in the presence of

triethylsilane (2.6 mL, 16.6 mmol) in CH_2Cl_2 (50 mL) at - 78 °C. After 20 min the reaction was

quenched by the subsequent addition of CH_3OH and triethylamine. After the reaction mixture

was washed with aq $NaHCO_3$, dried, and concentrated, the residue was purified by column

chromatography (1:2 EtOAc-hexanes) to provide compound **20** (2.0 g, 3.55 mmol, 71%) as a

slightly yellow oil. ^{1}H NMR (300 MHz, $CDCl_3$): δ 7.79–6.92 (14 H, m, aromatics), 5.14 (1H, d, J

$= 8.3$ Hz, *H*-1), 4.75 (1H, d, $J = 12.2$ Hz, –C*H*Ph), 4.64 (1H, d, $J = 12.0$ Hz, –C*H*Ph), 4.58 (1H, d,

$J = 12.0$ Hz, –C*H*Ph), 4.53 (1H, d, $J = 12.2$ Hz, –C*H*Ph), 4.24 (1H, dd, $J = 8.4, 10.8$ Hz, *H*-3),

4.15 (1H, dd, $J = 8.4, 10.8$ Hz, *H*-2), 3.81 (4H, m, *H*-4, *H*-6a, O–CH$_2$–CH$_2$), 3.66 (1H, m, *H*-5),

3.45 (1H, m, *H*-6), 3.11 (2H, m, C*H*₂N₃), 1.66 (2H, m, CH₂–C*H*₂–CH₂). ¹³C NMR(75 MHz, CDCl₃): δ 138.0, 137.6, 133.8, 128.4, 128.0, 127.7, 127.6, 127.3, 123.2, 131.4, 98.2, 78.6, 74.2, 74.2, 74.0, 73.6, 70.3, 68.1, 55.2, 47.8, 28.7 .

3-Azidopropyl (2,3,4,6-Tetra-*O*-benzyl-α-D-galactopyranosyl)-(1→3)- (4-*O*-acetyl-2,6-di-*O*-benzoyl-β-D-galactopyranosyl)-(1→4)-3,6-di-*O*-benzyl-2-deoxy-2-phtalimido-β-D-glucopyranoside (17) [33] One-pot procedure: Compound **18** (0.58 g, 1.0 mmol) and **19** (0.50 g, 1.0 mmol) were dissolved in CH₂Cl₂ (50 mL), powdered 4Å MS (500 mg) was added, and the reaction mixture was cooled to -40°C. IDCT (500 mg, 1.1 mmol) was added, and the reaction mixture was brought to 0°C. The reaction mixture was kept at 0°C for 1 h. The reaction mixture was cooled to -60°C, then NIS (450 mg, 2.0 mmol in 5 ml CH₂Cl₂) and TfOH (200 μL, 2.0 mmol) was added. After the reaction was kept at -60°C for 10 min, **20** (0.55 g, 1 mmol in 5 mL CH₂Cl₂) was added. The mixture was slowly warmed to 0°C, after which Et₃N (2 mL) was added. Standard workup and purification gave compound **17** (0.59 g, 37%) as a colorless oil. *R*f 0.60 (Hexane/EtOAc, 2:1 v/v). ¹H NMR (300 MHz, CDCl₃): δ 8.10-6.83 (44H, m, aromatics), 5.54 (2H, m, *H*-2', *H*-4'), 5.14 (1H, d, *J* = 3.3 Hz, *H*-1"), 5.00 (1H, d, *J* = 8.5 Hz, *H*-1), 4.91 (1H, d, *J* = 12.4 Hz, -C*H*Ph), 4.78 (1H, d, *J* = 8.1 Hz, *H*-1'), 4.74 (1H, d, *J* = 11.4 Hz, -C*H*Ph), 4.63 (2H, s, -C*H*Ph), 4.62 (1H, d, *J* = 11.8 Hz, -C*H*Ph), 4.55 (1H, d, *J* = 12.0 Hz, -C*H*Ph), 4.51 (1H, d, *J* = 12.4 Hz, -C*H*Ph), 4.44 (1H, d, *J* = 11.8 Hz, -C*H*Ph), 4.42 (1H, d, *J* = 11.8 Hz, -C*H*Ph), 4.35 (1H, d, *J* = 12.0 Hz, -C*H*Ph), 4.29 (3H, m, 2x-C*H*Ph, *H*-3), 4.22 (1H, dd, *J* = 6.5, 11.3 Hz, *H*-6'a), 4.13 (2H, m, H-6'b, *H*-2), 4.05 (1H, dd, *J* = 8.5, 9.9 Hz, *H*-4), 3.99 (1H, dd, *J* = 3.4, 10.2 Hz, *H*-3'), 3.91 (1H, dd, *J* = 3.3, 10.2 Hz, *H*-2"), 3.85 (1H, bt, *J* = 6.9 Hz, *H*-5"), 3.75 (1H, m, O-C*H*H-CH₂), 3.67 (2H, m, *H*-5', *H*-6a), 3.58 (2H, m, *H*-6b, *H*-3"), 3.41 (1H, m, *H*-5), 3.38 (2H, m, *H*-6"a, O-CH*H*-CH₂), 3.25 (1H, dd, *J* = 1.2, 2.6 Hz, *H*-4"), 3.21 (1H, dd, *J*=5.9, 9.4 Hz, *H*-6"b),

3.08 (2H, m, CH$_2$-C*H$_2$*-N$_3$), 1.81 (3H, s, COC*H$_3$*), 1.64 (2H, m, CH$_2$-C*H$_2$*-CH$_2$). ^{13}C NMR (75 MHz, CDCl$_3$): δ 170.2, 166.0, 164.6, 138.7, 138.4, 138.1, 138.0, 131.5, 129.3, 129.7, 133.7-123.2, 100.8, 98.3, 94.1, 78.8, 78.3, 76.9, 75.5, 74.8, 74.7, 74.5, 73.5, 73.3, 73.2, 73.1, 72.3, 71.4, 71.0, 69.8, 69.2, 67.8, 65.9, 65.0, 61.7, 55.7, 48.0, 28.8, 20.4.

3-Azidopropyl (2,3,4,6-Tetra-*O*-benzyl-α-D-galactopyranosyl)-(1→3)- (2-*O*-acetyl-β-D-galactopyranosyl)-(1→4)-2-acetamido-3,6-di-*O*-benzyl-2-deoxy-β-D-glucopyranoside (49) [33]
To a solution of **17** (320 mg, 0.21 mmol) in dry *n*-BuOH (2 mL) was added NH$_2$NH$_2$ (1 mL), and the mixture was heated to 90°C and stirred overnight. After concentration and coevaporation with toluene (20 mL), the resulting solid was dissolved in pyridine (2 mL), and Ac$_2$O (200 μL, 2.12 mmol) was added. After 3 hr, the reaction mixture was concentrated and then concentrated from toluene. The resulting oil was dissolved in dry CH$_3$OH (2 mL) and a catalytic amount of KOBu was added. After reaction overnight, TLC analysis (EtOAc/Hexane, 2:1 v/v) showed full consumption of the starting material into one lower running spot. The reaction mixture was neutralized with Amberlite IR 120 H$^+$-resin, filtered, and concentrated. The crude product was purified by column chromatography (EtOAc/Hexane, 1:2 v/v), affording the title compound **49** (234 mg, 0.19 mmol, 92%) as a white foam. R_f 0.40 (EtOAc/Hexane, 2:1 v/v). ^{1}H NMR (300 MHz, CDCl$_3$): δ (ppm) 7.28 (30H, m, aromatics), 6.03 (1H, d, *J*=8.5 Hz, *H*-1), 5.10 (1H, t, *J*=8.3 Hz, *H*-2'), 4.91 (1H, d, *J*=11.4 Hz, -C*H*Ph), 4.86 (1H, d, *J*=11.5 Hz, -C*H*Ph), 4.74 (4H, bs, -C*H*Ph), 4.59 (5H, m, -C*H*Ph, *H*-1"), 4.42 (3H, m, -C*H*Ph), 4.33 (1H, d, *J*=8.4 Hz, *H*-1'), 4.07 (1H, dd, *J*=9.6, 3.7 Hz, *H*-3'), 3.90 (2H, m, *H*-4, *H*-6"a), 3.83 (3H, m, *H*-6a, *H*-5", *H*-3), 3.73 (4H, m, *H*-2, *H*-2", *H*-6b, *H*-6'a), 3.69 (1H, d, *J*=3.3 Hz, *H*-4'), 3.61 (2H, m, *H*-6'b, *H*-5), 3.50 (3H, m, *H*-3', O-C*H$_2$*-CH$_2$), 3.34 (3H, m, *H*-5', CH$_2$-C*H$_2$*-N$_3$), 2.02 (3H, s, COC*H$_3$*), 1.89 (3H, s, COC*H$_3$*), 1.78 (2H, m, CH$_2$-C*H$_2$*-CH$_2$).

3-Azidopropyl (2,3,4,6-Tetra-*O*-benzyl-α-D-galactopyranosyl)-(1→3)-β-D-galacto pyranosyl-(1→4)-2-acetamido-3,6-di-*O*-benzyl-2-deoxy-β-D-glucopyranoside (50) [33] To a solution of **49** (234 mg, 0.19 mmol) in dry CH_3OH (2 mL) was added NaOMe solution and the mixture was refluxed for 16 h after which TLC analysis ($CH_3OH/CHCl_3$, 1:9 v/v) showed full conversion of the starting material into one lower running spot. The reaction mixture was neutralized by the addition of Amberlite IR 120 H^+-resin, filtered, and concentrated under reduced pressure. Column chromatography gave compound **50** (210 mg, 0.18 mmol, 94%) as a white foam. R_f 0.56 ($CH_3OH/CHCl_3$, 1:9 v/v). ^{1}H NMR (300 MHz, $CDCl_3$): δ (ppm) 7.31 (30H, m, aromatics), 4.90 (3H, m, -C*H*Ph), 4.85 (1H, d, *J*=8.2 Hz, *H*-1), 4.74 (2H, s, -C*H*Ph), 4.67 (1H, d, *J*=11.6 Hz, -C*H*Ph), 4.59 (4H, m, -C*H*Ph, *H*-1'), 4.47 (3H, m, -C*H*Ph), 4.34 (1H, d, *J*=7.6 Hz, *H*-1"), 4.28 (1H, t, *J*=3.3 Hz, *H*-3"), 4.13 (1H, dd, *J*=10.2, 6.0 Hz, *H*-2), 3.99 (3H, m, *H*-3, *H*-4, H-6"a), 3.88 (3H, m, *H*-6a, *H*-6'a, *H*-6b), 3.74 (1H, bs, *H*-4'), 3.62 (6H, m, *H*-5, *H*-6'b, *H*-6"b, *H*-5", O-C*H₂*-CH₂), 3.38 (3H, m, CH₂-C*H₂*-N₃, *H*-3'), 3.28 (1H, m, *H*-5'), 1.88 (3H, s, COC*H₃*), 1.80 (2H, m, CH₂-C*H₂*-CH₂). ^{13}C NMR (75 MHz, $CDCl_3$): δ (ppm) 170.80, 138.18, 138.02, 137.92, 137.76, 137.51, 137.39, 102.25, 100.38, 95.87, 80.14, 79.21, 78.97, 76.22, 75.89, 75.05, 74.69, 74.68, 74.53, 74.35, 73.15, 73.14, 72.53, 71.6, 70.01, 69.65, 68.85, 68.29, 66.19, 65.72, 62.19, 55.19, 47.93, 28.77, 22.82. HRMS calcd for $C_{65}H_{76}N_4O_{16}$ (M+Na): 1191.5153. Found: 1191.5141.

3-Aminopropyl α-D-galactopyranosyl-(1→3)-β-D-galactopyranosyl-(1→4)-2-acetamido-2-deoxy-β-D-glucopyranoside (16) [33] Pd/C (10 wt. % on activated carbon, 100 mg) was added to a solution of 47 (154 mg, 0.13 mmol) in ^{t}BuOH/H₂O (2 mL, 11:4 v/v) and HCl (1 M in H₂O, 500 μL), after which H₂ was bubbled through the solution for 1 hr followed by stirring under an H₂ atmosphere for 16 hr. TLC analysis (EtOAc/pyridine/AcOH/H₂O, 8:7:1.6:1

v/v) showed full transformation of the starting material into one lower running spot. The mixture was filtered, concentrated in vacuo, and lyophilized to afford compound 16 (96 mg, 0.13 mmol, quant.) as a white powder. R_f 0.32 (EtOAc/pyridine/AcOH/H_2O, 8:7:1.6:1 v/v). ^{1}H NMR (300 MHz, D_2O): δ (ppm) 5.15 (bs, 1H, H-1"), 4.54 (2H, m, H-1, H-1'), 4.18 (2H, H-1", H-4'), 4.03-3.95 (m, 4H), 3.89-3.47 (m, 16H), 3.09 (t, 2H, CH$_2$-CH_2-NH$_2$, J=6.4 Hz), 2.06 (s, 3H, Ac), 1.96 (m, 2H, CH$_2$-CH_2-CH$_2$). ^{13}C NMR (75 MHz, D_2O): δ (ppm) 176.0, 104.4, 102.7, 97.1, 80.4, 78.9, 76.6, 76.3, 75.2, 73.8, 72.4, 71.2, 70.9, 70.8, 69.8, 69.5, 66.5, 62.6, 61.7, 65.6, 39.2, 28.3, 23.8. HRMS calcd for $C_{23}H_{42}O_{16}N_2$ (M+H): 603.2607. Found: 603.2646.

Acetic acid 4,5-diacetoxy-2-acetoxymethyl-6-{3,5-diacetoxy-2-[4-acetoxy-2- acetoxy-methyl-5-actylamino-6-(3-amino-propoxy)-tetrahydro-pyran-3-yloxy]-6-acetoxymethyl-tetrahydro-pyran-4-yloxy}-tetrahydro-pyran-3-yl ester (12) To solution of **16** (60 mg, 0.1 mmol) in acetic acid (5 mL) was added AcCl (10 μL). The mixture was stirred at rt for 24 h and concentrated in vacuo. The crude product was purified by column chromatography (CH_2Cl_2: CH_3OH=20:1) to afford the compound 12 (55 mg, 56%). ^{1}H NMR (300 MHz, CDCl$_3$): δ 5.72 (1H, d, J = 9 Hz, NHAc), 5.43 (bs, 1H, H-1"), 5.23-5.01 (4H, m), 4.49 (2H, m, H-6"), 4.45 (2H, m, H-1, H-1'), 4.19-4.02 (6H, m), 3.76 (4H, m), 3.64-3.54 (4H, m), 3.35 (2H, t, J=6.4 Hz, CH$_2$-CH_2-NH$_2$), 2.14-2.05 (30H, s, 10 X CH_3), 1.88 (2H, m, CH$_2$-CH_2-CH$_2$); ^{13}C NMR (75 MHz, CDCl$_3$): δ (ppm) 170.8, 170.7, 170.6, 170.5, 170.4, 170.3, 170.3, 170.1, 169.9, 169.3, 101.3, 101.2, 93.6, 77.4, 75.3, 72.9, 72.3, 71.0, 69.9, 67.8, 67.3, 67.0, 66.6, 66.2, 64.8, 62.5, 61.4, 61.2, 53.0, 48.2, 36.8, 29.9, 29.4, 29.1, 23.4, 21.1, 21.0, 20.9, 20.8, 20.7, 20.6. HRMS calcd for $C_{41}H_{60}$ N_2O_{25} Na (M+Na): 1003.3383. Found: 1003.3400.

O-Propargyl-tetra(ethylene glycol) (35) [34] To a solution of tetra(ethylene glycol) (1, 2 g, 5.30 mmol) in 20 mL of THF was added NaH (60% w/w in mineral oil, 272 mg, 11.34 mmol, 1.1

equiv.) at 0 °C with frequent venting. After stirring for 15 min, propargyl bromide (80% in toluene, 1.68 mL, 11.34 mmol, 1.1 equiv) was added slowly, and the mixture was stirred at 0 °C for 2 h and then 23 °C for an additional 2 h. The reaction mixture was passed through a silica gel column eluted with EtOAc to give the purified product **35** (1.552 g, 65%) as a clear oil. ^{1}H NMR (300 MHz, CDCl$_3$) δ: 4.16 (d, 2 H, J = 2.4 Hz, OCH_2C≡CH), 3.65-3.61 (m, 14 H, -(OCH_2CH_2)O-), 3.56 (t, 2 H, J = 4.4 Hz, OCH$_2$CH_2OH), 2.75 (br. s, 1 H, -OH), 2.40 (t, 1 H, J = 2.4 Hz, OCH$_2$C≡CH).

O-Propargyl-tetra(ethylene glycol) tosylate (36) [34] *p*-Toluenesulfonyl chloride (1 g, 5.4 mmol) and DMAP (25 mg, 0.2 mmol) were added to a solution of **2** (1.044 g, 4.5 mmol) in 1:1 pyridine-CH$_2$Cl$_2$ (10 mL). After 5 h, the solution was poured into ice-water (20 mL), and the aqueous phase was extracted with dichloromethane (3 × 20 mL). The combined organic phases was washed with NH$_4$Cl (20 mL) and brine (20 mL), dried over anhydrous Na$_2$SO$_4$, and concentrated. The yellow oil was chromatographed on silica gel (EtOAc:hexane 3:1) to yield **36** (1.404 g, 81%) as a clear oil. ^{1}H NMR (300MHz, CDCl$_3$) δ: 7.75 (d, 2 H, J = 8.4 Hz, aromatics), 7.26 ((d, 2 H, J = 8.4 Hz, aromatics), 4.19 (d, 2 H, J = 2.4 Hz, OCH_2C≡CH), 4.16 (t, 2 H, J = 7.8 Hz, OCH$_2$CH_2OTs), 3.70-3.55 (m, 14 H, (OCH_2CH_2)O), 2.54 (s, 3 H, Ph-CH_3), 2.52 (t, 1 H, J = 2.4 Hz, OCH$_2$C≡CH).

Methyl 3,4,5-trihydroxybenzoate (33) To solution of Gallic acid (3.4 g, 20 mmol) in acetone (100 mL) was added CH$_3$I (2.8g, 20 mmol) and K$_2$CO$_3$ (3.0 g, 22mmol). The mixture was stirred and refluxed under stirring for 10 h and allowed to cool to temperature. The solid was filtered off and the filtrate was evaporated under reduced pressure. The residue was recrystallized from ethanol to afford **33** (3.0 g, 81%) as a white solid. ^{1}H NMR (300MHz, CDCl$_3$) δ 7.06 (s, 2 H, aromatics), 3.86 (s, 3 H, CH$_3$).

3,4,5-Tris-(2-{2-[2-(2-prop-2-ynyloxy-ethoxy)-ethoxy]-ethoxy}-ethoxy)-benzoic acid methyl ester (37) To a solution of methyl gallate **33** (184 mg, 1 mmol) in DMF(25mL) was added potassium carbonate (1.4 g, 10 mmol) and tosylated **36** (1.5 g, 4.0 mmol) dissolved in DMF (5 mL). The mixture was stirred at 80 °C for 24 h and allowed to cool to room temperature. The solid was filtered off and the filtrate was evaporated under reduced pressure, coevaporated with *tert*-BuOH, and the remaining residue was partitioned between CH_2Cl_2 and water. The organic layer was separated and washed with H_2O, brine solution, and dried over $MgSO_4$. After removing the solvent, the crude material was purified by silica gel chromatography using a gradient of 1:3 to 2:1(v/v) EtOAc/hexanes to give 630 mg (77 %) of **37** as a pure colorless oil. ^{1}H NMR (300MHz, $CDCl_3$) δ: 7.25 (s, 2 H, aromatics), 4.18-4.15 (6H, m, PhOCH_2), 3.84 (s, 3 H, CH_3), 3.82 (6H, m, OCH_2-alkyne), 3.68- 3.58 (42H, m, CH_2), 2.41 (3H, m, alkyne); ^{13}C (75MHz, $CDCl_3$) δ: 166.7, 152.4, 142.7, 125.1, 109.1, 79.8, 74.7, 72.6, 72.6, 71.0, 70.9, 70.8, 70.7, 70.6, 70.5, 69.8, 69.7, 69.2, 69.0, 61.9, 58.5. HRMS calcd for $C_{23}H_{42}O_{16}N_2$ (M+H): 849.3885. Found: 849.3873.

3,4,5-Tris-(2-{2-[2-(2-prop-2-ynyloxy-ethoxy)-ethoxy]-ethoxy}-ethoxy)-benzoic acid (38) To solution of methyl ester **37** (410 mg, 0.5 mmol) in CH_3OH was added 0.5 M NaOH (10 mL), the mixture was stirred at room temperature overnight. After treatment with H^+ resin, the filtrate was first evaporated to remove methanol. The pure product **38** was obtained as yellow oil (400 mg, 99%). ^{1}H NMR (300MHz, $CDCl_3$) δ: 7.27 (s, 2 H, aromatics), 4.14-4.13 (6H, m, PhOCH_2), 3.80-3.78 (6H, m, OCH_2-alkyne), 3.63- 3.58 (42H, m, CH_2), 2.38 (3H, m, alkyne); ^{13}C (75MHz, $CDCl_3$) δ: 165.6, 151.1, 141.5, 124.1, 108.4, 78.7, 78.6, 73.7, 73.6, 71.4, 69.8, 69.7, 69.6, 69.5,69.4, 69.3, 68.6, 68.0, 67.7, 57.3. HRMS calcd for $C_{23}H_{42}O_{16}N_2$ (M+H): 835.3728. Found: 835.3710.

Methyl 5-acetamido-3,5-dideoxy-D-*glycero*-β-D-*galacto*-non-2-ulopyranosonate (40) [35]

5-N-Acetylneuraminic acid **39** (5.0 g, 16.2 mmol) was dissolved in CH_3OH (500 ml, HPLC grade) and ion exchange resin Amberlite® IR 120-H (20 g) was added. The mixture was stirred overnight under argon atmosphere, filtered and the resin washed with CH_3OH. After evaporation of the solvent, compound **40** was obtained white foam (4.4 g, 84%). ^{1}H-NMR (300 MHz, CD_3OD) δ: 3.98-4.06 (2 H, m), 3.78- 3.82 (2 H, m), 3.77 (3 H, s, OC*H₃*), 3.59-3.71 (2 H, m), 3.47 (1 H, dd, J = 9.2 Hz, J = 1.2 Hz), 2.20 (1 H, dd, $J_{3ax,3eq}$ = 12.8 Hz, $J_{3eq,4}$ = 5.0 Hz, *H*-3eq), 2.0 (3 H, s, COC*H₃*), 1.88 (1 H, dd, $J_{3ax,3eq}$ = 12.8 Hz, $J_{3ax,4}$ = 11.6 Hz, *H*-3ax). ^{13}C -NMR (100 MHz, CD_3OD) δ: 22.6, 40.7, 53.1, 54.4, 64.9, 67.9, 70.2, 71.7, 72.1, 96.7, 171.8.

Methyl 5-acetamido-4,7,8,9-tetra-*O*-acetyl-3,5-dideoxy-D-*glycero*-β-D-*galacto*-non-2-ulopyranosylonate chloride (41) [36] A solution of **40** (1.1 g, 3.4 mmol) in AcCl (100 mL) was cooled to 0°C. The mixture was stirred overnight at RT, degassed (water pump) and evaporated to yield compound **41** (1.8 g, quantitative) as a white foam. ^{1}H NMR (300 MHz, $CDCl_3$) δ: 5.69 (1 H, d, $J_{NH,5}$ = 10 Hz, N*H*), 5.48 (1 H, dd, $J_{7,8}$ = 6.8 Hz, $J_{7,6}$ = 2.3 Hz, H-7), 5.36-5.44 (1 H, m, H-4), 5.17 (1 H, td, $J_{8,7}$ = 6.8 Hz, $J_{8,9a}$ = 6 Hz, $J_{8,9b}$ = 2.6 Hz, H-8), 4.35-4.47 (2 H, m, *H*-9b, *H*-5), 4.16-4.26 (1 H, m, *H*-6), 4.07 (1 H, dd, $J_{9a,9b}$ = 12.5 Hz, $J_{9a,8}$ = 6 Hz, *H*-9a), 3.88 (3 H, s, OC*H₃*), 2.78 (1 H, dd, $J_{3ax,3eq}$ = 13.9 Hz, $J_{3eq,4}$ = 4.8 Hz, *H*-3eq.), 2.26 (1 H, dd, $J_{3ax,3eq}$ = 13.9 Hz, $J_{3ax,4}$ = 11.3 Hz, *H*-3ax), 2.05, 2.06, 2.08, 2.15 (12 H, 4s, COC*H₃*), 1.92 (3 H, s, NHCOC*H₃*). ^{13}C-NMR (75 MHz, $CDCl_3$) δ: 21.4, 2.15, 21.6, 21.7, 23.8, 41.3, 49.3, 54.4, 62.7, 67.5, 69.4, 70.7, 74.6, 97.3, 166.3 (C-1), 170.4, 170.6, 171.1, 171.3, 171.6.

Methyl 5-acetamido-4, 7,8,9-tetra-O-acetyl-2,6-anhydro-3,5-dideoxy-u-glycero-D-galacto-non-2-enonate (42) [37] To a solution of **41** (450 mg, 1 mmol) in dry dichloromethane (100 mL) was added triethylamine (5 mL) with stirring. After 1 h, the solution was evaporated to

dryness and the residue chromatographed in a silica gel column with solvent (Hexane: EtOAC, 1:

1) as eluent to give 290 mg (62%) of **42** as a dry foam. ^{1}H NMR (300 MHz, CDCl$_3$) δ 8.17-8.21

(2 H, m, aromatics), 7.63-7.65 (2 H, m, aromatics), 5.26-5.30 (2 H, m, *H-7, H-8*), 5.21 (1 H, d,

$J_{NH,5}$ = 9.2, N*H*), 4.88 (1 H, ddd, $J_{4,5}$ = 14.2, $J_{4,3ax}$ = 10.1, *H-4*), 4.32 (1 H, dd, $J_{9b,9a}$ = 11.7, $J_{9b,8}$ =

2.2, *H-9b*), 4.08-4.10 (1 H, m, *H-9a*), 4.01 (1 H, q, $J_{5,6}$ + $J_{5,NH}$ = 29.0, *H-5*), 4.00 (1 H, m, *H-6*),

3.60 (3 H, s, C*H$_3$*), 2.87 (1 H, dd, $J_{3eq,3ax}$ = 12.8, $J_{3eq,4}$ = 4.6, *H-3eq*), 2.16 (3 H, s, COC*H$_3$*), 2.09

(1 H, m, *H-3ax*), 2.06 (3 H, s, COC*H$_3$*), 2.04 (3 H, s, COC*H$_3$*), 2.03 (3 H, s, COC*H$_3$*), 1.88 (3 H,

s, COC*H$_3$*)

Methyl 5 -acetamido-2,6 -anhydro-3,5 -dideoxy- 9-p-toluenesulfonyl-D-glycero-D-galactonon-2 -enonate (43) [38] To a solution of methyl 5-acetamido-4,7,8,9-tetra-O-acetyl-2,6-anhydro-3,5-dideoxy-D-glycero-D-galacto-non-2-enonate **42** (110 mg, 0.24 mmol) in dry

CH$_3$OH (10 mL) was added NaOCH$_3$ (13 mg, 0.25 mmol), and the mixture was stirred for 1 h at

room temperature. The mixture was neutralized by the addition of Dowex 50W resin. To this

mixture was added H$_2$O (2 mL), and the mixture was filtered and concentrated. To a solution of

this residue in pyridine (20 mL) was added *p*-toluenesulfonyl chloride (42 mg, 0.22 mmol) at

room temperature, and the mixture was stirred for 4 h. Next, CH$_3$OH (5 mL) was added to the

mixture, which was then concentrated in vacuo. Purification of the residue on a column of silica

gel (19:1 EtOAc–CH$_3$OH) yielded **43** (75 mg, 69%). ^{1}H NMR (300 MHz, D$_2$O) δ 7.39-7.74 (4H,

m, aromatics), 5.87 (1H, m, *H-3*), 4.35 (1H, m, *H-4*), 4.24 (1H, m, *H-6*), 4.00-4.06 (2H, m, *H-5*

and *H-9a*), 3.89 (1H, m, *H-8*), 3.86 (1H, m, *H-9b*), 3.71 (3H, s, OC*H$_3$*), 3.44 (1H, m, *H-7*), 2.41

(3 H, s, COC*H$_3$*),

Methyl 5-Acetamido-2,6-anhydro-9-azido-3,5,9-trideoxy-D-glycero-D-galacto-non-2-enonic acid (44) [39] To a solution of **43** (230 mg, 0.5 mmol) in DMF (2 mL) was added sodium

azide (241 mg, 3.71 mmol) and the mixture was stirred at 70 °C. After 7 h, it was allowed to cool to room temperature. Purification of the mixture on a column of silica gel (49:1 EtOAc-CH$_3$OH) yielded azide derivative **44** (107 mg, 65%). ^{1}H NMR (300 MHz, D$_2$O) δ 5.91 (1 H, d, J = 2.64 Hz, *H*-3), 4.40 (1H, m, *H*-4), 4.31 (1H, m, *H*-6), 4.11 (1H, m, *H*-5), 3.93 (1H, m, *H*-8), 3.76 (3 H, s, OC*H*$_3$), 3.54 (1 H, dd, J = 2.64, 13.2 Hz, *H*-9a), 3.51 (1H, m, *H*-7), 3.37 (1 H, dd, J = 6.6, 13.2 Hz, *H*-9b), 2.03 (3 H, s, COC*H*$_3$).

Methyl 5-Acetamido-4,7,8-tri-*O*-acetyl-2,6-anhydro-9-azido-3,5,9-trideoxy-D-glycero-D-galacto-non-2 -enonic acid (15). To solution of **44** (66 mg, 0.2 mmol) in pyridine (5 mL) was added acetic anhydride (1 mL) and the mixture was stirred at rt for 12 h. solvent was removed in vacuo, and residue was purified by column chromatography on silica gel (eluant: hexane: EtOAc 1:3) to give **15** (80 mg, 87%). ^{1}H NMR (300 MHz, CDCl$_3$) δ 6.26 (1H, m, N*H*Ac), 5.90 (1H, d, J = 2.4 Hz, *H*-3), 5.50 (1H, m, *H*-4), 5.46 (1H, m, *H*-7), 5.14 (1H, m, *H*-8), 4.36 (1H, m, *H*-6), 4.34 (1H, d, J = 5.4Hz, *H*-5), 3.89 (1H, dd, J = 3, 12 Hz, *H*-9), 3.76 (3H, s, OC*H*$_3$), 3.43 (1H, dd, J = 3, 12 Hz, *H*-9), 2.09, 2.06, 2.04, 1.86 (12H, s, 4 X C*H*$_3$); ^{13}C-NMR (75 MHz, CDCl$_3$) δ: 169.9, 169.4, 169.2, 160.5, 144.1, 107.3, 71.7, 67.3, 66.9, 51.6, 49.0, 45.5, 22.1, 19.9, 19.8, 19.7. HRMS calcd for C$_{18}$H$_{24}$N$_4$O$_{10}$Na (M+Na): 479.1390. Found: 479.1415.

Methyl (phenyl 5-acetanzido-4,7,8,9-tetra-O-acetyl-3,5-dideoxy-2-thio-β-D-glycero-galacto-2-nonuZopyranosid)onafe (45) [37] A mixture of **41** (500 mg, 1mmol) in anhydrous dichloromethane (10 mL) was added thiophenol (120 mg, 1.1 mmol) and TEA (0.1 mL). The mixture was kept overnight at room temperature, then diluted with CH$_2$Cl$_2$ (150 mL), washed with saturated aqueous NaHCO$_3$ (30 mL), dried (MgSO$_4$), and concentrated. The residue was eluted from a column of silica gel with 70: 1 CH$_2$Cl$_2$-CH$_3$OH to give **45** (450 mg, 73%). ^{1}HNMR (300 MHz, CDCl$_3$) δ 7.64, 7.10, and 6.99 (5 H, 3 m, aromatics), 5.72 (1 H, m, *H*-7), 5.44 (1 H,

m, *H*-8), 5.35 (1 H, m, *H*-4), 5.00 (1 H, m, *H*-9), 4.61 (1 H, m, *H*-6), 4.38 (1 H, m, *H*-9), 3.26 (3 H, s, OC*H*$_3$), 2.80 (1 H, m, *H*-3eq), 2.01 (1 H, m, *H*-3ax), 1.92, 1.88, 1.67, 1.63, and 1.60 (15 H, s, 5 COC*H*$_3$).

Methyl (5-acetamido-4,7,8,9-tetra-*O*-acetyl-3,5-di-deoxy-D-*glycero*-D-*galacto*-non-2-ulopyranosyl)onate] phenyl sulfone (3) and methyl (2,6-anhydro-5-acetamido-4,7,8,9-tetra-*O*- acetyl-3,5-dideoxy-D-*glycero*-D-*galacto*-non-2-ene)onate (46) [40] A catalytic amount of ruthenium trichloride hydrate (3 mg) was added to a vigorously stirred biphasic solution of **45** (300 mg, 0.5 mmol) and sodium metaperiodate (430 mg, 2 mmol) in CCl$_4$ (2 mL), acetonitrile (2 mL), and water (3 mL). After 5 min at room temperature, the yellow mixture was diluted with CH$_2$Cl$_2$ (100 mL), washed with H$_2$O (20 mL), dried (MgSO$_4$), and concentrated. The residue was eluted from a column of silica gel with EtOAc to give **46** (280 mg, 91%). ^{1}H NMR (300 MHz, CDCl$_3$) δ 7.97, 7.00, and 6.94 (5 H, m, aromatics), 5.79 (1 H, m, *H*-4), 5.76-5.70 (2 H, m, *H*-7,8), 5.23 (1 H, m, *H*-6), 4.89 (1H, m, *H*-9a), 4.50 (1 H, m, *H*-5), 4.39 (1 H, m, *H*-9), 3.36 (1 H, m, *H*-3eq), 3.05 (3 H, s, OC*H*$_3$), 2.14 (1 H, m, *H*-3ax), 2.00, 1.91, 1.71, 1.61, and 1.60 (15 H, s, 5 COC*H*$_3$).

Methyl 5-acetamido-4,7,8,9-tetra-O-acety-2,6-anhydro-3,5-dideoxyl-2-(C-1-hydroxy-acet-l-yl)-D-erythro-L-monno-nononate (47) Compound **46** (120 mg, 0.2 mmol) was dried under high vacuo for 4 h, then dissolved in degassed anhydrous THF (10 mL) and acetone (10 μL). SmI$_2$ (4 equiv., freshly prepared from Sm and ICH$_2$CH$_2$I, 0.1 M in THF) was added in one portion at room temperature with vigorous stirring. After 10 min, the reaction mixture was directly filtered, and the filtrate was concentrated under reduced pressure, then purified on silica gel column with EtOAc as eluent to afford the product **47** (90 mg, 89%). ^{1}H NMR (300 MHz, CDCl$_3$): δ 5.52-5.60 (1H, m, *H*-8), 5.40-5.45 (1H, m, *H*-7), 5.30 (1H, br, N*H*), 4.80 (1H, ddd, *J* =

12.5, 8.9Hz, *H*-4), 4.38 (1H, dd, *J* = 1.2Hz, 11.6Hz, *H*-9b), 4.00-4.29 (3H, m, *H*-5, *H*-6, *H*-9a), 3.80 (3H, s, COOC*H*₃), 2.55 (1H, dd, *J* = 2.1Hz), 1.98, 2.02, 2.03, 2.11, 2.18 (15H, 5s, 5 COC*H*₃), 1.95(1H, t, *J* = 12.5Hz, *H*-3ax), 1.20, 1.30(6H, 2s, C(C*H*₃)₂). ¹³C-NMR (75 MHz, CDCl₃) δ: 171.1, 170.9, 170.5, 170.2, 85.6, 74.4, 73.5, 70.5, 69.2, 68.1, 62.8, 52.5, 49.3, 33.4, 29.4, 24.9, 24.7, 23.1, 21.3, 21.3, 21.0, 20.8. HRMS calcd for C₂₃H₃₅NO₁₃Na (M+Na): 556.2006. Found: 556.2020.

5-Acetylamino-4-hydroxy-2-(1-hydroxy-1-methyl-ethyl)-6-(1,2,3-trihydroxy-propyl)-tetrahydro-pyran-2-carboxylic acid methyl ester (48). To a solution of methyl 5-acetamido-4,7,8,9-tetra-O-acetyl-2,6-anhydro- 3,5-dideoxy- D-glycero-D-galacto-non-2-enonate **47** (100 mg, 0.2 mmol) in dry CH₃OH (10 mL) was added NaOMe (13 mg, 0.25 mmol), and the mixture was stirred for 1 h at room temperature. The mixture was neutralized by the addition of Dowex 50W resin. Filtered and concentrated in vacuo. Purification of the residue on a column of silica gel (15:1 EtOAc–CH₃OH) yielded **48** (63 mg, 87%).¹H NMR (300 MHz, CD₃OD): δ 3.86-381 (2H, m, *H*-9 and *H*-8), 3.79 (3H, OC*H*₃), 3.68-3.55 (3H, m), 3.51-3.46 (2H, m), 2.57 (1H, dd, *J* = 4.5, 5.7 Hz, *H*-3eq), 1.99 (3H, s, C*H*₃CO), 1.98 (1H, dd, *J* = 4.5, 5.7 Hz, *H*-3ax), 1.22 (3H, s, C*H*₃), 1.17 (3H, s, C*H*₃); ¹³C-NMR (75 MHz, CD₃OD) δ: 174.1, 173.3, 85.7, 74.5, 73.4, 71.6, 69.1, 68.3, 68.2, 63.3, 52.8, 51.9, 34.9, 21.6, 21.5. HRMS calcd for C₁₅H₂₇NO₉Na (M+Na): 388.1584. Found: 388.1600.

4-Acetoxy-5-acetylamino-6-(1,2-diacetoxy-3-azido-propyl)-2-(1-hydroxy-1-methyl-ethyl)-tetrahydro-pyran-2-carboxylic acid methyl ester (13) To a solution of **48** (55 mg, 0.15 mmol) in pyridine (10 mL) was added *p*-toluenesulfonyl chloride (42 mg, 0.16 mmol) at room temperature, and the mixture was stirred for 4 h. Next CH₃OH (5 mL) was added to the mixture, which was then concentrated in vacuo. The residue was dissolved in DMF (2 mL) was added

sodium azide (100 mg, 1.6 mmol) and the mixture was stirred at 70 °C. After 7 h, it was allowed to cool to room temperature. Next a mixture of CH_2Cl_2 and CH_3OH (10: 1, 20 mL) was added to the reaction mixture, the resulting mixture was filtered to remove all solids and the filtrate was concentrated in vacuo. The residue was dissolved in pyridine (10 mL), and acetic anhydride (1 mL) was added. The mixture was stirred at rt for 12 h, the solvent was removed in vacuo, and the residue was purified by column chromatography on silica gel (EtOAc) to give **13** (31 mg, 41% in 3 steps). ^{1}H NMR (300 MHz, $CDCl_3$): δ 5.37-5.23 (3H, m, *H*-7, *H*-8, N*H*), 4.74 (1H, m, *H*-4), 4.02-3.91 (2H, *H*-5, *H*-6), 3.73 (3H, s, OC*H*$_3$), 3.49 (1H, dd, *J* = 2.7, 6.9 Hz, *H*-9), 3.24 (1H, dd, *J* = 2.7, 6.9 Hz, *H*-9), 2.75 (1H, s, O*H*), 2.43 (1H, dd, *J* = 5.4, 12.9 Hz, *H*-3eq), 2.19- 2.03 (9H, s, 3 X OC*H*$_3$), 1.96 (1H, dd, *J* = 5.4, 12.9 Hz, *H*-3ax), 1.81 (3H, s, C*H*$_3$), 1.20 (3H, s, C*H*$_3$), 1.15 (3H, s, C*H*$_3$); ^{13}C-NMR (75 MHz, $CDCl_3$) δ: 170.0, 169.6, 169.4, 169.3, 169.1, 84.3, 73.2, 72.3, 69.2, 68.5, 67.2, 51.4, 50.1, 48.4, 32.1, 23.7, 23.6, 22.1, 20.2, 19.9, 19.8. HRMS calcd for $C_{21}H_{32}N_4O_{11}Na$ (M+Na): 539.1965. Found: 539.1981.

Compound (51) To solution of **8** (6.0 mg, 0.0067 mmol) and **13** (14 mg, 0.027 mmol) in DMF was added CuI (0.2 mg, 0.001 mmol) and (1.2 mg, 0.01 mmol) at room temperature, and the mixture was stirred for 48 h. The solvent was removed in vacuo. The residue was purified by silica gel column chromatography (CH_2Cl_2: CH_3OH, 15: 1, v/v) to afford **51** (10.6 mg, 68%). ^{1}H NMR (500 MHz, $CDCl_3$): δ 7.64 (3H, s, triazole), 7.30 (2H, s, aromatics), 5.73-5.67 (3H, N*H*Ac), 5.39-5.33 (3H, m, *H*-8), 5.26-5.23 (6H, *H*-7, *H*-9), 4.83-4.73 (3H, m, *H*-4), 4.14-4.10 (6H, m, *H*-5, *H*-6), 4.05-3.99 (6H, m, PhOC*H*$_2$), 3.77-4.42 (64 H, m, C*H*$_2$, *H*-9), 2.48-2.44 (3H, m, *H*-3eq), 2.10-1.74 (39 H, s, 12 X C*H*$_3$, *H*-3ax), 1.26-1.16 (18H, 6 X C*H*$_3$); ^{13}C NMR(75 MHz, $CDCl_3$): δ 171.3, 170.7, 170.5, 170.5, 152.4, 145.1, 143.3, 130.2, 123.8, 110.3, 109.1, 86.0, 76.8, 74.6, 74.5, 74.1, 72.5, 71.2, 71.1, 70.9, 70.8, 70.7, 70.6, 70.5, 69.8, 69.7, 69.0, 64.5, 52.7, 50.5, 49.6, 33.5,

32.9, 32.1, 31.9, 30.3, 29.9, 29.6, 29.5, 25.1, 25.0, 23.3, 22.9, 21.1, 21.0, 14.3. HRMS calcd for $C_{103}H_{156}N_{12}O_{50}Na$ (M+Na): 2383.9931. Found: 2384.0640.

Compound (11) To solution of **51** (9.5 mg, 0.004 mmol) and **12** (6.0 mg, 0.006 mmol) in CH_2Cl_2 was added DCC (5.0 mg, 0.024 mmol), DMAP (0.5 mg) and DIPEA (1.2 mg, 0.01 mmol) at room temperature, and the mixture was stirred for 12 h. The solvent was removed in vacuo and the residue was purified by column chromatography on silica gel (CH_2Cl_2: CH_3OH, 10: 1 v/v) to afford **11** (8.0 mg, 61%). ^{1}H NMR (500 MHz, CDCl$_3$): δ 7.64 (3H, s, triazole), 7.34 (2H, s, aromatics), 5.75-5.68 (5H, N*H*Ac), 5.38 (1H, bs, *H*-1"), 5.32-5.26 (3H, m, *H*-8), 5.18-5.07 (4H, m), 4.83-4.79 (3H, m, *H*-4), 4.66-4.63 (3H, m, *H*-1, *H*-1', *H*-6"), 4.52-4.45 (4H, m, *H*-6", C*H*$_2$), 4.20-4.04 (16H, m, *H*-5, *H*-6, PhOC*H*$_2$), 3.84-3.64 (72H, m), 3.10-3.09 (6H, m, CH$_2$-C*H*$_2$-NH$_2$), 2.57-2.53 (3H, m, *H*-3eq), 2.10-1.70 (71H, 22 X C*H*$_3$, *H*-3ax, CH$_2$-C*H*$_2$-CH$_2$), 1.23-1.15 (18H, 6 X C*H*$_3$). HRMS calcd for $C_{144}H_{214}N_{14}O_{74}Na$ (M+Na): 3346.3311. Found: 3346.7588.

Compound (9) To solution of **11** (6.6 mg, 0.002 mmol) in CH_3OH (5 mL) was added 1N LiOH (1 mL), and the mixture was stirred for 24 h at rt. The mixture was neutralized by the addition of Dowex 50W resin and filtrated to remove the resin. The filtrate was concentrated in vacuo. Purification of the residue on with size exclusion chromatography afford **9** (2.4 mg, 50 %). ^{1}H NMR (500 MHz, D$_2$O): δ 7.94 (3H, s, triazole), 7.03 (2H, s, aromatics), 5.06 (1H, bs, *H*-1"), 4.74-4.59 (7H, m, *H*-8), 4.55-4.49 (6H, m, *H*-1, *H*-1', *H*-6", *H*-4), 4.46-4.39 (4H, m, H-6", C*H*$_2$), 4.15-3.93 (4H, m, *H*-7, C*H*$_2$), 3.90-3.76 (16H, m, *H*-5, *H*-6, PhOC*H*$_2$), 3.74-3.32 (60 H, m, C*H*$_2$), 2.54-2.53 (5H, m, *H*-3, CH$_2$-C*H*$_2$-NH$_2$), 2.14 (9H, 3X C*H*$_3$), 1.92 (3H, s, C*H*$_3$), 1.80-1.75 (5H, m, *H*-3, CH$_2$-C*H*$_2$-CH$_2$), 1.16-1.12 (18H, s, 6 X C*H*$_3$).

Compound (52) To solution of **8** (6.0 mg, 0.0067 mmol) and **15** (13.6 mg, 0.03 mmol) in DMF was added CuI (0.2 mg, 0.001 mmol) and (1.2 mg, 0.01 mmol) at room temperature, and

the mixture was stirred for 48 h. The solvent was removed in vacuo. The residue was purified by column chromatography on silica gel (CH_2Cl_2: CH_3OH, 20: 1) to afford **52** (9.5 mg, 65%). ^1H NMR (500 MHz, $CDCl_3$): δ 7.73-7.70 (3H, s, triazole), 7.29 (2H, s, Ph), 6.65 (3H, m, N*H*Ac), 5.89 (3H, m, *H*-3), 5.54 (3H, m, *H*-4), 5.46 5.46 (3H, m, *H*-7), 5.14 (3H, m, *H*-8), 4.53-4.35 (8H, m), 4.14-4.05 (7H, m), 3.73-3.52 (52 H, m, C*H*$_2$), 2.14-1.62 (45 H, s, 15 X C*H*$_3$); ^{13}C NMR(75 MHz, $CDCl_3$): δ 171.1, 170.9, 170.6, 170.5, 161.8, 152.4, 145.0, 124.3, 110.0, 109.1, 76.8, 73.7, 72.5, 71.0, 70.8, 70.7, 70.6, 69.9, 69.7, 69.3, 69.1, 68.2, 64.5, 53.6, 52.9, 49.7, 46.3, 29.9, 23.2, 21.1, 20.9, 20.8. HRMS calcd for $C_{94}H_{132}N_{12}O_{47}Na$ (M+Na): 2203.8206. Found: 2203.9280

Compound (14) To solution of **52** (8.7 mg, 0.004 mmol) and **12** (6.0 mg, 0.006 mmol) in CH_2Cl_2 was added DCC (5.0 mg, 0.024 mmol), DMAP (0.5 mg) and DIPEA (1.2 mg, 0.01 mmol) at room temperature, and the mixture was stirred for 12 h. The solvent was removed in vacuo and the residue was purified by silica gel column chromatography (CH_2Cl_2: CH_3OH, 15: 1, v/v) to afford **14** (6.9 mg, 55%). ^1H NMR (500 MHz, $CDCl_3$): δ 7.78 (3H, s, triazole), 7.29 (2H, s, Ph), 6.65 (3H, m, N*H*Ac), 5.98 (3H, m, *H*-3), 5.83 (1H, m, N*H*Ac), 5.61-5.45 (6H, m), 5.35-5.26 (19H, m), 5.12-5.10 (5H, m), 4.66-4.64 (6H, m), 4.55-4.44 (12H, m), 4.21-4.06 (14H, m), 84-3.63 (58 H, m, C*H*$_2$), 2.22-1.89 (68H, m, 22 X C*H*$_3$, CH_2-C*H*$_2$-CH_2). HRMS calcd for $C_{135}H_{190}N_{14}O_{71}Na$ (M+Na): 3166.1585. Found: 3166.2336.

Compound (10) To solution of **14** (6.2 mg, 0.002 mmol) in CH_3OH (5 mL) was added 1N LiOH to adjust pH = 10, and the mixture was stirred for 24 h at rt. The mixture was neutralized by the adding of Dowex 50W resin and Filtrated to remove the resin. The filtrate was concentrated in vacuo. Purification of the residue on with size exclusion chromatography to afford 10 (2.7 mg, 60%). ^1H NMR (500 MHz, D_2O): δ 7.97-7.94 (3H, s, triazole), 7.28 (2H, s, aromatics), 5.61 (3H, m, *H*-3), 5.06 (1H, d, *J* = 3 Hz, *H*-1"), 4.67-4.58 (10H, m, *H*-8, *H*-4), 4.55-

4.47 (6H, m, *H*-1, *H*-1', *H*-6'', *H*-4), 4.46-4.43 (4H, *H*-6'', C*H₂*), 4.37 (3H, m, *H*-6), 4.23-4.07 (10H, m, PhOC*H₃*), 3.97-3.81 (6H, m, *H*-5, *H*-6), 3.79-3.33 (58 H, m, C*H₂*), 2.89 (2H, m, CH₂-C*H₂*-NH₂), 1.95-1.92 (12H, 4 X C*H₃*), 1.80 (2H, m, CH₂-C*H₂*-CH₂).

2.4 REFERENCES

1. R. G. Webster, W. J. Beam, O. T. Gorman, T. M. Chambers, Y. Kawaoka, *Microbiol. Rev.* 1992, 56, 152.

2. Litman G, Cannon J, Dishaw L . *Nat Rev Immunol*, 2005, **5** (11), 866

3. Pancer Z, Cooper M. "The evolution of adaptive immunity". *Annu Rev Immunol* **24**, 497

4. Mullis; Kary B, US 7,422,746

5. Galili U, Macher BA, Buehler J, Shohet SB. *J Exp Med* 1985, 162, 573

6. Oriol RYeY, Koren E, Cooper DKC. *Transplantation* 1993, 56, 1433

7. Good AH, Cooper DK, Malcolm AJ, Ippolito RM, Koren E, Neethling FA et al. *Transplant Proc* 1992, 24, 559

8. Galili U, Mandrell RE, Hamadeh RM, Shohet SB, Griffiss JM. *Infect Immun* 1988, 56, 1730

9. J. J. Skehel, D. C. Wiley, *Annu. Rev. Biochem.* 2000, 69, 531

10. C. Liu, M. C. Eichelberger, R. W. Compans, G. M. Air, *J. Virol.* 1995, 69, 1099

11. Seok-Ki Choi, Shelly Lee, and George M. Whitesides *J. Org. Chem.*, 61 (25), 8739

12. J. N. Varghese, J. L. McKimm-Breschkin, J. B. Caldwell, A. A. Kortt, P. M. Colman, *Proteins Struct. Funct. Genet.* 1992, 14, 327

13. J. C. Dyason, M. von Itzstein, *Aust. J. Chem.* 2001, 54, 663

14. J. N. Varghese, V. C. Epa, P. M. Colman, *Protein Sci.* 1995, 4, 1081

15. D. M. Andrews, C. D. Shaw, S. Swanson, *Eur. J. Med. Chem.* 1999, 34, 563

16. M. Mammen *et al.*, *Angew. Chem. Int. Ed. Engl.* 1998, **37**, 2755

17. Z. Zhang, I.R. Ollmann, X.-S. Ye, R. Wischnat, T. Baasov and C.-H. Wong, *J. Am. Chem. Soc.* 1999, 121, 734

18. K.M. Koeller and C.-H. Wong, *Chem. Rev.* 2000, 100, 4465

19. P. Fügedi and P.J. Garegg, *Carbohydr. Res.* 1986, 149, c9

20. P. Konradsson, U.E. Udodong and B. Fraser-Reid, *Tetrahedron Lett.* 1990, 31, 4313

21. A. Linde, *Antiviral Res.* 2001, 51, 81

22. Spiro, R. G. & Bhoyroo, V. *J. Biol. Chem.* 1984, 239, 9858

23. G. Vic, J.J. Hasting, O.W. Howarth and D.H.G. Crout, *Tetrahedron: Asymmetry* 1996, **7**, 709

24. Baeschlin, Daniel K.; Green, Luke G.; Hahn, Michael G.; Hinzen, Berthold; Ince, Stuart J.; Ley, Steven V. *Tetrahedron: Asymmetry* 2000, 11, 173.

25. Scott W., Rainier, Jon D. *Org. Lett.* 2007, 9, 2227

26. Janczuk, Adam J., *Carbohydr. Res.* 2002, 337, 1247

27. Fernandez-Mayoralas, Alfonso, *Carbohydr. Res.* 1989, 188, 81

28. Stick, Robert V., *Tetrahedron: Asymmetry* 2005, 16, 321

29. Kumar, Rishi; Eur. J. of Org. Chem. 2005, (1), 74

30. Ellervik, Ulf, Magnusson, Goeran. *Carbohydr. Res.,* 1996, 280, 251

31. Sarkar, Kakali; *J. Carbohydr. Chem.* 2003, 22, 95

32. Nilsson, Marianne; *J. Carbohydr. Chem.* 1990, 9, 14

33. Litjens, Remy; *J. Carbohydr. Chem.* 2005, 24, 755

34. Sun, Xue-Long; Stabler, Cheryl L.; Cazalis, Chrystelle S.; Chaikof, Elliot L. *Bioconj. Chem.*, 2006, 17, 52.

35. Fitz, Wolfgang; Rosenthal, Peter B.; Wong, Chi-Huey. *Bioorg. Med. Chem.* 1996, 4, 1349.

36. Malapelle, Adeline; Abdallah, Zouleika; Doisneau, Gilles; Beau, Jean-Marie. *Angew. Chem., Int. Ed.* 2006, 45, 6016.

37. Narine, Arun A.; Watson, Jacqueline N.; Bennet, Andrew J. *Biochemistry*. 2006, 5, 9319.

38. Hiroya Kamei, Yasuhiro Kajihara and Yoshisuke Nishi. *Carbohydr. Res.,* 1999, 315, 243

39. Von Itzstein, Laurence Mark; Wu, Wen Yang; Phan Tho Van; Danylec, Basil; Jin, Betty. PCT Int. Appl, 1992: 449151

40. Marra, Alberto; Sinay, Pierre. *Carbohydr. Res.*, 1989, 187, 35.

CHAPTER 3

VISUALIZING METABOLICAL-LABELED GLYCOCONJUGATES OF LIVING

CELLS BY COPPER-FREE AND FAST HUISGEN CYCLOADDITIONS[*]

Reprinted here with permission of publisher

ABSTRACT

Cu^I-free click: 4-Dibenzocyclooctynol reacts, in the absence of a Cu^I catalyst, exceptionally fast with azido-containing saccharides and amino acids to give stable triazoles. A biotin-modified derivative is ideally suited for visualizing and tracking glycoconjugates of living cells that are metabolically labeled with azido-containing monosaccharides

Keywords: carbohydrates · glycoconjugates · click chemistry · azide · bioorthogonal
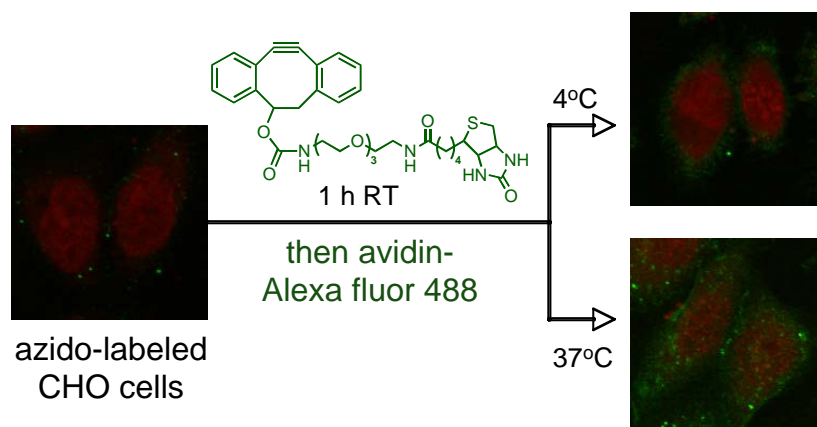
3.1 INTRODUCTION

Azides, which are extremely rare in biological systems, are emerging as attractive chemical handles for bioconjugation.[1-5] In particular, the Cu^I catalyzed 1,3-dipolar cyclization of azides with terminal alkynes to give stable triazoles[6, 7] has been employed for the tagging of a variety of biomolecules,[8-12] activity-based protein profiling,[13] and the chemical synthesis of microarrays and small molecule libraries.[14]

An attractive approach for installing azides into biomolecules is based on metabolic labeling whereby an azide-containing biosynthetic precursor is incorporated into biomolecules using the cells' biosynthetic machinery.[15] This approach has been employed for tagging proteins, glycans, and lipids of living systems with a variety of reactive probes. These probes can facilitate the mapping of saccharide-selective glycoproteins and identify glycosylation sites.[16] Alkyne probes

have also been used for cell surface imaging of azide-modified bio-molecules and a particularly attractive approach involves the generation of a fluorescent probe from a non-fluorescent precursor by a [3+2] cycloaddition.[17]

The cellular toxicity of the Cu^I catalyst has precluded applications wherein cells must remain viable,[18] and hence there is a great need for the development of Cu^I free [3+2] cycloadditions.[19-21] In this respect, alkynes can be activated by ring strain and for example constraining an alkyne within an eight membered ring creates 18 kcal mol^{-1} of strain, much of which is released in the transition state upon [3+2] cyclcoaddition with an azide.[19, 20] As a result, cyclooctynes such as **1** react with azides at room temperature without the need of a catalyst (**Figure 3.1**). The strain-promoted cycloaddition has been used to label biomolecules without observable cyto-toxicitiy.[20] The scope of the approach has, however, been limited due to a slow rate of reaction.[22] Appending electron-withdrawing groups to the octyne ring can increase the rate of strain-promoted cycloadditions, however, currently Staudinger ligation with phosphine **2** offers the most attractive reagent for cell surface labeling of azides.
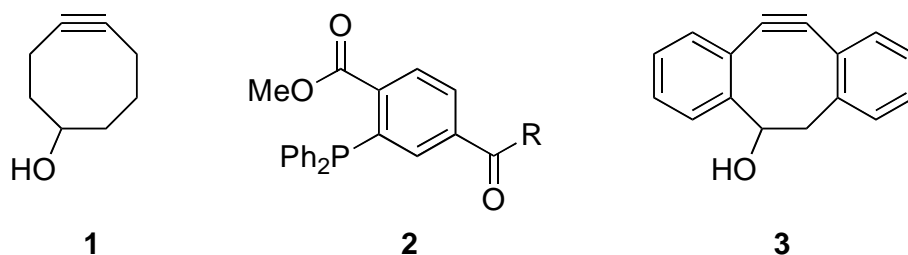
Figure 3.1 Reagents for labeling of azido-containing biomolecules.

It was envisaged that 4-dibenzocyclooctynols such as compound **3** would be ideal for the labeling of azides of living cells because the aromatic rings are expected to impose additional ring strain and conjugate with the alkyne, thereby increasing the reactivity of the alkyne in metal-free [2+3] cycloadditions with azides. The compound should, however, have excellent stability

because the ortho-hydrogens of the aromatic rings shield the alkyne from nucleophilic attack. Furthermore, the hydroxyl of **3** provides a handle for the incorporation of tags such as fluorescent probes and biotin.

3.2 RESULTS AND DISCUSSION

Compound **3** could be easily prepared from known[23, 24] 3-hydroxy-1,2:5,6-dibenzocycloocta-1,5,7-triene (**4**) by protection of the hydroxyl as a *t*-butyldimethyl silyl (TBS) ether using TBSCl in pyridine to give **5**, which was brominated with bromine in chloroform to provide di-bromide **6** in a yield of 60% (**Scheme 1**). Although the TBS protecting group was lost during the latter transformation, the bromination was low yielding when performed on alcohol **4**. Dehydro-bromination of **6** by treatment with LDA in THF at 0°C[25] gave the target cyclooctyne **3** in a yield of 45%.
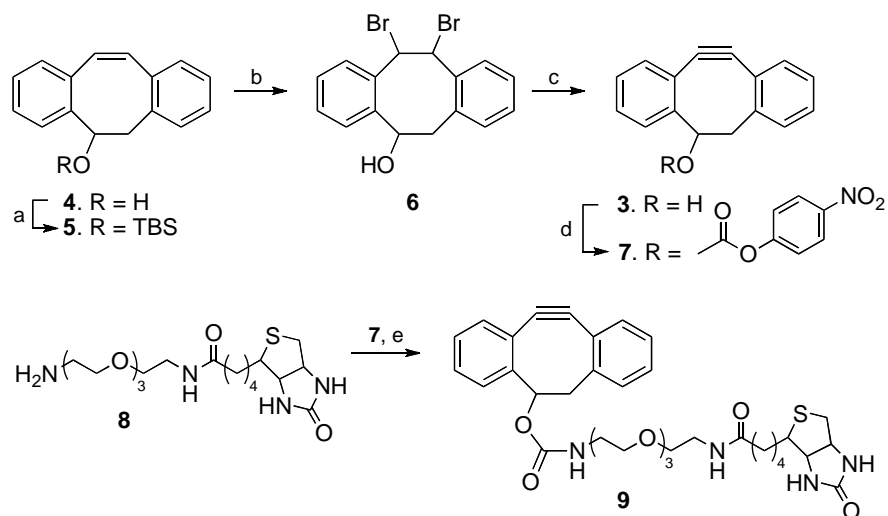
Scheme 3.1 Reagents and conditions. a) TBSCl, pyridine; b) Br$_2$, CHCl$_3$; c) LDA, THF; d) 4-nitrophenyl chloroformate, pyridine, DCM; e) DMF, Et$_3$N.

Compound **3** has an excellent shelf life and remained intact after treatment with nucleophiles such as thiols and amines. However, upon exposure to azides a fast reaction took place and gave the corresponding triazoles in high yield. For example, triazoles **10-13** were obtained in

quantitative yields as mixtures of regioisomers by reaction of the corresponding azido-containing sugar and amino acid derivatives with **3** in methanol for 30 min (**Figure 3.2**). The progress of the reaction of **3** with benzyl azide in methanol and in a mixture of water/acetonitrile (1/4, v/v) was monitored by ^{1}H NMR by integration of the benzylic proton signals and second-rate order constants of 0.17 and 2.3 $M^{-1}s^{-1}$, respectively were determined. The rate constant in acetonitrile/water is approximately three orders of magnitude faster than that of cyclooctyne **1**.

Having established the superior reactivity of **3**, attention was focused on the preparation of a derivative of 4-dibenzocyclooctynol (**9**) (**Scheme 3.1**), which is modified with biotin. Such a reagent should make it possible to visualize biomolecules after metabolic labeling cells with an azido-containing biosynthetic precursor, followed by cycloaddition with **9** and treatment with avidin modified with a fluorescence probe. Alternatively, biotinylation of glycoconjugates with **9** should make it possible to isolate these derivatives for glycocomics studies using avidin immobilized to a solid support. Compound **9** could easily be prepared by a two-step reaction involving treatment of **3** with 4-nitrophenyl chloroformate to give activated intermediate **7**, followed by immediate reaction with **8**.
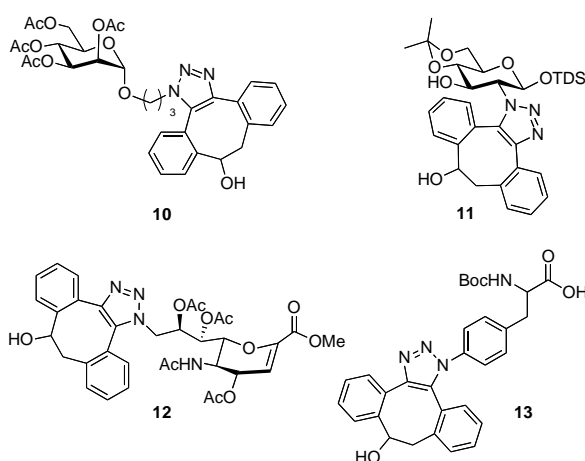
Figure 3.2 Metal free cycloadditons of compound **3** with azido-containing amino acid and saccharides.

Next, Jurkat cells were cultured in the presence of 25 μM of *N*-azidoacetylmannosamine (Ac$_4$ManNAz) for 3 days to metabolically introduce *N*-azidoacetyl-sialic acid (SiaNAz) moieties into glycoproteins.[26] As a negative control, Jurkat cells were employed that were grown in the absence of Ac$_4$ManNAz. The cells were exposed to 30 μM of compound **9** for various time periods and after washing, the cells were stained with avidin-FITC for 15 min at 4°C. The efficiency of the two-step cell surface labeling was determined by measuring the fluorescence intensity of the cell lysates. For comparison, the cell surface azido moieties were also labeled by Staudinger ligation with biotin-modified phosphine **2** followed by treatment with avidin-FITC. The labeling with **9** was almost complete after an incubation time of 60 min (**Figure 3.3a**). Interestingly, under identical conditions phosphine **2**[22] gave significantly lower fluorescent intensities indicating that cell surface labeling by Staudinger ligation is slower and less efficient. In each case, the control cells exhibited very low fluorescence intensities demonstrating that background labeling is negligible. It was found that the two-step labeling approach with **9** had no effect on cell viability as determined by morphology and exclusion of trypan blue.
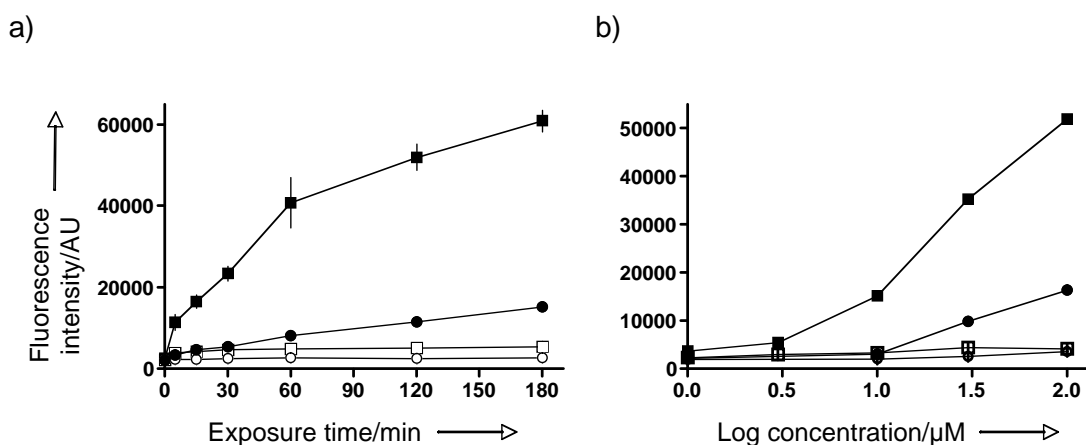
Figure 3.3 Cell surface labeling with compounds **2** and **9**. Jurkat cells grown for 3 days in the absence or presence of Ac$_4$ManNAz (25 μM) were incubated (a) with compounds **2** and **9** (30 μM) for 0 - 180 min or (b) with compounds **2** and **9** (0 - 100 μM) for 1 h at room temperature.

Next, cells were incubated with avidin-FITC for 15 min at 4°C, after which cell lysates were assessed for fluorescence intensity. Samples are indicated as follows: blank cells incubated with **2** (○) or **9** (□) and Ac$_4$ManNAz cells incubated with **2** (●) or **9** (■). AU indicates arbitrary fluorescence units.

The concentration dependency of the cell surface labeling was studied by incubation cells with various concentrations of **2** and **9** followed by staining with avidin-FTIC (**Figure 3.3b**). As expected, cells displaying azido moieties showed a dose-dependent increase in fluorescence intensity. Reliable fluorescent labeling was achieved at a concentration of 3 μM of **9**, however optimal results were obtained at concentrations ranging from 30 to 100 μM. No increase in labeling was observed at concentrations higher than 100 μM due to limited solubility of **9**.

Next, attention was focused on visualizing azido-containing glycoconjugates of living cells by confocal microscopy. Thus, adherent Chinese hamster ovary (CHO) cells were cultured in the presence of Ac$_4$ManNAz (100 μM) for three days. The resulting cell surface azido moieties were reacted with **9** (30 μM) for 1 h, and then visualized with avidin-Alexa fluor 488 for 15 min at 4°C. As expected, staining was only observed at the cell surface (**Figure 3.4**) and importantly, the labeling procedure was equally efficient when performed at ambient temperature or 4°C. Furthermore, blank cells exhibited very low fluorescence staining, confirming that background labeling is negligible.
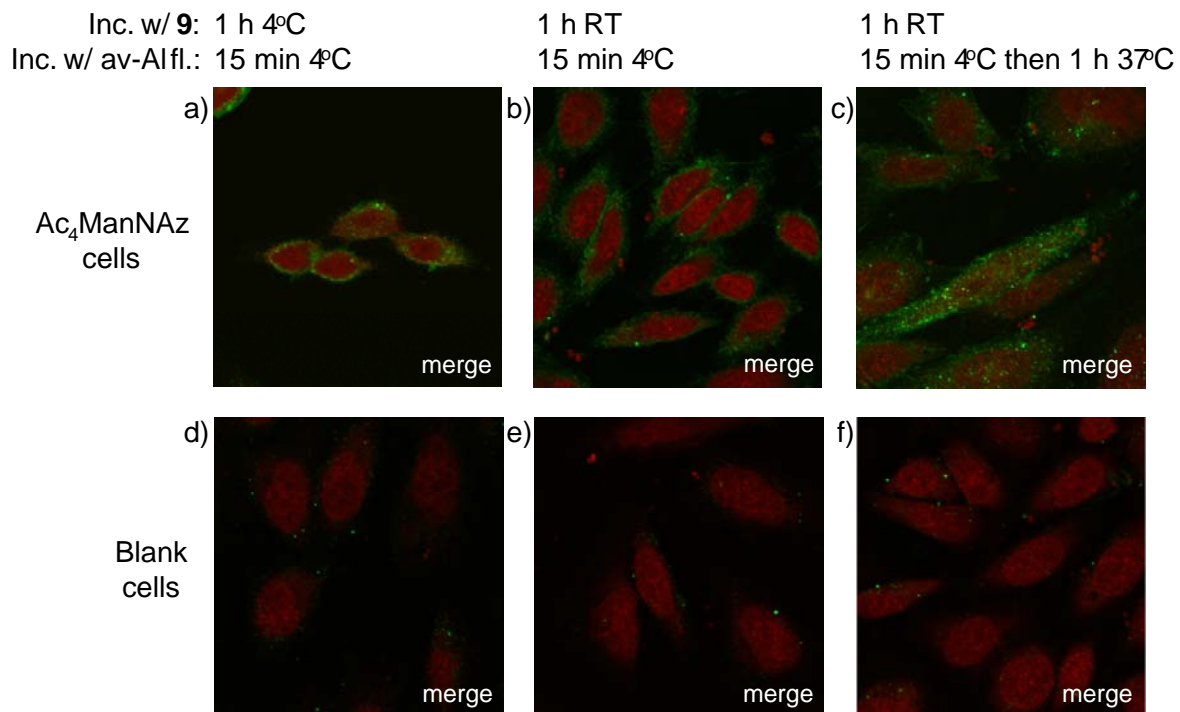
Figure 3.4 Fluorescence images of cells labeled with compound **9** and avidin-Alexa fluor 488. CHO cells grown for 3 days in the absence (d - f) or presence (a - c) of $Ac_4ManNAz$ (100 µM) were incubated with compound **9** (30 µM) for 1 h at 4°C (a, d) or room temperature (b, c, e, f). Next, cells were incubated with avidin-Alexa fluor 488 for 15 min at 4°C and, after washing, fixing, and staining for the nucleus with TO-PRO, imaged (a, b, d, e) or after washing incubated for 1 h at 37°C before fixing, nucleus staining, and imaging (c, f).

Cell surface glycoconjugates are constantly recycled by endocytosis and to monitor this process, metabolically labeled cells were reacted with **9** and avidin-Alexa fluor 488 using the standard protocol and incubated at 37°C for 1 h before examination by confocol microscopy. It was observed that a significant quantity of labeled glycoproteins had been internalized into vesicular compartments.

At the completion of these studies, Bertozzi and coworkers reported a difluorinated cyclooctyne (DIFO) that reacts with azides at almost the same reaction rate as compound **3**.[27]

DIFO linked to Alexa fluor was employed to investigate the dynamics of glycan trafficking. It was found that after incubation for 1 h, labeled glycans co-localized with markers for endosomes and Golgi.

CONCLUSIONS

4-Dibenzocyclooctynols such as **3** and **9** have several advantageous features such as ease of chemical synthesis and the possibility to further enhance the rate of cycloaddition by functionalization of the aromatic moieties. Modifying the aromatic rings may also offer an exciting opportunity to obtain reagents that become fluorescent upon [3+2] cycloaddition with azido-containing compounds, which will make it possible to monitor in real time the trafficking of glycoproteins and other biomolecules in living cells. These novel results constitute a significant step-forward for the selective functionalization and ligation of biological entities. Thus, cyclooctyne-based ligations could become important tools in chemical biology but also in some specific areas of materials science, where the use of transition-metal catalysts is problematic. In addition, these novel reactions appear as appealing "biologically friendly" complementary tools in the growing set of straightforward "click" reactions.

3.3 EXPERIMENTAL PROCEDURES

General Methods and Materials Chemicals were purchased from Aldrich and Fluka and used without further purification. Dichloromethane was distilled from CaH_2 and stored over molecular sieves 4 Å. Pyridine was distilled from P_2O_5 and stored over molecular sieves 4 Å. THF was distilled form sodium. All reactions were performed under anhydrous conditions under an atmosphere of Argon. Reactions were monitored by TLC on Kieselgel 60 F254 (Merck). Detection was by examination under UV light (254 nm) or by charring with 5% sulfuric acid in methanol. Flash chromatography was performed on silica gel (Merck, 70-230 mesh). Iatrobeads

(60 μm) were purchased from Bioscan. ^{1}H NMR (1D, 2D) and ^{13}C NMR were recorded on a Varian Merc 300 spectrometer and on Varian 500 and 600 MHz spectrometers equipped with Sun workstations. ^{1}H and ^{13}C NMR spectra were recorded in CDCl$_3$, and chemical shifts (δ) are given in ppm relative to solvent peaks (^{1}H, δ 7.24; ^{13}C, δ 77.0) as internal standard for protected compounds. Negative ion matrix assisted laser desorption ionization time of flight (MALDI-TOF) were recorded on a VOYAGER-DE Applied Biosystems using dihydrobenzoic acid as a matrix. High-resolution mass spectra were obtained using a VOYAGER-DE Applied Biosystems in the positive mode by using 2,5-dihydroxyl-benzoic acid in THF as matrix.

3-*tert*-Butyl-dimethylsilyl-oxy-1,2:5,6-dibenzocycloocta-1,5,7-triene (**5**) To a stirred solution of **4** (2.2 g, 10 mmol) in a mixture of CH$_2$Cl$_2$ (20 mL) and pyridine (5 mL) was added *tert*-butyl dimethyl silyl chloride (3.0 g, 20 mmol). After stirring for 6 h at room temperature, the reaction mixture was diluted with water and extracted with CH$_2$Cl$_2$ (40 mL). The combined organic extracts were washed with water, brine and dried (MgSO$_4$). The solvents were evaporated under reduced pressure and the residue was purified by silica gel column chromatography (hexane/ethyl acetate, 7/1, v/v) to afford **5** (2.9 g, 87%). ^{1}H NMR (300 MHz, CDCl$_3$): δ 7.60 (1 H, aromatics), 7.32-7.11 (7 H, aromatics), 6.93 (1 H, d, J = 7.5 Hz, C*H*=CH), 6.85 (1 H, d, J = 7.5 Hz, C*H*=CH), 5.51 (1 H, dd, J = 6.3, 9.6 Hz, C*H*OSi), 3.54 (1 H, dd, J = 6.3, 9.6 Hz, C*H$_2$*), 3.21(1 H, dd, J = 6.3, 9.6 Hz, C*H*), 0.96 (3 H, s, C*H$_3$*), 0.95 (3 H, s, C*H$_3$*), 0.94 (3 H, s, C*H$_3$*), 0.10 (3 H, s, C*H$_3$*), 0.07 (3 H, s, C*H$_3$*); ^{13}C NMR (75 MHz, CDCl$_3$): δ 148.0, 141.6, 140.8, 139.2, 138.3, 135.5, 135.0, 134.9, 133.0, 131.9, 131.6, 130.9, 130.8, 130.2, 77.0, 52.1, 34.5, 30.7, 30.5, 23.1, 5.8, 0.1; MALDI HRMS: m/z 359.1811 [M + Na^{+}]. Calcd for C$_{22}$H$_{28}$NaOSi 359.1807.

3-Hydroxy-7,8-dibromo-1,2:5,6-dibenzocyclooctene (6) A solution of bromine (0.8 g, 5 mmol) in CHCl$_3$ was added dropwise to a solution of **5** (1.7g, 5 mmol) in CHCl$_3$ (30 mL) at 0°C. The reaction mixture was stirred at room temperature for 12 h until the reaction was complete (monitored by TLC). The resulting mixture was washed with aqueous saturated sodium thiosulfate solution (15 mL), and dried (MgSO$_4$). The solvents were evaporated under reduced pressure and the residue was purified by silica gel column chromatography (hexane/CH$_2$Cl$_2$, 7/1, v/v) to afford **6** (1.2 g, 60%). ^{1}H NMR (300 MHz, CDCl$_3$): δ 7.54-7.47 (2 H, aromatics), 7.31-6.72 (6 H, aromatics), 5.77 (1 H, d, J = 5.4 Hz, C*H*Br), 5.22 (1 H, dd, J = 3.6, 15.9 Hz, C*H*OH), 5.19 (1 H, d, J = 5.4 Hz, C*H*Br), 3.50 (1 H, dd, J = 3.6, 15.9 Hz, C*H*$_2$), 2.75(1 H, dd, J = 3.6, 15.9 Hz, C*H*$_2$); ^{13}C NMR (75 MHz, CDCl$_3$): δ 141.3, 140.0, 137.2, 134.0, 133.4, 131.5, 131.3, 130.9, 127.8, 126.2, 123.7, 121.3, 76.5, 70.0, 62.3, 32.2; MALDI HRMS: m/z 402.9313 [M + Na$^+$]. Calcd for C$_{16}$H$_{14}$Br$_2$NaO 402.9309.

3-Hydroxy-7,8-didehydro-1,2:5,6-dibenzocyclooctene (3) To a solution of **6** (1.1 g, 3 mmol) in tetrahydrofuran (50 mL) was added dropwise lithium diisopropylamide in tetrahydrofuran (2.0 M), (5 mL) under an atmosphere of Argon at room temperature. The reaction mixture was stirred for 2h at rt, after which it was poured into ice water (50 mL) and the resulting mixture was extracted with CH$_2$Cl$_2$ (2 x 100 mL). The combined extracts were washed with water, brine and dried (MgSO$_4$) and the solvents were evaporated under reduced pressure. The residue was purified by silica gel column chromatography (hexane/ethyl acetate, 5/1, v/v) to afford **3** (0.30 g, 45%).^{1}H NMR (300 MHz, CDCl$_3$): δ 7.67 (1 H, aromatics), 7.37-7.18 (7 H, aromatics), 4.57 (1 H, dd, J = 2.1, 14.7 Hz, C*H*OH), 3.04 (1 H, dd, J = 2.1, 14.7 Hz, C*H*$_2$), 2.86(1 H, dd, J = 2.1, 14.7 Hz, C*H*$_2$); ^{13}C NMR (75 MHz, CDCl$_3$): δ 154.5, 150.6, 128.6, 127.1, 1127.0, 126.0, 125.8, 125.1, 124.7, 123.0, 122.7, 121.7, 111.9, 109.6, 74.2, 47.7.

Carbonic acid, 7, 8-didehydro-1,2:5,6-dibenzocyclooctene-3-yl ester, 4-nitrophenyl ester

(7) To a solution of **3** (0.22 g, 1 mmol) in CH_2Cl_2 (30 mL) was added 4-nitro-phenyl chloroformiate (0.4 g, 2 mmol) and pyridine (0.4 ml, 5 mmol). After stirring 4 h at ambient temperature, the reacting mixture was washed with brine (2 x10 mL), and the organic layer was dried ($MgSO_4$). The solvents were evaporated under reduced pressure. And the residue was purified by silica gel column chromatography (hexane/ethyl acetate, 10/1, v/v) to afford gives **7** (0.34 g, 89%). ^1H NMR (300 MHz, $CDCl_3$): δ 8.23-8.18 (2 H, aromatics), 7.56-7.54 (2 H, aromatics), 7.46-7.18 (8 H, aromatics), 5.52 (1 H, dd, J = 3.9, 15.3 Hz, C*H*OH), 3.26 (1 H, dd, J = 3.9, 15.3 Hz, C*H₂*), 2.97 (1 H, dd, J = 3.9, 15.3 Hz, C*H₂*); ^{13}C NMR (75 MHz, $CDCl_3$): δ 154.5, 150.7, 149.1, 148.7, 129.0, 127.4, 127.3, 126.7, 126.5, 125.5, 125.2, 124.3, 124.0, 122.6, 122.4, 120.8, 120.6, 120.2, 112.2, 108.5, 80.6, 44.8; MALDI HRMS: m/z 408.0852 [M + Na^+]. Calcd for $C_{23}H_{15}NNaO_5$ 408.0848

Compound: Carbonic acid,7,8-didehydro-1,2:5,6-dibenzocyclooctene-3-yl ester，8'-biotinylamine-3',6'-dioxaoctane 1'-amide (9) To a solution of **8** (37 mg, 0.1 mmol) and NEt_3 (30 mg, 0.3 mmol) in DMF (10 mL) was added the **7** (39 mg, 0.1 mmol) under an atmosphere of Argon. After stirring the reaction mixture overnight at ambient temperature, the solvent was removed under reduced pressure and the residue was purified by silica gel column chromatography (CH_2Cl_2/CH_3OH, 20/1, v/v) to afford **9** (44 mg, 71%). ^1H NMR (500 MHz, CD_3OD): δ 7.59 (1 H, aromatics), 7.42-7.33 (7 H, aromatics), 5.44, (1 H, dd, J = 5.0, 14.1 Hz, C*H*OH), 4.60, 4.46 (m, 2H, C*H*NH), 4.24 (s, 4H, OC*H₂*C*H₂*O), 3.72 (m, 4H, OC*H₂*), 3.64 (m, 2H, C*H₂*NH), 3.55 (m, 1H, C*H*S), 3.33 (dd, 1H, $J1$ = 12.0 Hz, $J2$ = 4.8 Hz, 1H, CH*Hexo*S), 3.23 (t, 2H, J = 6 Hz, C*H₂*–NH₂), 3.22, (1 H, dd, J = 5.0, 14.1 Hz, C*H₂*), 2.88, (1 H, dd, J = 5.0, 14.1 Hz, C*H₂*), 2.68 (d, 1H, J = 12.45 Hz, CH*Hendo*S), 2.20 (t, 2H, J = 7.5 Hz, *CH₂*CO), δ 1.4 (m, 6H,

biotin-C*H₂*; . ¹³C NMR (75 MHz, CD₃OD): δ 175.0, 164.9, 156.9, 152.5, 151.3, 129.9, 128.2, 128.1, 127.2, 127.1, 126.0, 125.7, 123.8, 121.2, 112.7, 109.8, 76.8, 70.2, 70.1, 69.8, 69.4, 62.1, 60.4, 55.8, 54.6, 46.0, 42.6, 40.6, 39.9, 39.1, 35.5, 28.6, 28.3, 25.6, 17.5, 16.1, 12.0; MALDI HRMS: m/z 643.2575 [M + Na⁺]. Calcd for $C_{33}H_{40}N_4NaO_6S$ 643.2566.

General procedure for click reactions with carbohydrates and peptides 3-Hydroxy-7,8-didehydro-1,2:5,6-dibenzocyclooctene (2.2 mg, 0.01 mmol) was dissolved in CH₃OH (1 mL) and an azide (3-azidopropyl 2,3,4,6-tetra-*O*-acetate-α-D-mannopyranoside, 1-*O*- [dimethyl(1,1,2-trimethylpropyl)silyl]-4,6-*O*-isopropylidene-2-azido-2-deoxy-β-glucopyranose, 4,7,8-tri-*O*-acetyl-5-acetamido-9-azido-2,3-anhydro-3,5,9-tri-deoxy-D-glycero-D-galacto-non-2-enonic methyl ester, and 4-azido-*N*-[(1,1-dimethylethoxy)carbonyl]-L-phenylalanine, 1.0 quivalent) was added. The reaction was monitored by TLC, and after stirring the reaction mixture for 30 min at room temperature, the reaction had gone to completion. The solvents were evaporated under reduced pressure and the residue was purified by silica gel column chromatography to afford the desired products **10-13** respectively in quantitative yields. Solvent systems of column chromatography**: 10** (hexane/ EtOAc, 1/1, v/v), **11** (hexane/ EtOAc, 2/1, v/v), **12** (hexane/ Acetone, 1/1, v/v), and **13** (CH₂Cl₂/CH₃OH, 20/1, v/v).

Compound 10: ¹H NMR (500 MHz, CDCl₃): δ 7.83 (1 H, m, aromatics), 7.58-6.99 (7H, m, aromatics), 5.33-4.98 (4H, m, 2-*H*, 3-*H*, 4-*H*, C*H*OH), 4.90-4.61 (1H, m, 1-*H*), 4.26,4.10 (2 H, m, 6-*H*), 3.93 (1 H, m, 5-*H*), 3.70-3.60 (2 H, m, OC*H₂*CH₂), 3.58-3.41 (2H, m, C*H₂*N), 3.31,3.20,3.06, 2.91 (2 H, m, CHOHC*H₂*), 2.35-1.94 (12H, m, C*H₃*CO), 1.38-1.14 (2H, m, C*H₂*CH₂N); ¹³C NMR (75 MHz, CDCl₃): δ 170.9, 170.2, 148.5, 146.9, 145.5, 144.9, 141.2, 139.3, 138.0, 136.7, 135.5, 133.8, 133.0, 132.3, 131.6, 130.3, 129.5, 129.0, 128.3, 127.7, 127.2, 126.5, 125.0, 124.2, 98.0, 97.4, 70.1, 69.5, 68.8, 66.2, 65.4, 64.9, 64.4, 62.6, 47.0, 45.1, 40.5,

32.1, 31.1, 30.6, 29.9, 22.9, 20.9, 14.3; MALDI HRMS: m/z 674.2330 [M + Na$^+$]. Calcd for C$_{33}$H$_{37}$N$_3$NaO$_{11}$ 674.2326.

Compound 11: ^{1}H NMR (500 MHz, CDCl$_3$): δ 7.80, 7.65 (1H, d, J =7.5 Hz, aromatics), 7.48-7.06 (7 H, aromatics), 5.82, 5.72, 5.60, 5.48 (1 H, d, J = 7.09 Hz, 1-H), , 5.13-4.60 (1H, m, CHOH), 4.40-4.20 (2 H, m, 2-H, 3-H), 4.10-3.90 (2H, m, 5-H, 6-H), 3.89-3.63 (1H, m, 6-H), 3.54-3.40 (2 H, m, 4-H, HCHCHOH), 3.07,2.66 (1H, m, HCHCHOH), 1.54-1.20 (6 H, m, CH(CH$_3$)C(CH_3)$_2$), 0.98-0.60 (13 H, m, 2 CH_3, CH(CH$_3$)$_2$), 0.35-0.19 (6H, m, Si(CH_3)$_2$); ^{13}C NMR (75 MHz, CDCl$_3$): δ 151.0, 149.2, 148.5, 148.0, 146.1, 145.3, 142.4, 141.6, 140.8, 139.4, 138.1, 136.6, 135.7, 134.9, 133.4, 132.4, 131.6, 130.6, 129.5, 128.9, 127.3, 103.5, 100.4, 99.8, 80.6, 73.3, 70.9, 69.3, 68.8, 65.5, 50.1, 46.6, 45.4, 44.4, 37.3, 33.3, 32.5, 28.4, 23.4, 22.6, 21.9, 4.6, 1.4, 0.7, 0.0; MALDI HRMS: m/z 630.2980 [M + Na$^+$]. Calcd for C$_{33}$H$_{45}$N$_3$NaO$_6$Si 630.2975.

Compound 12: ^{1}H NMR (500 MHz, CDCl$_3$): δ 7.95-7.69 (1 H, m, aromatics), 7.60-7.03 (7 H, m, aromatics), 6.77-6.26 (1 H, m), 5.98-8.81(1H, m), 5.80-5.61 (1 H, m), 5.58-5.33 (1 H, m), 5.32-5.16 (2 H, m), 5.16-4.94 (1 H, m), 4.93-4.80 (1 H, m), 4.69-4.34 (1 H, m), 4.24-4.06 (1 H, m), 3.95-3.60 (3H, m), 3.53-2.90 (2 H, m), 2.32-1.57 (12 H, m); ^{13}C NMR (75 MHz, CDCl$_3$): δ 169.6, 160.5, 147.8, 145.5, 145.1, 144.6, 143.9, 140.5, 138.7, 138.2, 137.1, 135.7, 134.5, 133.5, 132.7, 132.2, 131.8, 131.2, 130.8, 129.5, 129.0, 128.3, 127.7, 127.2, 126.5, 125.9, 124.8, 122.7, 108.0, 107.5, 75.1, 69.6, 68.8, 67.1, 66.6, 52.8, 51.7, 47.3, 46.4, 45.3, 28.7, 28.3, 22.0, 19.8; MALDI HRMS: m/z 699.2282 [M + Na$^+$]. Calcd for C$_{34}$H$_{36}$N$_4$NaO$_{11}$ 699.2278.

Compound 13: ^{1}H NMR (300 MHz, CD$_3$OD): δ 7.8-6.8 (12H, m, aromatics), 5.33, 5.17 (1H, dd, J= 5.1, 10.5 Hz CHOH), 4.37 (1H, m, CHCOOH), 3.8, 3.23 3.77, 3.20 (2H, m, CH_2CHOH), 3.21, 2.93 (2H, m, CH_2CHNH), 1.35(9H, m, C(CH_3)$_3$); ^{13}C NMR (75 MHz,

CD$_3$OD): δ 156.6, 145.1, 414.3, 139.6, 139.4, 138.0, 137.3, 136.1, 135.3, 135.0, 133.7, 133.4, 132.1, 131.7, 130.6, 130.3, 130.0, 129.5, 129.2, 128.8, 128.3, 128.0, 127.6, 126.9, 126.6, 126.6, 126.2, 125.3, 125.1, 124.8, 79.4, 76.8, 76.2, 68.6, 58.5, 54.9, 46.2, 40.5, 37.1, 29.6, 29.3, 27.5; MALDI HRMS: m/z 549.2118 [M + Na$^+$]. Calcd for C$_{30}$H$_{30}$N$_4$NaO$_5$ 549.2114.

(a) *N*-Boc-3,6-dioxaoctane-1,8-diamine. A solution of di-*tert*-butyl dicarbonate (di-Boc) (6 g, 28 mmol, 0.5 equiv) in CH$_2$Cl$_2$ (100 mL) was added dropwise to a mixture of tris(ethylene glycol)-1,8-diamine (7.6 g, 56 mmol) and diisopropylethylamine (10 mL, 57 mmol) at room temperature over a period of 2h. The reaction mixture was stirred for 6 h, after which it was concentrated *in vacuo*. Purification by flash silica gel chromatography (CH$_2$Cl$_2$/CH$_3$OH, 10/1, v/v) afforded products (4.1 g, 58%). ^{1}H NMR (300 MHz, CD$_3$OD): δ 3.6 (s, 4H), 3.54 (t, 2H), 3.53 (t, 2H), 3.24 (t, 2H), 2.8 (t, 2H), 1.4 (s, 9H); MALDI HRMS: m/z 271.1641 [M + Na$^+$]. Calcd for C$_{11}$H$_{24}$N$_2$NaO$_4$ 271.1634.

(b) *N*-Boc-*N*'-biotinyl-3,6-dioxaoctane-1,8-diamine. A solution of vitamin H (Biotin) (2.2 g, 9 mmol), O-Benzotriazol-1-yl-*N,N,N′,N′*-tetramethyluronium hexapfluorophosphate (HBTU) (3 g, 8 mmol), and DIPEA (1.8 mL, 10 mmol) in DMF (100 mL) was stirred for 10 min at room temperature before being adding dropwise to a solution of *N*-Boc-3,6-dioxaoctane-1,8-diamine (1.5 g, 6 mmol, 1.0 equiv). The reaction mixture was stirred for 1 h at room temperature, after which the DMF was removed *in vacuo* to give an oil. The residue was purified by flash silica gel chromatography (CH$_2$Cl$_2$/CH$_3$OH, 25/1, v/v) to afford Comop (2.0 g , 90%). ^{1}H NMR (300 MHz, CD$_3$OD): δ 4.5 (m, 1H), 4.3 (m, 1H), 3.6 (s, 4H), 3.54 (tt, 4H), 3.39 (t, 2H), 3.26 (t, 2H), 2.9 (dd, 1H), 2.7 (d, 1H), 2.2 (t, 2H), 1.7-1.5 (m, 8H), 1.4 (s, 9H); MALDI HRMS: m/z 497.2416 [M + Na$^+$]. Calcd for C$_{21}$H$_{38}$N$_4$NaO$_6$S 497.2410.

(c) *N*-Biotinyl-3,6-dioxaoctane-1,8-diamine. *N*-Boc-*N*'-biotinyl-3,6-dioxaoctane-1,8-

diamine (1.9 g, 4 mmol) was dissolved in 50% TFA in CH_2Cl_2 (20 mL) and stirred for 1 h at room temperature. The solvents were evaporated under reduced pressure to give an oil, which was purified by flash silica gel chromatography (CH_2Cl_2/CH_3OH, 10/1, v/v) to afford **7** (1.3 g, 92%). ^{1}H NMR (300MHz, DMSO-d$_6$): δ 7.85 (t, 1H, $J = 5.7$ Hz, N*H*CO), 6.42, 6.35 (s, 2H, N*H*), 4.29, 4.11 (m, 2H, C*H*NH), 3.5 (s, 4H, OC*H$_2$*C*H$_2$*O), 3.3 (m, 4H, OC*H$_2$*), 3.16 (m, 2H, C*H$_2$*NH), 3.10 (m, 1H, C*H*S), 2.81 (dd, 1H, $J1 = 12.0$ Hz, $J2 = 4.8$ Hz, 1H, CH*Hexo*S), 2.64 (t, 2H, $J = 6$ Hz, C*H$_2$*–NH$_2$), 2.52 (d, 1H, $J = 12.45$ Hz, CH*Endo*S), 2.06 (t, 2H, $J = 7.5$ Hz, C*H$_2$*CO), 1.6 (s, 2H, N*H$_2$*), δ 1.4 (m, 6H, biotin-C*H$_2$*); ^{13}C NMR (75 MHz, DMSO-d$_6$): δ 171.9, 160.6, 71.7, 71.6, 69.5, 69.1, 64.4, 59.2, 55.0, 54.2, 40.7, 38.4, 35.1, 28.4, 28.1, 25.2; MALDI HRMS: m/z 397.1892 [M + Na$^+$]. Calcd for $C_{16}H_{30}N_4NaO_4S$ 397.1885

Reagents for biological experiments

Synthetic compounds **2** and **9** were reconstituted in DMF and stored at –80°C. Final concentrations of DMF never exceeded 0.56% to avoid toxic effects.

Cell surface azide labeling and detection by fluorescence intensity

Human Jurkat cells (Clone E6-1; ATCC) were cultured in RPMI 1640 medium (ATCC) with Lglutamine (2 mM), adjusted to contain sodium bicarbonate (1.5 g L^{-1}), glucose (4.5 g L–1), HEPES (10 mM), and sodium pyruvate (1.0 mM) and supplemented with penicillin (100 umL^{-1})/ streptomycin (100 μg mL^{-1}; Mediatech) and fetal bovine serum (FBS, 10%; Hyclone). Cells were maintained in a humid 5% CO_2 atmosphere at 37°C. Jurkat cells were grown in the presence of peracetylated *N*-azidoacetylmannosamine (Ac4ManNaz; 25 μM final concentration) for 3 days, leading to the metabolic incorporation of the corresponding *N*-azidoacetyl sialic acid (SiaNAz) into their cell surface glycoproteins. Jurkat cells bearing azides and untreated control cells were incubated with the biotinylated compounds **2** and **9** (0-100 μM) in labeling buffer

(DPBS, supplemented with FBS (1%)) for 0-180 min at room temperature. The cells were washed three times with labeling buffer and then incubated with avidin conjugated with fluorescein (Molecular Probes) for 15 min at 4°C. Following three washes and cell lysis, cell lysates were analysed for fluorescence intensity (485 ex / 520 em) using a microplate reader (BMG Labtech). Data points were collected in triplicate and are representative of three separate experiments. Cell viability was assessed at different points in the procedure with exclusion of trypan blue.

Cell labeling and detection by fluorescence microscopy

Chinese hamster ovary (CHO) cells (Clone K1; ATCC) were cultured in Kaighn's modification of Ham's F-12 medium (F-12K) with L-glutamine (2 mM), adjusted to contain sodium bicarbonate (1.5 g L^{-1}) and supplemented with penicillin (100 u mL^{-1}) / streptomycin (100 μg mL^{-1} and FBS (10%). Cells were maintained in a humid 5% CO_2 atmosphere at 37°C. CHO cells were grown in the presence of Ac4ManNaz (100 μM final concentration) for 3 days to metabolically incorporate SiaNAz into their cell surface glycoproteins. CHO cells bearing azides and untreated control cells were then transferred to a glass coverslip and cultured for 36 h in their original medium. Live CHO cells were treated with the biotinylated compound **9** (30 μM) in labeling buffer (DPBS, supplemented with FBS (1%)) for 1 h at 4°C or at room temperature, followed by incubation with avidin conjugated with Alexa Fluor 488 (Molecular Probes) for 15 min at 4°C. Cells were washes 3 times with labeling buffer and fixed with formaldehyde (3.7% in PBS) or incubated for 1 h at 37°C before fixation. The nucleus was labeled with the far redfluorescent TO-PRO-3 dye (Molecular Probes). The cells were mounted with PermaFluor (Thermo Electron Corporation) before imaging. Initial analysis was performed on a Zeiss Axioplan2 fluorescent microscope. Confocal images were acquired using a 60X (NA1.42) oil

objective. Stacks of optical sections were collected in the *z* dimensions. The step size, based on the calculated optimum for each objective, was between 0.25 and 0.5 μm. Subsequently, each stack was collapsed into a single image (*z*-projection). Analysis was performed offline using ImageJ 1.39f software (National Institutes of Health, USA) and Adobe Photoshop CS3 Extended Version 10.0 (Adobe Systems Incorporated), whereby all images were treated equally.

Figure 3.5 Toxicity assessment of cell labeling procedure and cycloaddition reaction with compound **9**. Jurkat cells grown for 3 days in the absence (a) or presence (b) of Ac4ManNAz (25 μM) were incubated with compound **9** (0 - 100 μM) for 1 h at room temperature. The cells were washed three times and then incubated with avidin conjugated with fluorescein for 15 min at 4°C, after which cells were washed three times. Cell viability was assessed at different points during the procedure with trypan blue exclusion; after incubation with **9** (black), after avidin-FITC incubation (grey), and after complete procedure (white). Treatment with $Cu^{I}Cl$ (1mM) under the same conditions let to approximately 98% cell death for both the blank and the $Ac_4ManNAz$ treated cells.
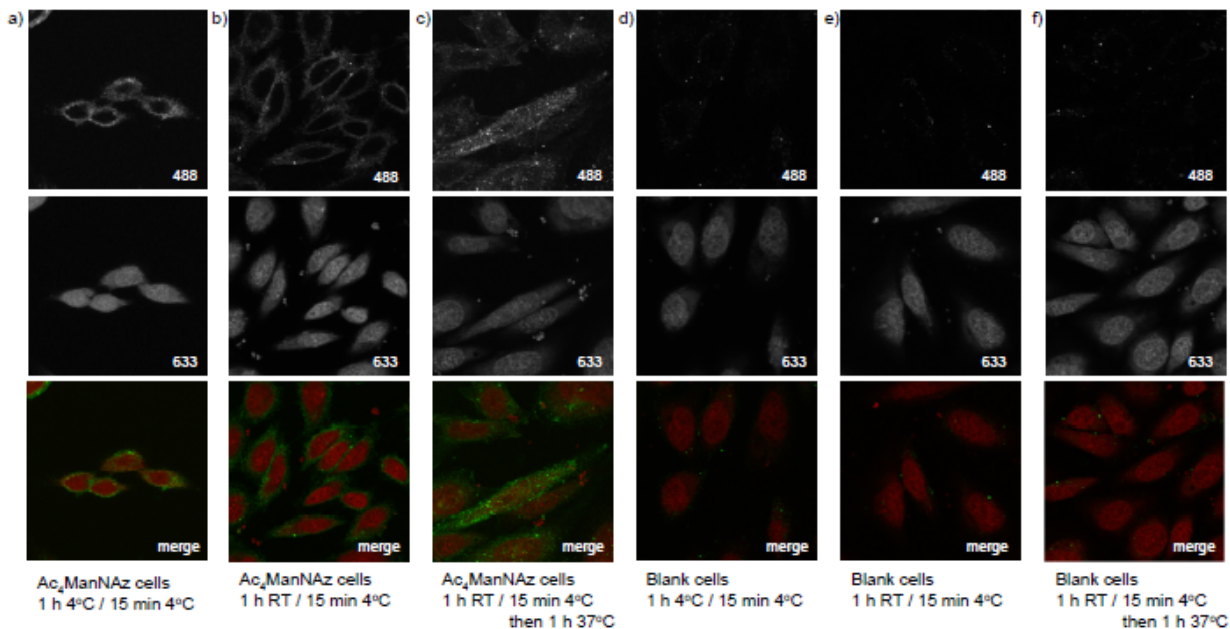
Figure3.6 Fluorescence images of cells labeled with compound **9** and avidin- Alexa fluor 488. CHO cells grown for 3 days in the absence (d-f) or presence (a-c) of Ac₄ManNAz (100 μM) were incubated with compound **9** (30 μM) for 1 h at 4°C (a, d) or room temperature (b, c, e, f). Next, cells were incubated with avidin-Alexa fluor for 15 min at 4°C and, after washing, fixing, and staining for the nucleus with TO-PRO, imaged (a, b, d, e) or after washing incubated for 1 h at 37°C before fixing, nucleus staining, and imaging (c, f).

3.4 REFERENCE

1. H. C. Kolb, K. B. Sharpless, *Drug Dis. Today* 2003, *8*, 1128

2. S. Dedola, S. A. Nepogodiev, R. A. Field, *Org. Biomol. Chem.* 2007, *5*, 1006

3. J. E. Moses, A. D. Moorhouse, *Chem. Soc. Rev.* 2007, *36*, 1249

4. H. Nandivada, X. W. Jiang, J. Lahann, *Adv. Mater.* 2007, *19*, 2197

5. P. Wu, V. V. Fokin, *Aldrichim. Acta* 2007, *40*, 7

6. V. V. Rostovtsev, L. G. Green, V. V. Fokin, K. B. Sharpless, *Angew. Chem. Int. Ed.* 2002, *41*, 2596

7. C. W. Tornoe, C. Christensen, M. Meldal, *J. Org. Chem.* 2002, *67*, 3057

8. J. W. Chin, T. A. Cropp, J. C. Anderson, M. Mukherji, Z. W. Zhang, P. G. Schultz, *Science* 2003, *301*, 964

9. Q. Wang, T. R. Chan, R. Hilgraf, V. V. Fokin, K. B. Sharpless, M. G. Finn, *J. Am. Chem. Soc.* 2003, *125*, 3192

10. Y. Kho, S. C. Kim, C. Jiang, D. Barma, S. W. Kwon, J. K. Cheng, J. Jaunbergs, C. Weinbaum, F. Tamanoi, J. Falck, Y. M. Zhao, *Proc. Natl. Acad. Sci.* 2004, *101*, 12479

11. J. Gierlich, G. A. Burley, P. M. E. Gramlich, D. M. Hammond, T. Carell, *Org. Lett.* 2006, *8*, 3639

12. A. J. Link, M. K. S. Vink, N. J. Agard, J. A. Prescher, C. R. Bertozzi, D. A. Tirrell, *Proc. Natl. Acad. Sci.* 2006, *103*, 10180

13. A. E. Speers, G. C. Adam, B. F. Cravatt, *J. Am. Chem. Soc.* 2003, *125*, 4686

14. X. L. Sun, C. L. Stabler, C. S. Cazalis, E. L. Chaikof, *Bioconjugate Chem.* 2006, *17*, 52

15. J. A. Prescher, C. R. Bertozzi, *Nat. Chem. Biol.* 2005, *1*, 13

16. S. R. Hanson, T. L. Hsu, E. Weerapana, K. Kishikawa, G. M. Simon, B. F. Cravatt, C. H. Wong, *J. Am. Chem. Soc.* 2007, *129*, 7266

17. K. Sivakumar, F. Xie, B. M. Cash, S. Long, H. N. Barnhill, Q. Wang, *Org. Lett.* 2004, *6*, 4603

18. A. J. Link, D. A. Tirrell, *J. Am. Chem. Soc.* 2003, *125*, 11164

19. R. B. Turner, P. Goebel, B. J. Mallon, A. D. Jarrett, *J. Am. Chem. Soc.* 1972, *95*, 790

20. N. J. Agard, J. A. Prescher, C. R. Bertozzi, *J. Am. Chem. Soc.* 2004, *126*, 15046

21. S. S. van Berkel, A. T. J. Dirks, M. F. Debets, F. L. van Delft, J. J. L. M. Cornelissen, R. J. M. Nolte, F. P. J. T. Rutjes, *Chembiochem* 2007, *8*, 1504

22. N. J. Agard, J. M. Baskin, J. A. Prescher, A. Lo, C. R. Bertozzi, *ACS Chem. Biol.* 2006, *1*, 644

23. M. E. Jung, A. B. Mossman, M. A. Lyster, *J. Org. Chem.* 1978, *43*, 3698

24. M. E. Jung, S. J. Miller, *J. Am. Chem. Soc.* 1981, *103*, 1984

25. G. Seitz, L. Pohl, R. Pohlke, *Angew. Chem.* 1969, *81*, 427-428; *Angew. Chem. Int. Ed.* 1969, *8*, 447

26. S. J. Luchansky, C. R. Bertozzi, *Chembiochem* 2004, *5*, 1706

27. J. M. Baskin, J. A. Prescher, S. T. Laughlin, N. J. Agard, P. V. Chang, I. A. Miller, A. Lo, J. A. Codelli, C. R. Bertozzi, *Proc. Natl. Acad. Sci.* 2007, *104*, 16793

CHAPTER 4

PROBING SIALYLATED GLYCANS *IN VIVO* USING NOVEL QUANTITATIVE PROTEOMICS

ABSTRACT

Sialic acids are widely expressed as terminal carbohydrates on glycoconjugates of eukaryotic cells. Sialylation is crucial for a variety of cellular functions, such as cell adhesion or signal recognition, and regulates the biological stability of glycoproteins. However, it is challenge to understand the signaling pathways and cellular mechanisms that regulate sialylation due to the difficulty of detecting and quantifying the modification. Therefore, developing strategies for investigating the sialylation will be useful for elucidating biological functions of glycans. Here, we demonstrate a novel quantitative isotopic and chemoenzymatic tagging (QUIC-Tag) for monitoring the dynamics of sialylation using quantitative mass spectrometry-based proteomics. This method, which combines selective, chemoenzymatic tagging of glycans with an efficient isotopic labeling strategy can also be cooperated with metabolic oligosaccharide engineering, which incorporate sugar with bioorthogonal chemical reporters into cellular glycoconjugates. These reporters are considered as handles for dynamics of glycans and isolating them for glyco-proteomic analysis. Here, we employed azide-functionalized mannosamine into living cell, which convert to azide functionalized sialic acid in cell-surface glycoconjugates *via* the biosynthetic pathway. As sialic acid is terminal glycan residues with a notably increased presence in cancers, this method will contribute to delineate the molecular basis for aberrant glycosylation in cancer and could ultimately be applied for diagnostic and therapeutic.

4.1 INTRODUCTION

Glycosylation, which is the enzymatic process that joins saccharides to generate glycans, either free or attached to proteins and lipids, is an important posttranslational modification affecting >50% of the proteins from eukaryotic cells.[1] Glycosylation generates one of four fundamental elements of all cells (along with proteins, nucleic acids, and lipids) and also offers a co-translational and post-translational modification mechanism that regulates the function and structure of membrane and secreted proteins. In living systems, it affects protein functions and metabolic turnover. Inside cells, it modulates protein folding, trafficking, and stability. At the cell surface, glycans take part in recognition events of molecules that are critical to biological and pathological processes such as: cell-cell interactions involved in metastasis, migration, and adhesion; host-pathogen interactions important to viral and bacterial infections; and initiation of immune response.[2] Aberrant glycosylation is often observed in pathological conditions such as inflammation and cancer metastasis.[3-7] In particular, altered terminal sialylation, an important glycosylation resulting from changes in expression locations and levels of sialyltransferases, is associated with tumor malignancy. Therefore, the field of glycomics has focused considerable attention on the development of methods for studying sialylated glycans in healthy and disease processes. Sialic acid, a monosaccharide with a nine-carbon backbone, is the N- or O-substituted derivatives of neuraminic acid. Sialic acids are discovered abroad distributed in animal tissues and in bacteria, in particular in glycoproteins and gangliosides. Sialic acids are important cell surface functional molecules because (i) they are the most abundant terminal parts of oligosaccharides on mammalian glycoconjugates, and (ii) the enzymes that take part in sialic acid metabolism are granting for simple unnatural substrates.[8-12] Sialic acids are biosynthesized from the six-carbon precursor N-acetylmannosamine (ManNAc).[13,14]

Several lines of evidence indicate an important role for sialic acid in the living systems. Sialic acid-rich glycoproteins bind selectin in living systems such as humans and other organisms. Cancer cells that can metastasize often bear a lot of sialic acid-rich glycoproteins, which help late-stage cancer cells enter the blood stream. Furthermore, sialic acid also performs an important function in Human Influenza infections. The influenza viruses express Hemagglutin Activity (HA) glycoproteins on their surface that bind to sialic acids found on human erythrocyte surface and the cell membranes of the upper respiratory tract. In addition, sialic acid-rich glycoconjugates on surface membranes produce a negative charge region on the cells' surface and to help keeping water at the cell surface, which contributes to cellular fluid uptake.

To understand the regulation of sialylation in cells will require the development of new tools to study the modification. The most common strategy for monitoring sialic acid levels involves immunoblotting cell lysates with general anti-sialic acid antibodies.[15,16] Although these antibodies are powerful tools, they do not permit to identify proteins of interest directly, detect only a subset of sialylated glycoconjugates and have finite sensitivity.[17] Recent successes demonstrate the role of mass spectrometry-based proteomics as an indispensable tool for molecular and cellular biology and for the emerging field of systems biology. These include the study of analyzing relative phosphorylation or protein expression levels in response to cellular stimulation. However, existing proteomics methods have limited sensitivity to study sialylation levels in vivo. Stable isotope labeling with amino acids in cell culture (SILAC) cannot be used to post-mitotic tissue samples due to requiring multiple cell divisions for isotope incorporation.[18] Therefore, new methods must be developed to probe the dynamics of sialylation in the living systems. To address this issue, we developed a novel method for the identification and quantification of sialylation in vivo in response to cellular stimulation. This strategy combines

mass spectrometry-based proteomics with metabolic labeling of glycans bearing a bioorthogonal chemical reporter such as the azide, which enables their visualization in cells and organisms as well as the enrichment of specific glycoprotein types for proteomic analysis. This strategy involves two steps. Cells or organisms are incubated with azido sugars which are integrated via the glycan biosynthetic machinery into glycoconjugates. The azido sugars, including azidoacetylmannosamine (ManNAz) and 9-azido sialic acid, are then covalently tagged with quantitative isotopic imaging probes or epitope tags, either ex vivo or in vivo, using an azide-orthogonal reaction. Using this strategy, we investigated the reversibility of aberrant sialylation in various cancer cells.

4.2 RESULTS AND DISCUSSION

QUIC-Tag strategy for sialylated glycoconjugates quantification

The ability to obtain glycoconjugate structures expressed on cell surfaces is an important tool to understand their biological roles. Previously, Hsieh-Wilson and coworkers demonstrated a chemoenzymatic reporter strategy for the biotinylation of glycoprotein and subsequent enrichment of glycopeptides from enzyme digest mixtures[19, 20] followed by structure analysis by mass spectrometry. In addition, the chemoenzymatic strategy could be combined with differential isotopic labeling to achieve high-throughput quantification of dynamics on specific proteins. This strategy, named QUIC-Tag, allows that cells are chemoenzymatically labeled and incorporated stable isotopes into target sialylated glycoconjugates for subsequent MS quantification. This isotopic labeling allows for complete resolution of isotopic envelopes even at higher charge states (+4) during MS analysis.

According to this fantastic strategy（Scheme 4.1）, we designed the new probes, which are connecting the cyclooctyne (copper-free click reagents) to biotin tag by a cleavable linker

(disulfide linker that can be cleaved with mercaptans, with or without eight deuterium labeling) to monitor the dynamics sialylation of living cells.
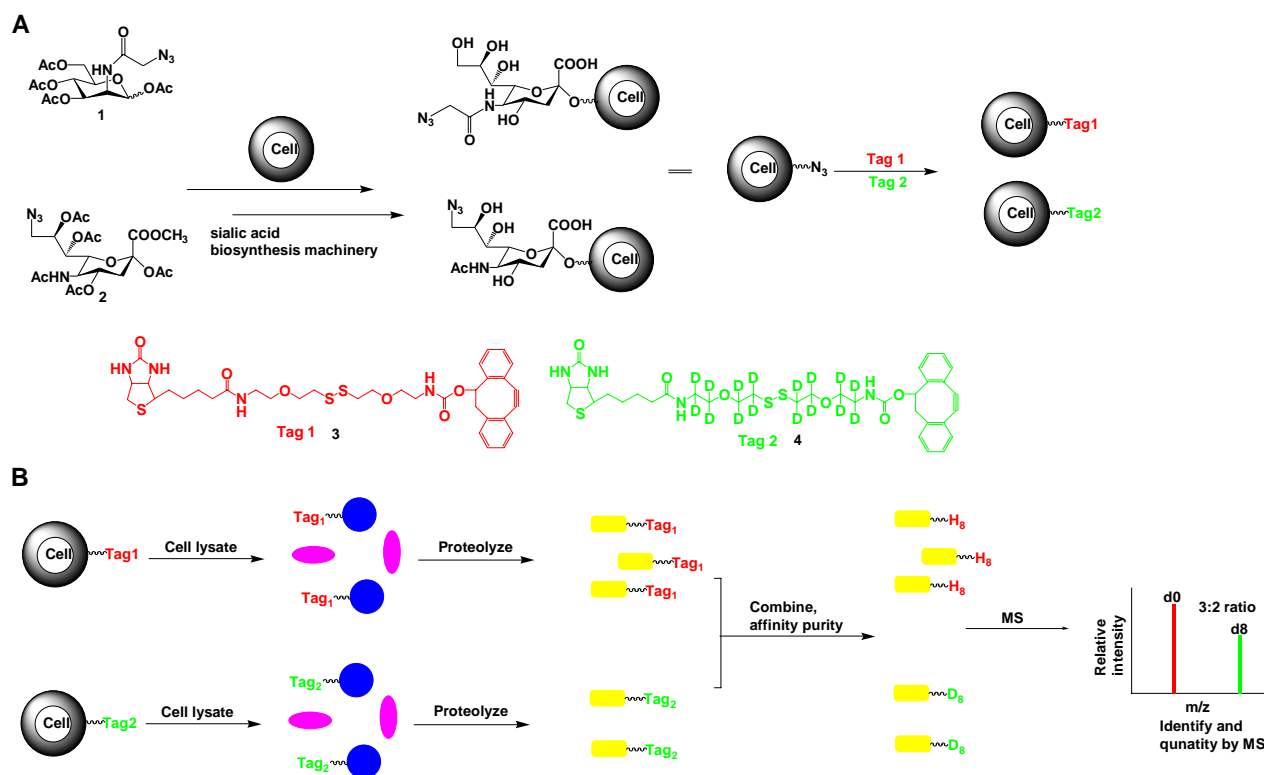
Scheme 4.1 QUIC-Tag strategy for quantitative sialic acid proteomics. (**a**) Biosynthetic incorporation of azide groups into cell surface-associated sialic acid, Ac$_4$ManNAz and 9-azido-9-deoxy-Neu5Ac2Me are metabolically converted to the corresponding cell surface sialoside. (**b**) Sialylated proteins are selectively tagged with 'light' or 'heavy' isotopes. The mixtures are combined, after cell lysing and proteolytically digesting, sialylated peptides of interest are specifically enriched by avidin chromatography for selective quantification by LC-MS.

Our approach is based on the fact that N-α-azidoacetylmannosamine is accepted by the CMP-sialic acid biosynthesis machinery (Scheme 4.1A). The resulting CMP-azidosialic acid is in turn recognized by sialic acid transferases, leading to the biosynthesis and cell surface expression of azidosialic acid containing glycoproteins. Once azide-derivatived glycoproteins are expressed,

the cyclooctyne-biotin probes (with or without D8-labled) are added individually into the cultured cells to react with the azide functionality to biotinylate the azidosialic acid-containing glycoproteins in physiological condition. After cell lysing and proteolytically digesting, the biotinylted glycopeptides (with or without D8-labled) can be pooled and purified by avidin chromatography. The purified glycopeptides are then debiotinylted by cleaving the disulfide-bond using mercaptans, followed by mass spectrometry analysis. Relative quantification of sialylation of cells is achieved by calculating the chromatographic peak area as determined by the MS response to every eluting glycosylated pair of peptide ions.

Synthesis of ManNAz and sialic acid Analogues.

$Ac_4ManNAz$ was synthesized by chemical approaches as a substrate of the CMP-sialic acid biosynthesis machinery so as to be expressed on cell surface as azidosialic acid. The synthesis started from mannosamine hydrochloride (**Scheme 4.2**)[22]. The mannosamine hydrochloride was deprotonated with sodium methoxide, followed by *N*-acetylation with iodoacetic anhydride in methanol. The $Ac_4ManNAz$ target compound was obtained by substituting halide with sodium azide, followed by *O*-acetylation. Compared the $Ac_4ManNAz$, 9-azido-9-deoxy-Neu5Ac$_2$Me seems to be more potent to hijack into sialic acid biosynthesis pathway sequent to be expressed into glycoprotein on cell surface. We used N-acetylneuraminic acid hydrochloride **8** as starting material to synthesize the target compound **2 (Scheme 4.3).** The synthetic process consists of the esterification of **8** with methanol and acidic resins, to give the methyl ester **9**, which is then treated with p-toluensulfonyl chloride in pyridine. The esterification of the primary alcoholic function occur at low temperature, but the 8-tosyl derivative was obtained as the main reaction product at >25 °C. The reason was assumed as room temperature promoted a kinetically controlled intramolecular transesterification. The 9-tosyl derivative **10** was purified by

124

chromatographic methods and were converted to the 9-azido derivative **11** by reaction with sodium azide in DMF. The target compound 9-azido-9- deoxy-Neu5Ac2Me was obtained by further *O*-acetylation. The synthesis of two azide-bearing ManNAc and sialic acid analogues was undertaken in an effort to identify site-tolerance of modification.
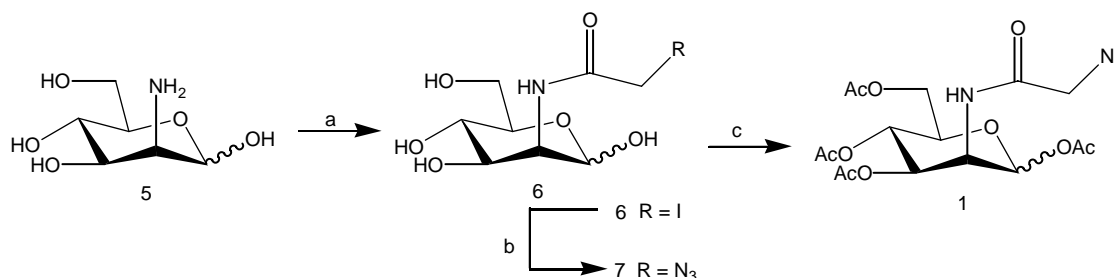
Scheme 4.2 Synthesis of Ac₄ManNAz. Reagents and conditions: a) Iodoacetic anhydride, NaOCH₃, CH₃OH, rt; b) NaN₃, CH₃OH, refluxing, 91%; c) Ac₂O, Py, rt, 95%.
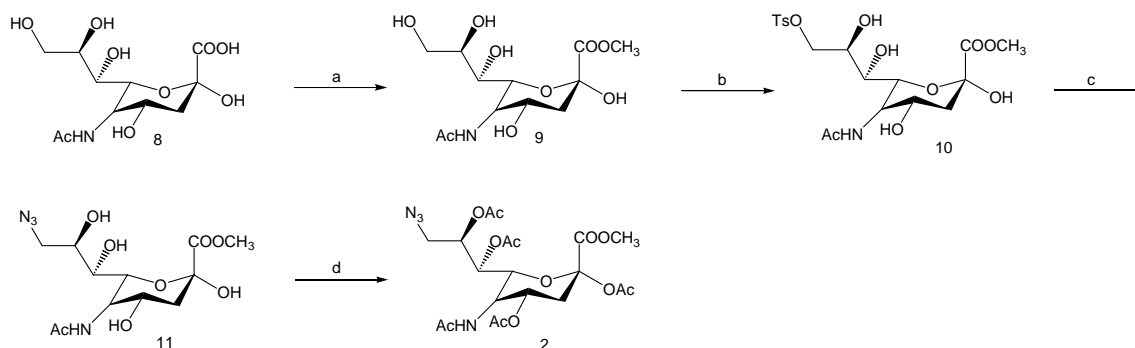
Scheme 4.3 Synthesis of 9-azido-9- deoxy-Neu5Ac2Me. Reagents and conditions: a) MeOH, ion exchange resin Amberlite® IR 120-H, rt, 84%; b) p-toluenesulfonyl chloride, Py, 0 °C, 77%; c) NaN3, DMF, 65 °C, 46%; d) Ac₂O, Py, rt, 81%.

Synthesis of QUIC-Tags and deuteriated QUIC-Tags

It was envisaged that the synthesis of target QUIC-Tag **3** and deuteriated QUIC-Tag **4** could be achieved by first synthesizing the protected (2-{2-[2-(2-tert-butoxycarbonylamino-ethoxy)-ethyldisulfanyl]-ethoxy}-ethyl)-carbamic acid tert-butyl ester linker **20** and **34** consisting of appropriately disulphate linkages and Boc protecting groups**.** These two linkers can easily be

synthesized by combining ether formation methods with a protection method using the tetrahydropyran (THP) group, which is often used for protection of alcohol moieties due to its stability and compatibility under various reaction conditions and reagents, such as metal hydrides, alkyllithiums, Grignard reagents, and catalytic hydrogenation. There are several known methods for the tetrahydropyranylation and depyranylation of alcohols. The most common reagent that can catalyze both transformations is p-toluenesulfonic acid (PTSA)[21,22] due to its milder reaction condition and higher yields. Therefore, this method has been utilized to synthesize the linkers **20** and **34**.

The synthesis of 2-(2-bromo-ethoxy)-tetrahydro-pyran **14** was achieved by reacting of dihydropyran with 2-bromoethanol in 80% overall yield (**Scheme 4.4**). Alkylation of the N-(2-Hydroxyethyl) phthalimide **15** with tetrahydropyranyl bromo derivative **14** gave THP-protected intermediate **16**. The tetrahydropyranyl moiety greatly enhanced the ease of purification. Cleavage of the protective tetrahydropyran with 1 N HCl in methanol yielded analogue **17**. The hydroxyl group of compound **17** was then converted to the corresponding bromide analogue **18** by treating with PBr₃ in good yield. Replacement of the bromide group in **18** by the thioacetate group could be carried out with KSAc, and (NBu^t)₄I in DMF, yielding the corresponding compound **19** in 80 % over yield. Removal of the acyl and phthalimide groups from **19** by treatment with hydrazine in ethanol at 80°C was straightforward. The protection of the deprotected **19** with N-Boc protecting group afforded important intermediate **20**. Removal of the Boc protective group with 20 % TFA in CH₂Cl₂ provided analogue **21**. It was found that the crude product was pure enough for the next reaction. Monobiotinylation of diamine **21** was achieved by treatment with 1 equivalent of biotin-NHS active ester **23**, followed by *N*-Boc protection of the other amine to provide compound **22.** The Boc moiety greatly improved the

ease of purification. Compound **22** was treated with 20% TFA to remove the Boc protecting group and was subsequently reacted with carbonic acid 7, 8- didehydro-1,2:5,6-dibenzocyclooctene-3-yl ester 4-nitrophenyl ester **24** to afford the target QUIC-Tag **3**. The QUIC-Tag **3** can also visualize azido-containing biomolecules by cycloaddition with azide group followed by treatment with avidin modified with a fluorescence probe.
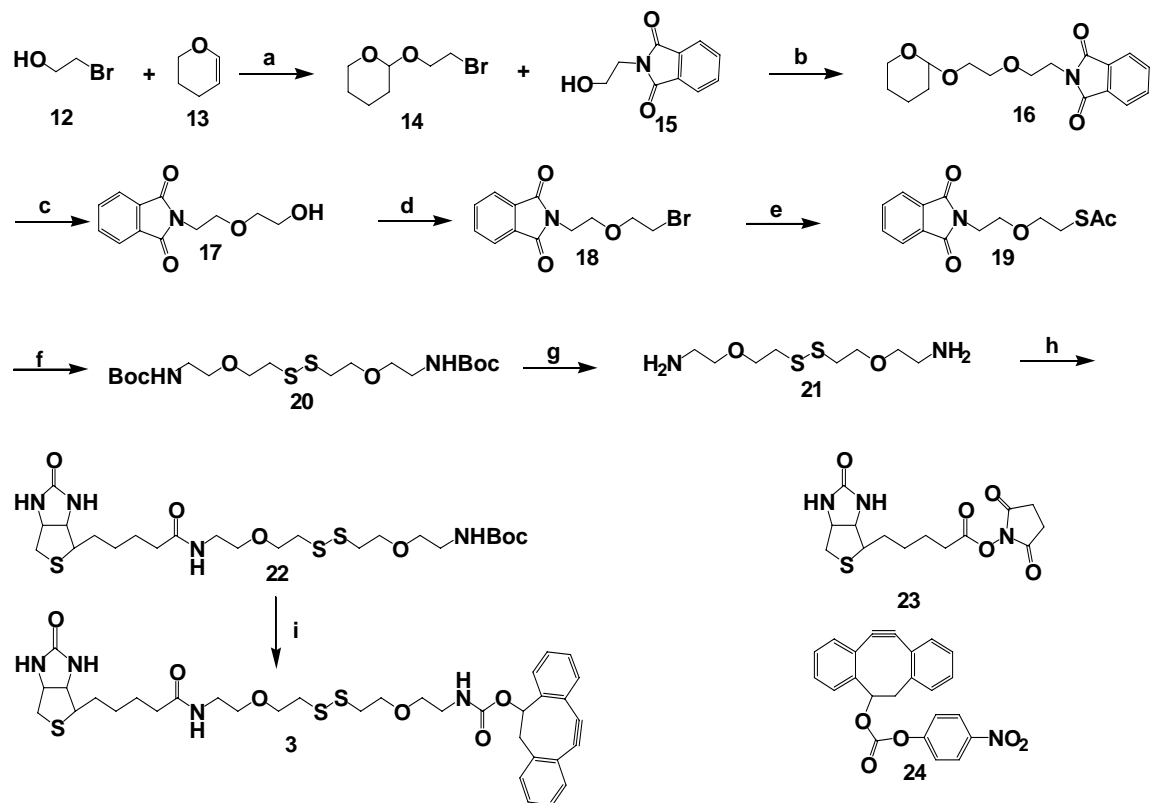
Scheme 4.4 Synthesis of QUIC-Tag. Reagents and conditions: a)TsOH, rt, 80%; b) NaH, DMF, rt, 77%; c) 1N HCl, CH$_3$OH, rt, 89%; d) 9, PBr$_3$, CH$_2$Cl$_2$, 0 ^{o}C,83%; e) KSAc, (NBu^t)$_4$I, DMF, 60 ^{o}C, 80%; f) i. NH$_2$NH$_2$, EtOH, refluxing, ii. (Boc)$_2$O, CH$_2$Cl$_2$, TEA, rt, 73% in two steps; g) 20% TFA in CH$_2$Cl$_2$, rt; (h) i. **24**, DMF, TEA, rt, ii. (Boc)$_2$O, DMF, TEA, rt, 61% in two steps; (i) i. 20% TFA in CH$_2$Cl$_2$, rt, ii. **25**, DMF, TEA, rt, 70% in two steps.

Deuteriated QUIC-Tag **4** was synthesized following the same reaction sequence as for QUIC-Tag **3** although with a slight modification. First, the 2-(2-bromo-ethoxy)-tetrahydro-

pyran-D4 **26** was synthesized by reaction of dihydropyran with 2-bromoethanol-D4 **25** in 81% overall yield (**Scheme 4.5**). Then compound **27** was synthesized from **26** by refluxing with phthalimide potassium salt. The protective tetrahydropyran group was cleaved with 1 N HCl in methanol to yield analogue **28**. Alkylation of the N-(2-Hydroxyethyl) phthalimide **28** with tetrahydropyranyl bromo derivative **26** by using NaH as a base gave THP-protected intermediate **29**. Removing the protective tetrahydropyran with 1 N HCl in methanol yielded analogue **30**. The hydroxyl group of compound **30** was then converted to the corresponding bromide analogue **31** by treatment with PBr$_3$ in good yield. The displacement of the bromide of **31** with a thioacetate group could be carried out using KSAc, and (NBu^t)$_4$I in DMF, yielding the corresponding compound **32** in 76 % over yield. The acyl and phthalimide groups were removed at same time by treatment with hydrazine in ethanol at 80°C followd by N-Boc protection to yield **33**. Removing of the Boc protective group with 20 % TFA in CH$_2$Cl$_2$ provide analogue **34**, the crude product is pure enough for the next step reaction. Monobiotinylation of diamine **34** was achieved by using 1 equivalent of biotin-NHS active ester **23**. The following N-Boc protecting of another amine group provide the compound **35**, in which the Boc moiety featly improved the ease of purification. Compound **35** was first treated with 20% TFA to remove the Boc protecting group and reacted with carbonate **24** to afford the target deuteriated QUIC-Tag **4**, which is the counterpart of QUIC-Tag **3**.
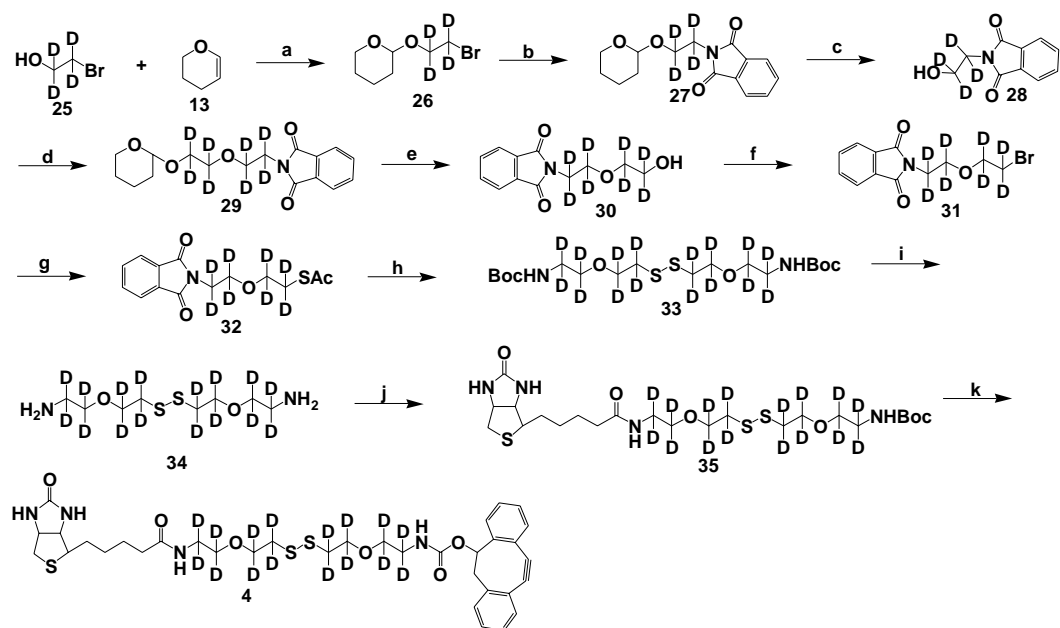
Scheme 4.5 Synthesis of deuteriated QUIC-Tag. Reaction conditions: a)TsOH, rt, 81%; b) phthalimide potassium salt, DMF 80 $^{\circ}$C, 86%; c) 1N HCl, THF, rt, 88%; d) 9, NaH, DMF, rt, 71%; e) 1N HCl, CH$_3$OH, rt, 80%; f) PBr$_3$, CH$_2$Cl$_2$, 0 $^{\circ}$C,83%; g) KSAc, (NBu^t)$_4$I, DMF, 60 $^{\circ}$C, 76%; h) i. NH$_2$NH$_2$, EtOH, refluxing, ii. (Boc)$_2$O, CH$_2$Cl$_2$, TEA, rt, 66% in two steps; i) 20% TFA in CH$_2$Cl$_2$, rt; j) i. **24**, DMF, TEA, rt, ii. (Boc)$_2$O, DMF, TEA, rt, 51% in two steps; k) i. 20% TFA in CH$_2$Cl$_2$, rt, ii. **25**, DMF, TEA, rt, 77% in two steps.

Probing the sialylated glyconconjugates using QUIC-Tag

Labeling of Cell-Surface Azido Glycans of Jurkat cells Using Biotinylated Conjugates.

Jurkat cells were cultured in the presence of 25 μM of N-azidoacetylmannosamine (Ac$_4$ManNAz) for 3 days to metabolically introduce N-azidoacetyl-sialic acid (SiaNAz) moieties into glycoproteins. As a negative control, Jurkat cells were employed that were grown in the presence of 25 μM of N-acetylmannosamine (Ac$_4$ManNAc). The cells were washed and labeled with QUIC-Tag **3** at different of concentrations (0, 3, 10 or 30 μM) for 60 min. In all cases, the cells were subsequently stained with FITC-labeled avidin and analyzed by flow cytometry. The

129

QUIC-Tag **3** displayed concentration-dependent reaction profiles with cell-surface-associated azides (shown in **Figure 4.1**). We were pleased to observe that QUIC-Tag **3** displayed only little bit background fluorescence labeling.
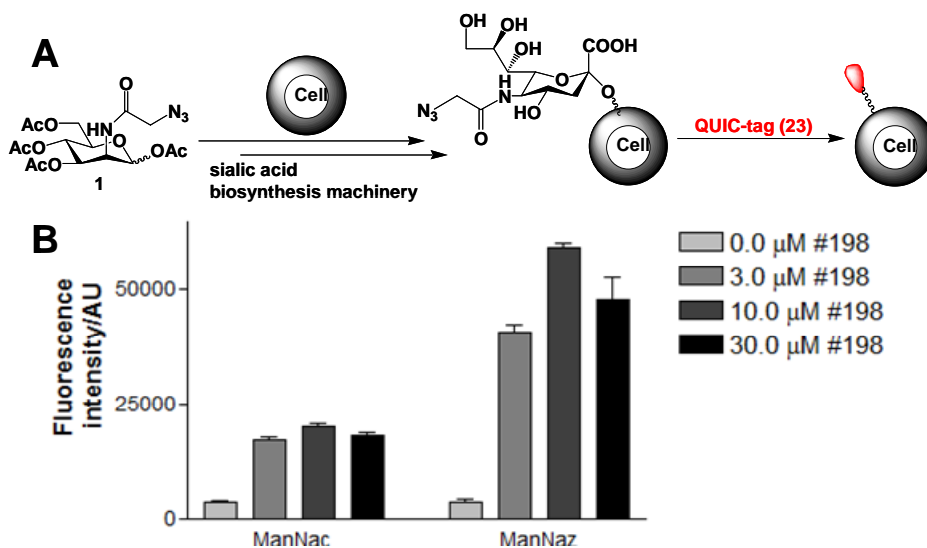
Figure 4.1 Labeling of cell-surface glycans of Jurkat cells with azido sugars and QUIC-Tag **3**. (**A**) Bioorthogonal chemical reporter strategy for two-step detection of glycans. Cells were first incubated with Ac₄ManNAz, which is metabolically converted to cell-surface SiaNAz residues, and subsequently reacted with QUIC-Tag **3** for visualization. (**B**) Jurkat cells were metabolically labeled with 25 μM Ac₄ManNAz (+Az) or no sugar (−Az) for 3 days. The cells were labeled with QUIC-Tag **3** for 60 min at 0, 3, 10, or 30 μM. The cells were then stained with FITC-labeled avidin and analyzed by flow cytometry. Shown in (**B**) is the mean fluorescence intensity (MFI) in arbitrary units (au).

We then studied the concentration-dependent efficacy of cell-surface azide labeling of QUIC-Tag **3** in a 60 min reaction at 0, 3, 10 or 30 μM (**Figure 4.2B**). The labeling concentration approximately at 10 μM showed best labeling. Finally, we tested the toxicity of QUIC-Tag **3**, and the results showed that the reagents did not cause cell apoptosis, indicating that QUIC-Tag **3** is not toxic to Jurkat cells.

Labeling of Cell-Surface Azido Glycans of CHO cells Using Biotinylated Conjugates.

We applied QUIC-Tag **3** to image cell-surface glycans in live CHO cells. The cells were incubated for 3 days with 25 μM Ac$_4$ManNAz, or 25 μM Ac$_4$ManNAc and in the absence of sugar as a negative control and labeled with QUIC-Tag **3** at different of concentrations (0, 3, 10 or 30 μM) for 60 min. Subsequently, the cells were treated with FITC-labeled avidin and imaged by epifluorescence microscopy. We observed that the labeling on the cell surface was clearly azide-dependent and QUIC-Tag concentration-dependent, although a somehow increased background fluorescence appeared in the negative control QUIC-Tag **3**. The results suggested that QUIC-Tag **3** can be used for live-cell imaging applications.
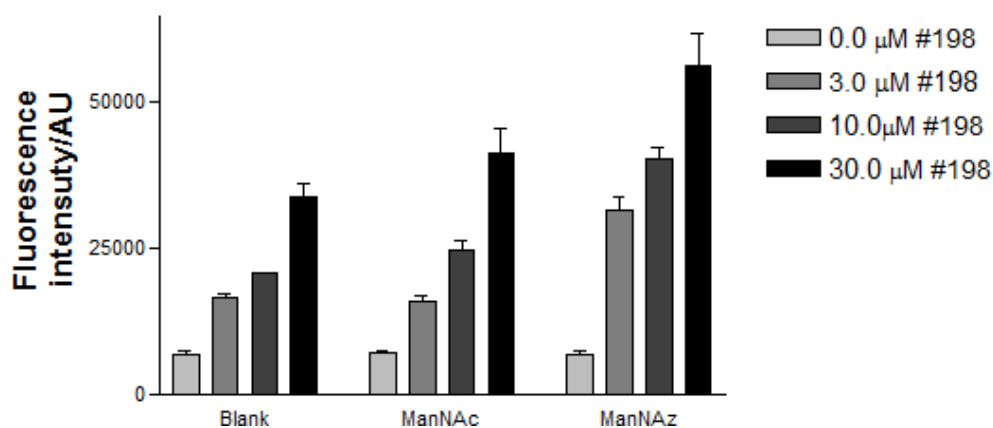
Figure 4.2 Labeling of cell-surface glycans of CHO cells with azido sugars and QUIC-Tag **3**. CHO cells were metabolically labeled with 25 μM Ac$_4$ManNAz (+Az) or 25 μM Ac$_4$ManNAc and no sugar (−Az) for 3 days. The cells were labeled with QUIC-Tag **3** for 60 min at 0, 3, 10 or 30 μM. The cells were then stained with FITC-labeled avidin and analyzed by flow cytometry. Shown in (**Figure 4.3**) is the mean fluorescence intensity (MFI) in arbitrary units (au).

We then studied the concentration-dependent efficacy of cell-surface azide labeling of QUIC-Tag **3** in a 60 min reaction at 0, 3, 10 or 30 μM (**Figure 4.2**). The labeling concentration at approximately 30 μM showed best labeling.

Future study

Finally, the cells, which were chemoenzymatically labeled with QUIC-Tags, can be lysated, proteolytically digested , and pooled as described in **Scheme 4.1**. Following avidin capture of the QUIC-Tag labeled peptides, we can debiotinylate and perform mass spectrometry analysis.

CONCLUSIONS

We demonstrated a novel quantitative proteomics method to study the dynamics of sialylation in vivo. Our QUIC-Tag strategy combines the ability to selectively biotinylate enriched sialylated proteins with a simple and efficient isotopic labeling strategy. When used with tandem mass spectrometry, the method permits straightforward identification and simultaneous quantification of individual sialylation. In particular, the chemoenzymatic tagging method does not disturb endogenous sialylation levels. Compared with other methods, the isotopic labeling strategy has some advantages including being fast, high yielding and inexpensive. Therefore, this strategy allows sialylation to be investigated in more physiological settings and in key cell types where the modification is most highly abundant.

4.3 EXPERIMENTAL PROCEDURES

General Methods and Materials

Chemicals were purchased from Aldrich and Fluka and used without further purification. Dichloromethane was distilled from CaH_2 and stored over molecular sieves 4 Å. Pyridine was distilled from P_2O_5 and stored over molecular sieves 4 Å. THF was distilled form sodium. All reactions were performed under anhydrous conditions under an atmosphere of Argon. Reactions were monitored by TLC on Kieselgel 60 F254 (Merck). Detection was by examination under UV light (254 nm) or by charring with 5% sulfuric acid in methanol. Flash chromatography was performed on silica gel (Merck, 70-230 mesh). Iatrobeads (60 μm) were purchased from Bioscan.

^{1}H NMR (1D, 2D) and ^{13}C NMR were recorded on a Varian Merc 300 spectrometer and on Varian 500 and 600 MHz spectrometers equipped with Sun workstations. ^{1}H and ^{13}C NMR spectra were recorded in CDCl$_3$, and chemical shifts (δ) are given in ppm relative to solvent peaks (^{1}H, δ 7.24; ^{13}C, δ 77.0) as internal standard for protected compounds. Negative ion matrix assisted laser desorption ionization time of flight (MALDI-TOF) were recorded on a VOYAGER-DE Applied Biosystems using dihydrobenzoic acid as a matrix. High-resolution mass spectra were obtained using a VOYAGER-DE Applied Biosystems in the positive mode by using 2,5-dihydroxyl-benzoic acid in THF as matrix.

***N*-Azidoacetylmannosamine (7)**[22] To a solution of mannosamine hydrochloride (**5**, 244 mg, 1.13 mmol) in dry CH$_3$OH (11 mL) was added 1 M NaOCH$_3$ in CH$_3$OH (1.13 mL). The reaction mixture was stirred for 1 h at rt, followed by the addition of iodoacetic anhydride (1.0 g, 2.8 mmol). The resulting solution was stirred for 8 h at rt under argon. To this was added H$_2$O (5 mL) and the solution was stirred for an additional 1 h. The solution was neutralized with sat. aq. NaHCO$_3$ (10 mL)and concentrated. The residue was filtered through a plug of silica gel eluting with 5:1 CHCl$_3$/CH$_3$OH. The crude product obtained was used in the next step without further purification. ^{1}H NMR (300 MHz, D$_2$O) δ 4.91 (1H, d, *J* = 1.4 Hz), 4.84 (1H, d, *J* = 1.6 Hz), 4.38 (1H, d, *J* = 4.3 Hz), 4.24 (1H, d, *J* = 4.6 Hz), 4.00-4.07 (1H, m), 3.83 (2H, br s), 3.80 (2H, d, *J* = 1.3 Hz), 3.78 (2H, d, *J* = 1.0 Hz), 3.53-3.62 (1H, m), 3.44-3.52 (1H, m), 3.34-3.41 (1H, m). ^{13}C NMR (75 MHz, D$_2$O) δ 176.1, 172.7, 92.9, 92.4, 76.3, 72.0, 71.9, 68.8, 66.7, 66.4, 60.3, 53.7, 48.8.

To a solution of **6** (392 mg, 1.13 mmol) in CH$_3$OH (2.3 mL) was added NaN$_3$ (734 mg, 11.3 mmol). The mixture was heated at reflux overnight and allowed to cool to rt and concentrated. The residue was filtered through a plug of silica gel eluting with 5:1 CHCl$_3$/CH$_3$OH. The crude

product obtained was further purified by silica gel column chromatography eluting with a slow gradient from 50:1 to 6:1 CHCl$_3$/CH$_3$OH. The fractions collected were concentrated and redissolved in a minimum amount of water. Lyophilization afforded **7** (271 mg, 91% in two steps) of a white powder. ^{1}H NMR (300 MHz, D$_2$O) δ 5.28 (1H, d, J = 3.4 Hz, *H*-1), 5.23 (1H, d, J = 1.7 Hz), 4.15 (4H, s, CH$_2$N$_3$), 4.02 (1H, d, J = 3.5 Hz), 3.99 (1H, d, J = 3.1 Hz), 3.94 (2H, dd, J = 2.3, 2.7 Hz), 3.89-3.91 (2H, m), 3.85-3.87 (2H, m), 3.77-3.83 (1H, m), 3.65-3.72 (1H, m), 3.56 (2H, t, J = 9.1 Hz). ^{13}C NMR (75 MHz, D$_2$O): δ92.8, 92.7, 76.3, 75.9, 71.9, 71.5, 70.5, 69.9, 68.7, 66.6, 66.4, 60.2, 54.2, 54.0, 53.2, 51.6, 51.5.

1,3,4,6-Tetra-*O*-acetyl-*N*-azidoacetylmannosamine (1)[22] A solution of **7** (25 mg, 0.095 mmol) in pyridine (2 mL) was cooled to 0 °C. To this solution was added Ac$_2$O (1.0 mL, 11 mmol) and a catalytic amount of DMAP. The reaction mixture was stirred for 10 h while warming to rt. The resulting light yellow solution was diluted with CH$_2$Cl$_2$ (100 mL) and washed with 1 N HCl (3 x 50 mL), sat. aq. NaHCO$_3$ (1 x 50 mL), H$_2$O (1 x 50 mL) and sat. aq. NaCl (1 x 50 mL). The combined aqueous layers were back extracted with CH$_2$Cl$_2$ (50 mL). The combined organic layers were dried over Na$_2$SO$_4$ and concentrated. The crude product was purified by silica gel column chromatography eluting with a gradient of 1:10 to 1:2 EtOAc/hexanes to afford 39 mg (95%) of a light yellow oil. ^{1}H NMR (300 MHz, CDCl$_3$) δ 6.37 (1H, d, J = 5.7 Hz, *H*-1), 5.78 (1H, t, J = 4.5 Hz, *H*-3), 5.21 (1H, t, J = 5.7 Hz, *H*-2), 5.15 (1H, t, J = 9.6 Hz, *H*-6), 4.29 (1H, dd, J = 4.5, 12.6 Hz, *H*-4), 4.13 (1H, dd, J = 2.4, 12.6 Hz, *H*-5), 3.93 (2H, s, C*H*$_2$N$_3$), 3.82 (1H, m, *H*-6), 2.12 (3H, s, COC*H*$_3$), 2.10 (3H, s, COC*H*$_3$), 2.05 (6H, s, 2 × COC*H*$_3$). ^{13}C NMR (75 MHz, CDCl$_3$): δ171.5, 170.8, 170.6, 169.2, 169.1, 168.6, 166.9, 92.1, 90.2, 72.9, 72.1, 72.0, 70.3, 69.8, 67.6, 67.4, 61.5, 61.4, 53.2, 52.5, 52.4, 51.2, 20.8, 20.8, 20.6, 20.6, 20.6, 20.5, 20.5.

5-Acetylamino-2,4-dihydroxy-6-(1,2,3-trihydroxy-propyl)-tetrahydro-pyran-2-carboxylic acid methyl ester (9)[23] 5-*N*-Acetylneuraminic acid **8** (5.0 g, 16.2 mmol) was dissolved in CH_3OH (500 ml, HPLC grade) and ion exchange resin Amberlite® IR 120-H (10 g) was added. The mixture was stirred overnight under argon atmosphere, then filtered to remove the resin. After evaporation of the , compound **9** was obtained as a white foam (4.4 g, 84%). ^{1}H NMR (300 MHz, D_2O) δ 3.98-4.06 (2 H, m), 3.78- 3.82 (2 H, m), 3.77 (3 H, s, OC*H₃*), 3.59-3.71 (2 H, m), 3.47 (1 H, dd, *J* = 9.2, 1.2 Hz), 2.20 (1 H, dd, *J* = 5, 12.8 Hz, *H*-3ax), 2.0 (3 H, s, NHCOC*H₃*) 1.88 (1 H, dd, *J* = 11.6, 12.8 Hz, *H*-3ax). ^{13}C NMR (75 MHz, D_2O) δ 171.8, 96.7, 72.1, 71.7, 70.2, 67.9, 64.9, 54.4, 53.1, 40.7, 22.6.

Methyl 5-acetamido-3,5-dideoxy-9-*O*-(*p*-toluenesulfonyl)-β-D-glycero-D-galacto-nonulopyranosonate (10)[23] *p*-toluenesulfonyl chloride (1.1 g, 6.0 mmol) was added to a solution of *N*-acctylneuraminic acid methyl ester (1.5 g, 4.5 mmol) in pyridine (20 mL) over 90 min. The reaction mixture was stirred at 0 °C for 12 h. The solvent was evaporated and the residue purified by silica gel column chromatography (CH_2Cl_2/CH_3OH, 2/1, v/v) to give the tosylate **10** (16.7 g, 77%). ^{1}H NMR (300 MHz, D_2O) δ 7.80 (2H, d, *J* = 8.4 Hz), 7.47 (2H, d, *J* = 8.1 Hz), 4.29 (1H, dd, *J* = 10.6, 2.4 Hz, *H*-9′), 4.19 (1H, dd, *J* = 10.6, 4.9 Hz, *H*-9), 4.05 (1H, m, *H*-8), 4.00 (1H, dd, *J* = 10.4, 0.9 Hz, *H*-6), 3.90-3.85 (2H, m, *H*-4, *H*-7), 3.81 (s, 3H, s, $CO_2C H_3$), 3.57 (1H, d, $J_{7,8}$ = 9.2 Hz, *H*-5), 2.44 (3H, s, Ar*CH₃*), 2.29 (1H, dd, $J_{3eq,3ax}$ = 12.0 Hz, $J_{3eq,4}$ = 4.9 Hz, *H*-3eq), 2.04 (3H, s, NHCOC*H₃*), 1.88 (1H, dd, $J_{3ax,3eq}$= 13.1 Hz, $J_{3ax,4}$ = 11.6 Hz, *H*-3ax). ^{13}C NMR (75 MHz, D_2O) δ 175.64, 172.03, 147.34, 131.25, 130.94, 128.54, 96.03, 73.25, 70.86, 68.36, 68.27, 67.28, 54.23, 52.78, 39.43, 22.80, 21.57.

Methyl 5-acetamido-9-azido-3,5,9-trideoxy-D-β-glycero-D-galacto-nonulopyranosonate (11) [23] The tosylate **10** (972 mg, 2.03 mmol) was dissolved in DMF (5 mL) and sodium azide

(1.06 g, 16.3 mmol) and molecular sieves (100 mg) were added. The mixture was stirred at 65 °C and the reaction progress was monitored by TLC. After 5.5 h, 20% CH_3OH in CH_2Cl_2 (5 mL) was added at rt and then filtered. Concentration of the filtrate and silica gel column chromatography of the residue (CH_2Cl_2/CH_3OH, 4/1, v/v) afforded the azide **11** (325 mg, 46%). ^1H NMR (300 MHz, D_2O) δ 4.10-4.04 (1H, m, *H*-7), 4.05 (1H, dd, J = 10.4, 1.1 Hz, *H*-4), 3.92 (1H, d, J = 10.2 Hz, *H*-5), 3.90-3.85 (1H, m, *H*-6), 3.85 (3H, s, OC*H*$_3$), 3.60 (1H, dd, J = 13.2, 2.8 Hz, *H*-8), 3.55 (1H, dd, J = 9.3, 1.0 Hz, *H*-9), 3.46 (1H, dd, J = 13.2, 6.0 Hz, *H*-9), 2.30 (1H, dd, J = 13.1, 4.9 Hz, *H*-3), 2.05 (3H, s, NHCOC*H*$_3$), 1.90 (1H, dd, J = 13.2, 11.6 Hz, *H*-3). ^{13}C NMR (75 MHz, D_2O) δ 175.51, 172.07, 96.03, 70.87, 69.67, 69.31, 67.36, 54.53, 54.20, 52.76, 39.36, 22.77. HRMS calcd for $C_{12}H_{20}N_4O_8Na$ (M + Na$^+$): 371.1179, found: 371.1156.

Methyl (5-acetamido-4,7,8-tri-*O*-acetyl-9-azido-3,5,9-trideoxy- D -glycero- D -galacto-2-nonulopyranoso)onate (2)[24] A solution of compound **11** (167 mg, 0.48 mmol) in pyridine (3 mL) was stirred with Ac_2O (2 mL) at 0 °C for 30 min, and then 10 h at room temperature. The mixture was dissolved in CH_2Cl_2 (20 mL) and washed with water, 1N HCl (5 mL), $NaHCO_3$ (5 mL), NaCl (5 mL), dried ($MgSO_4$), and concentrated. The residue was purified with silica gel column chromatography (CH_2Cl_2/CH_3OH, 50:1, v/v) to give **2** (200 mg, 81%) as a white powder. ^1H NMR (300 MHz, $CDCl_3$) δ 5.63 (1 H, s1 H, AcNH), 5.41 (1 H, dd, *H*-7), 5.25 (1 H, m, *H*-4), 4.90 (1 H, m, *H*-8), 4.18 (1H, m, *H*-5), 4.08 (1H, dd, $J_{5,6}$ = 10.6 Hz, $J_{6,7}$ = 2.0 Hz, *H*-6), 3.83 (1 H, dd, $J_{8,9b}$ = 2.6 Hz, *H*-9b), 3.80 (3H, s, CO_2C*H*$_3$), 3.37 (1 H, dd, $J_{8,9a}$ = 8.0 Hz, $J_{9a,9b}$ =13.4 Hz, *H*-9a), 2.52 (1H, dd, $J_{3ax,3eq}$ = 13.0 Hz, $J_{3eq,4}$ = 5.0 Hz, H-3*eq*), 2.17 (3H, s, O_2CC*H*$_3$), 2.07(3H, s, O_2CC*H*$_3$), 2.04(3H, s, O_2CC*H*$_3$), 1.89 (3H, s, C*H*$_3$CONH).^{13}C NMR (75 MHz, $CDCl_3$) δ 171.0, 170.9, 170.6, 170.2, 167.9, 84.7, 72.5, 72.1, 69.3, 68.5, 62.4, 52.9, 49.5, 36.9, 23.2, 21.0, 20.9, 20.8. HRMS calcd for $C_{20}H_{28}N_4O_{12}Na$ (M + Na$^+$): 539.1601, found: 539.1589.

2-(2-Bromo-ethoxy)-tetrahydr-pyran (14) 3,4-Dydro-2H-pyran (2.7 mL, 30 mmol) was added to a flame-dried flask containing *p*-TSA (26 mg, 1.4 mmol) and freshly distilled CH_2Cl_2 (20 mL) under nitrogen. The reaction was allowed to stir for 10 min before the dropwise addition of 2-bromoethanol (1.4 mL, 20 mmol). The reaction mixture was then allowed to stir for an additional 18 h at ambient temperature. Sodium hydrogen carbonate (1.50 g) was added to the reaction mixture and stirring was continued for a further 50 min before filtering. The filtrate was evaporated under reduced pressure and the resultant oil was subjected to silica gel column chromatography (hexane/EtOAc, 10: 1, v/v) to give 2-(2-bromoethoxy)tetrahydropyran **14** as a colorless oil (3.3 g, 80%). ^{1}H NMR (300 MHz, $CDCl_3$) δ 4.60 - 4.63 (1H, m, C*H*), 3.93 - 3.99 (1H, m, OC*H*$_2$), 3.81 - 3.86 (1H, m, OC*H*$_2$), 3.70 - 3.75 (1H, m, OC*H*$_2$), 3.41 - 3.50 (3H, m, C*H*$_2$, OC*H*$_2$), 1.73 - 1.83 (1H, m, C*H*$_2$), 1.65 - 1.71 (1H, m, C*H*$_2$), 1.47 - 1.58 (4H, m, C*H*$_2$).^{13}C NMR (75 MHz, $CDCl_3$) δ 98.9, 67.6, 62.3, 30.9, 30.5, 25.4, 19.3.

2-{2-[2-(Tetrahydro-pyran-2-yloxy)-ethoxy]-ethyl}-isoindole-1,3-dione (16) A mixture of sodium hydride (360 mg, 15 mmol) and 2-(2-hydroxy-ethyl)-isoindole-1,3-dione **15** (1 g, 5 mmol) in dry DMF (20 mL) was stirred for 2 h under argon. 2-(2-bromoethoxy)tetrahydropyran (2.0 g, 10 mmol) was then added slowly and stirring was continued for 12 h at room temperature. The mixture was poured into ice-water and extracted with CH_2Cl_2, and the extract was washed with water, dried ($MgSO_4$), and concentrated. The oily residue was purified by silica gel column chromatography (hexane/EtOAc, 5/1, v/v) to give pure **16** (1.2 g, 77%). ^{1}H NMR (300 MHz, $CDCl_3$) δ 7.76 (2H, m, Phth*H*), 7.65 (2H, m, Phth*H*), 4.49 (1H, m, C*H*), 3.77 (1H, m, C*H*$_2$), 3.75 (4H, m, C*H*$_2$), 3.62 (2H, m, O C*H*$_2$), 3.46 (2H, m, C*H*$_2$N), 3.36 (1H, m, OC*H*$_2$), 1.35-1.72 (6H, m, C*H*$_2$). ^{13}C NMR (75 MHz, $CDCl_3$) δ 168.5, 134.1, 132.4, 123.4, 99.0, 70.2, 68.1, 66.7, 62.3, 37.6, 30.7, 25.6, 19.6. HRMS calcd for $C_{17}H_{21}NO_5Na$ (M + Na$^+$): 342.1317, found: 342.1309.

2-[2-(2-Hydroxy-ethoxy)-ethyl]-isoindole-1,3-dione (17) A solution of **16** (1.5 g, 5 mmol) in 30 mL of CH_3OH was treated with 5 mL of 1N HC1, and was stirred for 8h at room temperature. The mixture was poured into ice-water and extracted with EtOAc, and the extract was washed with water, dried ($MgSO_4$), and concentrated. The oily residue was purified by silica gel column chromatography (hexane/EtOAc, 1/ 1, v/v) to give pure **17** (1.6 g, 89%). ^{1}H NMR (300MHz, $CDCl_3$) δ 7.85 (2H, m, Phth$H$), 7.73 (2H, m, Phth$H$), 3.91 (2H, t, J = 5.3 Hz, CH_2N), 3.75 (2H, t, J = 5.3 Hz, OCH_2CH$_2$N), 3.69 (2H, m, CH_2OH), 3.61 (2H, m, CH_2CH$_2$OH). ^{13}C NMR (75 MHz, $CDCl_3$) δ 168.7, 134.3, 132.3, 123.6, 72.4, 68.6, 62.0, 37.8. HRMS calcd for $C_{17}H_{21}NO_5Na$ (M + Na $^+$): 342.1317, found: 342.1309.

2-[2-(2-Bromo-ethoxy)-ethyl]-isoindole-1,3-dione (18) To solution of **17** (1.1 g, 5 mmol) in CH_2Cl_2 (20 mL) was added PBr$_3$ (2.6 g, 10 mmol) and the reaction was cooled by an ice bath under argon atmosphere. The resulting mixture was stirred for 6 h. Solvents were evaporated and the residue was purified by silica gel column chromatography (hexane/EtOAc, 6/1, v/v) to give pure **18** (1.2 g, 83%). ^{1}H NMR (300MHz, $CDCl_3$) δ 7.78 (2H, m, Phth$H$), 7.67 (2H, m, Phth$H$), 3.84 (2H, t, J = 5.3Hz, CH_2), 3.74 (2H, t, J = 5.1 Hz, OCH_2CH$_2$N), 3.72 (2H, t, J = 6.0 Hz, CH_2CH$_2$Br), 3.33 (2H, t, J = 6.0 Hz, CH$_2$CH_2Br). ^{13}C NMR (75 MHz, $CDCl_3$) δ 168.5, 134.2, 132.3, 123.5, 70.7, 68.0, 37.4, 30.4. HRMS calcd for $C_{12}H_{12}BrNO_3Na$ (M + Na $^+$): 319.9898, found: 319.9891.

Thioacetic acid 2-[2-(1,3-dioxo-1,3-dihydro-isoindol-2-yl)-ethoxy]-ethyl ester (19)
Compound **18** (1.1 g, 4 mmol) was dissolved in 20 ml of dried DMF at 0 °C. After that potassium thioacetate (1.0 g, 8 mmol) and NBu$_4$I (20 mg) were added. The deep red mixture was stirred for 3 h at 60 °C, diluted with CH_2Cl_2 (60 ml) and washed three times with water. The organic phase was dried over $MgSO_4$ and the solvent was coevaporated with toluene. The light

yellow crude product was purified by silica gel column chromatography (hexane/EtOAc, 4/1, v/v) to give pure **19** (0.93 g, 80%). ^{1}H NMR (300MHz, CDCl$_3$) δ 7.78 (2H, m, Phth$H$), 7.67 (2H, m, Phth$H$), 3.84(2H, t, J = 5.7 Hz, CH_2N), 3.64 (2H, t, J = 5.7 Hz, OCH_2CH$_2$N), 3.51 (2H, t, J = 6.6 Hz, CH_2CH$_2$SAc), 2.95 (2H, t, J = 6.6 Hz, CH$_2$CH_2SAc), 2.17 (3H, s, CH_3). ^{13}C NMR (75 MHz, CDCl$_3$) δ 195.6, 168.4, 134.1, 132.4, 123.7, 123.5, 69.4, 67.8, 37.5, 30.6, 29.1. HRMS calcd for C$_{14}$H$_{15}$NO$_3$SNa (M + Na [+]): 300.0670, found: 300.0661.

(2-{2-[2-(2-tert-Butoxycarbonylamino-ethoxy)-ethyldisulfanyl]-ethoxy}-ethyl)-carbamic acid tert-butyl ester (20) Compound **19** (0.88 g, 0.3 mmol) was dissolved in EtOH (30 mL) and NH$_2$NH$_2$ (320 mg, 10 mmol) was added. The reaction was refluxed for 18 h. When the reaction was complete (TLC, MeOH), the solvent was removed. The residue was co-evaporated three times from MeOH. A mixture of di-*tert*-butyl dicarbonate (6.6 g, 3 mmol)**,** TEA (2 mL) and dry CH$_2$Cl$_2$ (40 mL) was added with cooling. The mixture was kept for 24 h at room temperature. The solvent was removed and the residue was purified by silica gel column chromatography (EtOAc) to give pure **20** (0.96 g, 73%). ^{1}H NMR (300MHz, CDCl$_3$) δ 3.64 (4H, t, J = 6.3 Hz, CH_2CH$_2$S), 3.46 (2H, t, J = 5.4 Hz, OCH_2CH$_2$N), 3.24 (2H, t, J = 5.4 Hz, OCH$_2$CH_2N), 2.82 (4H, t, J = 6.3 Hz, CH$_2$CH_2S), 1.38 (18H, s, CH_3). ^{13}C NMR (75 MHz, CDCl$_3$) δ 156.2, 79.6, 70.2, 69.4, 40.6, 38.8, 28.6.   HRMS calcd for C$_{18}$H$_{36}$N$_2$O$_6$S$_2$Na (M + Na [+]): 463.1912, found: 463.1903.

2-{2-[2-(2-Amino-ethoxy)-ethyldisulfanyl]-ethoxy}-ethylamine (21) Compound **19** (0.88 g, 2 mmol) was dissolved in 20% TFA in CH$_2$Cl$_2$ (20 mL) and stirred for 1 h at room temperature. The solvents were evaporated under reduced pressure, and the residue was co-evaporated three times from toluene to produce an oily residue, which was sufficiently pure for the next reaction step.

{2-[2-(2-{2-[5-(2-Oxo-hexahydro-thieno[3,4-d]imidazol-4-yl)-pentanoylamino]-ethoxy}-ethyldisulfanyl)-ethoxy]-ethyl}-carbamic acid tert-butyl ester (22) To solution of compound **21** (140 mg, 0.06 mmol) in DMF (10 mL) and TEA (0.1 mL) was added a solution of Biotin-NHS **23** (100 mg, 0.03 mmol) in DMF (10 mL) at 0 °C. The mixture was stirred for 12 h at 0 °C. The reaction was monitored with TLC (TLC, MeOH). A mixture of di-*tert*-butyl dicarbonate (0.66 g, 3 mmol), TEA (0.2 mL) and dry CH_2Cl_2 (10 mL) was added with cooling. The resulting reaction mixture was kept for 24 h at room temperature. The solvent was removed and the residue was purified by silica gel column chromatography (CH_2Cl_2/CH_3OH, 4: 1, v/v) to give pure **22** (100 mg, 61%).^{1}H NMR (300MHz, $CDCl_3$) δ 4.97 (1H, m, C*H*N), 4.37 (1H, m, C*H*N), 3.64 (4H, m, C*H_2*), 3.48 (2H, m, C*H_2*S), 3.24 (1H, m), 3.05 (2H, t, *J* = 6.0 Hz, CH_2CH_2S), 2.82 (2H, t, J = 6.0 Hz, CH_2CH_2S), 2.2 (2H, m, C*H_2*), 1.32-1.52 (6H, m, C*H_2*), 1.38 (9H, s, C*H_3*). ^{13}C NMR (75 MHz, $CDCl_3$) δ172.3, 161.1, 155.0, 78.3, 75.6, 68.9, 68.6, 68.1, 67.9, 60.9, 59.3, 54.5, 52.6, 40.9, 39.5, 39.3, 38.1, 37.4, 34.9, 27.4. HRMS calcd for $C_{23}H_{42}N_4O_6S_3Na$ (M + Na$^+$): 589.2164, found: 589.2155.

Compound 3 Compound **22** (28 mg, 0.05 mmol) was dissolved in 20% TFA in CH_2Cl_2 (5 mL) and stirred for 1 h at room temperature. The solvents were evaporated under reduced pressure to give an oily residue, which was co-evaporated three times from dry toluene. A mixture of **24** (38 mg, 0.1 mmol) and NEt_3 (30 mg, 0.3 mmol) in DMF (10 mL) was added with cooling. After stirring the reaction mixture overnight at ambient temperature, the solvent was removed under reduced pressure and the residue was purified by silica gel column chromatography (CH_2Cl_2/CH_3OH, 10:1, v/v) to afford **3** (22 mg , 70%). ^{1}H NMR (300MHz, $CDCl_3$) δ 7.29-7.55 (8H, m, aromatics), 5.51 (1H, m, C*H*OH), 4.30, 4.49(2H, m, C*H*NH), 3.66-3.80 (4H, m), 3.58 (4H, m, C*H_2*), 3.43 (4H, m, C*H_2*), 3.20 (1H, m, C*H_2*), 2.93 (1H, m, C*H_2*),

2.91-2.95 (4H, m, CH_2S), 2.74 (1H, m), 2.2 (2H, m, CH_2), 1.36-1.72 (6H, m, CH_2). ^{13}C NMR (75

MHz, CD122.8, Cl$_3$) δ 154.5, 151.0, 150.0, 128.9, 127.1, 126.9, 126.1, 126.0, 125.8, 125.2,

124.9, 120.3, 111.9, 108.9, 75.8, 75.6, 68.7, 68.6, 68.0, 67.8, 60.8, 59.2, 54.6, 45.2, 39.9, 39.6,

38.1, 37.6, 37.5, 34.9, 28.7, 27.2, 27.1, 24.6. HRMS calcd for C$_{36}$H$_{46}$N$_4$O$_6$S$_2$Na (M + Na $^+$):

735.2321, found: 735.2315.

2-(2-Bromo-ethoxy)-tetrahydr-pyran-D4 (26) 3,4-Dihydro-2H-pyran (2.7 mL, 30 mmol)

was added to a flame-dried flask containing *p*-TSA (26 mg, 1.4 mmol) and freshly distilled

CH$_2$Cl$_2$ (20 mL) under argon. The reaction was allowed to stir for 10 min before the dropwise

addition of 2-bromoethanol-D4 **25** (2.5 g, 20 mmol). The reaction mixture was then allowed to

stir for additional 12 h at ambient temperature. NaHCO$_3$ (2.0 g) was added to the reaction

mixture and stirring was continued for a further 1 h before filtering. The filtrate was evaporated

under reduced pressure and the resultant oil was subjected to silica gel column chromatography

(hexane/EtOAc, 9/1, v/v) to give 2-(2-bromoethoxy) tetrahydropyran-D4 **26** as a colorless oil

(3.4 g, 81%). ^{1}H NMR (300 MHz, CDCl$_3$) δ 4.66 (1H, m, C*H*), 3.88 (1H, m, C*H$_2$*), 3.51 (1H, m,

C*H$_2$*), 1.83 (1H, m, C*H$_2$*), 1.72 (1H, m, C*H$_2$*), 1.52 - 1.63 (4H, m, C*H$_2$*).^{13}C NMR (75 MHz,

CDCl$_3$) δ 99.0, 66.8, 62.4, 30.9, 30.6, 30.4, 25.5, 19.4. HRMS calcd for C$_{17}$H$_{21}$NO$_5$Na (M + Na

$^+$): 342.1317, found: 342.1309.

2-[2-(Tetrahydro-pyran-2-yloxy)-ethyl]-isoindole-1,3-dione-D4 (27) Compound **26** (2.1 g,

1 mmol) was dissolved in 100 ml acetone and heated to reflux. Phthalimide potassium salt (5.8 g,

2 mmol) was added in 4 parts to the boiling solution during 6 h. After an additional 24 h, the

solution was cooled to room temperature and a white solid, KBr, was removed by filtration and

the acetone was evaporated. The resultant oil was subjected to silica gel column chromatography

(hexane/EtOAc, 5/1, v/v) to give product **27** as a colorless oil (2.4 g, 86%). ^{1}H NMR (300 MHz,

CDCl$_3$) δ 7.75 (2H, m, Phth*H*), 7.63 (2H, m, Phth*H*), 4.56 (1H, m, C*H*), 3.64 (1H, m, C*H*$_2$), 3.36 (1H, m, C*H*$_2$), 1.35 - 1.69 (6H, m, C*H*$_2$). ^{13}C NMR (75 MHz, CDCl$_3$) δ 168.3, 134.0, 132.3, 123.3, 98.2, 63.3, 62.2, 37.4, 30.5, 25.5, 19.3. HRMS calcd for C$_{15}$H$_{13}$D$_4$NO$_4$Na (M + Na $^+$): 302.1302, found: 302.1296.

2-(2-Hydroxy-ethyl)-isoindole-1,3-dione-D4 (28) A solution of **27** (1.7 g, 0.6 mmol) in 20 mL of CH$_3$OH was treated with 3 mL of 1N HC1, and was stirred for 8 h at room temperature. The mixture was poured into ice-water and extracted with EtOAc, and the extract was washed with water, dried (MgSO$_4$), and concentrated. The oily residue was purified by silica gel column chromatography (hexane/EtOAc, 2/1, v/v) to give pure **28** (1.1 g, 88%). ^{1}H NMR (300 MHz, CDCl$_3$) δ 7.68 (2H, m, Phth*H*), 7.59 (2H, m, Phth*H*), 3.96 (1H, s, O*H*). ^{13}C NMR (75 MHz, CDCl$_3$) δ 168.7, 133.9, 131.7, 123.0, 48.9, 48.3. HRMS calcd for C$_{10}$H$_5$D$_4$NO$_3$Na (M + Na $^+$): 218.0727, found: 218.0719.

2-{2-[2-(Tetrahydro-pyran-2-yloxy)-ethoxy]-ethyl}-isoindole-1,3-dione-D8 (29) A mixture of sodium hydride (360 mg, 15 mmol) and 2-(2-Hydroxy-ethyl)-isoindole-1,3-dione-D4(**28**) (1 g, 5 mmol) in dry DMF (20 mL) was stirred for 2 h under argon. 2-(2-Bromoethoxy) tetrahydropyran-D4 (**26**) (1.0 g, 5 mmol) was then added slowly and stirring was continued for 12 h at room temperature. The mixture was poured into ice-water and extracted with dichloromethane, and the extract was washed with water, dried (MgSO$_4$), and concentrated. The oily residue was purified by silica gel column chromatography (hexane/EtOAc, 5/1, v/v) to give pure (**29**) (1.1 g, 71%). ^{1}H NMR (300 MHz, CDCl$_3$) δ 7.76 (2H, m, Phth*H*), 7.65 (2H, m, Phth*H*), 4.49 (1H, m, C*H*), 3.77 (1H, m, C*H*$_2$), 3.75 (1H, m, C*H*$_2$), 3.36 (1H, m, OC*H*$_2$), 1.34-1.72 (6H, m, C*H*$_2$). ^{13}C NMR (75 MHz, CDCl$_3$) δ 168.5, 134.1, 132.4, 123.4, 99.0, 70.2, 68.1, 66.7, 62.2, 37.6, 30.7, 25.6, 19.6. HRMS calcd for C$_{17}$H$_{13}$D$_8$NO$_5$Na (M + Na $^+$): 350.1811, found: 350.1802.

2-[2-(2-Hydroxy-ethoxy)-ethyl]-isoindole-1,3-dione-D8 (30) A solution of **29** (0.75 g, 2.5 mmol) in 10 mL of CH_3OH was treated with 2 mL of 1N HC1, and was stirred for 8h at room temperature. The mixture was poured into ice-water and extracted with EtOAc, and the extract was washed with water, dried ($MgSO_4$), and concentrated. The oily residue was purified by silica gel column chromatography (hexane/EtOAc, 1/1, v/v) to give pure **30** (0.72 g, 80%). ^1H NMR (300MHz, $CDCl_3$) δ 7.78 (2H, m, Phth*H*), 7.65 (2H, m, Phth*H*). ^{13}C NMR (75 MHz, $CDCl_3$) δ 167.4, 132.8, 131.0, 122.6, 70.2, 66.4, 62.0, 35.9. HRMS calcd for $C_{12}H_5D_8NO_4Na$ (M + Na $^+$): 266.1236, found: 266.1228.

2-[2-(2-Bromo-ethoxy)-ethyl]-isoindole-1,3-dione-D8 (31) To solution of **30** (0.55 g, 2.5 mmol) in CH_2Cl_2 (10 mL) was added PBr_3 (1.3 g, 5 mmol), the reaction mixture was cooled by an ice bath under argon atmosphere. The resulting mixture was stirred for 8 h at 0 °C. The solvents were evaporated in vacuo and the residue was purified by silica gel column chromatography (hexane/EtOAc, 6/1 v/v) to give pure **31** (0.6 g, 83%). ^1H NMR (300MHz, $CDCl_3$) δ 7.78 (2H, m, Phth*H*), 7.67 (2H, m, Phth*H*). ^{13}C NMR (75 MHz, $CDCl_3$) δ 167.2, 133.2, 131.3, 122.5, 68.5, 65.8, 35.5, 28.6. HRMS calcd for $C_{12}H_4D_8BrNO3Na$ (M + Na $^+$): 328.0392, found: 328.0383.

Thioacetic acid 2-[2-(1,3-dioxo-1,3-dihydro-isoindol-2-yl)-ethoxy]-ethyl ester (32) Compound **31** (0.6 g, 2 mmol) was dissolved in 10 ml of dried DMF at 0 °C. Potassium thioacetate (0.5 g, 4 mmol) and NBu_4I (20 mg) were added to the solution. The deep red mixture was stirred for 3 h at 60 °C, diluted with CH_2Cl_2 (40 mL) and washed three times with water. The organic phase was dried over $MgSO_4$ and the solvent was coevaporated with toluene. The light yellow crude product was purified by silica gel column chromatography (hexane/EtOAc, 4/1, v/v) to give pure **32** (0.44 g, 76%). ^1H NMR (300MHz, $CDCl_3$) δ 7.78 (2H, m, Phth*H*), 7.67

(2H, m, Phth*H*), 2.17 (3H, s, C*H*$_3$). ^{13}C NMR (75 MHz, CDCl$_3$) δ 194.4, 167.2, 132.9, 131.1, 122.2, 68.4, 66.8, 35.9, 30.8, 29.4. HRMS calcd for C$_{14}$H$_7$D$_8$NO$_4$SNa (M + Na $^+$): 324.1113, found: 324.1106.

(2-{2-[2-(2-tert-Butoxycarbonylamino-ethoxy)-ethyldisulfanyl]-ethoxy}-ethyl)-carbamic acid tert-butyl ester- D16 (33) Compound **32** (0.44 g, 0.15 mmol) was dissolved in EtOH (20 mL). NH$_2$NH$_2$ (160 mg, 5 mmol) was added to the solution. The reaction was refluxed for 12 h. When the reaction was complete (TLC, CH$_3$OH), the solvent was removed under reduced pressure. The residue was co-evaporated three times from methanol. A mixture of di-tert-butyl dicarbonate (3.3 g, 1.5 mmol)**,** TEA (1 mL) and dry CH$_2$Cl$_2$ (10 mL) was added with cooling. The mixture was kept for 24 h at room temperature. The solvent was removed and the residue was purified by silica gel column chromatography (EtOAc) to give pure (**33**) (0.43 g, 68%). ^{1}H NMR (300MHz, CDCl$_3$) δ 1.38 (18H, s, C*H*$_3$). ^{13}C NMR (75 MHz, CDCl$_3$) δ 154.9, 27.4. HRMS calcd for C$_{18}$H$_{20}$D$_{16}$N$_2$O$_6$S$_2$Na (M + Na $^+$): 479.2900, found: 479.2893.

2-{2-[2-(2-Amino-ethoxy)-ethyldisulfanyl]-ethoxy}-ethylamine-D16 (34) Compound **33** (0.43 g, 1mmol) was dissolved in 20% TFA in CH$_2$Cl$_2$ (10 mL) and stirred for 1 h at room temperature. The solvents were evaporated under reduced pressure, and the residue was co-evaporated three times from toluene to give an oily residue, which was sufficiently pure for next step reaction.

{2-[2-(2-{2-[5-(2-Oxo-hexahydro-thieno[3,4-d]imidazol-4-yl)-pentanoylamino]-ethoxy}-ethyldisulfanyl)-ethoxy]-ethyl}-carbamic acid tert-butyl ester –D16 (35) To a solution of compound **34** (140 mg, 0.06 mmol) in DMF (10 mL) and TEA (0.1 mL) was added a solution of Biotin-NHS **23** (100 mg, 0.03 mmol) in DMF (10 mL) at 0 °C. The mixture was stirred for 12 h at 0 °C, the reaction was monitored with TLC (CH$_3$OH). A mixture of di-*tert*-butyl dicarbonate

(0.66 g, 3 mmol)**,** TEA (0.2 mL) and dry CH_2Cl_2 (10 mL) was added with cooling. The mixture was kept for 24 h at room temperature. The solvent was removed, and the residue was purified by silica gel column chromatography (CH_2Cl_2/CH_3OH, 4/1, v/v) to give pure **35** (80 mg, 51%).^{1}H NMR (300MHz, $CDCl_3$) δ 4.45 (1H, m, C*H*N), 4.27 (1H, m, C*H*N), 3.10 (1H, m), 2.85 (1H, m), 2.68 (1H, m), 2.16 (2H, m, C*H*$_2$), 1.52-1.62 (6H, m, C*H*$_2$), 1.38 (9H, s, C*H*$_3$). HRMS calcd for $C_{23}H_{26}D_{16}N_4O_6S_3Na$ (M + Na$^+$): 605.3152, found: 605.3144.

Compound 4 Compound **35** (14 mg, 0.025 mmol) was dissolved in 20% TFA in CH_2Cl_2 (5 mL) and stirred for 1 h at room temperature. The solvents were evaporated under reduced pressure to give an oily residue, which was co-evaporated three times from dry toluene. A mixture of **24** (38 mg, 0.1 mmol) and TEA (30 mg, 0.3 mmol) in DMF (10 mL) was added to the oily residuewith cooling. After stirring the reaction mixture overnight at ambient temperature, the solvent was removed under reduced pressure and the residue was purified by silica gel column chromatography (CH_2Cl_2/CH_3OH, 10/1, v/v) to afford **4** (12 mg , 77%). ^{1}H NMR (300MHz, $CDCl_3$) δ 7.29-7.55 (8H, m, aromatics), 7.29-7.55 (8H, m, aromatics), 5.51 (1H, m, C*H*OH), 4.57(2H, m, C*H*NH), 3.43 (1H, m), 3.19 (1H, m), 2.85 (1H, m), 2.2 (2H, m, C*H*$_2$CO), 1.35-1.72 (6H, m, SCHC*H*$_2$C*H*$_2$C*H*$_2$). ^{13}C NMR (75 MHz, $CDCl_3$) δ 154.6, 151.0, 150.0, 128.9, 127.0, 126.1, 125.2, 124.9, 122.8, 120.2, 111.9, 108.9, 75.6, 59.3, 52.4, 45.1, 30.9, 28.6, 28.3, 21.6, 20.0. HRMS calcd for $C_{35}H_{28}D_{16}N_4NaO_6S_3$ (M + Na$^+$): 751.3309, found: 751.3301.

Jurkat cell-Surface Labeling of Azide-Bearing Glycans with QUIC-Tag 3 Human Jurkat cells (Clone E6-1; ATCC) were cultured in RPMI 1640 medium (ATCC) with L-glutamine (2 mM), adjusted to contain $NaHCO_3$ (1.5 g L^{-1}), glucose (4.5 g L^{-1}), HEPES (10 mM), and sodium pyruvate (1.0 mM) and supplemented with penicillin (100 u mL^{-1})/ streptomycin (100 μg mL^{-1}; Mediatech) and fetal bovine serum (FBS, 10%; Hyclone). Cells were maintained in a humid 5%

CO$_2$ atmosphere at 37$^\text{o}$C. Jurkat cells were incubated for 3 days in media containing 25 μM Ac$_4$ManNAz or 25 μM of N-acetylmannosamine (Ac$_4$ManNAc) as a negative control, leading to the metabolic incorporation of the corresponding N-azidoacetyl sialic acid (SiaNAz) and sialic acid, respectively, into their cell surface glycoproteins. Jurkat cells bearing azides and control cells were incubated with the QUIC-Tag **3** (0, 3, 10 or 30 μM) in labeling buffer (DPBS, supplemented with FBS (1%)) for 60 min at room temperature. The cells were washed three times with labeling buffer and then incubated with avidin conjugated with fluorescein (Molecular Probes) for 15 min at 4$^\text{o}$C. Following three washes and cell lysis, cell lysates were analysed for fluorescence intensity (485 ex / 520 em) using a microplate reader 9 (BMG Labtech). Data points were collected in triplicate and are representative of three separate experiments. Cell viability was assessed at different points in the procedure with exclusion of trypan blue.

CHO cell-Surface Labeling of Azide-Bearing Glycans with QUIC-Tag 3. Chinese hamster ovary (CHO) cells (Clone K1; ATCC) were cultured in Kaighn's modification of Ham's F-12 medium (F-12K) with L-glutamine (2 mM), adjusted to contain NaHCO$_3$ (1.5 g L^{-1}) and supplemented with penicillin (100 u mL^{-1}) / streptomycin (100 μg mL^{-1} and FBS (10%). Cells were maintained in a humid 5% CO$_2$ atmosphere at 37$^\text{o}$C. CHO cells were grown in the presence of Ac4ManNaz (100 μM final concentration) or 25 μM of N-acetylmannosamine (Ac$_4$ManNAc) and without sugars as a negative control for 3 days to metabolically incorporate SiaNAz into their cell surface glycoproteins. CHO cells bearing azides and control cells were then incubated with the QUIC-Tag **3** (0, 3, 10 or 30 μM) in labeling buffer (DPBS, supplemented with FBS (1%)) for 60 min at room temperature. The cells were washed three times with labeling buffer and then incubated with avidin conjugated with fluorescein (Molecular Probes) for 15 min at 4$^\text{o}$C. Following three washes and cell lysis, cell lysates were analysed for fluorescence intensity (485

ex / 520 em) using a microplate reader 9 (BMG Labtech). Data points were collected in triplicate and are representative of three separate experiments. Cell viability was assessed at different points in the procedure with exclusion of trypan blue.

4.4 REFERENCES

1. Apweiler, R.; Hermjakob, H.; Sharon, N. *Biochim. Biophys. Acta.* 1999, 1473, 4.

2. Varki A, Cummings R, Esko JD, Freeze H, Hart GW, Marth J (1999) Essentials of Glycobiology (Cold Spring Harbor Lab Press, Cold Spring Harbor, NY), pp 1–635.

3. Axford JS, *Biochim Biophys Acta,* 1999, 1455, 219.

4. Dube DH, Bertozzi CR *Nat Rev Drug Discov* 2005, 4 ,477.

5. Mackiewicz A, Mackiewicz K *Glycoconj J* 1995, 12, 241.

6. Meezan E, Wu HC, Black PH, Robbins PW *Biochemistry* 1969, 8, 2518.

7. Turner GA *Clin Chim Acta* 1992, 208, 149.

8. R. E. Kosa, R. Brossmer, H.-J. Gross, *Biochem. Biophys. Res. Commun.* 1993, 190, 914

9. W. Fitz and C.-H. Wong, *J. Org. Chem*, 1994, 59, 8279.

10. S. L. Shames, et al., *Glycobiology*, 1991, 1, 187.

11. M. A. Sparks, et al., *Tetrahedron* 1993, 49, 1.

12. C.-H. Lin, T. Sugai, R. L. Halcomb, Y. Ichikawa, C.-H. Wong, *J. Am. Chem. Soc.* 1992, 114, 10138.

13. L. Warren, Bound Carbohydrates in Nature (Cambridge Univ. Press, New York, 1994).

A. Varki, *FASEB J.* 1991, **5**, 226

14. Kneass, Z.T. & Marchase, R.B. *J. Biol. Chem.* 2004, 279, 45759

15. Zachara, N.E. et al. *J. Biol. Chem.* 2004, 279, 30133

16. Khidekel, N. et al. *J. Am. Chem. Soc.* 2003, 125, 16162

17. Ross, P.L. et al. *Mol. Cell. Proteomics*, 2004, 3, 1154

18. Tai, H.C., Khidekel, N., Ficarro, S.B., Peters, E.C. & Hsieh-Wilson, L.C. *J. Am. Chem. Soc.* 2004, 126, 10500

19. Khidekel, N., Ficarro, S.B., Peters, E.C. & Hsieh-Wilson, L.C. *Proc. Natl. Acad. Sci. USA,* 2004, 101, 13132

20. K.F. Bernady, M.B. Floyd, J.F. Poletto and M.J. Weiss, *J. Org. Chem*. 1979, 44, 1438.

21. E.J. Corey, H. Niwa and J. Knolle, *J. Am. Chem. Soc*. 1978, 100, 1942.

22. Eliana Saxon, Sarah J. Luchansky, Howard C. Hang, Chong Yu, Sandy C. Lee, and Carolyn R. Bertozzi.*J. Am. Chem. Soc.*, 2002, 124, 14893

23. Fitz, Wolfgang; Rosenthal, Peter B.; Wong, Chi-Huey. *Bioorganic & Medicinal Chemistry*. 1996, 4, 1349.

24. Kiyoshi; Kimura, Fuyuki; Sano, Kimihiko; Suzuki, Yasuo; Achiwa, Kazuo. Carbohydrate Research. 1998, 312, 183.

CHAPTER 5

A MICELLAR NANO-DELIVERY SYSTEM

-selective drug delivery at the subcellular level

ABSTRACT

Two essential criteria are required for an efficacious drug. First, a chemical compound has to have the desired biological effect. Second, it has to be able to reach the target area. A modular, multi-functional drug delivery system emerges to meet these two criteria to promise simultaneously to enhance the effectiveness and reduce undesirable side-effects.

Nanoparticles have garnered attention as attractive systems for drug delivery. Even though nanoparticles are exceptionally small, they are much larger than single molecules. For example, block copolymer micelles are usually spherical supramolecular assemblies (10 to 100 nm) of amphiphilic block copolymers that possess a core-shell architecture. The core of the micelles acts as a loading space for hydrophobic drugs and the shell is a brush-like protective corona that ensures water dispersity.

Research in this field has increasingly focused on enhancing stability of the micellar assembly, prolonging circulation times and controlling release of the drug for optimal targeting. With that in mind, we are developing novel multifunctional micellar nanosystems for various applications.

5.1 INTRODUCTION

Drug delivery has evolved into an interdisciplinary and independent field of research and is gaining the attention of pharmaceutical scientists. The targeted and safe drug delivery system can

improve the performance of some classical medicines which have been on the market, moreover, will have implications for the development and success of new therapeutic strategies. However, the delivery of highly efficacious therapeutic compounds can be hindered by their poor solubility, stability, and toxicity. To ameliorate problems, many innovative technologies for effective drug delivery have been developed,[1-9] including nanotechnology.

We are involved in a program that employs nanoparticles as scaffolds for the attachment of the various modules to provide a multifunctional drug delivery device.[10-13] These modules include targeting devices for specific cell types, cell permeation molecules, and cell-signaling peptides for selective transport to organelles. Further enhancement of selectivity will be achieved by employing prodrugs that will only be activated when the targeted location has been reached. In this way, misdirected molecules will not induce unwanted side reactions. Thus, the long-term aim of these studies is to develop a sophisticated drug delivery device that will target specific cell types, facilitate internalizations into cells and direct drugs to a particular organelle to achieve high local concentrations, as well as induce the drug activity after reaching the target area to reduce the unwanted toxicity.

The small molecule disadvantage

Since the early 1990's, the strategy of small molecule drug discovery has changed dramatically. Molecular biology and genomics provide opportunities to identify and express many new important biological targets. Chemists have developed combinatorial approaches to prepare large libraries of compounds, which can be screened for biological activities by high throughput assays. In addition, structural biologists have developed powerful new tools such as molecular docking algorithms, homology modeling of proteins, mapping protein-binding sites by NMR and high throughput protein X-ray crystallography, which allow an unprecedented level of

rational design of prospective drugs.[14-16] Despite these technological developments, small molecule drugs discovery does not seem to be getting easier because many interesting lead compounds fail in clinical trials due to lack of selectivity or drug resistance. Clearly, new technological platforms should be developed to endow a small molecule drug candidate with features to increase selectivity. The following project intends to break new ground by aiming to use biological systems as blueprints in the discovery of drugs with exquisite selectivity. In particular, a flexible and multifunctional nanoscale device is developed for selective delivery of small molecule drugs to organelles of particular cell or tissue types.

Selectivity in biological recognition processes

Delicate selectivity of proteins and enzymes for their cognate ligands and substrates has long been regarded as a hallmark of biological processes. However, the emerging evidences indicate many possibilities for cross interactions between proteins and molecules arising from the similarities in structures of metabolites and flexibility binding of protein active sites. For example, structural and computational studies have shown that unrelated groups of proteins may share steric or electrostatic features, allowing groups of ligands with complementary features to be accommodated. Indeed, docking studies have indicated that particular enzymes can recognize a number of endogenous metabolites. Promiscuity has also been observed experimentally for a number of proteins and enzymes, including human serum albumin, chemotrypsin, bovine carbonic anhydrase, L-asparaginase, alkaline phosphatase and glycosyltranferases.

Protein glycosylation is an important example of biosynthetic fidelity controlled by compartmentalization.[17] Many glycosyltransferases can utilize common saccharide acceptors to produce different products. As a result, the location of glycosidases and glycosyltransferases in the secretory pathway is an important determinant of the type of biosynthesized oligosaccharide.

Not surprisingly, major changes in the glycome are induced by a loss of some chaperones and multi-protein complexes that alter glycosyltransferase trafficking between the ER and the Golgi[18]. In addition, there is evidence that intracellular trafficking of glycosides and glycosyltransferases is controlled by phosphorylation of their cytoplasmic tail. The biosynthesis and catabolism of glycoproteins is also spatially separated to avoid undesirable crossreactions. For example, glycoproteins destined for degradation are internalized by clathrin-mediated endocytosis to give early endosomes, which are transported to lysomes. The latter organelle contains many glycosidases with broad substrate specificity that can degrade a wide range of glycoproteins. Thus, catabolic enzymes would destroy newly synthesized glycoproteins if both processes were not strictly separated. Interestingly, many putative drugs that are aimed at targeting glycosidases of the ER or Golgi have failed in preclinical or clinical trials due to unwanted inhibition of lysosomal enzymes.

Overcoming the small molecule disadvantage

It is clear that the reliability of biomolecular recognition relies on a number of processes such as optimizing protein-ligand interactions, cell specific expression of proteins and enzymes, multi-protein complex formation and compartmentalization of enzymes and substrates in specific organelles.[19] A drug delivery device will incorporate a module that will bind to protein or ligand that is specific for a particular tissue or cell type. Humanized antibodies, small peptides, oligosaccharides and aptamers have already been used to deliver drugs to specific tissues or tumors.[20-21] Targeting to other types of diseased tissue is much less well developed. Thus, there is an urgent need to identify functionalities that can bind to particular cells of the musculoskeletal system to selectively deliver drugs to hasten bone healing and prevent muscle atrophy. Interestingly, the cell permeation peptide (CPP) of Tat can deliver a wide variety of functional

biomolecules into cells. Furthermore, a number of structural analogs of the Tat peptide have been developed with improved properties. Thus, it is proposed that attachment of a CPP to a drug delivery device will ensure internalization by cells. Selective targeting and uptake may also be achieved by employing ligands of the cell surface receptor. For example, compounds attached to Pam$_3$CysSK^4, which is a ligand for Toll-like receptor 2 (TLR2),[22] can selectively be endocytosed by immune cells that express this receptor.

Particles that are internalized by endocytosis may become trapped in endosomes and lysosomes, preventing travel to the required subcellular location. Therefore, the delivery device may need to contain a module that will facilitate escape from these compartments. In this respect, small peptide domains of viral proteins that are rich in histidines have been found to facilitate endosomal escape.[23] The escape mechanism is that the histidines mediate an acid-dependent fusion and leakage of negatively charged liposomes after protonation of the imidazole group of histinyl monomers.

After escape from endosomes, the delivery device will direct drug molecules to the target organelle. Many proteins contain short signal peptides that facilitate retention or retrieval to particular cellular compartments. During the past decade, the structures of many retention and retrieval peptides have been elucidated. The attentions have been focused on selective delivery of glycosidase and glycosyltransferase inhibitors to the ER and Golgi for the treatment of a wide variety of diseases such as cancer, inflammation and congenital disorders.[24] Accordingly, a unique aspect of our research is to exploit nature's strategies for protein trafficking to guide the delivery device to a particular subcellular location.

It is anticipated that side effects of a drug may be minimized when it is endowed with multiple approaches to achieve exquisite selectivity. Also, an imaging module such as a

fluorescence tag, a quantum dot or an MRI agent can be incorporated. A fluorescence probe will make it possible to track the device in cell based systems whereas an MRI imaging agent such as iron oxide will be able to determine tissue distributions in animals. The use of an MRI contrast may also make it possible to combine a drug delivery with therapeutic imaging.[25-27]

It is envisaged that nanoparticles will provide attractive scaffolds for the attachment of the various modules to give multifunctional delivery devices.[10-13] Furthermore, by using appropriate chemistries, it will be possible to modify nanoparticles in a controlled manner with a variety of modules.[28] An important goal of our study is to establish the appropriate configurations of multifunctional nanoparticles for spatially controlled delivery of (pro)drugs. Another major object is to develop chemical technologies for the modular assembly of such nanoparticles. However, no chemical technologies are available for the controlled attachment of different chemical entities to a nanoscale device that can carry multiple copies of a putative (pro)drug. Here, dendrimers, gold nanoparticles, self-assembled micellar copolymers and cationic liposomes will be considered as nanoparticle platforms. These materials are sufficiently small so as to be transported to a particular organelle.

In principle, (pro)drugs can either be attached to exterior functionalities of nanoparticles or entrapped in interior spaces. An exterior attachment will be attractive for polar drugs to create multivalent surfaces. Actually, the multivalent binding events, in which multiple ligands on one entity simultaneously interact with multiple receptors on a complementary entity, are widespread in nature. The best studied manifestations of multivalency include dramaticly increased functional affinities and enhanced selectivities. Thus, it is anticipated that multivalently presented drug candidates on nano-particles will bind with a high avidity to membrane-bound enzymes and receptors. Compared to polar drugs, lipophilic drugs can be entrapped in interior

spaces of dendrimers and micelles. In this case, it will be important that entrapped drugs are able to escape from the device after entry to cell. The goal can be achieved by employing nanomaterials that are able to be selectively metabolized within the intracellular environment.

Nanoscale drug delivery devices require to be carefully evaluated for safety issues such as antigenic and cytotoxicity properties. Furthermore, to achieve therapeutic concentrations, it is important to avoid that the nanoparticles are taken up by the liver. In this respect, several studies have shown that particles covered with polyethylene glycol (PEG) moieties can produce long circulating materials.[29-34] Polymeric micelles with poly(ethylene oxide) (PEO) as the hydrophilic block forming the corona of the micelles can avoid uptake by the reticuloendothelial system (RES) and thus remain in blood circulation for a prolonged time.[1-3] A wide range of polymeric materials has been utilized as hydrophobic block or charged block in complexes to form the core of the micelles, the choice depending on compatibility between the polymers and incorporated drugs.[2] Poly(ethyleneoxide)-*b*-poly(ε-caprolactone) (PEO-*b*-PCL) diblock copolymer micelles have been explored as a drug delivery system.[35-36] PCL is a well-known biodegradable polymer which has been utilized in various biomedical applications because of its excellent biocompatibility and degradability. It has been reported that PEO-*b*-PCL micelles are effective carriers for lipophilic drugs, such as dihydrotestosterone.[35-37]

Research plan: preparation of KDEL functional micelles for targeting Glycosidase Inhibitors to ER

In our research, we are planning to design selective delivering of α-glycosidase inhibitors to the ER for the treatment of a wide variety of diseases such as cancer, inflammation and congenital disorders. Glycosidases play a very important role in various biological processes, such as intestinal digestion, post-translational modification of glycoproteins and the lysosomal

catabolism of glycoconjugates.[38] The prospect of modifying or blocking these processes by using glycosidase inhibitors has attracted a lot of attention, since some sugar-mimic alkaloids show potential antidiabetic, antiviral and anticancer effects.[39] The enzymatic cleavage of the glycosidic bond liberates a sugar hemiacetal with either retention or inversion of the substrate. (**Scheme 5.1**)[40]
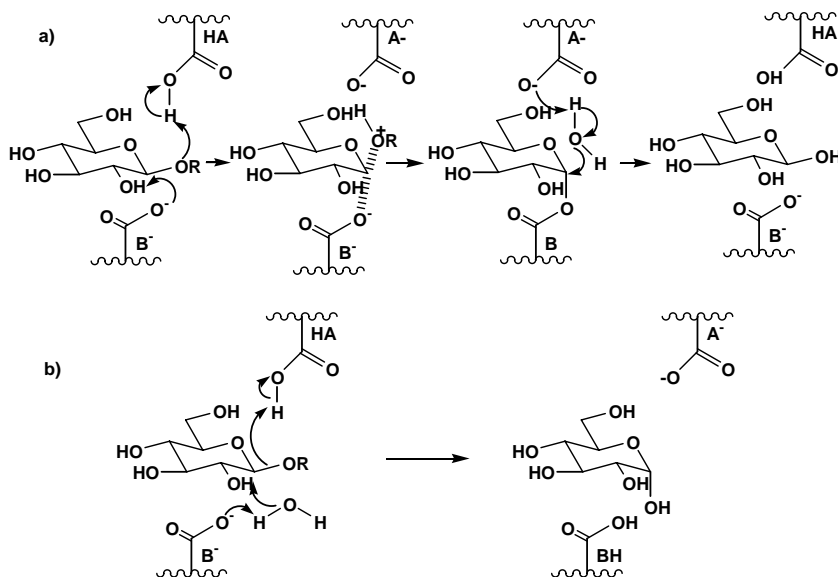
Scheme 5.1 a) Catalytic mechanism for configuration retaining glycosidases; b) Catalytic mechanism for configuration inverting glycosidases

α-mannosidase is a type of glycosidase which hydrolyzes mannose. Lack of α-mannosidase function causes mental and physical deterioration. Thus α-mannosidase inhibitors have been evaluated as anti-cancer agents by many scientists.

A number of α-mannosidase inhibitors have been obtained from natural sources or synthesized chemically (Shown in **Figure 5.1**). The first reported glycoprotein processing α-mannosidase inhibitor was the indolizidine alkaloid swainsonine (1). This compound originally showed inhibition of the lysosomal α-mannosidase and caused similar symptoms with those of the lysosomal storage disease α-mannosidosis when it was administered to animals.

Deoxymannojirimycin (**2**) was first isolated from the seeds of the legume *Lonchocarpus sericeus*. In animal cells, Deoxymannojirimycin inhibited Golgi mannosidase IA/B and caused the accumulation of glycoproteins containing a high mannoside sugar. Mannojirimycin (**3**) has been proposed as an intermediate in the biosynthesis of Deoxymannojirimycin.

Kifunensine (**4**) is an alkaloid produced by the actinomycete, *Kitasatsporia kifunese* and corresponds in structure to the cyclic oxamide derivative of 1-amino Deoxymannojirimycin. This alkaloid is a potent inhibitor of the Golgi mannosidase I, but is as a very weak inhibitor of jack bean α-mannosidase in ER as Kifunensine. Golgi mannosidase I inhibition by Kifunensine is 100 times greater than by deoxymannojirimycin.[41]
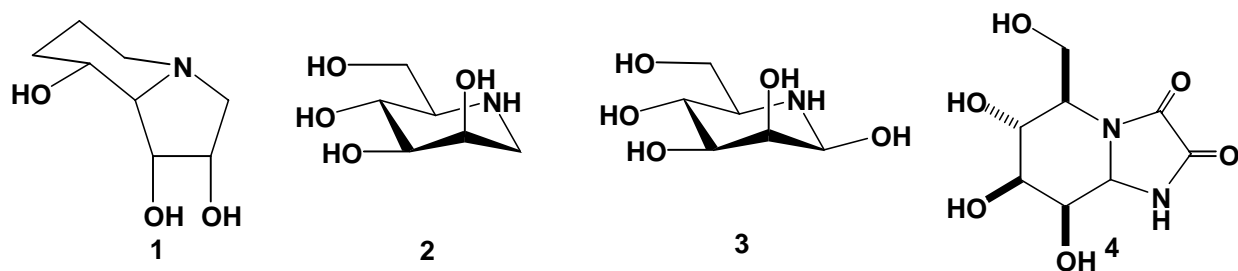
Figure 5.1 α-Mannosidase Inhibitors

Kifunensine is a potent naturally occurring class I α-mannosidase inhibitor. Kifunensine inhibits both human ER α-1,2-mannosidase I (ER Man I) and Golgi α-mannosidase IA,IB and IC (Golgi Man IA/IB/IC). ER Man I plays an important role in the quality control of glycoprotein folding within the ER, a process that is commonly referred to as ER Associated Degradation (ERAD). A large number of genetic diseases are related to the processes of ERAD.

Recently, several studies have verified that Kifunensine inhibits ER Man I leading to blockage of the degradation of mutant glycoproteins including the T cell receptor subunit CD3-δ, tyrosinase, and α2-plasmin inhibitor. In contrast, the disposal of misfolded glycoproteins was accelerated by the overexpression of ER Man I. Surprisingly, acceleration of the "disposal clock"

by ER Man I overexpression also activated a large disposal of wild-type glycoproteins. Thus, a model was designed in which glycan trimming to $Man_8GlcNAc_2$ moieties in the context of partly folded or misfolded polypeptide structures acts as the rate-determining step in generating the signal for glycoprotein disposal. In this model, ER Man I occupies a unique intersection **(Figure 5.2)** of both catabolic and glycoprotein biosynthetic pathways and defines the binary decision for the fate of nascent glycoproteins toward folding or disposal.

These results indicate that inhibition of ER Man I may serve as a possible approach for the treatment of genetic diseases that take place as a direct result of the processes of ERAD. As a result of its potent inhibition of ER Man I, Kifunensine delivers a superb means for the study and regulation of this important enzyme and its role in ERAD. However, Kifunensine also inhibits Golgi Man I, an enzyme that is required for the maturation of *N*-linked glycoproteins into hybrid and complex type glycoproteins. Thus, there is a need to synthesize a selective drug delivery system that can selectively deliver kifunensine to ER and selectively inhibit ER Man I over Golgi Man I in order to successfully study the mechanism of ER Man I and to help in the development of novel therapeutic agents for the treatment of genetic diseases related to ERAD.[42]
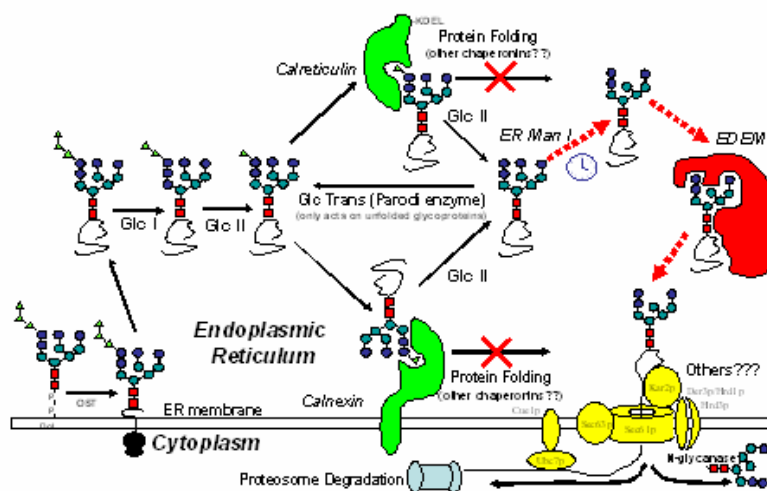
Figure 5.2 Processed glycans influence the rate and targeting of misfolded proteins for ERAD

Secretory proteins, mostly glycoproteins, are transported by the ER and from there throughout the cell are marked with an address tag called a signal sequence. The majority of ER resident proteins are retained in the ER through a retention motif. This motif is carboxy-terminal tetrapeptide KDEL (Lys-Asp-Glu-Leu).[43]

Therefore, we planed to design a drug delivery system carrying KDEL as a targeting motif and kifunensine as a therapeutic motif.

We have developed an efficient method for the preparation of ligand-modified micellar nanoparticles that can entrap lipophilic compounds (drugs). In this method, poly(ethylene glycol) (PEG) capped with an azide is copolymerized with ε-caprolactone to form block copolymer PEG-*b*-PCL. Ligands can be attached to the block copolymer by click reaction between azide of the polymer and an alkyne of a modified ligand. In this way, we have attached a KDEL signal peptide ligand to the polymers. The addition of the amphiphilic copolymers to an aqueous solution results in the formation of micelle, and interior of the micelles trap lipophilic α-Mannosidase inhibitors kifunensine. Thus, the liposomes modified by a KDEL signal peptide ligand have the potential to be developed as selective drug delivery devices which can selectively deliver kifunensine into the ER.[43]
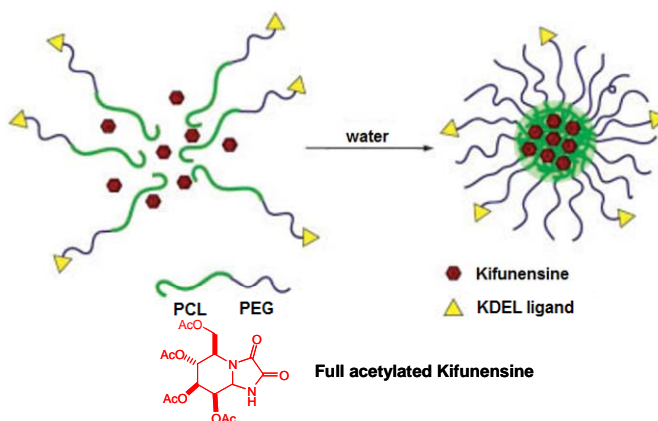
Figure 5.3 Preparation of Kifunensine loading KDEL-modified micelles

5.2 RESULTS AND DISCUSSION

Synthesis of PEG$_{45}$-*b*-PCL$_{23}$ Block Copolymers and Rhodamine-Conjugated Copolymers

We used an amphiphilic block copolymer of poly(ε-capro-lactone)-b-poly(ethylene glycol) (PCL-*b*-PEG) for the micelle formation. PEG$_{45}$-*b*-PCL$_{23}$ block copolymers and rhodamine-conjugated copolymers were synthesized as shown in **Scheme 5.2**. This copolymer was synthesized by a cationic ring opening polymerization of ε-caprolactone using mono-methoxy-terminated PEG (2 k) as a macroinitiator and Sn(Oct)$_2$ as a catalyst. In order to produce uniform length polymers, the mono-methoxy-terminated PEG macroinitiators had polydispersity indices (PMI) below 1.1. The synthesized polymers were then dissolved in THF, recovered by precipitation into cold hexane, and dried under vacuum at room temperature. Molecular weights were analyzed by the PEG analysis by NMR. The number average molecular weight(M_n) of the PEG$_{45}$-*b*-PCL$_{23}$ block copolymer was determined by the PEG analysis ^{1}H-NMR. The ^{1}H-NMR spectrum of the labeled polymer is shown in **Figure 5.4**. The methylene protons of the ethylene oxide units of the PEG correspond to the singlet at 3.7 ppm. The methylene peaks of the caprolactone appear at 4.1, 2.3, 1.63, and 1.37 ppm. The molar ratio of ethylene oxide units to caprolactone units can be calculated based on the ratios of their peak areas. Therefore, the degree of polymerization of the caprolactone can be obtained relative to the degree of polymerization of ethylene oxide. In our case, the calculated degree of polymerization of the caprolactone is 23. The molecular weight based on the degree of polymerization of caprolactone and ethylene oxide from NMR is 4600 g/mol.

As shown in **Scheme 5.2**, the rhodamine-conjugated PEG$_{45}$-*b*-PCL$_{23}$ block copolymers (PEG$_{45}$-*b*-PCL$_{23}$-Rh) were synthesized by employing a modified version of an existing procedure.

In PEG$_{45}$-*b*-PCL$_{23}$ block copolymers, the functional group at the end of PEG chain is methoxy, while the functional group at the end of PCL chain is hydroxy. The hydroxy group can react with the isothiocyanate group of Rhodamine B. Therefore, tetramethylrhodamine can be attached to the end of the PCL chain. The success of the conjugation of tetramethylrhodamine to the block copolymer can be proven by ^{1}H NMR (**Figure 5.4**). The signal of methyl protons of tetramethylrhodamine is found at 1.84 ppm. The ratios of peak areas of the methyl group in tetramethylrhodamine to those of the methylene groups in PEG or PCL were used to analyze the molar ratio of tetramethylrhodamine to block copolymer chains. The average molar ratio is 0.86, suggesting that 86% of the polymer chains may be functionalized.
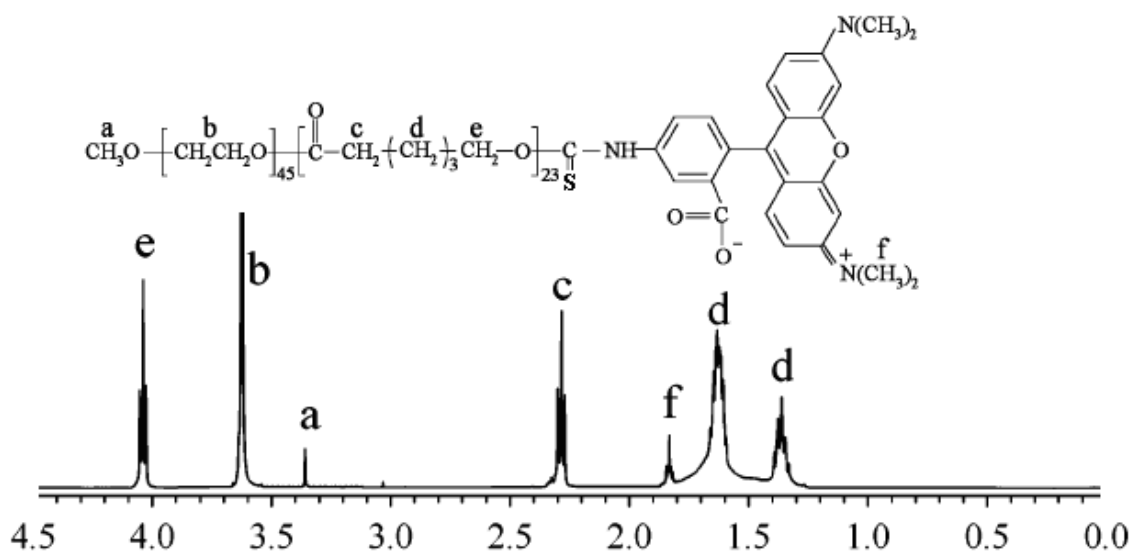
Figure 5.4 ^{1}H-NMR spectrum of PEG$_{45}$-*b*-PCL$_{23}$-Rh in CDCl$_3$
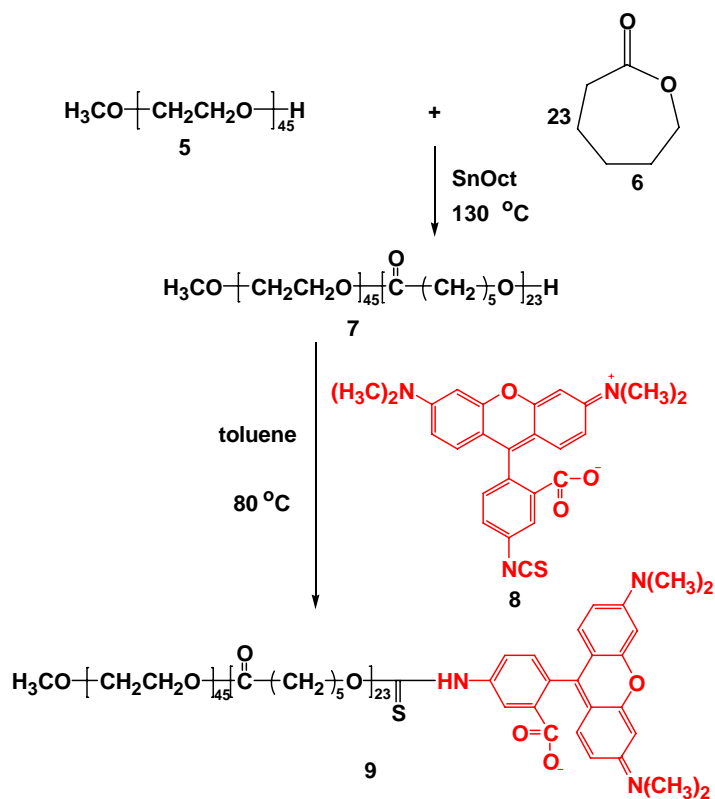
Scheme 5.2 Synthesis of PEG-*b*-PCL copolymer and Rhodamine-Conjugated PEG-*b*-PCL copolymer.

Preparation and characterization of fluorogenic micelles

Micelles only can form when the surfactant concentration is higher than the critical micelle concentration (CMC), and the temperature of the system is greater than the critical micelle temperature, or Krafft temperature. The formation of micelles is based on thermodynamics: micelles can form spontaneously due to a balance between enthalpy and entropy. Although assembling surfactant molecules together reduces their entropy, the hydrophobic force induces micelle formation in aqueous condition.

Rhodamine-conjugated block copolymer (40%) was mixed with the of the unlabeled block copolymer (60%) to prepare the rhodamine-labeled micelles. The sizes and morphologies of labeled micelles were studied by both cryo-TEM and AFM. As shown in **Figure 5.5**, labeled

micelles are generally spheroidal. The average diameters of labeled micelles were 35 ± 3 nm, which suggests that the size distributions of labeled micelles are narrow. It should be noted that only the spherical units were counted in the calculation of average sizes from TEM micrographs, because some of the elongated aggregates are probably the results of the attachment of two or more micelles during deposition.
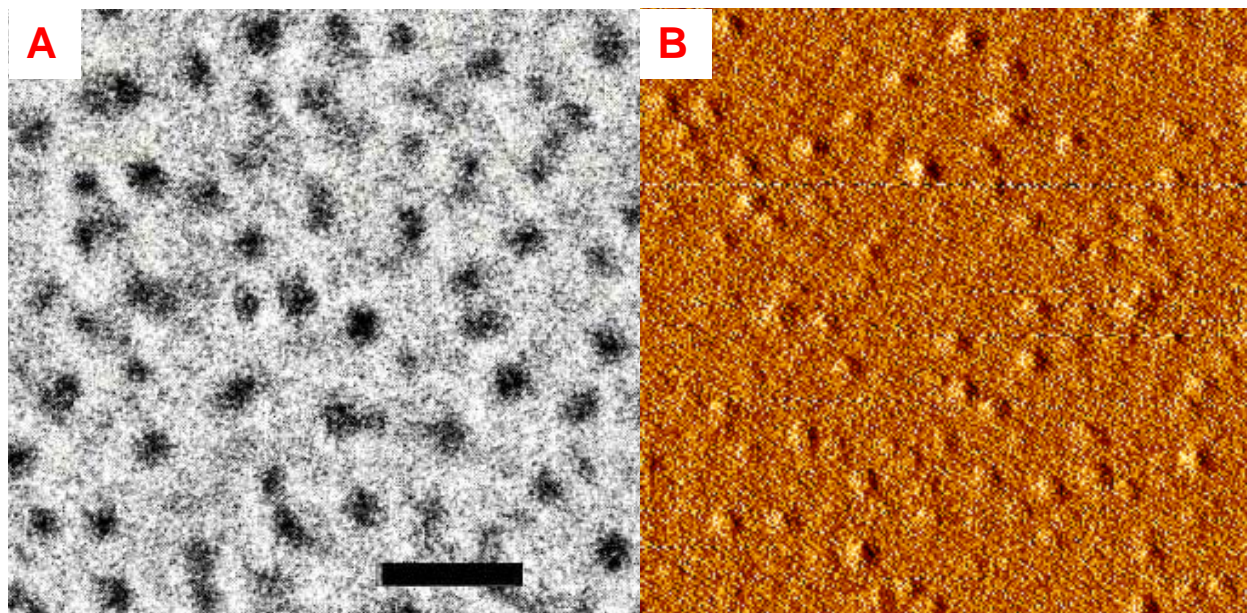
Figure 5.5 TEM and AFM of micelles, scale bar in **Figure 5A** indicates 100 nm

Internalization of micelle into Human adenocarcinoma epithelial cells (HeLa229 cells) and Murine embryonic fibroblasts (NIH/3T3 cells)

To determine whether micelles with a PEG corona are internalized by cells, we used fluorescent micelles (referred to as TMRCA-PCL-b-PEG micelles) made from red-fluorescent, TMRCA-labeled PCL-b-PEO block copolymer (40%) and nonlabeled PCL-b-PEO block copolymer (60%). The model cell system was Human adenocarcinoma epithelial cells (HeLa229 cells) and Murine embryonic fibroblasts (NIH/3T3 cells).[48] Fluorescence from TMRCA-PCL-b-PEO micelles was detected in the cytoplasmic but not the nuclear compartment (**Figure 5.6**). Furthermore, washing the cells with an acidified buffer and phosphate-buffered saline did not

eliminate the fluorescence, since the rhodamine molecules are chemically linked to the PEO_{45}-*b*-PCL_{23} block copolymers. The results provide direct evidence for internalization of the block copolymer micelles into cells.
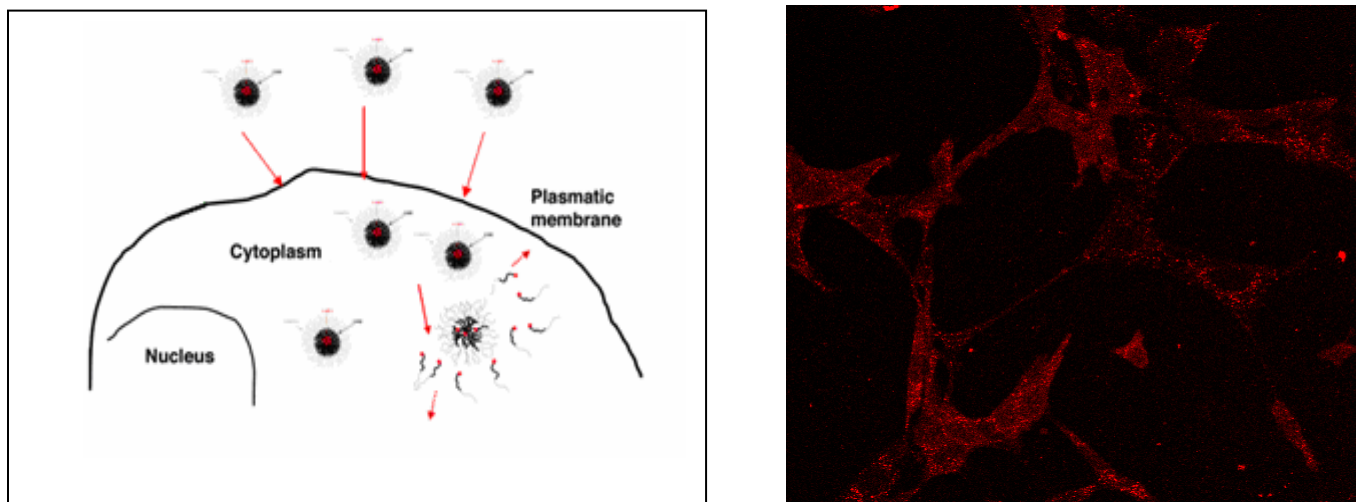
Figure 5.6 Internalization and localization of labeled micelles in cells

Synthesis of Azide-PEO$_{45}$-*b*-PCL$_{25}$-Rhodamine Block Copolymers

Azide-PEO$_{45}$-*b*-PCL$_{25}$-Rhodamine Block Copolymers were synthesized as shown in **Scheme 3**. Our initial objective was to demonstrate a route to synthesize azide-PEG-OH building blocks commencing with commercially available starting materials. An uncapped 2K average molecular weight PEG diol (Aldrich) was selected and subjected to desymmetrization (**Scheme 5.3**). Monotosylated PEG can be isolated from ditosylate and PEG diol, and the resulting monotosylate was converted to azide-PEG-OH via nucleophilic displacement with sodium azide. The azide-PEG proved highly versatile for production of numerous Block Copolymers. Azide-PEG-*b*-PCL was synthesized by a one-pot cation ring opening polymerization at 130 °C under argon stream adopting a previously reported method for the preparation of PEG-*b*-PCL with some modifications (**Scheme 5.3**). The synthesized polymers were then dissolved in THF, recovered by precipitation by cold hexane, and dried under vacuum at room temperature. The

number average molecular weight (M_n) of azide-PEG$_{45}$-b-PCL$_{25}$ block copolymer was determined by ^{1}H NMR (**Figure 5.7**).
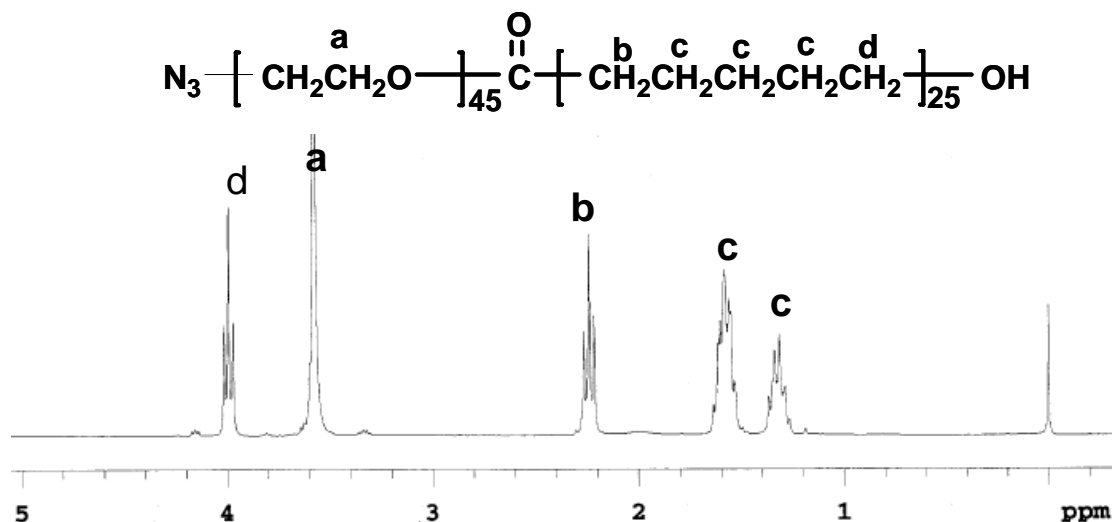
Figure 5.7 ^{1}H-NMR spectrum of N$_3$-PEG$_{45}$-b-PCL$_{25}$ in CDCl$_3$

Azide-PEG$_{45}$-b-PCL$_{25}$-Rhodamine Block Copolymers were synthesized by employing a modified version of an existing procedure (**Scheme 5.3**). In azide-PEG$_{45}$-b-PCL$_{25}$ block copolymers, the functional group at the end of PEG chain is azide, while the functional group at the end of PCL chain is hydroxyl, which can react with the isothiocyanate group in rhodamine B. Therefore, rhodamine B can be attached to the end of the PCL chain. The success of the conjugation of rhodamine B to the block copolymer can be proven by ^{1}H NMR (**Figure 5.8 B**). The signal of methyl protons of tetramethylrhodamine is found at 1.84 ppm. The ratios of peak areas of the methylene group in tetramethylrhodamine to those of the methylene groups in PEG or PCL were used to analyze the molar ratio of tetramethylrhodamine to block copolymer chains. The average molar ratio is 0.77, suggesting that 77% of the polymer chains may be functionalized.
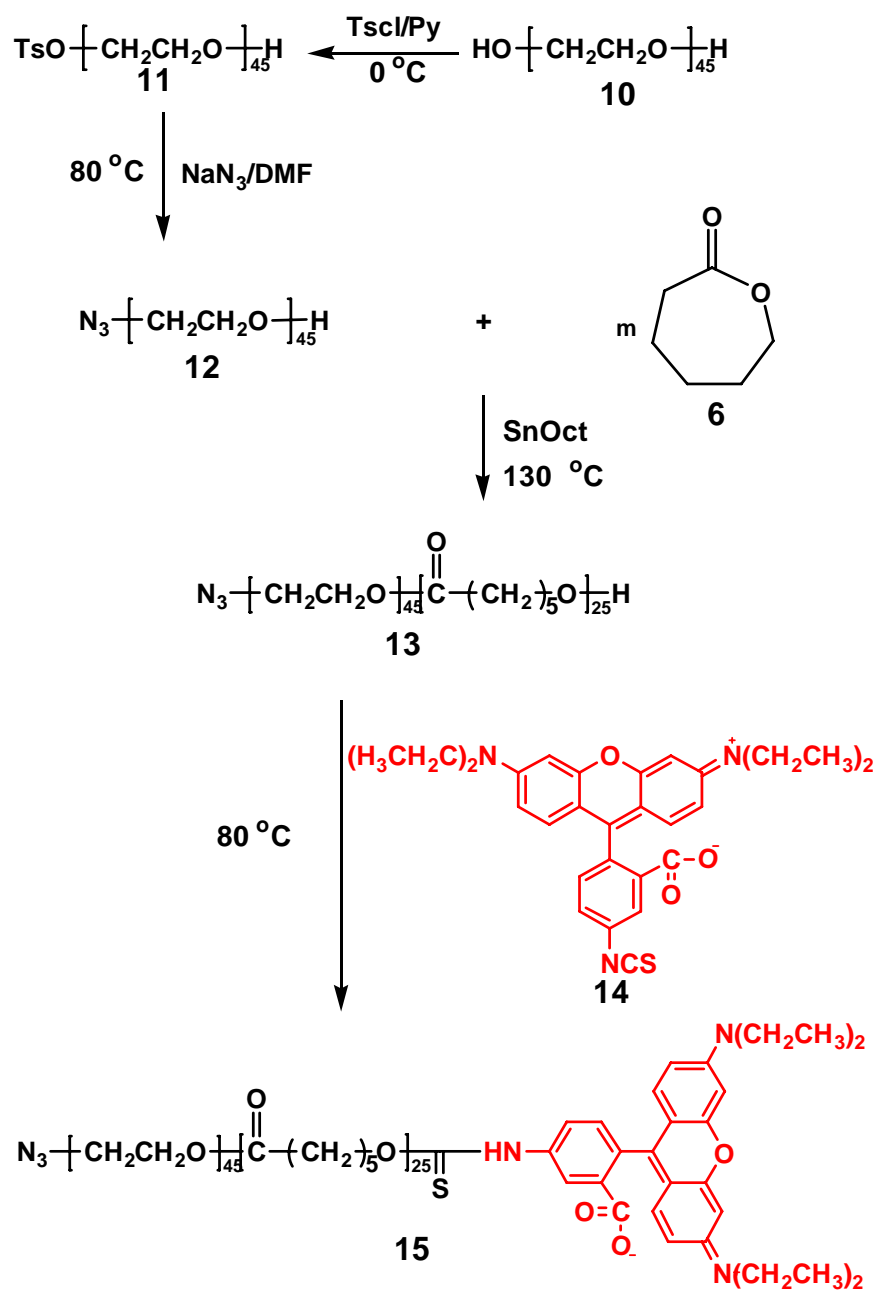
Scheme 5.3 Synthesis of Azide-PEO$_{45}$-*b*-PCL$_{23}$ Copolymer and Azide-PEO$_{45}$-*b*-PCL$_{23}$
-Rhodamine Block Copolymer.
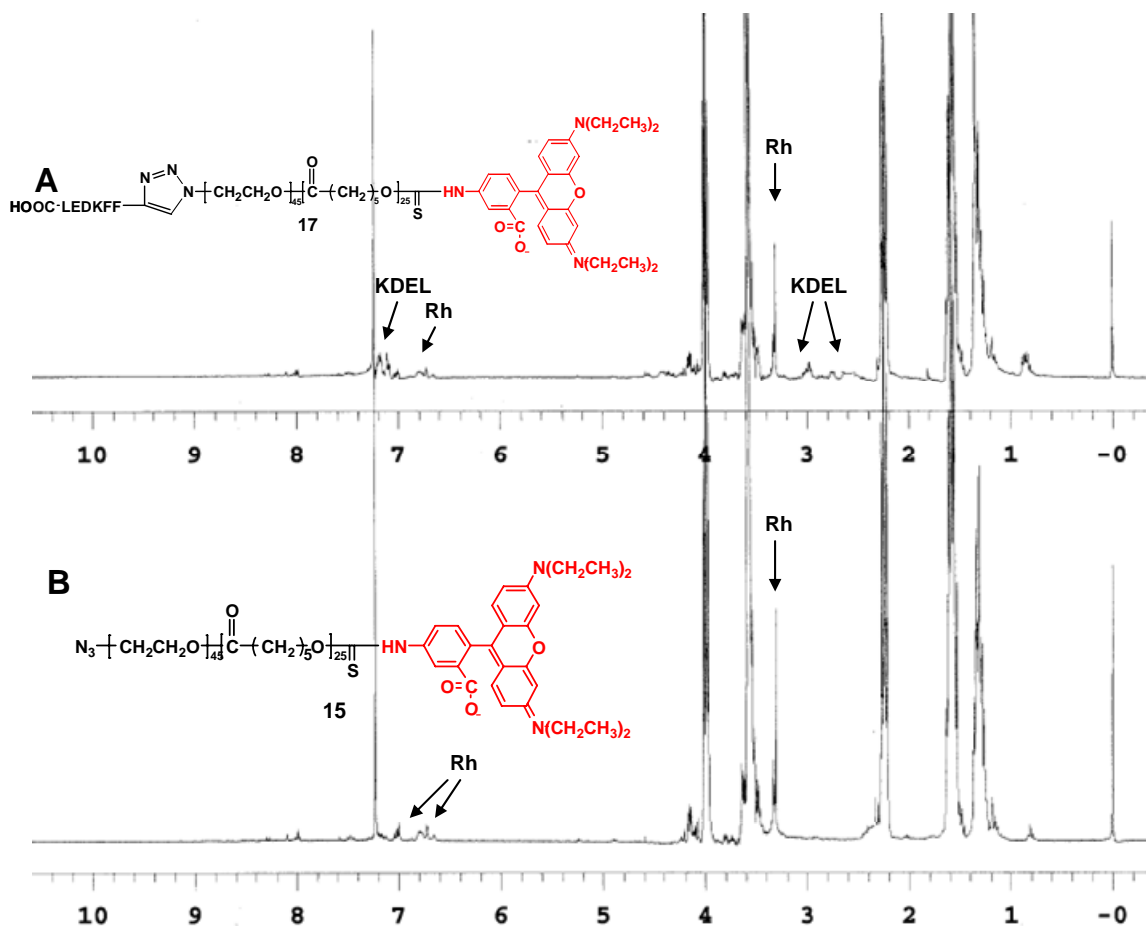
Figure 5.8 ^{1}H-NMR spectrum of N_3-PEG$_{45}$-b-PCL$_{25}$-Rh and KDEL- PEG$_{45}$-b-PCL$_{25}$-Rh in CDCl$_3$

Synthesis of KDEL signal peptide

The C-terminal KDEL peptide is an important retrieval signal of the luminal ER proteins that have escaped to the Golgi apparatus and other post-ER compartments. The KDEL receptor is concentrated in the intermediate compartment, as well as in the Golgi stack. After binding to this receptor, the proteins are transported to the ER by the way of retrograde vesicle flow. In order to target to the ER, we synthesized the peptide sequence FFKDEL-COOH (Phe-Phe-Lys-Asp-Glu-Leu) containing this ER retention motif as shown in **Scheme 5.4**.[50] The peptide was synthesized on an acid sensitive HMPB resin that is cleaved by treatment with 50% TFA in CH$_2$Cl$_2$ for 30

minutes. After the coupling was complete and the conjugate was cleaved from the resin, the protecting group also can be removed at same time, and the signal peptides with the alkyne functional group were formed.
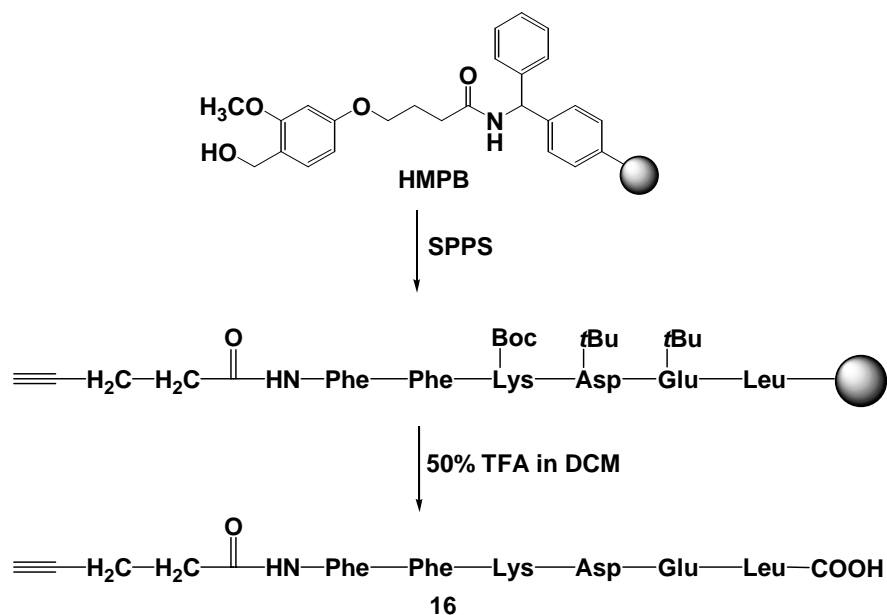
Scheme 5.4 Preparation of the KDEL signal peptide

KDEL signal peptides were conjugated with azide-PEg$_{45}$-*b*-PCL$_{25}$-Rhodamine Block Copolymers via click reaction (scheme 5).

Given the success in using "click chemistry" in the bioconjugation[51], we hypothesized that the "spring-loaded" nature of click reaction between an organic azide and a terminal alkyne would permit exhaustive reaction between polymers and signal peptides via routine method. The synthetic appeal of click reactions relies upon their high yields, simple reaction conditions, tolerance of oxygen and water, and simple product isolation. While these reactions occur between two highly energetic moieties, they exhibit quite narrow chemoselectivity. To apply the click chemistry concept to polymers, we could prove it useful for polymer modifications. The success of the conjugation of the KDEL signal peptide to the azide-PEg$_{45}$-*b*-PCL$_{25}$-Rhodamine can be proven by ^{1}H NMR (**Figure 5.8 A**).
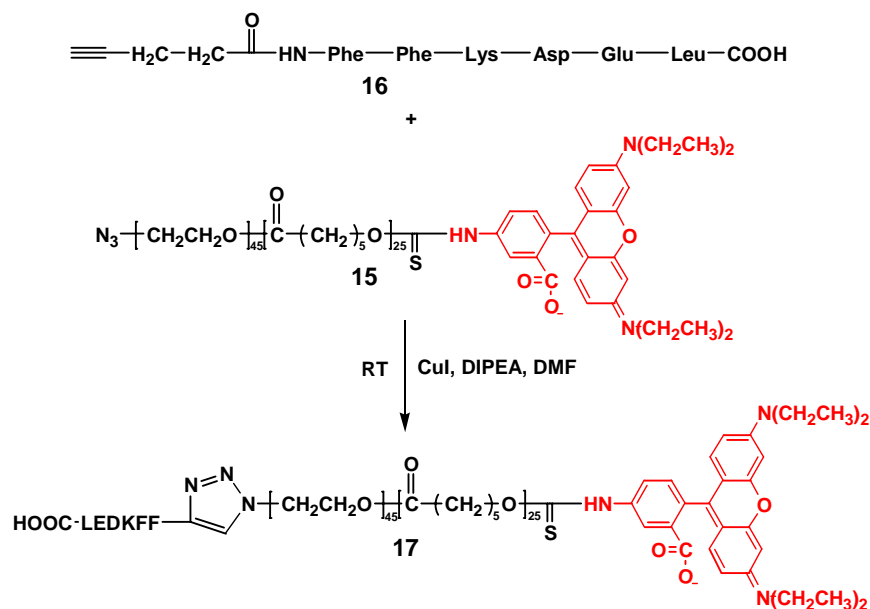
Scheme 5.5 Click reaction between KDEL signal peptides and Azide-PEO$_{45}$-*b*-PCL$_{23}$-Rhodamine Block Copolymers

Preparation and Characterization of Rhodamine loaded KDEL-modified micelles.

The copolymer with KDEL signal peptides were dissolved in acetone to provide a 2 mg/mL polymer concentration. The solution was then added dropwise to dd-water under a moderate stirring at 25 °C, followed by evaporation of acetone under vacuum. As shown in **Figure 5.9,** an average diameter of the prepared micelles were 40 ± 2 nm measured by TEM, the micelles are generally spheroidal. The results suggest that the sizes of both micelles with and without KDEL signal peptide do not change too much.

Internalization of KDEL-modified micelle into Human adenocarcinoma epithelial cells (HeLa229 cells) and Murine embryonic fibroblasts (NIH/3T3 cells)

The cellular uptake of rhodamine loaded KDEL-modified micelles by HeLa229 cells and NIH/3T3 cells was investigated by fluorescent spectroscopy and confocal microscopy techniques and was compared to the uptake of rhodamine loaded PEO-*b*-PCL micelles. Although all cells can survive during internalization of the negative control micelle (free of KDEL) into Hela229

cells and NIH/3T3 cells studies, unfortunately all cells were dead after incubation with the KDEL-modified micelle. The reason for this hasn't been clear by now. Perhaps the KDEL signal peptides are toxic to the cells. Further studies, aimed at understanding the reasons for cell-toxicity and at finding a solution to this problem, are currently underway.
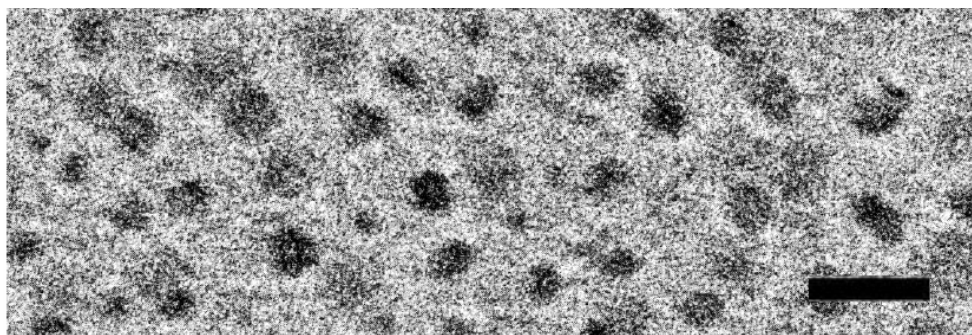
Figure 5.9 Transmission electron micrograph (TEM) of micelles of Signal Peptide-PEO$_{45}$-*b*-PCL$_{25}$-Rh, scale bar indicates 100 nm

CONCLUSION

A KDEL containing a model peptide was conjugated to the surface of micelles as a ligand that can work as an address tag, which can enhance the micellar delivery of encapsulated hydrophobic glycosidase and glycosyltransferase inhibitors into the ER.[49] Toward this goal, PEG-*b*-PCL copolymers bearing azide groups on the PEG end were synthesized. The azide group on the PEG of the PEO-*b*-PCL polymer can react with a KDEL-containing linear peptide with alkyne group by click reaction. Therefore KDEL was conjugated on the surface of the PEO-*b*-PCL micelles. A hydrophobic fluorescent probe, rhodamine, was covalently loaded in polymeric micelles to imitate hydrophobic drugs loaded in micellar carriers. The cellular uptake of rhodamine loaded KDEL-modified micelles by HeLa229 cells and NIH/3T3 cells was investigated by fluorescent spectroscopy and confocal microscopy techniques and was compared to the uptake of rhodamine loaded PEG-*b*-PCL micelles (as the irrelevant ligand decorated micelles). Although internalization of KDEL-modified micelles into cells failed, we believed that

we will find a method to overcome this problem based on additional studies. We have demonstrated that KDEL-peptide-PEO-*b*-PCL conjugate-micelles were successfully prepared by using the click reaction, which has opened a new door for the development of multifunctional micellar drug delivery systems.

5.3 EXPERIMENTAL PROCEDURES

^{1}H-NMR spectra were recorded in $CDCl_3$ or D_2O on a Varian Merc-300 or Varian Inova-500 spectrometers equipped with Sun workstations at 300K. TMS (δ_H=0.00) or D_2O (δ_H=4.67) was used as the internal reference. ^{13}C-NMR spectra were recorded in $CDCl_3$ or D_2O at 75MHz on Varian Merc-300 spectrometer, respectively using the central resonance of $CDCl_3$ (δ_C=77.0) as the internal reference. COSY, HSQC, HMBC and TOCSY experiments were used to assist assignment of the products. Mass spectra were obtained on Applied Biosystems Voyager DE-Pro MALDI-TOF (no calibration) and Bruker Daltonics 9.4T (FTICR, external calibration with BSA). Optical rotatory power was obtained on Jasco P-1020 polarimeter at 300 K. Chemicals were purchased from Aldrich or Fluka and used without further purification. DCM was distilled from calcium hydride; THF from sodium; CH_3OH from magnesium and iodine. Aqueous solutions are saturated unless otherwise specified. All the reactions were performed under anhydrous conditions under argon and monitored by TLC on Kieselgel 60 F254 (Merck). Detection was by examination under UV light (254 nm) and by charring with 10 % sulfuric acid in methanol. Silica gel (Merck, 70-230 mesh) was used for chromatographies. Iatrobeads 6RS-8060 was purchased from Bioscan..

Synthesis of PEG$_{45}$-*b*-PCL$_{23}$ Block Copolymers and Rhodamine-Conjugated Copolymers PEG$_{45}$-*b*-PCL$_{23}$ block copolymers were synthesized as reported.[60] A predetermined volume (12.0 mL) of ε-caprolactone monomer was placed in a flask containing an amount (9.0 g)

of PEG under an argon atmosphere. Then, a drop of SnOct was added. After cooling to liquid-nitrogen temperature, the flask was evacuated for 12 h, sealed off, and kept at 130°C for 24 h. The synthesized polymers were dissolved in THF, recovered by precipitation by cold hexane, and dried under vacuum at room temperature. The degree of polymerization of the PCL was caculated by ^{1}H NMR relative to the degree of polymerization of the PEG.

The rhodamine-conjugated PEG_{45}-b-PCL_{23} block copolymers (PEG_{45}-b-PCL_{23}-Rh) were synthesized by using a modified reported procedure[61]: Dried PEG_{45}-b-PCL_{23} block copolymers (20mg) and tetramethylrhodamine-5-isothiocyanate (10mg) were dissolved in 10 mL of freshly distilled toluene under an argon atmosphere. After heating at 80 $^\circ$C for 12 h, the toluene was removed under in *vacuo* to give an oil, the residue was purified with Sephadex LH 20 size-exclusion chromatography using CH_2Cl_2/CH_3OH (1:1 v/v) as the eluent to remove unconjugated rhodamine. The rhodamine-conjugated block copolymers were obtained. ^{1}H NMR was used to determine the amount of rhodamine in the conjugated block copolymers.

Preparation and characterization of Labeled Micelles Block copolymer mixture consisting of PEG_{45}-b-PCL_{23}/PEG_{45}-b-PCL_{23}-Rh (molar ratio: 3/2) (15 mg) was dissolved in DMF (1mL) and stirred for 4 h. Micelle formation was induced by addition of nanowater 2mL (1 drop/10 seconds). Micelles were transferred to a dialysis bag and dialyzed against nanopure H_2O for one hour. The water was exchanged and the procedure repeated 3 times. Subsequently the water was changed every 3 hours for the following 12 hours. The content of TMRCA in micelles was determined by spectrofluorometry using a fluorescence spectrometer Excitation was set to 545 nm and peak emission was registered at 573 nm.

Cryogenic Transmission Electron Microscopy (Cryo-TEM) was carried out on an FEI Tecnai 20 electron microscope operated with a CCD camera operating at an acceleration voltage

of 120 kV. Cryo-TEM samples were prepared utilizing a custom-built chamber often referred to as the controlled environment vitrification system (CEVS).[35,38] All of the samples were prepared at room temperature (23 °C). In the CEVS, the sample in the form of a droplet was placed on a copper EM grids precoated with a thin film of Formvar and then coated with carbon. It was then soaked by a filter paper, resulting in the formation of thin liquid films of 10-300 nm thickness freely spanning across the micropores in a carbon-coated lacelike polymer layer supported by a meshy metal grid. After 30 min detainment, the sample grid assembly was rapidly vitrified with solid nitrogen at its melting temperature (90 K). The sample was kept under liquid nitrogen until it was loaded into a cryogenic sample holder.

Cell labeling and detection by fluorescence microscopy

Human adenocarcinoma epithelial cells (HeLa229 cells; ATCC) were cultured in Eagle's minimum essential medium with Earle's BSS L-glutamine (2 mM) (EMEM), adjusted to contain sodium pyruvate (1.0 mM), nonessential amino acids (0.1 mM), sodium bicarbonate (1.5 g L^{-1}) and supplemented with penicillin (100 u mL^{-1}) / streptomycin (100 μg mL^{-1} and FBS (10%). Murine embryonic fibroblasts (NIH/3T3 cells; ATCC) were cultured in Dulbecco's modified Eagle's medium with L-glutamine (4 mM), adjusted to contain glucose (4.5 g L^{-1} and sodium bicaebonate (1.5 g L^{-1}) and supplemented with penicillin (100 u mL^{-1}) / streptomycin (100 μg mL^{-1} and FBS (10%). Cells were maintained in a humid 5% CO_2 atmosphere at 37°C.

Cells were grown in 12-well plates on circular glass coverslips as 50,000 cells/well (HeLa cells/well) or 100,000 cells/well (NIH/3T3 cells) and cultured overnight in their appropriate medium. Slides with adherent live cells at 30% confluency were incubated with micelles conjugated rhodamine for 24 hours. Cells were washes 3 times with DPBS and fixed with formaldehyde (3.7% in PBS). The cells were mounted with PermaFluor (Thermo Electron

Corporation) before imaging. Initial analysis was performed on a Zeiss Axioplan2 fluorescent microscope. Confocal images were acquired using a 60X (NA1.42) oil objective. Stacks of optical sections were collected in the z dimensions. The step size, based on the calculated optimum for each objective, was between 0.25 and 0.5 μm. Subsequently, each stack was collapsed into a single image (z-projection). Analysis was performed offline using ImageJ 1.39f software (National Institutes of Health, USA) and Adobe Photoshop CS3 Extended Version 10.0 (Adobe Systems Incorporated), whereby all images were treated equally.

Synthesis of N$_3$-PEG$_{45}$-OH (13) TsCl (1.9 g, 10.0 mmol) was added to a solution of an uncapped PEG diol (20.0 g, average molecular weight 2000, 10.0 mmol) in pyridine (100 mL). The resulting mixture was stirred at 0 ℃ for 12 h. The precipitate was filtered and the solvent was evaporated. The residue in anhydrous DMF (30.0 mL) was stirred with sodium azide (1.3 g, 20.0 mmol) at 80 °C for 8 h. CH$_2$Cl$_2$ (250 mL) was added and the resulting solution was washed with water (25 mL). The organic layer was dried over MgSO$_4$, and the solvents were removed under vacuum. The crude product was purified by silica gel chromatography (CH$_2$Cl$_2$/CH$_3$OH, 10/1, v/v) to afford a pure product, the two-step yield was 58%. ^{1}H NMR (CDCl$_3$, 300 MHz) δ 3.87 (2H, m, CH_2OH), 3.83–3.60 (180H, m, CH_2O), 3.41 (2H, m, CH_2N$_3$).

Synthesis of azide-PEG$_{45}$-b-PCL$_{25}$ (13) and azide-PEG$_{45}$-b-PCL$_{25}$-Rhodamine Block Copolymers (15) Azide-PEG-b-PCL was synthesized by a one-pot cation ring opening polymerization at 130 °C under a stream of argon adopting a previously reported method[29] for the preparation of PEG-b-PCL with some modifications. Briefly, a predetermined volume (3.3 mL) of ε-caprolactone monomer was placed in a flask containing a preweighed amount (2.5 g) of azide-PEG-OH under a nitrogen atmosphere. Then a drop of SnOct was added. After cooling to liquid-nitrogen temperature, the flask was evacuated, sealed off, and kept at 130 °C for 24 h. The

synthesized polymers were then dissolved in THF, recovered by precipitation into cold hexane, and dried under vacuum at room temperature. The number average molecular weight (M_n) of azide-PEO$_{45}$-b-PCL$_{25}$ block copolymer was determined by ^{1}H NMR. ^{1}H NMR (CDCl$_3$, 300 MHz) δ 4.10-4.02 (50H, m, CH$_2$CH_2OH), 3.80- 3.58 (180H, m, CH_2O), 2.26-2.20 (50H, m, CH_2C=O), 1.65-1.55 (100H, m, CH_2), 1.30-1.22 (50H, m, CH_2).

Azide-PEG$_{45}$-b-PCL$_{25}$-Rhodamine Block Copolymers were synthesized by employing a modified version of an existing procedure. 200 mg of the dried PEG$_{45}$-b-PCL$_{25}$ block copolymers and 100 mg of tetraethylrhodamine-4/5-isothiocyanate were dissolved in 50 mL of freshly distilled toluene under an argon atmosphere. After heating at 80 °C for 12 h, the reaction mixture was purified with Sephadex LH 20 size-exclusion chromatography using CH$_2$Cl$_2$/CH$_3$OH (1:1 v/v) as the eluent to remove unconjugated rhodamine. The rhodamine-conjugated block copolymers were obtained. ^{1}H NMR was used to determine the amount of rhodamine in the conjugated block copolymers.

Synthesis of KDEL signal peptide (16) The C-terminal KDEL peptide was synthesized by SPOS on HMPB resin using Fmoc based strategy. Fmoc-Leucine (1.76 g, 5mmol) was dissolved in CH$_2$Cl$_2$ (20 ml) at 0 °C and DIPC (0.315 g, 2.5 mmol) was added. The solution was warmed to rt and the solvent was removed. The activated amino acid was dissolved in DMF and added to HMPB resin (0.42 g, 0.5 mmol) along with DMAP (60 mg, 0.05 mmol) to the manual peptide reactor and the reaction was agitated with a stream of N$_2$ for 10 hrs. The resin was washed with DMF and the N-terminal Fmoc was removed with 20% piperidine in DMF. The deprotection was monitored by Kaiser test. The resin was washed repeatedly with DMF to remove remaining piperidine. The subsequent Fmoc protected amino acids glutamic acid, aspartic acid, lysine, phenyl alanine (2 times) and pentynoic acid were coupled using the following general procedure.

175

Amino acid (3 eq.), PyBOP (3 eq.), HOBt (3 eq.), and DIPEA (6 eq.) were added to the reactor

and kept for 3 h. The peptide was finally cleaved from the resin using 50%TFA, 2.5%H_2O, 2.5%

TIS in CH_2Cl_2. HR MALDI-TOF MS: *m/z* calcd. $[M+Na]^+$ 900.4119, found 900.4123

Click Reaction of azide-PEG$_{45}$-*b*-PCL$_{25}$-Rhodamine Block Copolymers with Propargyl

FFKDEL peptide. The azide-PEG$_{45}$-*b*-PCL$_{25}$-Rhodamine polymers were reacted with the ER

targeting peptide **16** via click reaction procedure. A solution of polymers **15** (M_n = 5000 g/mol,

150 mg, 0.0300 mmol) and DIPEA (2.2 mg, 0.017 mmol) in DMF (10 mL) was purged with

argon for 1 hour and transferred via syringe to a vial containing CuI (3.2 mg, 0.017 mmol) and

ER targeting peptide **16** (45.0 mg, 0.06 mmol) under a nitrogen atmosphere. The reaction

mixture was stirred at 25 °C for 24 hours in the absence of oxygen. The reaction mixture was

exposed to air, and the solution was passed through a column of the celite. DMF was removed

under vacuum, and the product was precipitated by hexanes. The resulting block copolymer was

were purified by LH-20 size exclusion chromatography using CH_2Cl_2/CH_3OH (1:1 v/v) as the

eluent. ^{1}H NMR was used to determine that the ER targeting peptide was conjugated to the block

copolymers successfully.

Preparation and Characterization of Rhodamine loaded KDEL-modified micelles.

Copolymer-KDEL conjugate **17** (10mg) was dissolved in 2 mL DMF and stirred for 4 hours.

The solution was added dropwise to water (10 mL) under moderate stirring at 25 °C. The

micelles was dialyzed against nanopure water for 1 h. The water was exchanged and the

procedure repeated 3 times. Subsequently the water was changed every 3 h for the following 12

h. The content of TMRCA in the micelles was determined by spectrofluorometry using a

fluorescence spectrometer. Excitation was set to 545 nm and peak emission was registered at

573 nm. Micelles were characterized by Cryo-TEM, which was carried out on an FEI Tecnai 20

electron microscope operated with a CCD camera operating at an acceleration voltage of 120 kV. Cryo-TEM samples were prepared as the methods mentioned above.

Cell labeling and detection by fluorescence microscopy

Human adenocarcinoma epithelial cells (HeLa229 cells; ATCC) were cultured in Eagle's minimum essential medium with Earle's BSS L-glutamine (2 mM) (EMEM), adjusted to contain sodium pyruvate (1.0 mM), nonessential amino acids (0.1 mM), sodium bicarbonate (1.5 g L^{-1}) and supplemented with penicillin (100 u mL^{-1}) / streptomycin (100 μg mL^{-1} and FBS (10%). Murine embryonic fibroblasts (NIH/3T3 cells; ATCC) were cultured in Dulbecco's modified Eagle's medium with L-glutamine (4 mM), adjusted to contain glucose (4.5 g L^{-1} and sodium bicaebonate (1.5 g L^{-1}) and supplemented with penicillin (100 u mL^{-1}) / streptomycin (100 μg mL^{-1} and FBS (10%). Cells were maintained in a humid 5% CO_2 atmosphere at 37°C.

Cells were grown in 12-well plates on circular glass coverslips as 50,000 cells/well (HeLa cells/well) or 100,000 cells/well (NIH/3T3 cells) and cultured overnight in their appropriate medium. Slides with adherent live cells at 30% confluency were incubated with micelles conjugated with KDEL and rhodamine for 24 hours. Cells were washes 3 times with DPBS and fixed with formaldehyde (3.7% in PBS). The cells were mounted with PermaFluor (Thermo Electron Corporation) before imaging. Initial analysis was performed on a Zeiss Axioplan2 fluorescent microscope. Confocal images were acquired using a 60X (NA1.42) oil objective. Stacks of optical sections were collected in the z dimensions. The step size, based on the calculated optimum for each objective, was between 0.25 and 0.5 μm. Subsequently, each stack was collapsed into a single image (z-projection). Analysis was performed offline using ImageJ 1.39f software (National Institutes of Health, USA) and Adobe Photoshop CS3 Extended Version 10.0 (Adobe Systems Incorporated), whereby all images were treated equally.

5.4 REFERENCES

1. R. Langer. *Science* 2001, 293, 58

2. D. D. Lasic, D. Papahadjopoulos. *Science* 1995, 267, 1275

3. D. E. Discher, A. Eisenberg. *Science* 2002, 297, 967

4. L. Zhang, K. Yu, A. Eisenberg. *Science* 1996, 272, 1777.

5. V. P. Torchilin. *Adv. Drug Deliv. Rev*. 2002, 54, 235.

6. W. M. Saltzman, Drug Delivery: Engineering Principles for Drug Therapy (Oxford Univ. Press, New York, 2001).

7. C. Allen, A. Eisenberg. J. Mrsic, D. Maysinger, *Drug Deliv.* 2000, 7, 139.

8. Y. Kakizawa, K. Kataoka. *Adv. Drug Deliv. Rev*. 2002, 54, 203.

9. K. Kataoka, A. Harada, Y. Nagasaki. *Adv. Drug Deliv. Rev.* 2001, 47, 113

10. Jain, K. K. *Drug. Dis. Today* 2005, 10, 1435

11. Service, R. F. *Science* 2005, 310, 1132

12. Klefenz, H. *Nanobiotechnology.* 2004, 4, 211

13. Duncan, R., Ringsdorf, H. & Satchi-Fainaro, R. *Polym. Sci*. 2006, 489

14. Mark S. Butler. *J. Nat. Prod.* 2004, 67, 2141

15. Kolb, H.C. & Sharpless, K.B. *Drug Discov. Today* 2003, 8, 1128

16. J.K. Hood and P.A. *Curr. Opin. Cell Biol.* 1999, 11, 241

17. Robert G. Spiro. *Glycobiology* 2002, l (12), 443

18. Lodish, Harvey, et al. Molecular Cell Biology 5th Edition. W. H. Freeman, 2003, pp. 659-666

19. Gunnar von Heijne. *Journal of membrane biology*, 1990, 115 (3), 195

20. Matthew L. Becker, Edward E. Remsen, Dipanjan Pan & Karen L. Wooley. *Bioconjugate Chem*, 2004, 15, 699

21. Fawell S, Seery J, Daikh T, Moore C, Chen L L, Pepinsky B, Barsoum J. *Proc Natl Acad Sci USA.* 1994, 91, 664

22. Buwitt-Beckmann U, Heine H, Wiesmuller KH, Jung G, Brock R, Akira S, Ulmer AJ *J Biol Chem* 2006, 281:9049–9057

23. Jingsong Zhu, Paul W. Luther, Oixin Leng & A. James Mixson. *Antimicrobial. Agents and Chemotherapy,* 2006, 50 (8), 2797

24. Farquhar, M. G., and G . E. Palade. *J. Cell Biol.* 1981, 91(3), 77

25. Bjornerud, A. & Johansson, L. *NMR Biomed.* 2004, 17, 465

26. Weissleder, R., Elizondo, G., Wittenberg, J., Rabito, C. A., Bengele, H. H. & Josephson, L. *Radiology* 1990, 175, 489

27. Wu, E. X., Tang, H. Y. & Jensen, J. H. *NMR Biomed.* 2004, 17, 478

28. Rostovtsev, V.V., Green, L.G., Fokin, V.V. & Sharpless, K.B. *Angew. Chem. Int. Edn. Engl.* 2002, 41, 2596

29. Laibin Luo, Joseph Tam, Dusica Maysinger & Adi Eisenberg. *Bioconjugate Chem*, 2002, 13, 1259

30. Benahmed, A., Ranger, M. and Leroux, J.-C. *Pharm. Res.* 2001, 18, 323

31. Nishiyama, N., Yokoyama, M., Aoyagi, T., Okano, T., Sakurai, Y., and Kataoka, K. *Langmuir* 1999, 15, 377-383.

32. Kabanov, A. V., Vinogradov, and Alakhov, V. Yu. *Bioconjugate Chem.* 1995, 6, 639-643.

33. Katayose, S., and Kataoka, K. *Bioconjugate Chem.* 1997, 8, 702

34. Harada, A. and Kataoka, K. *Science* 1999, 283, 65

35. Allen, C., Yu, Y., Maysinger, D., and Eisenberg, A. *Bioconjugate Chem.* 1998, 9, 564-572.

36. Allen, C., Han, J., Yu, Y., Maysinger, D., and Eisenberg, A. *J. Controlled Release* 2000, 63,

275

37. Annette Rosler, Guido W.M. Vandermeulen & Harm-Anton Klok. *Advanced drug Delivery Reviews* 2001, 53, 95

38. B. Ganem, *Acc. Chem. Res.* 1996, 29, 340

39. B. Winchester, G. W. J. Fleet, *Glycobiology*, 1992, 2 199

40. D. E. Koshland, *Biol. Rev.* 1953, 28, 416

41. N. Asano, A. Kato, A. A. Watson, *Mini. Rev. Med. Chem.* 2001, 1, 145

42. Y. Wu, M. T. Swulius, K. W. Moremen, R. N. Sifers, *Proc. Natl. Acad. Sci. U.S.A.* 2003, 100, 8229

43. E. H. W. Pap, T. B. Dansen, R. van Summeren and K. W. A. Wirtz.Exp. *Cell Res.,* 2001, 265, 288.

44. D. Vaudry, P. J. Stork, P. Lazarovici, L. E. Eiden.*Science* 2002, 296, 1648.

45. C. Allen, D. Maysinger, A. Eisenberg *Coolids Surf.* B 1999,16, 3

46. M. H. Dufresne, E. Fournier. B. T. Gattefosse, vol. 96, Gattefosse, Saint-Priest, 2003, pp. 87-102

47. D. L. Taegarden, D. S. Baker. *Eur. J. Pharm. Sci.* 2004, 15,115

48. L. A. Greene, A. S. Tischler. *Proc. Natl. Acad. Sci. U.S.A.* 1976, 73, 2424.

49. Toyoshima C, Nakasako M, Nomura H, Ogawa H. *Nature* 2000, 405, 647

50. Heather A. Behannaa and Samuel I. Stupp. *Chem. Commun.,* 2005, 4845

51. R. K. O'Reilly, M. J. Joralemon, C. J. Hawker and K. L. Wooley, *Chem.–Eur. J.*, 2006, 12, 6776; R. K. O'Reilly, M. J. Joralemon, C. J. Hawker and K. L. Wooley. *J. Polym. Sci., Part A: Polym. Chem.*, 2006, 44, 5203; M. J. Joralemon, R. K. O'Reilly, C. J. Hawker and K. L. Wooley. *J. Am. Chem. Soc.*, 2005, 127, 16892

52. Jennifer A Prescher & Carolyn R Bertozzi, *Nature Chemical Biology* 2005, 1, 13

53. V. V. Rostovtsev, L. G. Green, V. V. Fokin and K. B. Sharpless. *Angew. Chem., Int. Ed.*, 2002, 41, 2596

54. Enochs, W. S., Harsh, G., Hochberg, F. & Weissleder, R. *J. MRI,* 1999, 9, 228

55. Harisinghani, M. G., Barentsz, J., Hahn, P. F., Deserno, W. M., Tabatabaei, S., van de Kaa, C. H., de la Rosette, J. & Weissleder, R. *New England Journal of Medicine* 2003, 348, 2491-U5.

56. Bulte, J. W. M. & Kraitchman, D. L. *NMR Biomed.* 2004, 17, 104

57. Song, H. T., Choi, J. S., Huh, Y. M., Kim, S., Jun, Y. W., Suh, J. S. & Cheon, J. *J. Am. Chem. Soc.* 2005, 127, 9992

58. Konda, S. D., Wang, S., Brechbiel, M. & Wiener, E. C. *Inv. Radiology* 2002, 37, 104

59. Hsu, A. R., Hou, L. C., Veeravagu, A., Greve, J. M., Vogel, H., Tse, V. & Chen, X. *Mol. Imaging Biol.* 2006, 8, 315

60. Bogdanov, B., Vidts, A., Bulcke, A. V. D., Verbeeck, R., and Schacht, E. *Polymer* 1998, *39*, 1631-1636.

61. Balestrieri, C., Camussi, G., Giovane, A., Iorio, E. L., Quagliuolo, L., and Servillo, L. *Anal. Biochem.* 1996, *233*, 145

CHAPTER 6

PREPARATION OF MULTIFUNCTIONAL MICELLAR MAGNETIC DRUG DELIVERY SYSTEMS

ABSTRACT

Polymeric micelles are nanoscopic (10 to 100 nm) colloidal particles that are self-assembled from an amphiphilic block or graft copolymers in aqueous media. Due to their unique core shell structure, small size and modifiable surface, polymeric micelles have been widely investigated as nanoscale drug delivery carriers. We are involved in a program that employs nanoparticles as scaffolds for the attachment of the various modules to provide a multifunctional drug delivery device. These modules include targeting devices for specific cell types, cell permeation enhancing molecules, and cell-signaling peptides for selective transport to organelles. In addition, different types of contrast reporter moieties for γ-scintigraphy, magnetic resonance imaging (MRI) and computed tomography (CT) can be incorporated into micelles to achieve medical diagnostic imaging. The aim of these studies is to develop a targeted drug delivery device combined with medical diagnostic imaging system. In this study, we have developed novel multifunctional super-paramagnetic polymeric micelles as a new class of magnetic resonance imagining (MRI) probe with remarkably high spin-spin (T_2) relaxivity and sensitivity. A biocompatible diblock poly(ε-caprolactone)-poly(ethylene glycol) (PCL-PEG, PCE) co-polymer is used to form monodisperse and shape specific microstructures. These freestanding polymer particles with uniform and precise spherical morphology can be used as carriers for drug and imaging agents for biomedical applications.

6.1 INTRODUCTION

Recently, remarkable progress has been made to establish polymer micelles as novel multifunctional systems of nanoscale construct with drug delivery and diagnostic imaging applications.[1-5] Polymer micelles are composed of amphiphilic block copolymers that contain distinguished hydrophobic and hydrophilic segments. The distinct chemical nature of the two blocks results in thermodynamic phase separation in aqueous solution and formation of a nanoscopic supramolecular core/shell structure (usually 10 to 100 nm in size). During the micellization process, the hydrophobic blocks associate to form the core region, whereas the hydrophilic blocks form the shell that separates the core from the aqueous medium[6]. This unique architecture enables the micelle core to serve as a nanoscopic depot for the therapeutic agents, and the shell consists of a brushlike protective corona that stabilizes the nanoparticles in aqueous solution.[6] Many hydrophobic drugs such as paclitaxel and doxorubicin have been successfully loaded inside the micelle core to improve drug solubility and pharmacokinetics.[2,3,31,32] In addition to therapeutic applications, polymeric micelles have also received increasing attention in diagnostic imaging applications. Superparamagnetic iron oxide (SPIO) has been reported to incorporate into micelles for the diagnostic imaging on tumor.

Super-paramagnetic polymeric micelles are a new class of magnetic resonance imaging (MRI) probes with remarkably high spin-spin (T_2) relaxivity and sensitivity and can be employed for therapeutic imaging combined with drug delivery. The basic advantages for the applications of super-paramagnetic polymeric micelles include ultrasensitive MRI detection, high drug-loading capacity, biodegradability, long blood circulation times, and controllable drug-release profiles. However, the ability to target to tumor and related cells remains a great challenge for developing micelle-mediated therapeutic imaging systems. The reason is that micelles not only

spontaneously accumulate at tumor sites with leaky vasculature by an enhanced permeability and retention (EPR) effect,[33] they are also found to accumulate in reticuloendothelial sites such as the spleen, liver, and kidney.[34] The insufficient delivery of micelles to tumor will reduce the therapeutic effect, and increase the toxic effect by nonspecific distributing to healthy tissues.

Therefore targeting delivery is a highly desirable methodology for diagnostic imaging because of enhanced efficacy and reduced dosage/toxicity. Receptor-targeting was used to deliver contrast-producing superparamagnetic iron oxide (IO) nanoparticle to receptor-expressed tumors for in vivo magnetic resonance (MR) imaging. Folate-based ligands are especially popular for targeted delivery of therapeutics and imaging agents to cancer tissues[35-38].

Folate is required by all cells for metabolism and survival. Eukaryotic cells are unable to produce folate and therefore must ingest it from the environment. There are two routes by which folate can enter a cell (**Figure 6.1**):
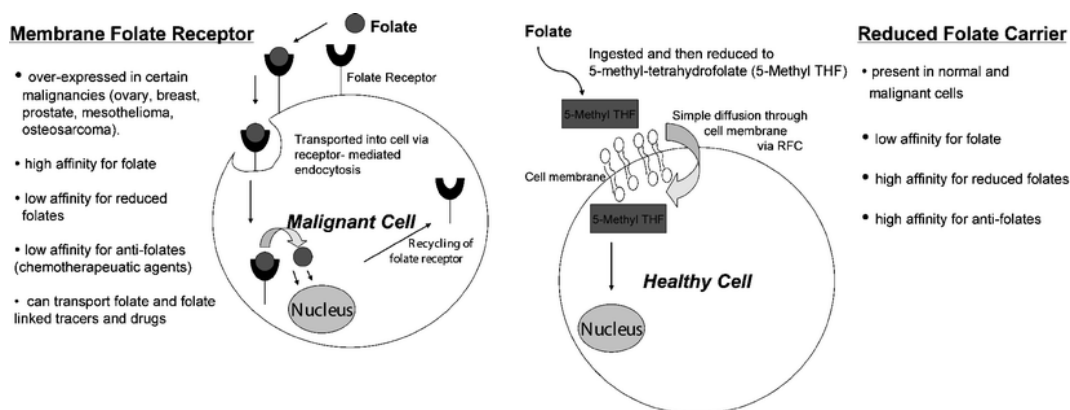
Figure 6.1 Mechanisms of folate entry into cells[39]

The major route of entry is through reduced folate carrier (RFC)[40]. RFC is a transmembrane protein that is ubiquitously expressed throughout development and in normal adult tissue. Upon oral ingestion of folate, the vitamin undergoes intestinal absorption and is rapidly taken up by the liver[41]. The reduced form of folate is then released by the liver and enters cells of normal organs via the RFC.

The other route of entry to cells is through folate receptor (FR). FR is a glycopolypeptide that binds folate with high affinity (Kd about $10^{-10}\,M$)[42] but not with its reduced form. FR remains relatively low levels of FR in normal tissues[49], but is over-expressed in various types of human carcinomas including ovarian, breast, colorectal and nasopharyngeal carcinomas in adults[43-45], as well as pediatric tumors such as choroid plexus tumors, ependymomas, osteosarcomas and leukemia[46-48]. Therefore this makes folate a valuable vehicle for conjugation with specific tracers for targeted delivery of therapeutics and imaging agents to inflammation sites or cancer tissues. The FR-targeted deliveries have relatively easy and cost-effective synthesis, potential broad applications for a large variety of tumors, and favorable tumor-to-background ratios.

Successful tumor-selective FR targeting has been reported both in vitro and in vivo with a variety of nanoparticles[50-52]. More recently, efforts have been directed toward the development of imaging probes that are detectable with MR imaging[53,54], which provides a noninvasive means for tumor detection with excellent soft-tissue contrast and anatomic resolution, without radiation exposure.

The aim of our study was to develop a FR-targeted super paramagnetic polymeric micelle (Figure 6.2) as a new class of drug delivery system with remarkably high spin-spin (T_2) relaxivity and sensitivity that allows combining treatment with disease monitoring. Super-paramagnetic iron oxide (SPIO) nanoparticles such as magnetite (Fe_2O_3) are known to exert a strong effect on T_2. The better detection sensitivity and slower kidney clearance of magnetic nanoparticles make them advantageous over Gd-based small molecular contrast agents. Currently, most T_2 contrast agents are composed of hydrophilic magnetite nanoparticles dispersed in a dextran matrix. However, our design is making magnetite particles encapsulated inside the

hydrophobic core of a Biodegradable poly(ε-caprolactone)-*b*-poly(ethylene glycol)(PCL-*b*-PEG, PCE) polymeric micelle whose surface is stabilized by a PEG shell (**Figure 6.2**). This novel micellar magnetic-resonance probe has a unique core-shell structure which enables the micelle core to serve as a nanoscopic depot for therapeutic agents, and the outer surface of the copolymer attached with cell-specific ligands (folate) for targeted cancer detection and therapy. It may provide a great opportunity to combine treatment with disease monitoring. We choose ovarian cancer with high levels of FR over-expression as a representative tumor in order to evaluate the feasibility of FR-targeted MR imaging. The concept of receptor-targeted imaging, however, would be applicable to other FR-positive tumors.
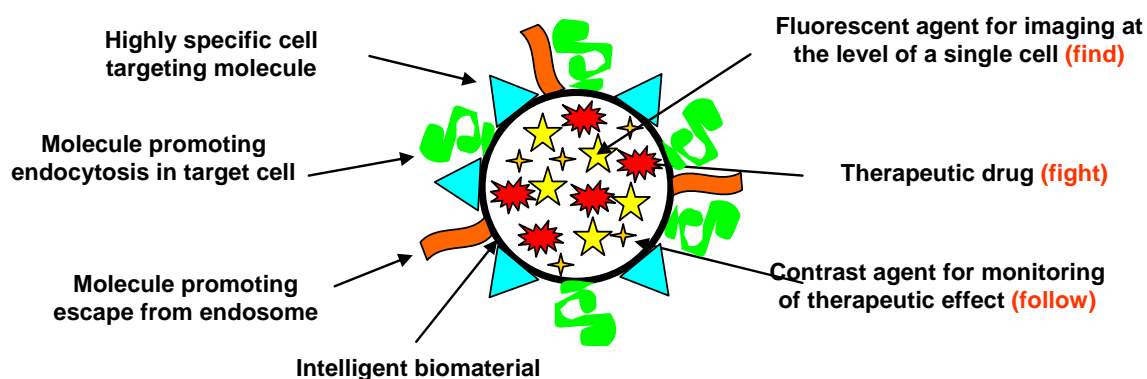
Figure 6.2 Multifunctional micellar drug delivery systems

6.2 RESULTS AND DISCUSSION

We used an amphiphilic diblock copolymer of poly(ε-capro-lactone)-*b*-poly(ethylene glycol) (PCL-*b*-PEG) for the micelle formation. This copolymer was synthesized by a ring opening polymerization of ε-caprolactone using mono-azido-terminated PEG (2 k) as a macroinitiator and $Sn(Oct)_2$ as a catalyst.[7] The feed ratio was controlled to achieve the final copolymer composition (PEG_{45}-*b*-PCL_{23}). The PCL segment has been demonstrated to form crystalline hydrophobic cores, which leads to stable micelle formation with a very low critical micelle concentration (CMC).[10] Hydrophobic, single magnetite (Fe_2O_3) nanocrystals were synthesized with precise

control of particle diameters (12 nm) following a published procedure by Sun et al.[11,12] Transmission electron microscopy (TEM) showed that the magnetic particles are mostly uniform in size distribution. Compared to previously studied hydrophilic magnetic particles that are synthesized through co-precipitation of ferrous (Fe^{2+}) and ferric (Fe^{3+}) ions in a basic aqueous phase,[8,13] our particles are covered with hydrophobic aliphatic chains from dodecylamine (DDA) during magnetic particle synthesis, which is essential for micelle encapsulation and ligand exchanging. Magnet-loaded polymeric micelles were formed using a solvent evaporation procedure.

Preparation and characterization of Single magnetite (γ-Fe_2O_3) nanocrystals

Magnetite (γ-Fe_2O_3) nanocrystals were synthesized with precise control of particle diameters (12 nm) utilizing a simple one-step synthesis. Structurally well-defined iron oxide nanocrystals with the shapes of mainly diamonds, triangles, and spheres were obtained from the thermal decomposition of $Fe(CO)_5$ in a hot solution (180 °C) containing capping ligand (dodecylamine (DDA)) under aerobic condition by precursor-to-capping ligand molar ratio of 1:1. During this thermolysis and air oxidation process, the color of the solution changed from initial orange to deep red-brown. After 9 h, the resulting solution was separated and analyzed. TEM analysis (**Figure 6.3A**) shows a mixture of diamond, sphere, and triangle-shaped nanocrystals all similar in size (~12 nm). High resolution transmission electron microscopy (HRTEM) images illustrate that these nanocrystals are high-quality single-crystalline maghemite (γ-Fe_2O_3) (**Figure 6.3C**). Spherical nanocrystals were isolated from the mixtures via a simple precipitation method. TEM image shows monodisperse nanocrystals of 12 nm (σ = 4.6%) (**Figure 6.3 B**).
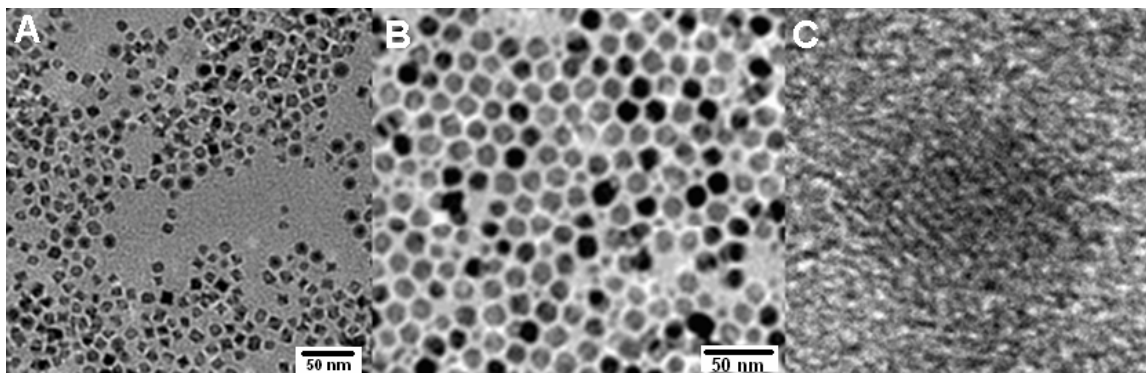
Figure 6.3 TEM images I (A) TEM image of ~ 12 nm γ-Fe$_2$O$_3$ nanocrystals which are the mixture of diamond, sphere, and triangle-shaped nanocrystals. (B) TEM image of γ-Fe$_2$O$_3$ spherical nanocrystals after the shape-selection process. (C) HRTEM image of spherical shaped nanocrystals, which indicates the particle composition is γ-Fe$_2$O$_3$.

End Group Functionalization of PEG$_{45}$-*b*-PCL$_{23}$ Block Copolymers via Click Reaction

We used an amphiphilic diblock copolymer of azido-terminated poly(ethylene glycol)-*b*-poly (ε-caprolactone) (N$_3$-PEG-*b*-PCL), which was developed to prepare for ligand-modifiable micellar nanoparticles that can entrap lipophilic compounds (drugs). In PEG$_{45}$-*b*-PCL$_{23}$ block copolymers (molecular weight of polymers was estimated to 4500 by NMR) the functional groups at the end of the PEG and PCL are azide and hydroxyl, respectively. The hydroxy group can react with the carboxylic group in 3,4-dihydroxyphenylacetic acid (**Scheme 6.1**), which is a robust anchor conjugating on the iron oxide shell of the nanocrystals. Although several functional groups have been utilized to immobilize on iron oxide nanocrystals, their binding strength and their ease of surface immobilization are very different. The spectroscopic studies showed that bidentate enediol ligands convert the under-coordinated Fe surface sites back to a bulk-like lattice structure with an octahedral geometry for oxygen-coordinated iron, which may result in tight binding to iron oxide[7]. Therefore, the polymer bearing the 3,4-dihydroxyphenylacetic acid terminal functional group can chelate to the surface of magnetic

nanoparticles. By further attaching folic acid to the surface of the copolymer, targeted cancer detection and therapy can be achieved. Recently, Couvreur *et al.* has demonstrated that in the case of the self assembly of folic acid-encoded micelles as drug delivery systems, the number and distribution of micelle surface ligands can have a significant affect on biodistribution, cytotoxicity, and anticancer activity.[28] Therefore, we hypothesized that the "spring-loaded" nature of the Cu(I)-catalyzed Huisgen [2 + 3] dipolar cycloaddition reaction (click reaction) between an organic azide and a terminal alkyne would permit exhaustive reaction between polymers and folic acid via a routine method. The azido-functionalized PEG$_{45}$-*b*-PCL$_{23}$ was reacted with propargyl folate at 25 °C in DMF according to **Scheme 6.1**. After catalyst removal, the end-functionalized polymers were purified by reprecipitation and size exclusion chromatography to remove unconjugated propargyl folate starting material and afford the functionalized polymer **5**.
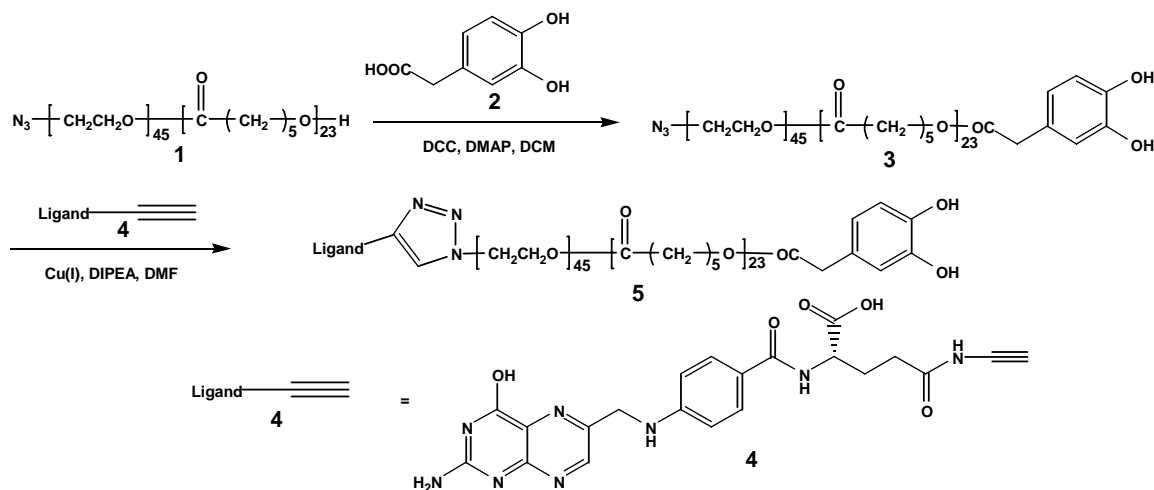
Scheme 6.1 Synthesis of functional PCE polymers

End group functionalization of N$_3$-PEG-*b*-PCL copolymer was characterized by ^{1}H NMR. **Figure 6.4B** shows the ^{1}H NMR spectrum of N$_3$-PEG-PCL copolymer bearing the 3,4-dihydroxyphenylacetic acid functional group at the end of the PCL in DMSO-d*6*. Resonances

of the PEG methylene protons (mainly at δ=3.42 ppm) and PCL protons (δ=1.35, 1.56, 2.24, and 3.98 ppm) were observed. The two small peaks at δ = 6.61 and 6.47 ppm was contributed by the proton resonance of the aromatic protons of 3,4-dihydroxyphenylacetic acid, and the intensity of the protons at δ =6.61 ppm confirms that the 3,4-dihydroxyphenylacetic acid group was successfully linked to copolymers . In addition, the azide functional group at the end of the PEG modification with folate was accomplished by CuAAC. ^{1}H NMR spectroscopy strongly suggests propargyl folate was successfully conjugated to PEG parts of polymers (**Figure 6.4A**). The small peak at δ = 8.63 was attributed to the proton resonance of the pteridine ring and small peaks at δ = 7.61 and 6.60 were belonged to proton resonance of the benzyl ring. All these NMR spectrum data strongly indicated that the desired bifunctional block copolymers **5** were successfully synthesized.
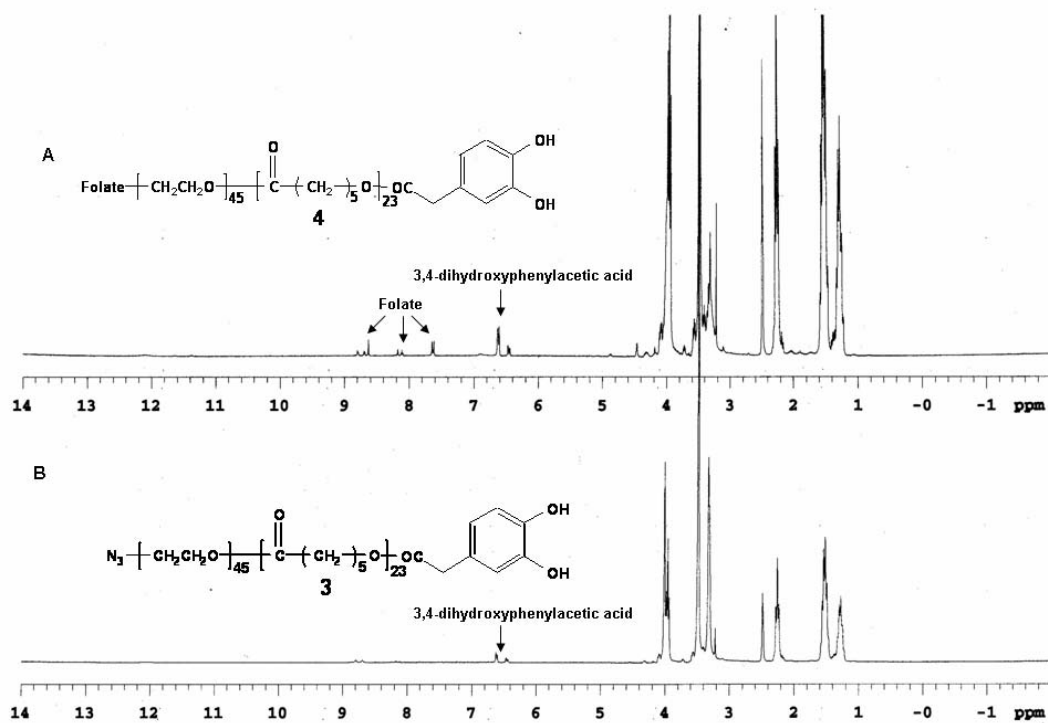
Figure 6.4 ^{1}H-NMR spectra of functional polymers

Preparation of Magnetite-Loaded Polymeric Micelles

Spherical nanocrystals are covered with DDA during SPIO synthesis, which is necessary for the ligand exchanging for further nanocrystal surface modification. SPIO-loaded polymeric micelles were formed using a solvent evaporation procedure, in which a cluster of SPIO particles was encapsulated inside the hydrophobic core of PCL-*b*-PEG micelles. It is notable that peptide-based copolymers had also been used to equip polymer micelles or vesicles for encapsulating both hydrophilic and hydrophobic maghemite nanocrystals.[14,15] In this case, we choose biocompatible and biodegradable folate functionalized PCL-b-PEG copolymer for the formation of FR-targeted SPIO-loaded micelles which specifically have bifunctions of combination of MR probes and targeting deliver system(**Figure 6.5**). PCL-*b*-PEG Copolymer was dissolved in dimethyl sulfoxide (DMSO), and a solution of magnetic nanoparticles in toluene (8 wt%) was added. Fe_2O_3 nanoparticles were reacted with polymer **5** under vigorous stirring overnight and then under sonication for 30 min to form Fe-O bonds that link polymer **5** to the Fe_2O_3 shell. After the reaction, the resulting Fe_2O_3 nanoparticles covered with polymers can be collected by centrifugation and free polymer can easily be removed. Fe_2O_3 nanoparticles were re-dissolved in DMSO, and the suspension was dispersed by sonication, and the well-dispersed suspension was added dropwise to water under ultrasonic dispersion. After 3 h, magnet-load polymeric micelles were prepared successfully. The obtained magnet-load polymer micelles were collected using centrifugation, and subsequently magnetic-separated. The obtained nanoparticles were washed with distilled water, centrifuged three times to remove some small molecules, and magnetic-separated twice to remove the micelles without magnets.

Magnet-loaded polymeric micelles were analyzed by direct cryogenic transmission electron microscopic (cryo-TEM) imaging of the microstructures in the form of thin vitreous hydrated

specimens to determine the size distribution in aqueous solution and magnet distribution in polymeric micelles. Analyses of cryo-TEM images lead to determination of the packing properties of the hydrophobic block in terms of the interfacial area per chain and the degree of chain stretching.
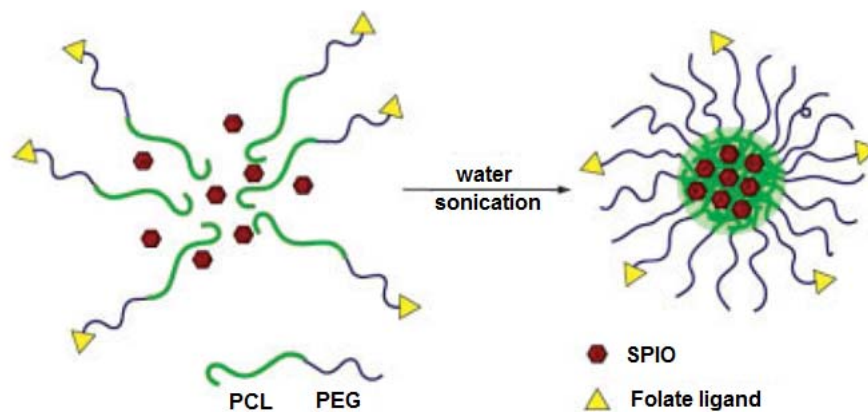
Figure 6.5 Preparation of magnet-loaded polymeric micelles

Figure 6.6 shows the average of hydrodynamic diameter of 12 nm magnet-loaded PCL-*b*-PEG micelles was 303±15 nm. The clustering of magnet nanoparticles in the micelle cores was verified with TEM and the mean magnetic nanoparticle loading number was 25. **Figure 6.7A** shows isolated clusters of magnetic nanoparticles on a carbon-coated grid at low magnification. Closer examination of a single micelle particle revealed the clustering of multiple 12 nm magnetic nanoparticles (**Figure 6.7B**). These aggregate structures represent the variation in magnet loading inside polymeric micelles, which may reflect the polydisperse nature of the PCL-b-PEG copolymer and the resulting micelles. Encapsulation of magnetic nanoparticles inside the hydrophobic micelle cores has the advantages of avoiding potential exposure of hydrophobic magnetic surfaces and adsorption of blood proteins (e.g., opsonin), and may allow an increased blood circulation.
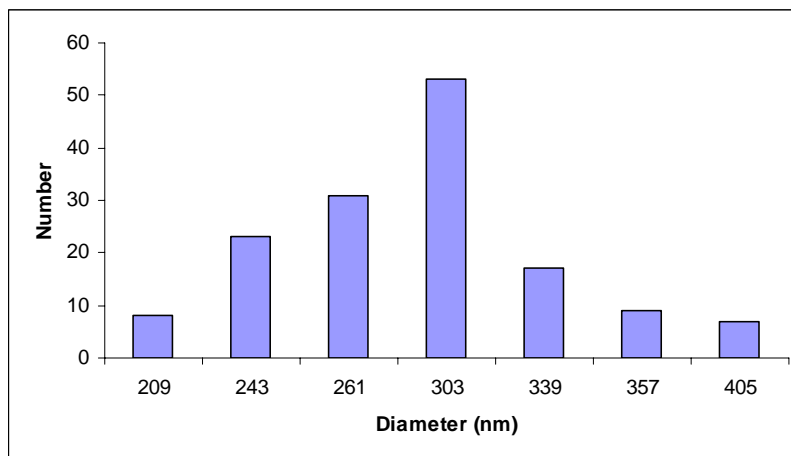
Figure 6.6 TEM shows the size distribution of 12 nm magnet-loaded micelles
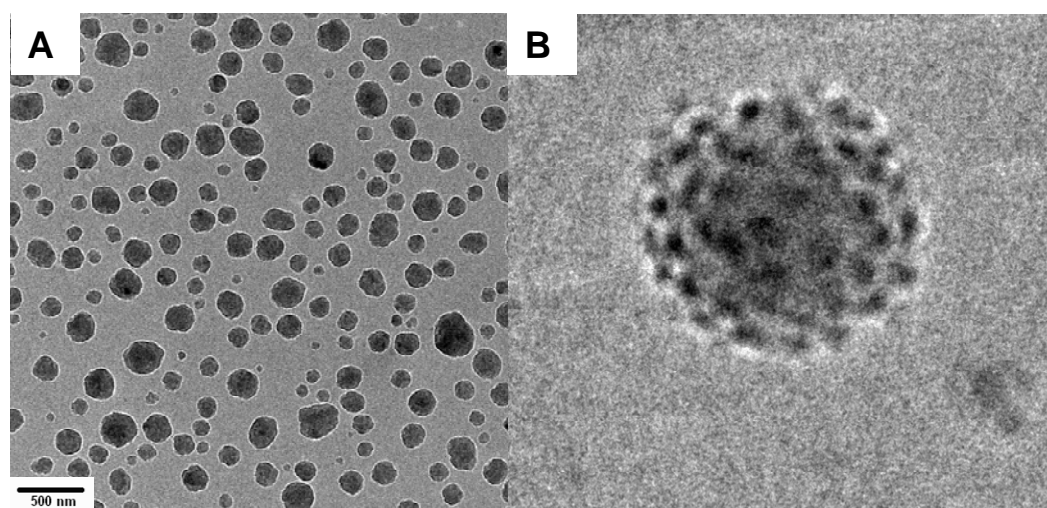
Figure 6.7 TEM images II (A) TEM of magnet-loaded micelles at low magnification. (B) TEM of micelles at high magnification.

CONCLUSION

In summary, we present the proof-of-concept for the use of magnet-load polymeric micelles for ultra-sensitive MRI detection. The clustering of magnetic particles inside the hydrophobic core of micelles can increase MRI relaxivity. The hydrophilic PEG corona gives a stable shell for protecting particles in aqueous solution. By further attaching cell-specific ligands (Folate) on the surface of the micelles, targeted cancer detection and therapy can be achieved. The unique FR-

targeted magnet-loaded micelles design expands the application of polymeric micelles, not only for encapsulating small organic molecules, but also for nanosize contrast reagents targeted to novel diagnostic and therapeutic applications.

6.3 EXPERIMENTAL PROCEDURES

^{1}H-NMR spectra were recorded in CDCl$_3$ or D$_2$O on a Varian Merc-300 or Varian Inova-500 spectrometers equipped with Sun workstations at 300K. TMS (δ_H=0.00) or D$_2$O (δ_H=4.67) was used as the internal reference. ^{13}C-NMR spectra were recorded in CDCl$_3$ or D$_2$O at 75MHz on Varian Merc-300 spectrometer, respectively using the central resonance of CDCl$_3$ (δ_C=77.0) as the internal reference. COSY, HSQC, HMBC and TOCSY experiments were used to assist assignment of the products. Mass spectra were obtained on Applied Biosystems Voyager DE-Pro MALDI-TOF (no calibration) and Bruker Daltonics 9.4T (FTICR, external calibration with BSA). Optical rotatory power was obtained on Jasco P-1020 polarimeter at 300 K. Chemicals were purchased from Aldrich or Fluka and used without further purification. DCM was distilled from calcium hydride; THF from sodium; CH$_3$OH from magnesium and iodine. Aqueous solutions are saturated unless otherwise specified. All the reactions were performed under anhydrous conditions under argon and monitored by TLC on Kieselgel 60 F254 (Merck). Detection was by examination under UV light (254 nm) and by charring with 10 % sulfuric acid in methanol. Silica gel (Merck, 70-230 mesh) was used for chromatographies. Iatrobeads 6RS-8060 was purchased from Bioscan.

Preparation and characterization of Single magnetite (γ-Fe$_2$O$_3$) nanocrystals

Preparation: In a typical synthesis of mixed shapes γ-Fe$_2$O$_3$ nanocrystals, 1.0 mmol of Fe(CO)$_5$ (0.13 mL) dissolved in 0.5 mL of (not deoxygenated) ortho-dichlorobenzene (ODCB) was rapidly injected into a hot solution containing 2.0 mL of ODCB and 1.0 mmol of

dodecylamine (DDA, 0.18 g). The resulting mixture was maintained at 180 $^{\circ}$C under aerobic conditions. During this process, the initial orange color of the solution gradually changes to slightly black. After 12 h, the resulting solution was cooled to room temperature and an approximately 10.0 ml toluene was added to adjust the solubility of the nanocrystals. The initial crop of nanocrystals containing mixtures of spheres, triangles and diamonds was isolated by centrifugation and redispersed in toluene. After adding ethanol into the remaining solution, resulting black flocculates were isolated by centrifugation. This second crop was identified as highly monodisperse spherical 12 nm γ-Fe$_2$O$_3$.

Characterization: TEM observations were carried out on an FEI Tecnai 20 electron microscope operated at 120 and 300 kV, respectively. The data were collected in transmission mode with N$_2$ gas-filled ionization chambers as detectors. Samples for TEM analysis were prepared by drying a dispersion of the γ-Fe$_2$O$_3$ particles in hexane on amorphous carbon coated copper grids. The TEM data showed that the SPIO particles are mostly uniform in size distribution. In addition, the measured particle lattice spacing matches very closely to the published 2004 J. Am. Chem. Soc for Diffraction Data for magnetic nanoparticles indicating the particle composition is γ-Fe$_2$O$_3$.

Synthesis of Alkyne-Functionalized Folic Acid (Propargyl Folate) (4) The synthesis of propargyl folate was accomplished by a method derived from literature reports of folate conjugation.[55] Folic acid (0.6 g, 0.0013 mol) was dissolved in DMF (10 mL) and cooled in a water/ice bath. *N*-Hydroxysuccinimide (160 mg, 0.0015 mol) and EDC (260 mg, 0.0015 mol) were added and the resulting mixture was stirred on an ice bath for 30 min to give a white precipitate. A solution of propargylamine (75 mg, 1.35 mmol) in DMF (5.0 mL) was added, and the resulting mixture was allowed to warm to room temperature and stirred for 24 h. The reaction

mixture was poured into water (50 mL) and stirred for 1 hour to form a precipitate. The orange-yellow precipitate was filtered, washed with acetone, and dried under vacuum for 6 h to yield 0.50 g of product (78% yield). ^{1}H NMR (DMSO-d_6, ppm): 8.64 (1H, s), 8.29–8.24 (1H, d, J = 5.2 Hz), 8.04–8.02 (1H, d, J = 7.8 Hz), 7.67–7.65 (2H, d, J = 8.3 Hz) 6.93 (2H, brs), 6.65–6.63 (2H, d, J = 8.4 Hz), 4.49–4.48 (2H, d, J = 5.2 Hz), 4.32–4.30 (1H, m), 3.84–3.81 (2H, m), 3.07–3.05 (1H, t, J = 2.6 Hz), 2.88 (1H, s), 2.72 (1H, brs), 2.31–2.20 (2H, m), 1.98–1.96 (1H, m), 1.87–1.85 (1H, m).

Synthesis of 3,4-dihydroxyphenylacetic acid functionalized polymer (3) To a solution of the 3,4-dihydroxyphenylacetic acid (200 mg, 1.2 mmol), N$_3$-PEG-b-PCL polymer (450 mg, 1.0 mmol) and DMAP (1 mg, 0.008 mmol) in CH$_2$Cl$_2$ (20 mL) at 0°C was added DCC (260 mg, 1.1 mmol). After being stirred at room temperature for 12 h, the mixture was diluted with ether and filtered through a pad of celite. The filtrate was concentrated and was precipitated into hexanes. The resulting block copolymer was purified by LH-20 size exclusion chromatography using CH$_2$Cl$_2$/CH$_3$OH (1:1 v/v) as the eluent.

Click Reaction of Azido-Terminated Polymers with Propargyl Folate (4) The azido-terminated polymers were reacted with propargyl folate **(4)** in a manner analogous to the following example procedure. A solution of N$_3$-PEG-b-PCL **(3)** (M_n = 4500 g/mol, 270 mg, 0.0600 mmol) and DIPEA (4.3 mg, 0.033 mmol) in DMF (5 mL) was purged with nitrogen for 1 hour and transferred via syringe to a vial equipped with a magnetic stir bar containing CuI (6.3 mg, 0.033 mmol) and propargyl folate (2) (30 mg, 0.063 mmol) under a nitrogen atmosphere. The reaction mixture was stirred at 25 °C for 2 days in the absence of oxygen. The reaction mixture was exposed to air, and the solution was passed through a column of the celite. DMF was removed under vacuum, and the product was precipitated into hexanes. The resulting folate-

terminated block copolymer (FA-PEG-*b*-PCL) (6) was dissolved in THF and filtered to remove excess propargyl folate. THF was removed under reduced pressure and the polymers were purified by LH-20 size exclusion chromatography using CH_2Cl_2/CH_3OH (1:1 v/v) as the eluent.

Formation of Magnet-Loaded Polymeric Micelles

Magnet-loaded polymeric micelles were prepared as follows in a typical example: 0.20 g folate-terminated block copolymer was dissolved in 6 mL of dimethyl sulfoxide (DMSO), and 0.3 ml magnetic nanoparticles solution in toluene (8 wt%) was added. The suspension was vigorously stirred overnight and it was ultrasound-dispersed for another 30 min to generate Fe-O bonds that link polymer **5** to the Fe_2O_3 shell. After the reaction, the resulting Fe_2O_3 nanoparticles covered with polymers can be collected by centrifugation and free polymer can be removed easily. Fe_2O_3 nanoparticles were dissolved in 5 ml DMSO again, and next, the well-dispersed suspension was dropped into 100 mL pure water under ultrasonic dispersion. After 3 h, the porous magnetic polymeric micelles were prepared successfully.

The obtained magnetic polymeric micelles were collected by centrifugation at a speed of 10,000 rpm, and then magnetic-separated. The composite micelles were washed with distilled water and centrifuged three times to wash off remaining small molecules, and magnetic-separated two times to remove the micelles without magnetism. Then, the samples were stored at 4 °C and all related measurements were conducted within two weeks.

Characterization of magnet-Micelles

Samples for TEM analysis were spread on an on amorphous carbon coated copper grids and were preserved in a frozen-hydrated state by rapid freezing, usually in liquid nitrogen temperature. By maintaining specimens at liquid nitrogen temperature or colder, they can be introduced into the high-vacuum of the electron microscope column. Cryogenic Transmission

Electron Microscopy (Cryo-TEM) was used to study size distribution in aqueous solution and magnet distribution in polymeric micelles. The mean hydrodynamic diameters were 300 nm for PCL-*b*-PEG micelles containing 12 nm SPIO particles (Figure S2E and S2F). in addition, TEM data showed that polymeric micelles containing 12 nm SPIO nanoparticles and cluster of SPIO nanoparticles were encapsulated in one micelle.

6.4 REFERENCES

1. V. P. Torchilin, *Adv. Drug Delivery Rev.* 2002, 54, 235.

2. H. Otsuka, Y. Nagasaki, K. Kataoka, *Adv. Drug Delivery Rev.* 2003, 55, 403.

3. M. L. Adams, A. Lavasanifar, G. S. Kwon, *J. Pharm. Sci.* 2003, 92, 1343.

4. B. Dubertrer, P. Skourides, D. J. Norris, V. Noireaux, A. H. Brivan-lou, A. Libchaber, *Science* 2002, 298, 1759.

5. S. Lecommandoux, Y. Gnanou, *Bioforum* 2004, 5, 38.

6. R. Savic, L. Luo, A. Eisenburg, D. Maysinger, *Science* 2003, 300, 615 – 618.

7. S. Muniyandy, B. Kessavan, and P. K. Sadasivan, *Int. J. Pharm.* 2004, 283, 71.

8. S. Rudge, C. Peterson, V. Cessely, J. Koda, S. Stevens and L. Catterall, *J. Control Rel.* 2001, 74, 335.

9. H. Yousef, P. Vinay, C. Ching-jen, *J. Magn. Mater.* 1999, 194, 254.

10. J. Richardson, P. Hawkins and R. Luxton, *Biosensors Bioelectronics.* 2001, 16, 989.

11. G. Zheng, B. Shu and S. Yan, Enzyme, *Microb. Technol.* 2003, 32, 776.

12. A. Spanova, B. Rittich, M. J. Benes and D. Horak, *J. Chromatogr. A* 2005, 1080, 93.

13. Enochs, W. S., Harsh, G., Hochberg, F. & Weissleder, R. *J. MRI* , 1999, 9, 228

14. Harisinghani, M. G., Barentsz, J. & Weissleder, R. *New England Journal of Medicine* 2003, 348, 2491-U5.

15. Bulte, J. W. M. & Kraitchman, D. L. *NMR Biomed.* 2004, 17, 104

16. J. Ren, H. Y. Hong, T. B. Ren and X. R. Teng, *Mater lett.* 2005, 59, 2655; L. Zhenghua and H. Leaf, *J. Control Rel.* 2004, 98, 437

17. D. Horak, *J. Polym. Sci. Part A: Polym. Chem.* 2001, 39, 3707

18. L. C. Santa Maria, M. A. S. Costa, F. A. M. Santos, S. H. Wang and M. R. Silva, *Mater. Lett.* 2006, 60, 270

19. Y. Deng, L. Wang, W. Yang, S. Fu and A. Elaissari, *J. Magn. Magn. Mater.* 2003, 257, 69

20. M. K. Chun, C. S. Cho and H. K. Choi, *Int. J. Pharm.* 2005, 288, 295

21. S. Guinebretiere, S. Briancon, J. Lieto, C. Mayor and H. Fessi, *Drug Develop. Res.* 2002, 57, 18

22. J. You, F. D. Cui, Q. P. Li, X. Han, Y. W. Yu and S. M. Yang, *Int. J. Pharm.* 2005, 288, 315

23. Y. Y. Yang, H. H. Chia and T. S. CHung, *J. Control Rel.* 2000, 69, 81

24. R. H. Mullar, S. Maaben, H. Weyhers, F. Specht and J. S. Lucks, *Int. J. Pharm.* 1996, 138, 85

25. J. Ren, H. Y. Hong, T. B. Ren and X. R. Teng, *Mater lett.* 2005, 59, 2655

26. L. C. De Santa Maria, M. C. A. M. Leite, M. A. S. Costa and J. M. S. Ribeiro et al., *Mater. Lett.* 2004, 58, 3001

27. S. B. Zhou, X. M. Deng and H. Yang, *Biomaterials* 2003, 24, 3563

28. Barbara Stella, Silvia Arpicco, Maria Teresa Peracchia, Didier Desmaële, Johan Hoebeke, Michel Renoir, Jean D'Angelo, Luigi Cattel, Patrick Couvreur, *J. Pharm. Sci.* 2000, 89(11), pp. 1452,.

29. Jinwoo Cheon, Sang Jun Oh, *J. Am. CHEM. SOC.* 2004, 126, 1950.

30. Sun, S.; Zeng H. *J. Am. Chem. Soc.* 2002, 124, 8204.

31. X. Shuai, T. Merdan, A. K. Schaper, F. Xi, T. Kissel, *Bioconjugate Chem.* 2004, 15, 441.

32. X. Shuai, H. Ai, N. Nasongkla, S. Kim, J. Gao, *J. Controlled Release* 2004, 98, 415.

33. K. Greish, J. Fang, T. Inustuka, A. Nagamitsu, H. Maeda, *Clin. Eur. Clin. Phamarcokinet.* 2003, 42, 1089

34. Y. Yamamoto, Y. Nagasaki, Y. Kato, Y. Sugiyama, K. Kataoka, *J. Controlled Release* 2001, 77, 27

35. Kamen, B. A.; Capdevila, A. *Proc. Natl. Acad. Sci. U.S.A.* 1986, *83*, 5983.

36. Rothberg, K. G.; Ying, Y.; Kolhouse, J. F.; Kamen, B. A.; Anderson, R. G. W. *J. Cell. Biol.* 1990, *110*, 637

37. Leamon, C. P.; Low, P. S. *Proc. Natl. Acad. Sci. U.S.A.* 1991, *88*, 5572–5576.

38. Low, P. S.; Henne, W. A.; Doorneweerd, D. D. *Acc. Chem. Res.* 2008, *41*, 120–129.

39. Wang, ZJ; Boddington, S; Wendland, M; Meirer, R; Corot, C and Daldrup-Link, H. *Pediatric Radiology*, 2008, 5, 529

40. Matherly LH, Goldman DI, *Vitam Horm* 2003, 66, 403

41. Sadasivan E, Rothenberg SP, da Costa M et al *Biochim Biophys Acta* 1986, 882, 311

42. Antony AC Folate receptors. *Annu Rev Nutr*, 1996, 16, 501

43. Ross JF, Chaudhuri PK, Ratnam M *Cancer*, 1994, 73, 2432

44. Toffoli G, Cernigoi C, Russo A et al, *Int J Cancer* 1997, 74, 193

45. Weitman SD, Lark RH, Coney LR et al, *Cancer Res*, 1992, 52, 3396

46. Patrick TA, Kranz DM, van Dyke TA et al, *J Neurooncol*, 1997, 32, 111

47. Yang R, Kolb EA, Qin J et al, *Clin Cancer Res,* 2007, 13, 2557

48. Wang H, Zheng X, Behm FG et al, *Blood*, 2007, 96, 3529

49. Shen F, Ross JF, Wang X et al, *Biochemistry*, 1994, 33, 1209

50. Bettio A, Honer M, Muller C et al. *J Nucl Med*, 2006, 47, 1153

51. Reddy JA, Xu LC, Parker N et al. *J Nucl Med*, 2004, 45, 857

52. Guo W, Hinkle GH, Lee RJ. *J Nucl Med*, 1999, 40, 1563

53. Konda SD, Aref M, Brechbiel M et al. *Invest Radiol*, 2000, 35, 50

54. Konda SD, Aref M, Wang S et al. *MAGMA* 2001, 12, 104

55. Priyadarsi De, Sudershan R. Gondi, and Brent S. Sumerlin, *Biomacromolecules*, 2008, 9, 1064

CHAPTER 7

CONCLUSIONS

We have successfully demonstrated the applications of click chemistry in three classes including drug discovery, bioconjugation, and materials science.

Two novel anti-influenza reagents based on the Altermune Method were synthesized by using the click reation in **Chapter 2**. These anti-influenza reagents are designed to stimulate the immune system to attack influenza viruses using a Linker Molecule, which can recognize the viruses and be recognized by immune system, and then redirect the immune response to influenza viruses.

A novel Cu^I-free reagent, 4-Dibenzocyclooctynol described in **Chapter 3**, was designed, synthesized and found to react exceptionally fast with azido-containing saccharides and amino acids to give stable triazoles in the absence of a Cu^I catalyst. Its biotin-modified derivative is ideally suited for visualizing and tracking glycoconjugates of living cells that are metabolically labeled with azido-containing monosaccharides.

In addition, quantitative isotopic and chemoenzymatic tagging (QUIC-Tag) was synthesized for the monitoring the dynamics sialylation *in vivo* using quantitative mass spectrometry-based proteomics in **Chapter 4**. This method combines selective, chemoenzymatic tagging of glycans with an efficient isotopic labeling strategy, and can also be used with metabolic oligosaccharide engineering, which incorporate sugar with bioorthogonal chemical reporters into cellular glycoconjugates. This method will help to delineate the molecular basis for aberrant glycosylation in cancer and ultimately can be applied for diagnostic and therapeutic.

Micellar nanoparticles are very important for drug delivery systems. We designed a novel KDEL functional micelles, which can enhance the micellar delivery of encapsulated hydrophobic glycosidase and glycosyltransferase inhibitors into the ER, in **Chapter 5**. It was demonstrated that KDEL-peptide-PEO-*b*-PCL conjugate micelles were successfully prepared by using the click reaction, which has open a new door for the development of multifunctional micellar drug delivery systems.

At last, magnet-loaded polymeric micelles for ultra-sensitive MRI detection were prepared in **Chapter 6**. The clustering of magnetic particles inside the hydrophobic core of micelles can increase MRI relaxivity. The hydrophilic PEG corona gives a stable shell for protecting particles in aqueous solution. By further attaching cell-specific ligands (Folate) on the surface of the micelles by using click reaction, targeted cancer detection and therapy can be achieved. The unique FR-targeted magnet-loaded micelles design expands the application of polymeric micelles, not only for encapsulating small organic molecules, but also for nanosize contrast reagents targeting to novel diagnostic and therapeutic applications.